Hydrodynamics

Infrastructure Victoria
Second Container Port Advice

59917507

Prepared for
AECOM

3 May 2017

Cardno®
Shaping the Future

Contact Information

Cardno Victoria Pty Ltd
ABN 47 106 610 913

Level 4 , 501 Swanston Street
Melbourne, VIC 3000

Telephone: (03) 8415 7777
Facsimile: (03) 8415 7788
International: +61 3 8415 7777

www.cardno.com.au

Author(s):
David Provis
Senior Principal, Oceanography

Approved By:
Phebe Bicknell
Experienced Engineer

Document Information

Prepared for	AECOM
Project Name	Infrastructure Victoria Second Container Port Advice
File Reference	59917507_R_01_Rev_0
Job Reference	59917507
Date	3 May 2017
Version Number	Revision 0 (Final)
Effective Date	3 May 2017
Date Approved:	3 May 2017

Document History

Version	Effective Date	Description of Revision	Prepared by:	Reviewed by:
V01	12 Dec 2016	Internal Draft	dgp	pjb
Rev A	22 Dec 2016	Draft for review by IV	dgp	pjb
Rev B	31 Jan 2017	Revision following review by I.V.	dgp	pjb
Rev C	27 Feb 2017	Revision following review by I.V.	dgp	pjb
Rev 0	3 May 2017	Final	dgp	pjb

Executive Summary

The Victorian Special Minister of State has asked Infrastructure Victoria to provide advice on the future capacity of Victoria's ports, focusing on the need for, timing and location of a second container port.

Currently all container shipping into Victoria is through the Port of Melbourne, which is Australia's largest container port. The Infrastructure Victoria Study is preparing advice on the ultimate capacity of the Port of Melbourne, when the port will reach capacity and when a second counter port will be required.

The Special Minister of State has also asked Infrastructure Victoria to assess two possible sites for the second container port, one at Hastings in Western Port and one at Bay West in Port Phillip Bay.

Bay West

The Bay West project (see Figure 2-3 and Figure 2-4) was modelled using an existing validated model. The model included the following features of the Project:

> An island at Bay West with dredged channel, turning basin and berth pockets all dredged to -16.5 m CD

> Great Ship Channel in the Entrance to Port Phillip widened from 245 m to 425 m at the existing depth of -17.3 m CD;

> South Channel deepened to -17.3 m CD within the existing toe lines;

> Turning area around Hovell Pile deepened to -17.8 m CD within the existing toe lines.

The impacts identified include those due to the dredging to widen the Entrance and deepen South Channel:

> An increase in tidal range in the body of the bay with the 2nd percentile, the level defining the lowest 2% of sea levels, decreasing by 3.7 mm and the 98th percentile, the level defining the highest 2% of sea levels, increasing by 6.3 mm. This is due mainly to the widening of the Great Ship Channel.

> An increase in the peak tidal currents in Port Phillip Heads of up to 10% in the areas where dredging occurs when the channel is widened, but generally much less than this. This is due mainly to the widening of the Great Ship Channel.

> An increase in the current speeds in a relatively small area in the turning area around Hovell Pile where peak speeds increase by up to 15% and speeds two hours after the peak flood also increase, but do not exceed the existing peak current speed. This is due mainly to the deepening of South Channel.

The current speeds in the vicinity of Bay West are low, with tidal currents less than 0.1 m/s; there are some local increases at the ends of the terminal island, but only over a small area and speeds remain below the expected threshold for sediment movement.

Waves in Port Phillip Heads were modelled for slack water, peak ebb and peak flood flow conditions and the impact of the project channel widening investigated.

> At slack water, there are some increases in wave height (1-2%) on the Lonsdale Bight beach due to refraction from the dredged area on Nepean Bank, as well as some increases and decreases in different areas of energy propagating into the south of the bay.

> At peak ebb flow, there is an increase in wave height south of the entrance due to the effects of the increased ebb-tide jet, there is some reduction in wave energy propagating into the south of the bay.

> At peak flood, there are small increases and decreases in difference areas of Lonsdale Bight beach, a reduction in energy propagating into the south of the bay with some localised increases, particularly around Observatory Point and just south of the shipping channel.

Sediment transport due to tidal currents was modelled qualitatively to identify potential changes:

> There is an increase in potential sediment transport towards the north east - in the turning area around Hovell Pile due to the increase in flood currents.

> Near the entrance where there is a potential increase in transport towards the Heads on the south side of the channel and into the bay on the north side.

> In general, the changes in wave energy propagation are small and unlikely to result in significant change to beach processes; however, there may be some local effects.

There is a potential for vessel-generated waves to impact on the beaches in the south east of the bay between Safety Beach and Rye. As larger vessels transit the channel, it may be necessary to reduce the speed-limit in sections of the channel to minimise the likelihood of the generation of large waves.

There is the potential for the currents generated by large vessels in the Yarra River to become an issue for moored vessels along the river.

Hastings

The development of a container port in Western Port, Port of Hastings, as shown in Figure 3-2, requires;

Construction of a land backed berth with extension to the north east.

Dredging of new berths and swing basin, the swing basin with depths -16.2 m CD and the berth pockets - 16.5 m CD.

Deepening existing channels with some minor re-aligning to facilitate access for larger vessels; the seaward section of the Western Channel would have a declared depth of -17.5 m CD, the remaining sections to Stony Point a declared depth of -17.0 m CD, the North Arm southern section would be -16.3 m CD, the northern section -16.2 m CD.

The impacts of the development were modelled using an existing model.

> The greatest change in tide levels is at Tooradin where there is an increase in tidal range; the 2nd percentile, the level defining the lowest 2% of sea levels, will decrease by 14.5 mm and the 98th percentile, the level defining the highest 2% of sea levels will increase by 15.9 mm.

> At Stony Point the corresponding levels change by about 6 mm decrease and increase respectively.

> There is no change at Corinella.

> Tidal current speeds do not change apart from immediately adjacent to the new berth extension where there are local increases, especially in the gaps in the terminal reclamation.

> The tidal divide north east of French Island migrates an average of 32 m to the south east, but with a variability over the month of simulation of from 0 to 62 m.

No wave modelling was undertaken as there is minimal dredging south of Sandy Point and thus no impact on swell propagation from Bass Strait

Qualitative modelling of changes in sediment transport indicated changes in the vicinity of the port area, particularly on the edge of the dredged area and immediately adjacent to the terminal reclamation.

Table of Contents

Appendices

Tables

Figures

1 Introduction

1.1 The Project

The Victorian Special Minister of State has asked Infrastructure Victoria to provide advice on the future capacity of Victoria's ports, focusing on the need for, timing and location of a second container port.

Currently all container shipping into Victoria is through the Port of Melbourne, which is Australia's largest container port. The Infrastructure Victoria Study is preparing advice on the ultimate capacity of the Port of Melbourne, when the port will reach capacity and when a second counter port will be required.

The Special Minister of State has also asked Infrastructure Victoria to assess two possible sites for the second container port, one at Hastings in Western Port and one at Bay West in Port Phillip Bay.

1.2 Scope of work

The scope of work for this report, as agreed with AECOM and Infrastructure Victoria, is

Using existing numerical models, run the following cases:

> The hydrodynamics of Port Phillip with existing channel configuration and depths;

> The hydrodynamics of Port Phillip with channel configuration and depths required for the Bay West scenario as specified by the Navigation Study (AECOM, 2016) and Concept Options Report (GHD, 2017);

> The wave transmission through Port Phillip Heads with existing channel configuration and depths;

> The wave transmission through Port Phillip Heads with channel configuration and depths required for the Bay West scenario as specified by others;

> The hydrodynamics of Western Port with existing channel configuration and depths;

> The hydrodynamics of Western Port with channel configuration and depths required for the Port of Hastings scenario as specified by others;

Based on the results of the modelling assess the impact of the proposed developments on the following:

> Sea level;

> Currents;

> Wave conditions;

> Sediment transport (using residual currents over a threshold as a proxy);

> The “null point” in Western Port.

Provide the results in a written report including discussion of the numerical models and their validation, model results and results of the impact assessment.

1.3 Qualifications

This study has used existing numerical models and measured data. No new model development or data collection has been undertaken. Model calibration and validation relies on work existing at the time of commencing the study.

2 Port Phillip Bay – Bay West

2.1 Port Phillip Bay

Port Phillip Bay is almost circular in shape and covers approximately 1,930 km^2 in area (Figure 2-1). The overall coastline stretches for 264 km. The hydrodynamics of the Bay vary significantly depending on the dominant driving forces in the various areas (Cardno Lawson Treloar, 2007a).

The Entrance to Port Phillip Bay is approximately 3 km wide and includes Nepean Bank, the Entrance Deep and Rip Bank. The Entrance has a very dramatic and complex bathymetry with a deep canyon, the Entrance Deep. Depths here are close to 100 m. The canyon curves around the relatively shallow Nepean Bank and is bounded on the sea-ward side by Rip Bank. Water entering or leaving Port Phillip Bay thus flows over areas of greatly varying depths and the result is a highly turbulent flow with large eddies. In the area between Nepean and Rip Banks, the surface layer moves in a general north-south direction, whilst deeper water follows the canyon of the Entrance Deep moving approximately in an east-west direction. This area is characterised by very strong tidal-currents and sometimes very rough wave conditions.

Immediately north of the Entrance and south of the main body of the Bay, lies the Great Sands. The Great Sands consist of a number of substantial sand bars and shallows that are dissected by deeper channels. The Great Sands form a flood-tide delta, restricting the exchange of water and sediments between the Entrance and the main body of the Bay. The southern body of Port Phillip covering The Entrance and The Great Sands are shown in Figure 2-2.

West of the main body of the Bay lies the Geelong Arm which leads to Corio Bay (Figure 2-1). The exchange between this area and the main body of the Bay is further restricted by shallow areas, through which the shipping channel to Geelong has been dredged.

Figure 2-1 Map of Port Phillip region.

Figure 2-2 Map of South Port Phillip region showing South Channel.

2.2 Scenario

The container port development considered for Port Phillip is an island terminal off the west coast of the bay, south of the mouth of the Werribee River. A shipping channel would be dredged to the south east to reach the deeper central section of the bay. Berth pockets and swing basin would be dredged adjacent to the seaward side of the island. The general layout of the development is shown in Figure 2-3.

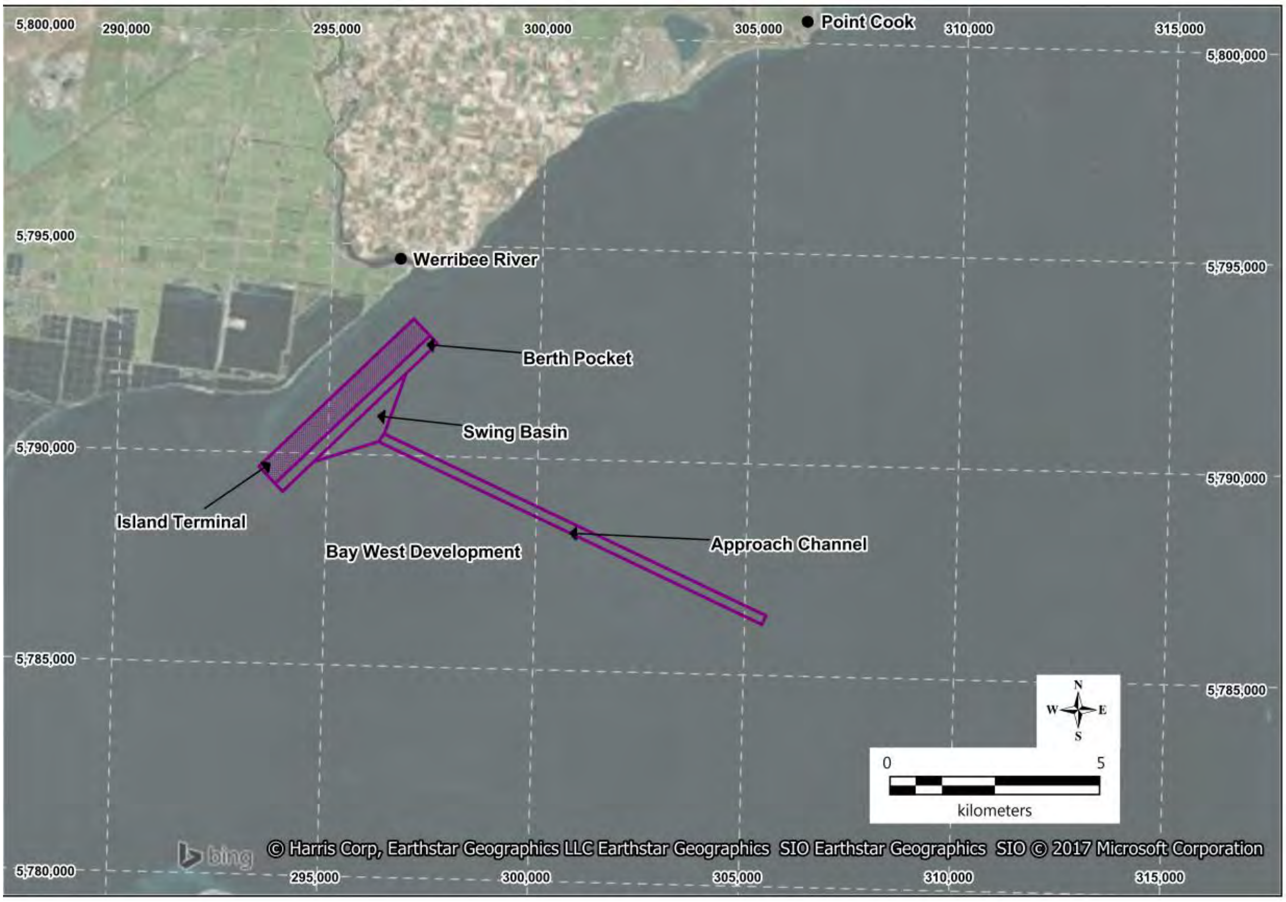

Figure 2-3 Map of the west of Port Phillip showing the preferred option for the Bay West Development.

The size of container vessels visiting Melbourne are currently limited to a length of 300 m, a beam of 40 m and a draught of 14 m. These vessels have some constraints in the Heads at times of strong currents or high waves, but in practice are able to transit the Heads most of the time.

In order to cater for the larger vessels projected to use the new facility, modifications may also be required to the great Ship Channel through Port Phillip Heads and South Channel.

Based on an underkeel clearance analysis and ship-simulation trials it was found (AECOM, 2016) that:

> Vessels 366 m long, with draught up to 14 m, can transit the Heads using existing channels when currents are low around slack water;

> Vessels 400 m long, with a draught of 14m, will require widening of the Great Ship Channel from 245 to approximately 425m by dredging to safely transit the Heads; and

> Vessels 400 m long with a draught of 15m would require widening and deepening of the Great Ship Channel to safely transit the Heads.

Based on AECOM (2016) and GHD (2017) a "Project" was defined for modelling. This included the following:

> An island at Bay West with dredged channel, turning basin and berth pockets as shown in Figure 2-3 all dredged to -16.5 m CD

> Great Ship Channel widened from 245 m to 425 m at the existing depth of -17.3 m CD;

> South Channel deepened to -17.3 m CD within the existing toe lines;

> Turning area around Hovell Pile deepened to -17.8 m CD within the existing toe lines.

The relevant areas of channel deepening are shown in Figure 2-4. The widening of the Great Ship Channel is shown in Figure 2-5 which demonstrates the extent and magnitude of the dredging required .

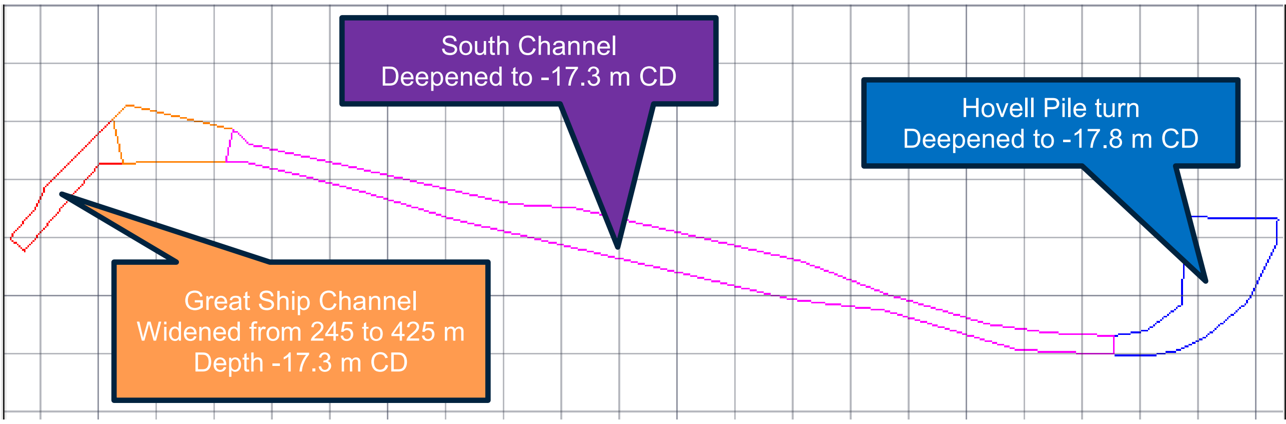

Figure 2-4 Changes in the shipping channel in the south of Port Phillip incorporated into the modelling (see Figure 2-2 for location details).

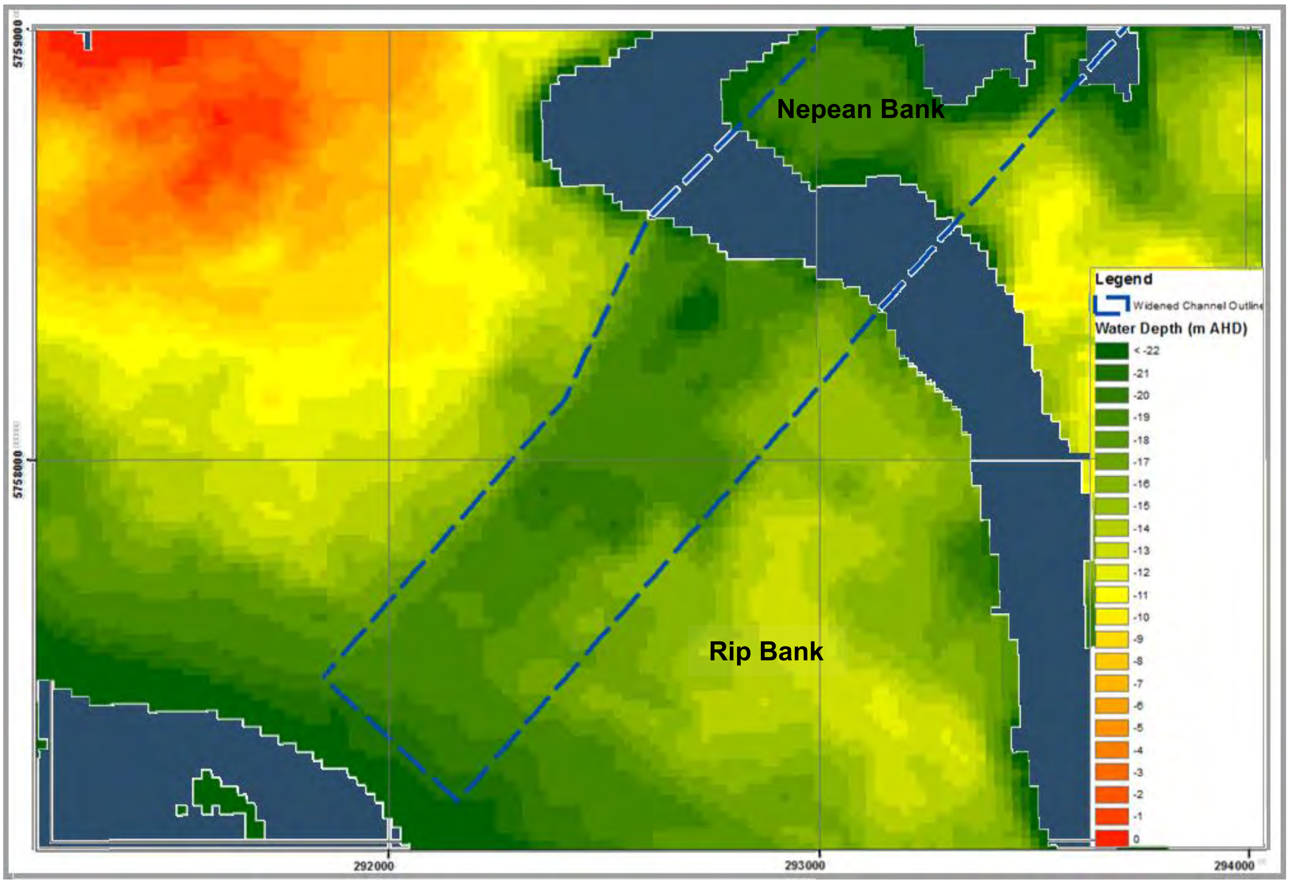

Figure 2-5 Great Ship Channel through Port Phillip Heads, showing existing bathymetry and the outline of possible modifications. Dark blue areas are deeper than 22 m, the limit of the LADS depth sounding system.

When assessing the impact of the potential works, termed the “Project” case, where possible, the changes due to the Bay West port development are separated from those due to dredging in Port Phillip Heads and South Channel. The dredging activities are further separated in discussion by reference to “widening” in the heads where this is the major cause and “dredging” in South Channel where this is considered to be the major cause of the change. There will be some interaction between the various changes, and they have

been modelled as a combined project, but where the impacts can be reasonably attributed to a particular action, this has been done.

2.3 Models

2.3.1 Hydrodynamics

2.3.1.1 Description

The numerical model used to calculate the hydrodynamics of Port Phillip, including the entrance and adjacent waters of Bass Strait, is a development of that used for the Channel Deepening Project (CDP) and described in Cardno Lawson Treloar (2007b). The model calculates the water level and current speed and direction over the model domain which is shown in Figure 2-6. A curvilinear grid with variable grid size is used in the horizontal and five layers are used in the vertical, each of a fixed thickness of 20 m vertically starting from 2 m above mean sea level, taken as 0.0 m AHD. (This is termed a “z-layer” modelling system).

The model uses the FLOW module of the Delft3D modelling system developed by Deltares of The Netherlands.

The bathymetry used in the model is primarily derived from data provided by PoMC for modelling after the completion of dredging for the CDP (Cardno, 2011). These data included survey from LADs and multibeam echo-soundings as well as historical survey data from the body of the bay. For offshore areas, not covered by PoMC surveys, the bathymetry was derived from the Australian Bathymetry and Topography Grid, Geoscience Australia (2009) which has a resolution of 9 arc seconds. (~ 250 m at the equator).

For the Project case, the bathymetry was modified to represent the conditions for the scenario described above. All other inputs were left unchanged.

The model extent and existing case bathymetry is shown in Figure 2-6.

The model was run for a two month simulation using the measured sea level from Lorne as the input boundary condition. No wind was applied to the model.

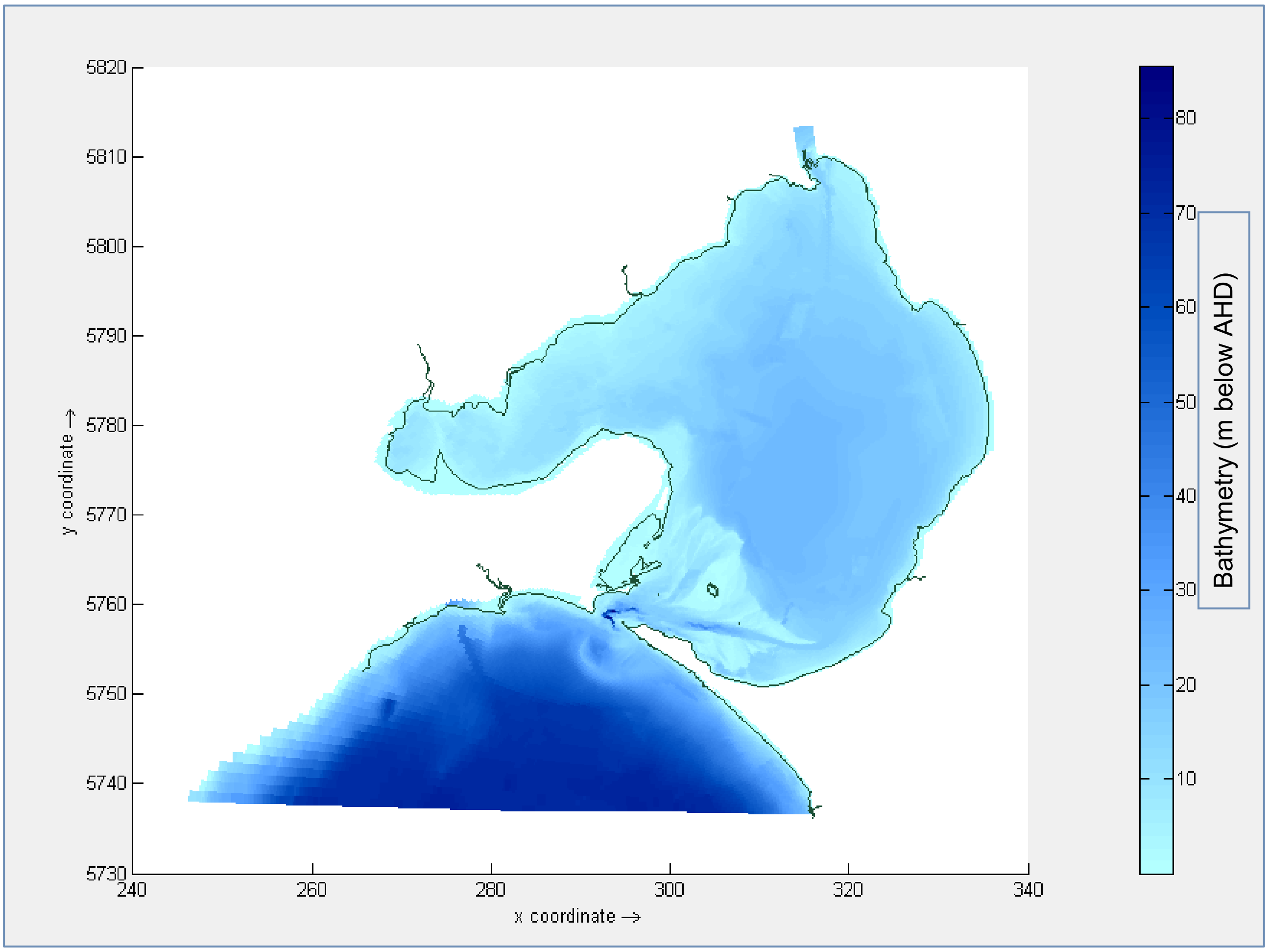

Figure 2-6 Model domain and bathymetry (in metres below 0.0 AHD)

2.3.1.2 Calibration and Validation

Further details of the model and the calibration and validation procedures are presented in Appendix A. Examples of the validation against measured data are shown in Figure 2-7, Figure 2-8 and Figure 2-9.

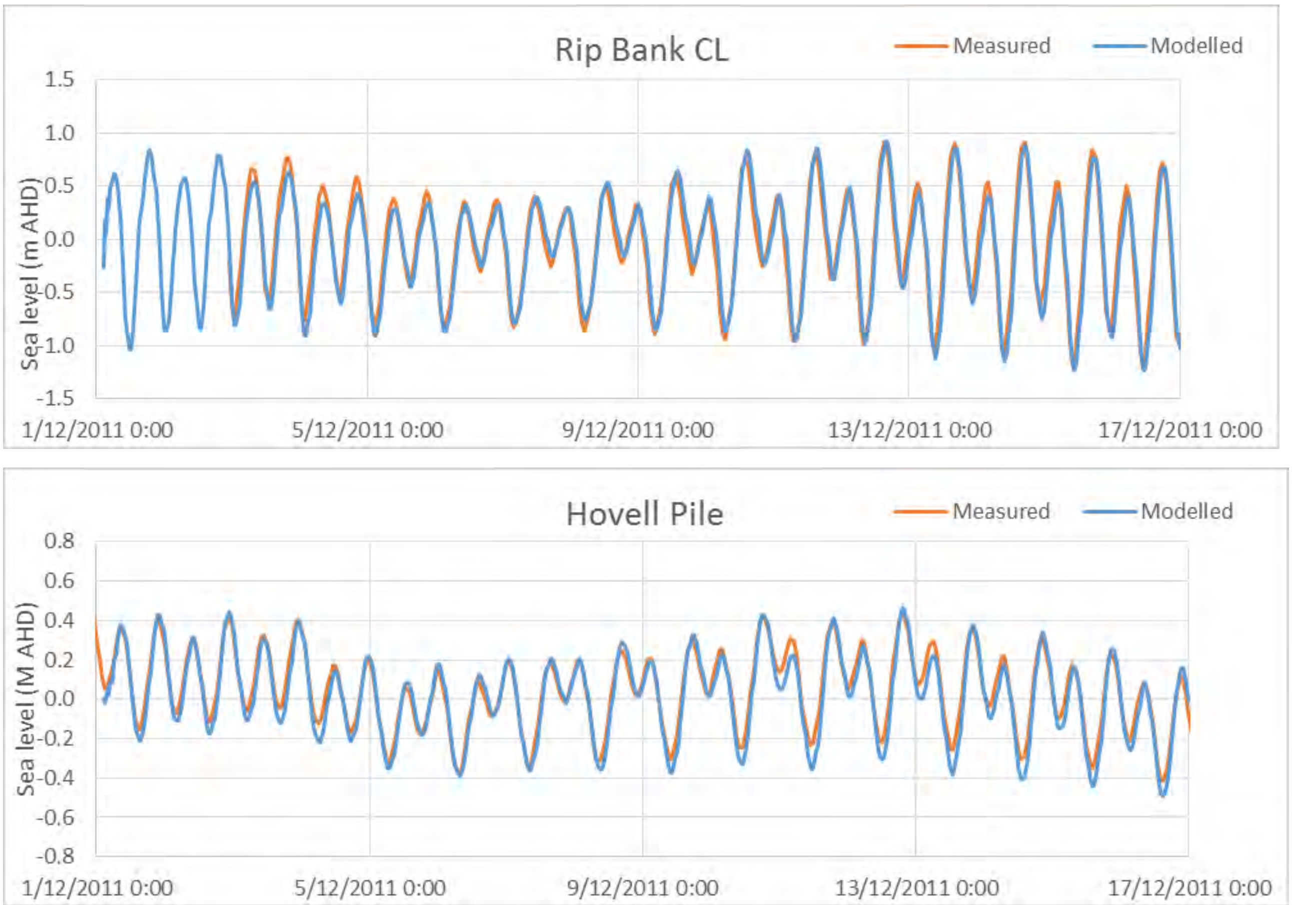

Figure 2-7 Port Phillip hydrodynamics model validation, examples of results for sea level (Cardno, 2016)

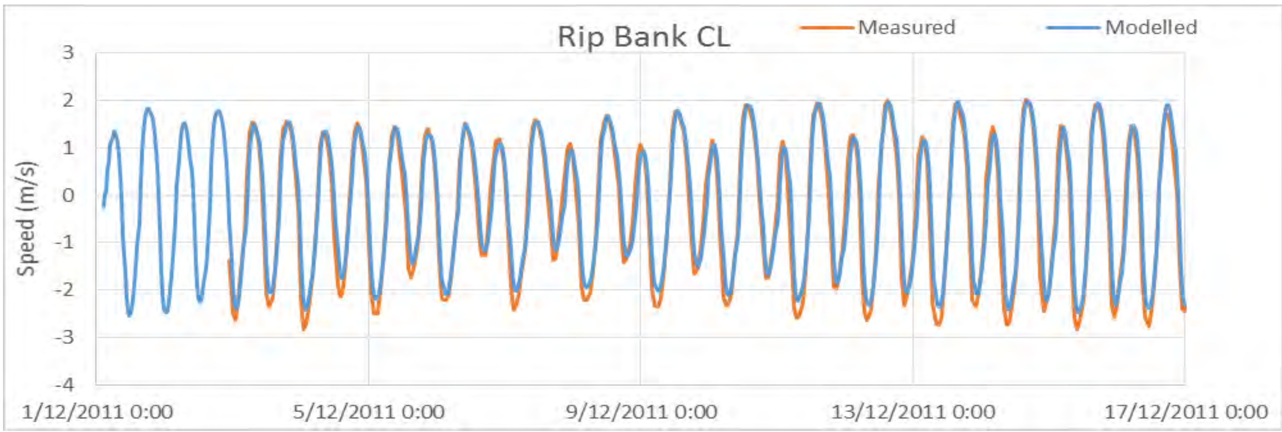

Figure 2-8 Port Phillip hydrodynamics model validation, examples of results for current speed (flood positive, ebb negative) for Rip Bank in Port Phillip Heads.

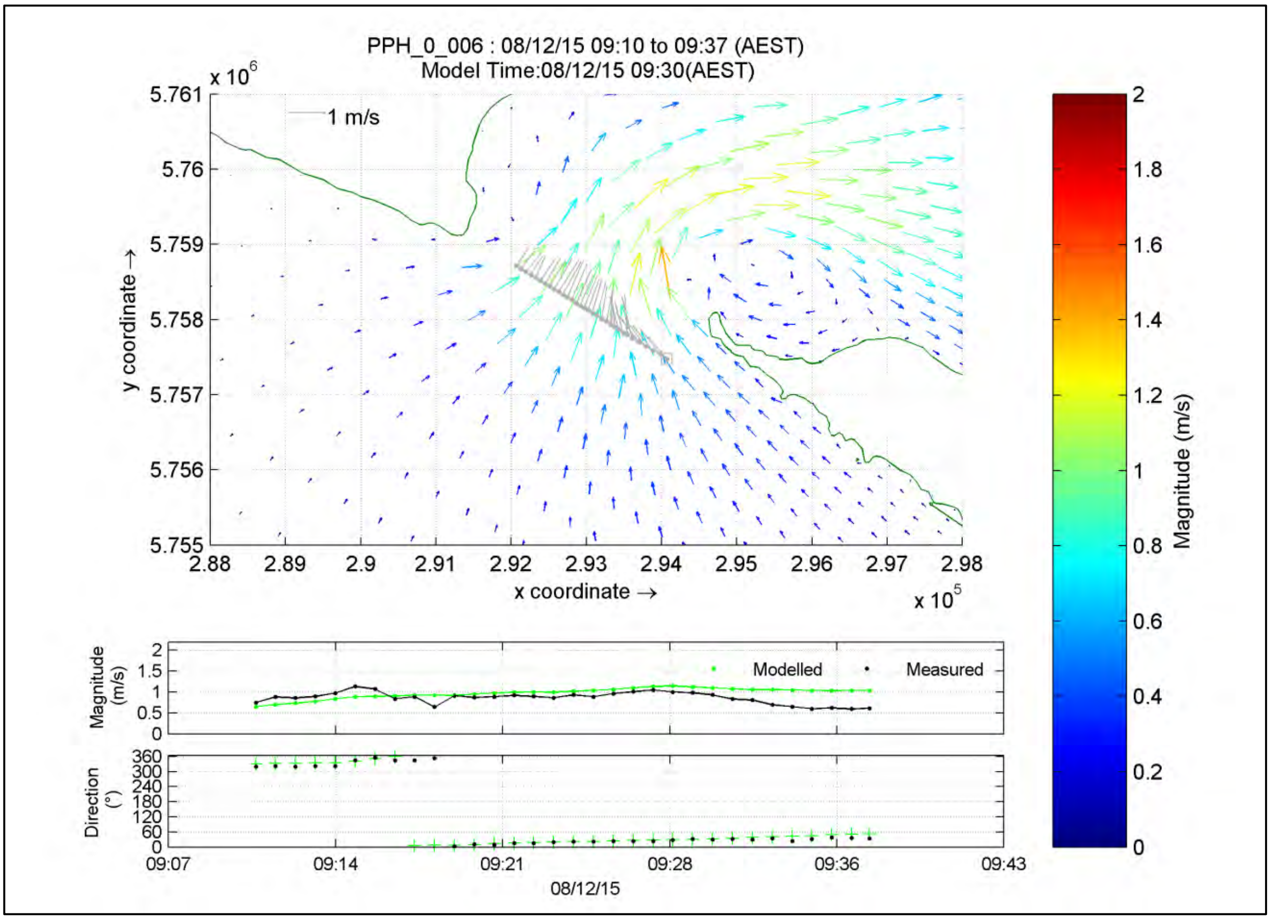

Figure 2-9 Port Phillip hydrodynamics model validation, examples of results for current vectors along a transect) in Port Phillip Heads compared with the modelled current field.

2.3.2 Waves

Wave modelling in Port Phillip was only undertaken for Port Phillip Heads. In this area, swell and wind-waves from Bass Strait propagate through the Heads into the south-western part of the bay. In the remainder of the bay, the waves are locally generated wind-waves and the scope of the investigation did not include modelling of these waves.

2.3.2.1 Description

The wave climate within Port Phillip Heads and adjacent waters was modelled using the Simulating WAves Nearshore (SWAN) III model (Ris et al., 1999). SWAN is a numerical wave model based on the wave-action balance equation. The model is capable of taking into account wind energy, white capping, depth-induced breaking, bottom friction, refraction by bathymetry and currents and wave-wave interaction. The model set up was that used for the Channel Deepening Project and described in Cardno Lawson Treloar (2007b). Which also describes the model calibration and validation.

The model bathymetry was revised using data from the Port of Melbourne Corporation hydrographic survey and 2010 airborne laser bathymetric survey (Cardno, 2011). The model was set up on a regular rectangular grid with a spacing of 50 m. Figure 2-10 shows the model extent and bathymetry.

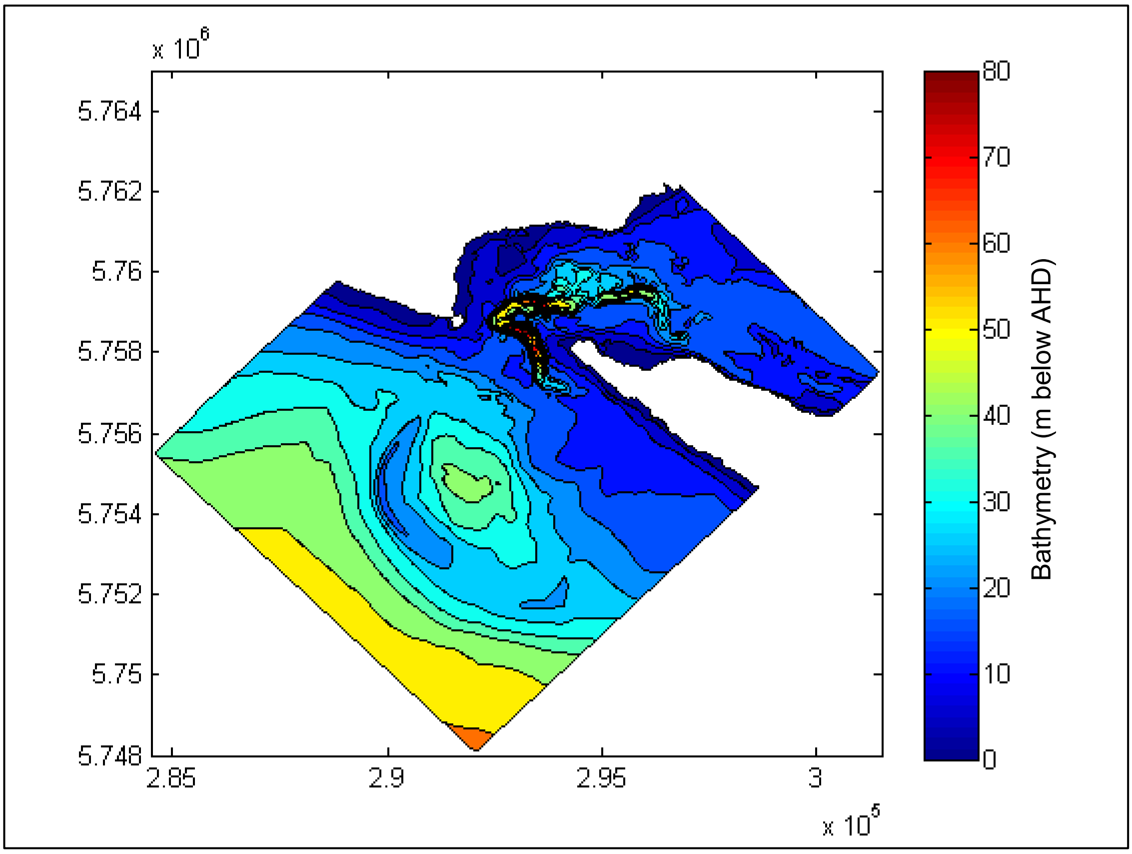

Figure 2-10 SWAN model grid and bathymetry, coordinates are metres in MGA.

The model was run for nine cases for each of the existing bathymetry and the widened channel case. Input wave conditions on the south-west boundary and part of the south east boundary was a JONSWAP spectrum with Hs = 1.7 m, Tp = 13 s. This represents the average incoming wave conditions in Port Phillip Heads. The average incoming wave direction varies slightly from year to year, but is close to 210°T. The model was run for incoming directions of 190°T, 210°T and 230°T to span the range of normal wave directions. Due to the significant impact of currents on wave propagation through the Heads, current fields were used to represent the peak ebb, peak flood and slack water. These currents were extracted from the hydrodynamic model and interpolated onto the SWAN model grid. The sea level associated with each current field was also applied for the relevant runs. Thus the three directions and three current cases results in nine model runs for each of the scenarios.

2.3.2.2 Calibration and Validation

No specific calibration or validation was undertaken for this investigation, but the validation is discussed in Cardno Lawson Treloar (2007b).

2.4 Impact Assessment

2.4.1 Sea-level

Following the experience of the Channel Deepening Project, it was anticipated that changes to the channels in the Heads and Great Sands will lead to small changes in the tidal range (increase in water level at high tide and decrease in water level at low tide) in Port Phillip. These changes were investigated by extracting time series of sea level from the model at a number of locations and analysing the change caused by the developments included in the model for the Project case. Data were extracted from the model at six-minute intervals and, for each time, the difference in sea level was plotted against the level in the existing case. The values were binned in 0.1 m increments and the mean and standard deviation of the values within that bin computed. An example of the resulting plot for Williamstown is shown in Figure 2-11.

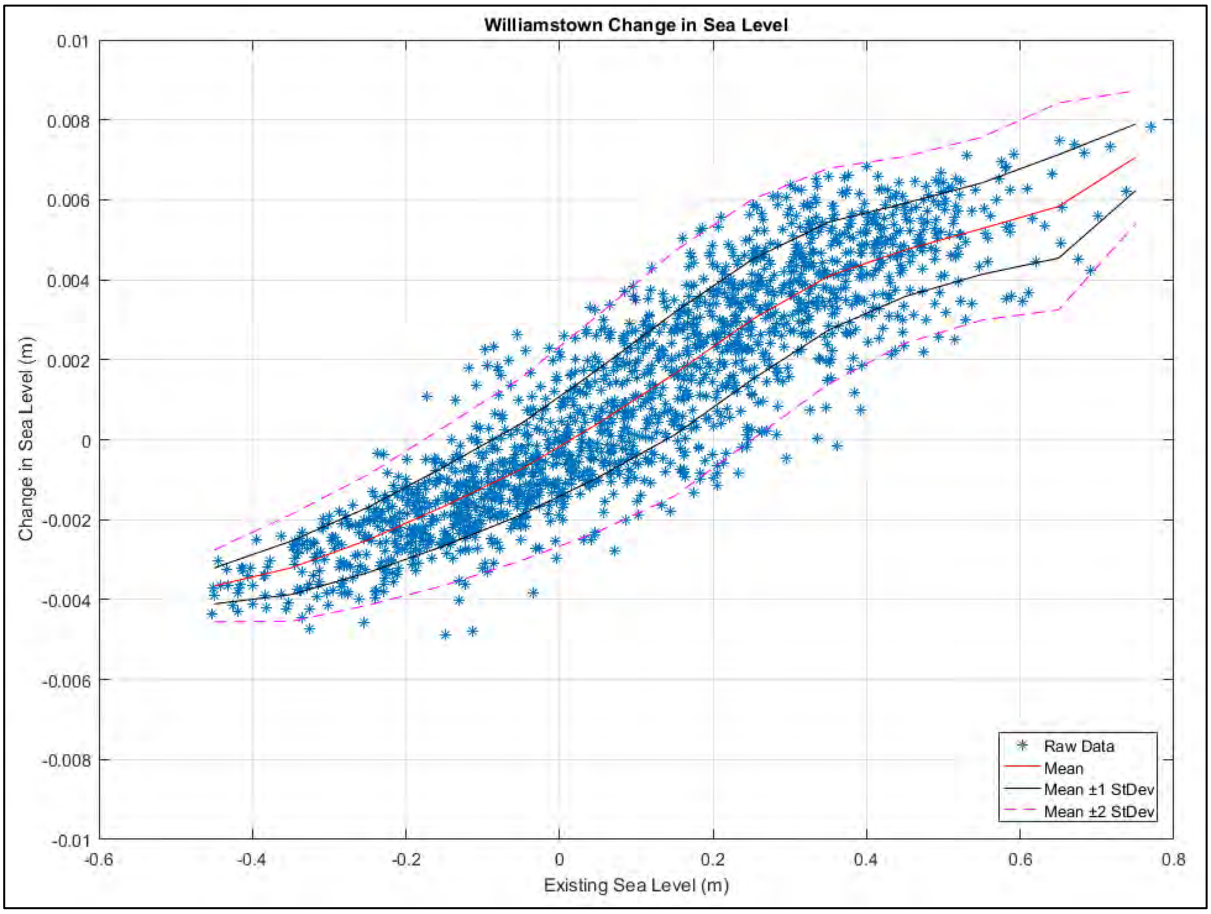

Figure 2-11 Change in sea level due to the Project case compared with existing sea level

In order to quantify the changes, percentiles of the distributions at a number of locations were extracted and are presented in Table 2-1.

Table 2-1 Impact of the Project on the distribution of sea levels (m) over the modelled period.

Location	2nd percentile	10th percentile	50th percentile	90th percentile	98th percentile
Queenscliff	-0.0059	-0.0040	0.0000	0.0027	0.0033
Hovell Pile	-0.0043	-0.0032	0.0002	0.0037	0.0050
Geelong	-0.0043	-0.0026	0.0007	0.0054	0.0069
Frankston	-0.0035	-0.0024	0.0009	0.0049	0.0061
Williamstown	-0.0037	-0.0025	0.0010	0.0051	0.0063

It can be seen from Table 2-1 that the 2nd percentile, the level defining the lowest 2% of sea levels, will decrease by 3.7 mm and the 98th percentile, the level defining the highest 2% of sea levels, will increase by 6.3 mm. These values are typical of those occurring around the bay, with some variation at Queenscliff. The changes are likely to be due predominantly to the widening of the great Ship Channel in the heads as this sis the major control on water entering or leaving Port Phillip. There may be a small contribution from the deepening of South Channel, but it is unlikely to be significant compared with that due to widening in the Heads.

The magnitude of these changes can be compared with the annual rates of change in sea level in Port Phillip attributed to climate change. At Williamstown, sea level has risen by an average of 2.3 mm each year for the

period 1965 to 2013 (Cardno, 2015) and continues to rise (BoM, 2016). Thus the change in high-tide levels due to the modelled dredging is approximately equivalent to three years of sea-level rise.

2.4.2 Currents

2.4.2.1 Port Phillip Heads

Changes in the currents in Port Phillip Heads due to the Project as modelled, in this case due to the widening of the Great Ship Channel, are identified in the first instance by plotting the difference in current speed. Figure 2-12 shows the difference in speed for the peak ebb flow and Figure 2-13 the difference at peak flood. The largest differences occur adjacent to the area of dredging on Nepean Bank with smaller changes in the dredged area on Rip Bank, especially for the ebb tide. Due to the large currents in this area, the differences are almost imperceptible in plots of current vectors. The current speeds near the area of greatest change are about 3 m/s and thus the changes in current speed are less than 10%. There are no perceptible changes in current direction and thus the changes have little significance for navigation.

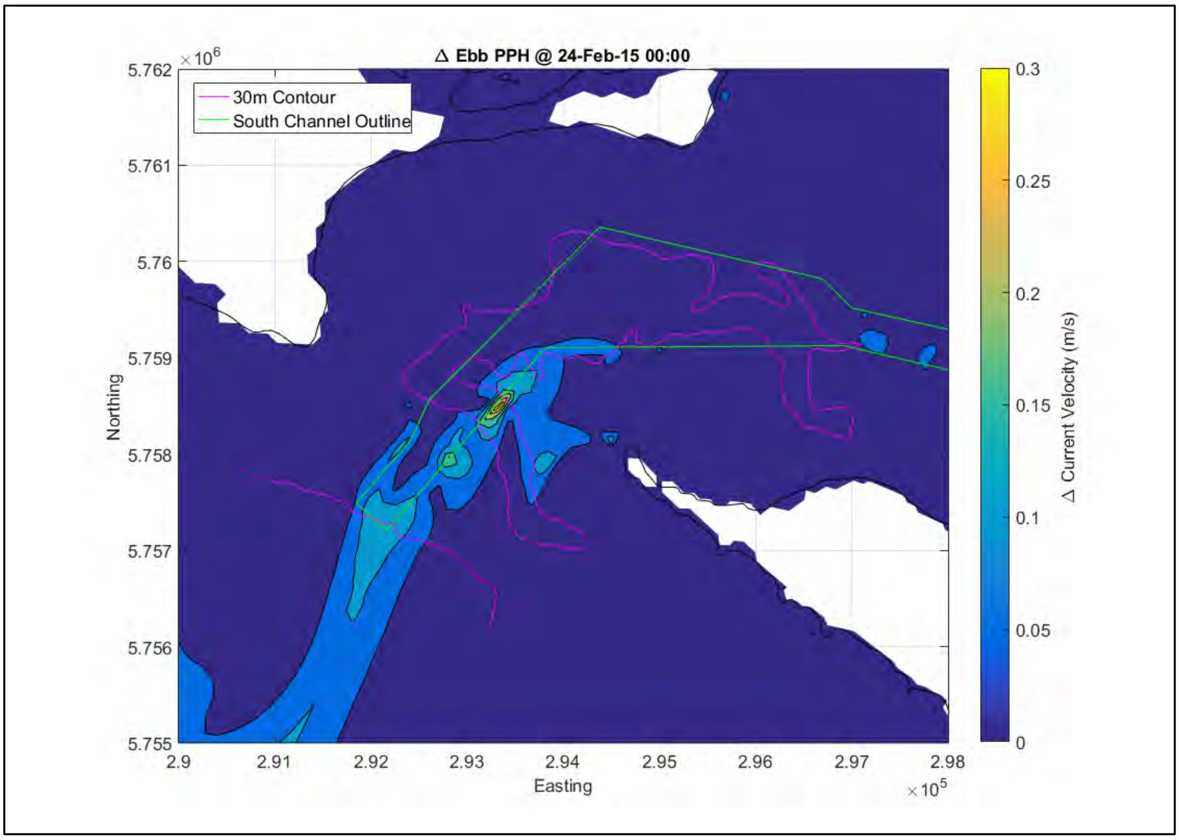

Figure 2-12 Difference in current speed at peak ebb flow, Port Phillip Heads, widened minus existing case. Background contour is 30 m depth.

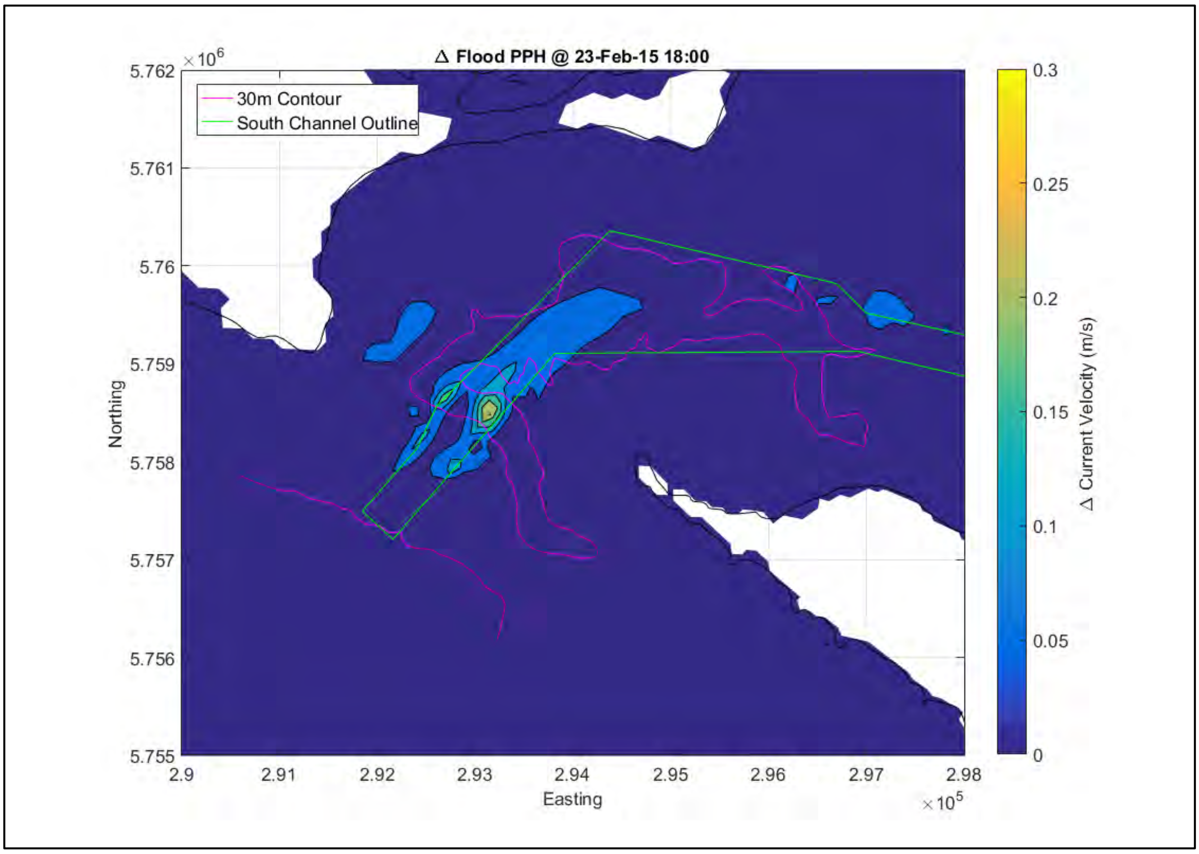

Figure 2-13 Difference in current speed at peak flood flow, Port Phillip Heads, widened minus existing case. Background contour is 30 m depth.

2.4.2.2 Hovell Pile

The other location of significant changes in current speed is at the eastern end of South Channel in the turning area around Hovell Pile. In this location, the speeds are increased due to the deepening of South Channel which results in increased flow through this section. The change in current speed for the ebb flow is shown in Figure 2-14 and for the flood flow in Figure 2-15.

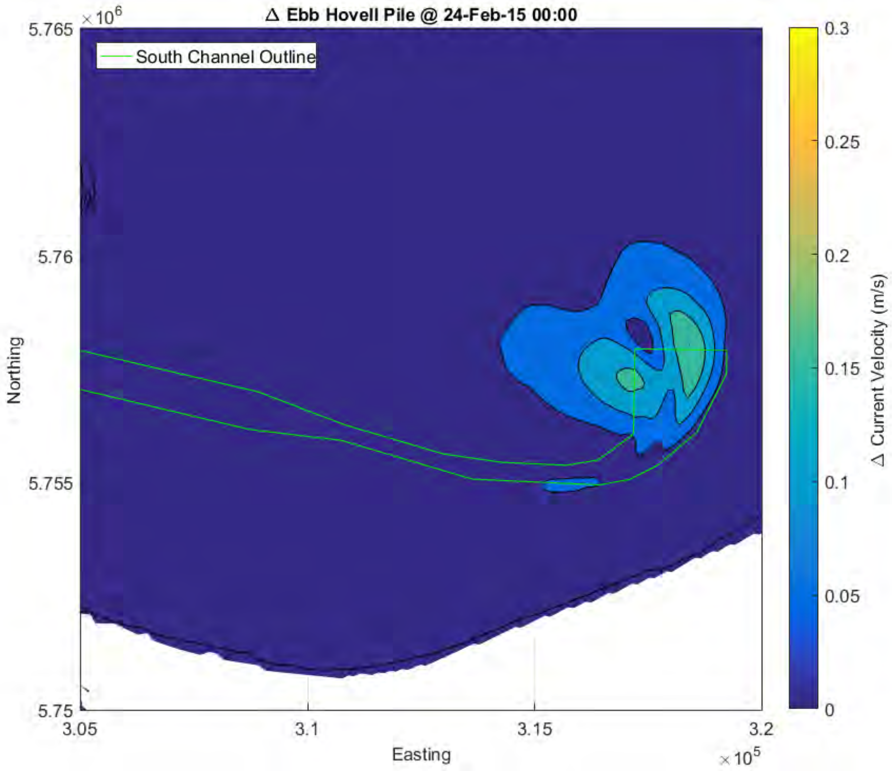

Figure 2-14 Difference in current speed at peak ebb flow, Hovell Pile, dredged minus existing case.

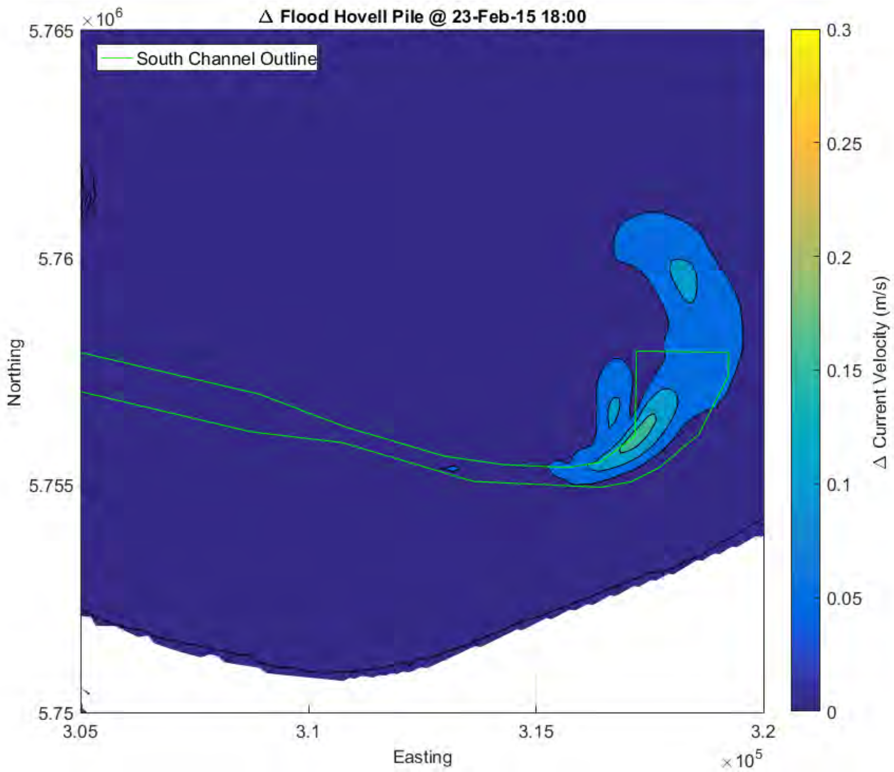

Figure 2-15 Difference in current speed at peak flood flow, Hovell Pile, dredged minus existing case.

The current vectors for the existing and dredged cases are shown for the peak ebb flow in Figure 2-16 and for the peak flood flow in Figure 2-17. The difference between existing and dredged case current vectors on

the peak ebb flow and peak flood flow at Hovell Pile about 0.15-0.2 m/s, with an increase in magnitude for the dredged case.

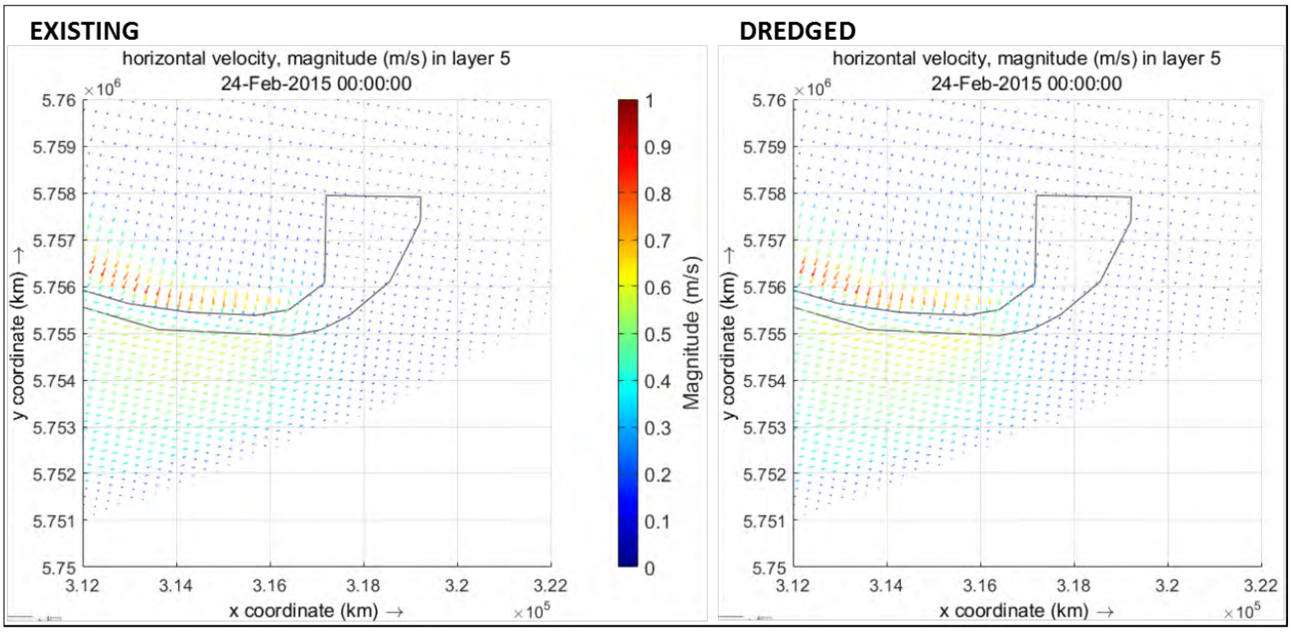

Figure 2-16 Current vectors at peak ebb flow, Hovell Pile, existing (left) and dredged case (right)

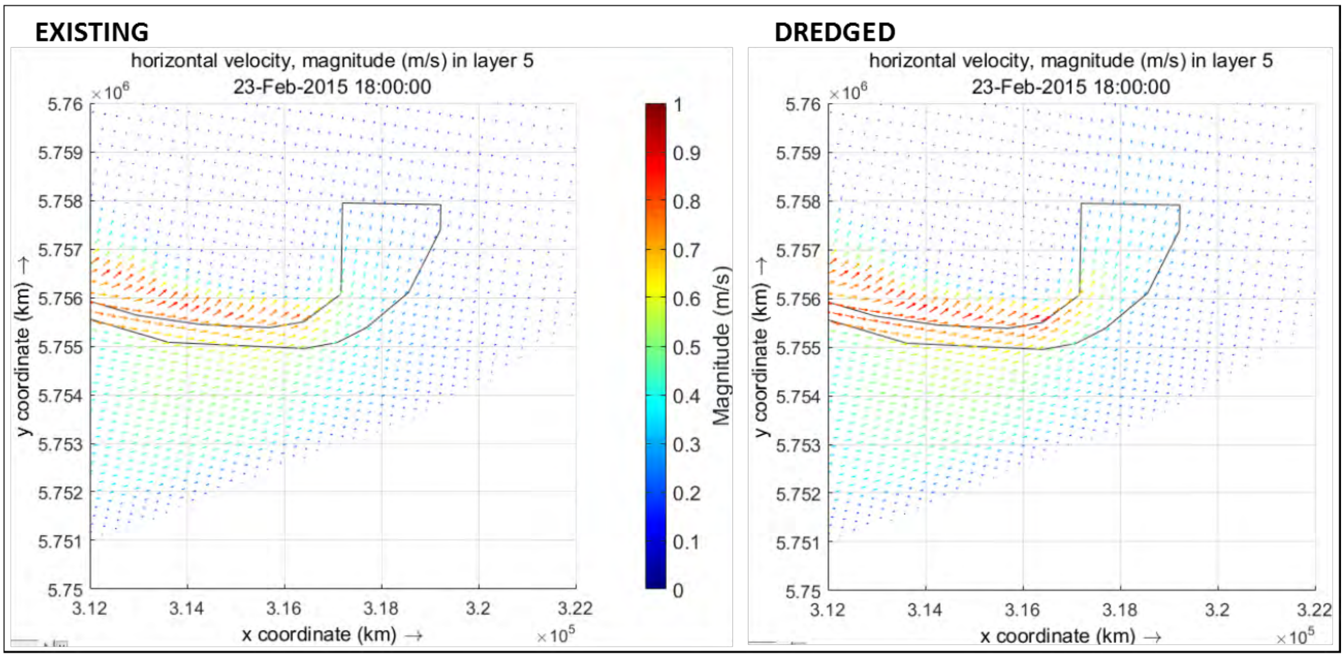

Figure 2-17 Current vectors at peak flood flow, Hovell Pile, existing (left) and dredged case (right)

The current vectors following the peak flood tide show larger changes, with a clear increase of approximately 0.25 m/s in magnitude within the channel. The easterly shift in the location of an eddy toward the end of the northern edge of the turning area is notable, and likely to be associated with the strong currents within the channel. The largest change occurs about 2-3 hours following the peak flood tide. Figure 2-18 shows the change in current speed at this time, with differences increasing up to approximately 0.3 m/s.

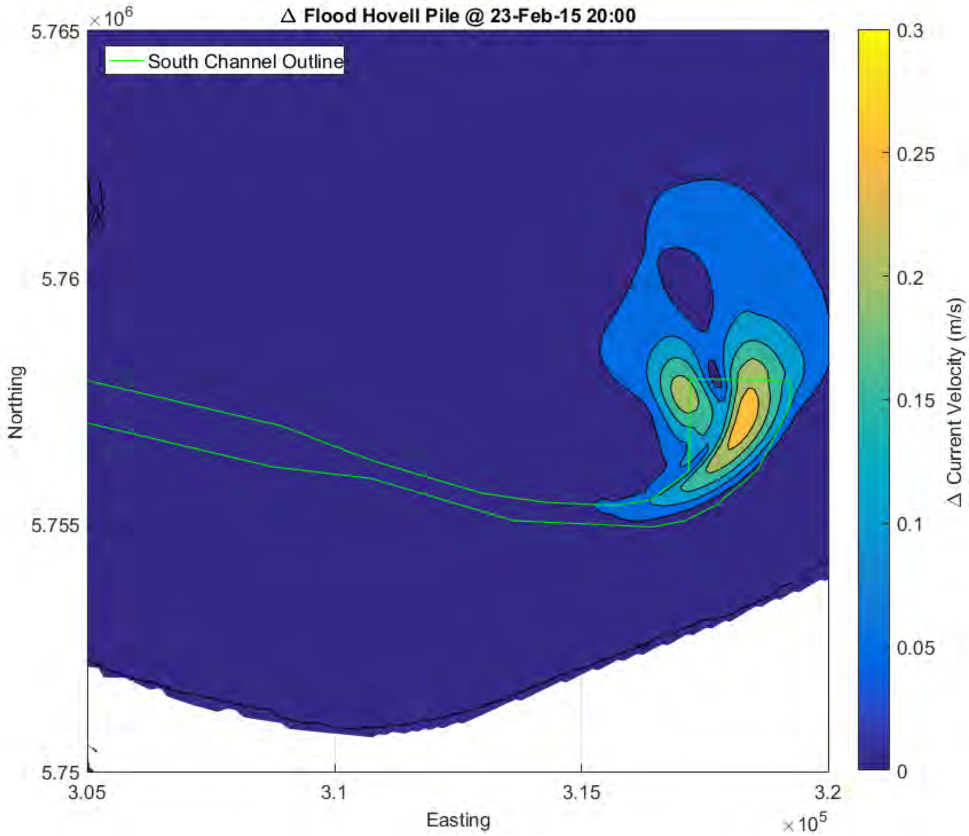

Figure 2-18 Difference in current speed at 2 hours after peak flood flow, Hovell, Bay West minus existing case.

The current vectors at the time of the greatest difference in current speed are shown in Figure 2-19. The increase in current speed in the turning area and the eastwards movement of the eddy in the dredged case compared with the existing conditions can be seen. Since this change does not occur at the time of peak flow, the change in maximum current-speed is smaller and the change is more related to the timing of the maximum flow. It is thought that the dredging of the channel results in an increased flow which has more momentum and thus the flow does not decrease as rapidly as in the non-dredged case when the tidal pressure gradient starts to reverse.

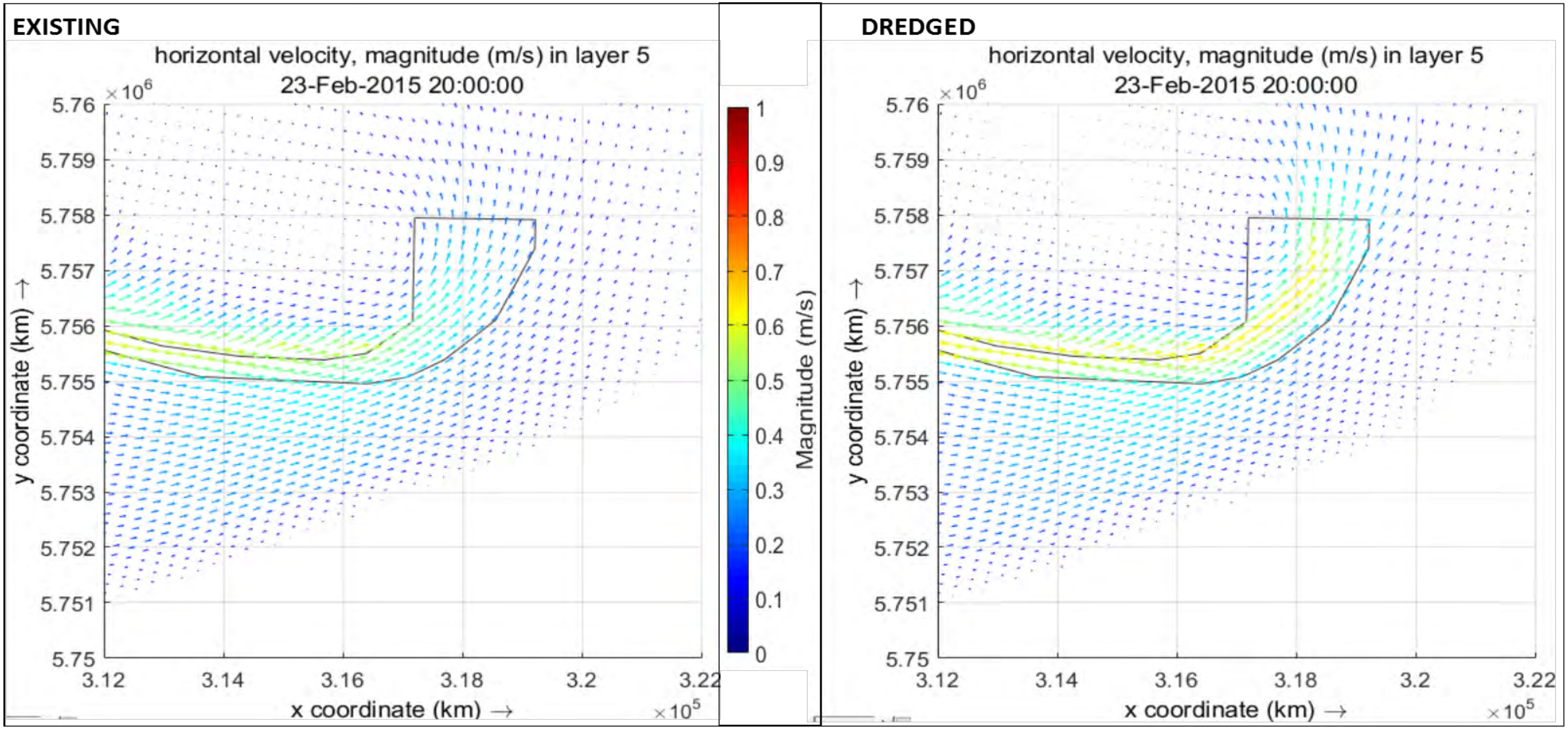

Figure 2-19 Current vectors at two hours after peak flood flow, Hovell Pile, existing (left) and dredged case (right).

2.4.2.3 Bay West

The effect of the Bay West development on currents was examined in the model. Due to the small velocities in the area, the changes in the currents are shown with respect to the whole bay. The results for the peak ebb flow are shown in Figure 2-20 and for the peak flood in Figure 2-21.

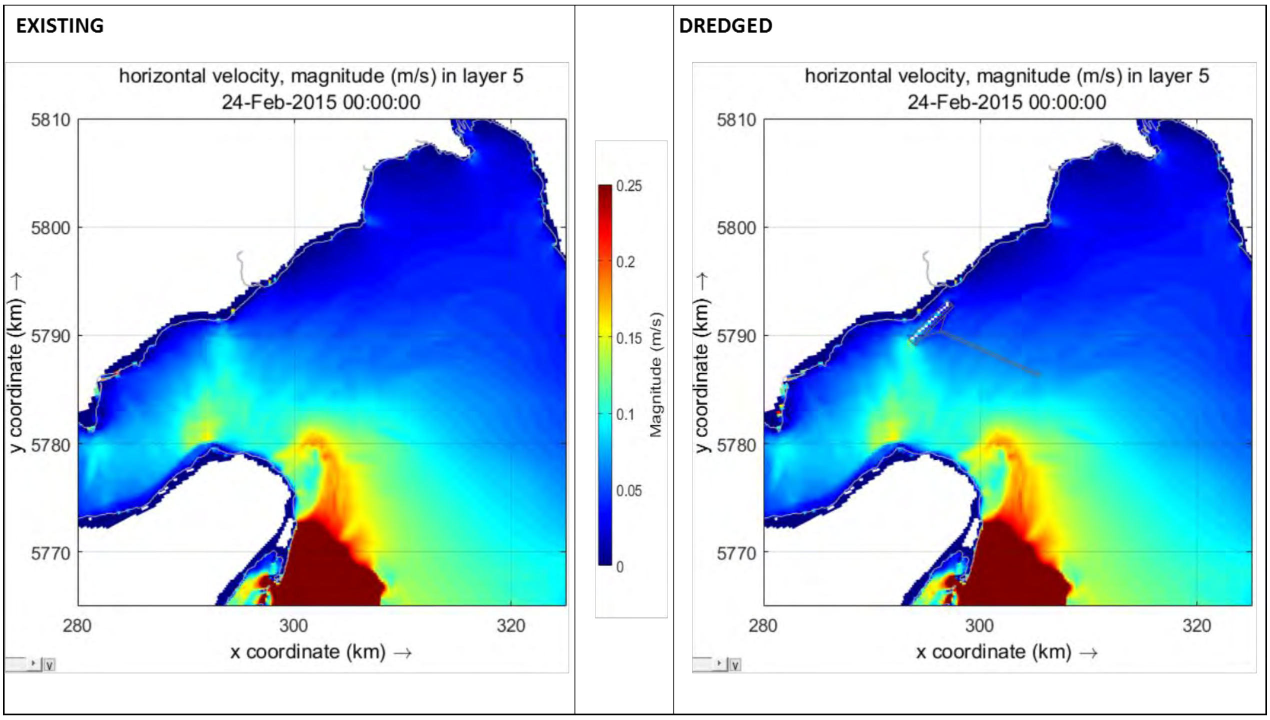

Figure 2-20 Magnitude of tidal currents at peak ebb flow for the Bay West project area, existing case (left) and Project case (right)

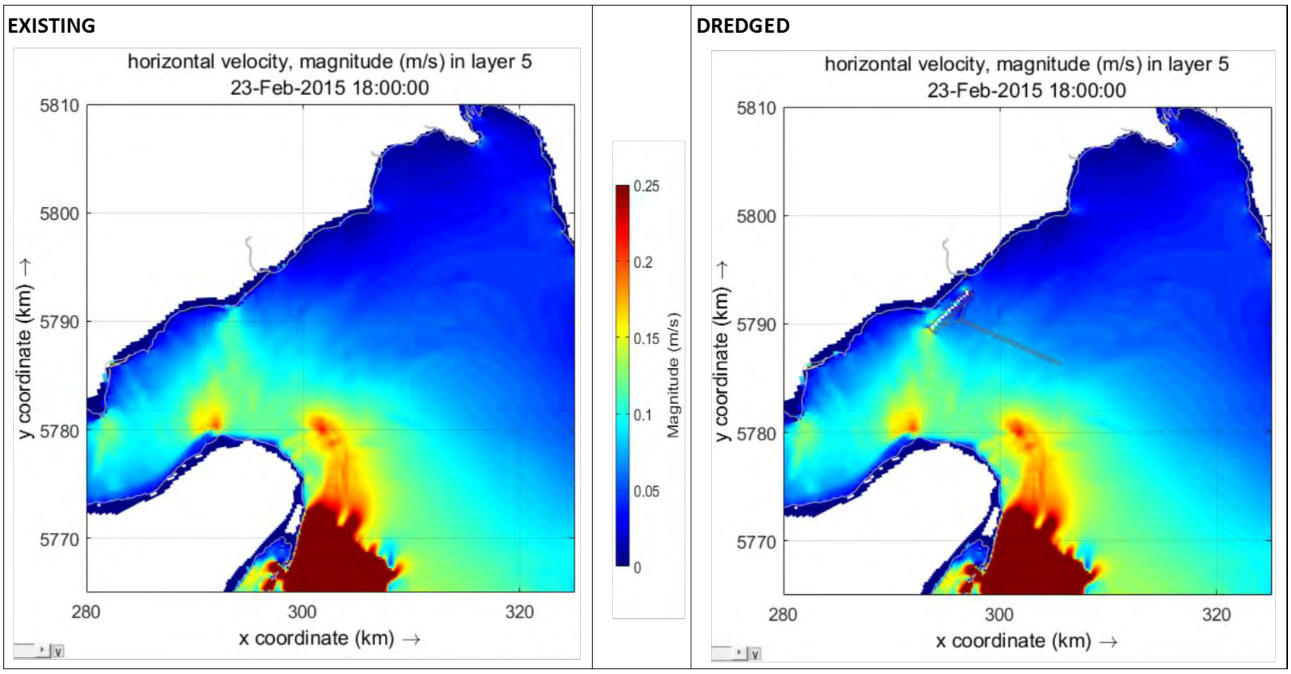

Figure 2-21 Magnitude of tidal currents at peak flood flow for the Bay West project area, existing case (left) and Project case (right)

The current speeds in the port area are below 0.1 m/s and the Project results in increased currents at the southern end of the terminal in the ebb-tide case and increased flow around the southern end and inshore of the terminal in the flood case with some increase at the northern end of the terminal in flood case. The speeds are still below the expected threshold for sediment movement, although this would need to be

confirmed in a more detailed investigation during detailed design. It is noted that there is a change in current speed along the dredged channel leading to the port, however, this is likely to be due to the model computing the depth-averaged currents and thus an increase in depth due to dredging will result in a change in the depth-averaged current speed. There is no observable change in the currents in the body of the Bay or along the northern edge of the Great Sands.

2.4.3 Waves

The wave conditions in Port Phillip Heads vary markedly with location and the tidal conditions. This is illustrated in Figure 2-22 which shows the wave height at slack tide, essentially no currents, Figure 2-23 which shows the wave height at peak ebb or outgoing tidal flow and Figure 2-24 which shows wave height at peak flood or ingoing tidal flow. At slack tide (Figure 2-22), the variations in wave height are due mainly to the bathymetry which leads to focussing of wave energy on Point Lonsdale and Rip Bank in the Heads as well as locations along the Bass Strait shoreline. There is relatively little propagation of wave energy through the Entrance into the south of Port Phillip.

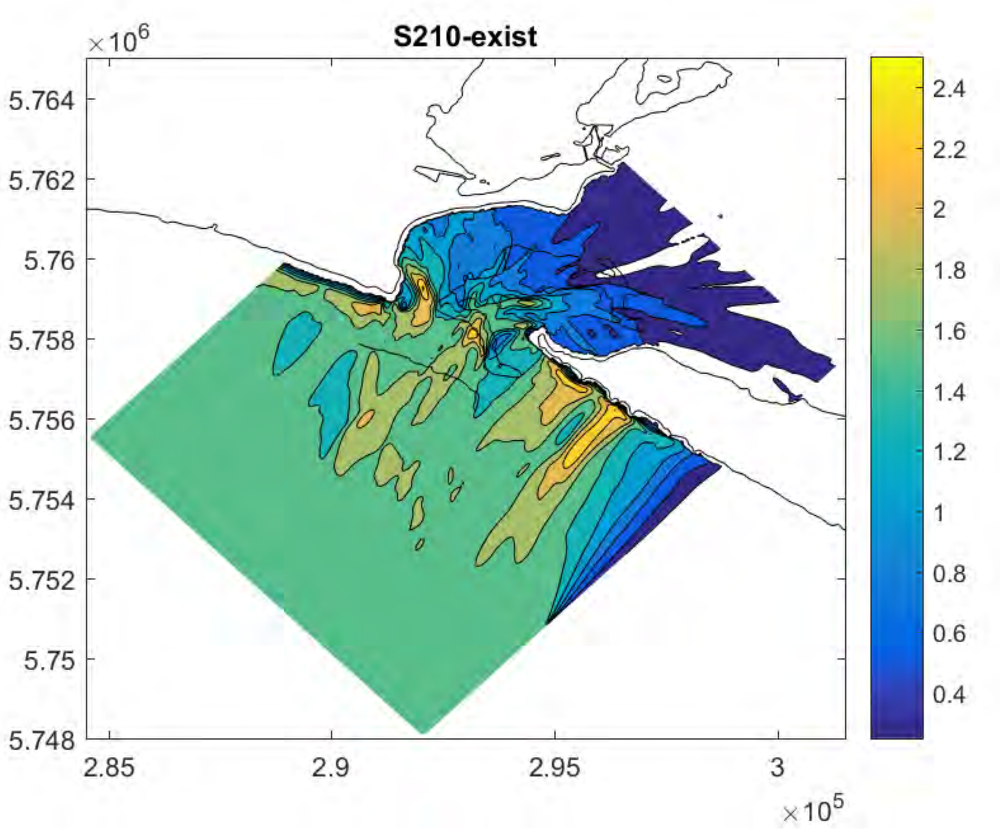

Figure 2-22 Modelled significant wave height (m) at slack water, incoming waves Hs = 1.7 m, Tp = 13 s direction 210°T, existing bathymetry.

At peak ebb tide (Figure 2-23), the outgoing current forms a jet south of the Entrance which leads to focussing of wave energy and steepening of waves and loss of energy through wave breaking. The focussing of wave energy on Point Lonsdale and Rip Bank in the Heads is still present, but not as strong as in the slack case. There is again relatively little propagation of wave energy through the Entrance into the south of Port Phillip.

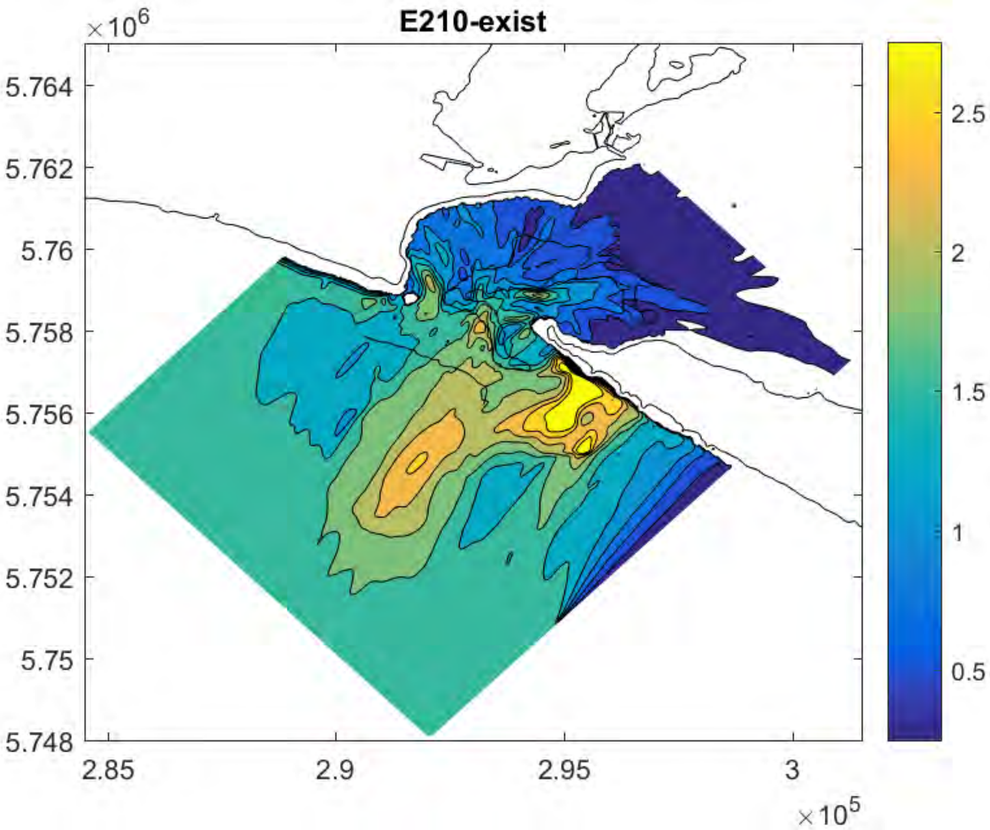

Figure 2-23 Modelled significant wave height (m) at peak ebb flow, incoming waves Hs = 1.7 m, Tp = 13 s direction 210°T, existing bathymetry.

At peak flood tide (Figure 2-24), the ingoing current is more uniform than the ebb and the absence of strong horizontal gradients in current speed avoids the focussing of the waves seen in the ebb case. There is focussing of wave energy on Point Lonsdale and Rip Bank as in the slack case, but slightly stronger. There is also focussing on Point Nepean. Again relatively little wave energy propagates through the Entrance into the south of Port Phillip, although more energy passes through the Heads on the flood tide than at slack or ebb tide.

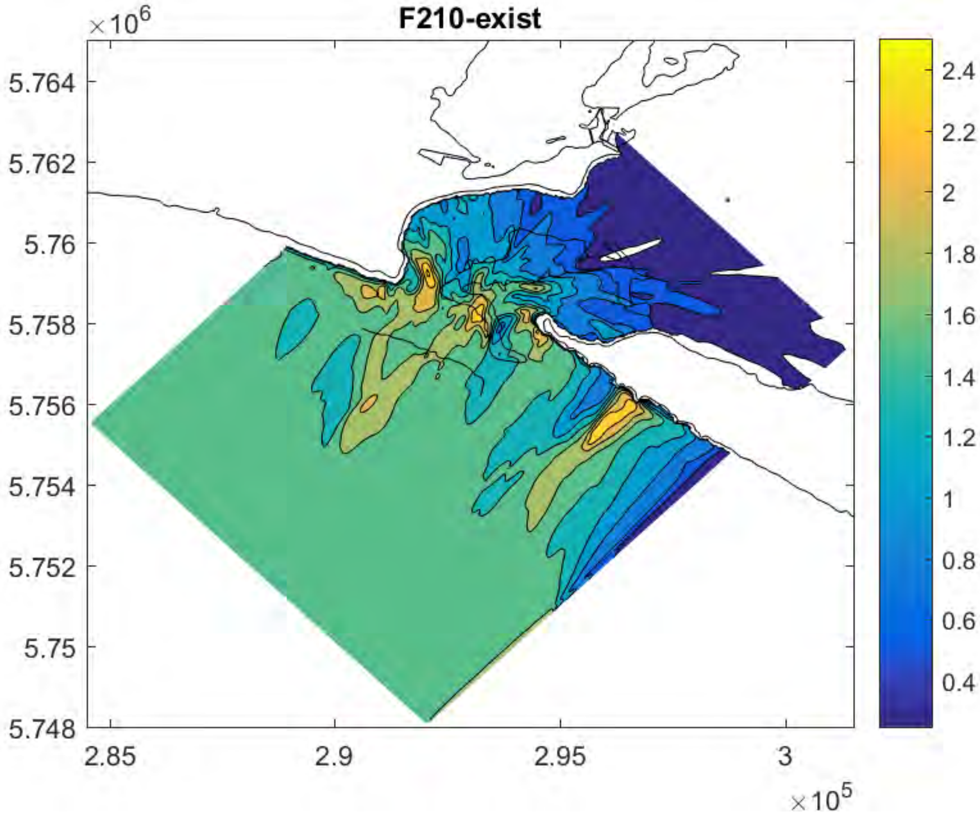

Figure 2-24 Modelled significant wave height (m) at peak flood flow, incoming waves Hs = 1.7 m, Tp = 13 s direction 210°T, existing bathymetry.

Changes in the wave propagation in the Heads has been assessed by considering the percentage change in significant height for each of the nine conditions. Examples for the cases illustrated above are shown in Figure 2-25 for the slack water case, Figure 2-26 for the peak ebb flow and Figure 2-27 for the peak flood.

The main differences in the slack-water case, Figure 2-25, are due to the widening of the channel and thus effects on waves propagating over the relatively small areas that are dredged in this case. The main effects are on portions of the Lonsdale Bight beach and some waves propagating into the south of the bay, although, as noted above, there is little wave energy in this area and thus the percentage change may overemphasise the actual change in wave height.

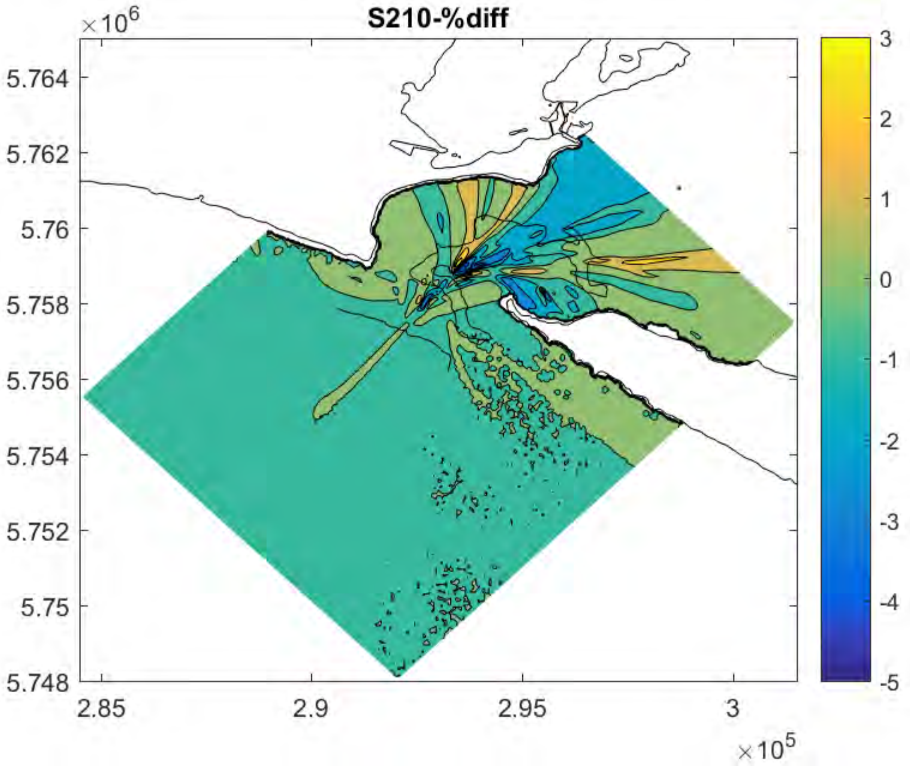

Figure 2-25 Difference in modelled significant wave height (dredged – existing) at slack water expressed as a percentage change from existing.

In the case of the peak ebb flow, Figure 2-26, the biggest percentage change results from the changes in the ebb-tide current jet which results in changes in the wave height south of the Entrance. There are also some reductions in wave height for waves propagating into the south of the bay.

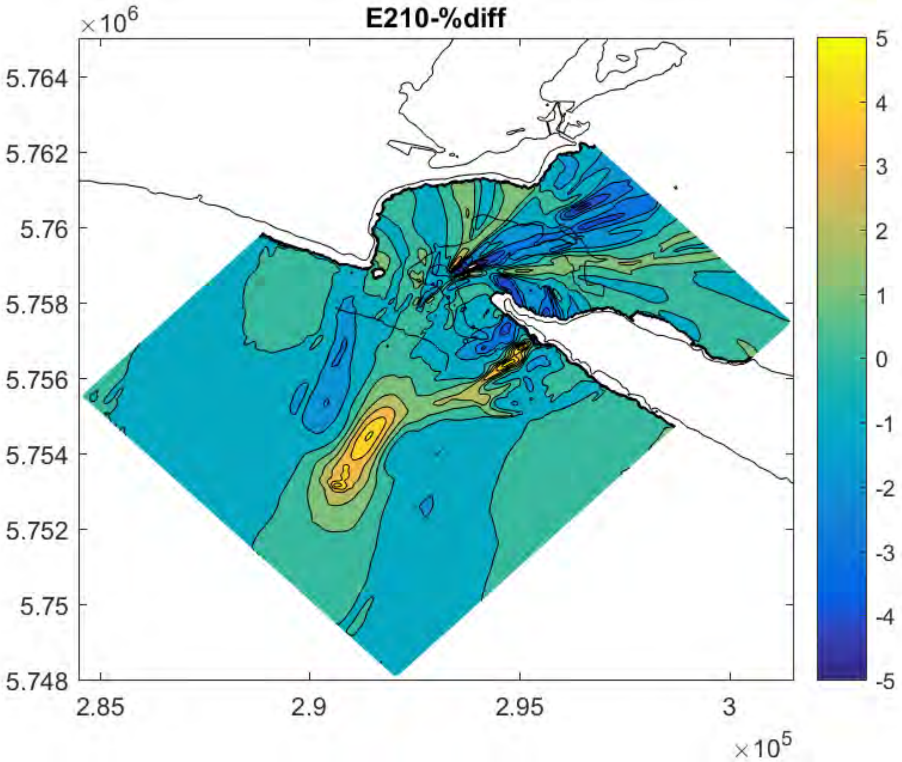

Figure 2-26 Difference in modelled significant wave height (dredged – existing) at peak ebb flow expressed as a percentage change from existing.

The changes for the peak flood flow, Figure 2-27,shows little change in the Entrance, but some changes in the south of the bay with small increases in wave height along the northern coast of Point Nepean. (The changes in Bass Strait in the south east of the model are a modelling artefact from the model boundary in this area.)

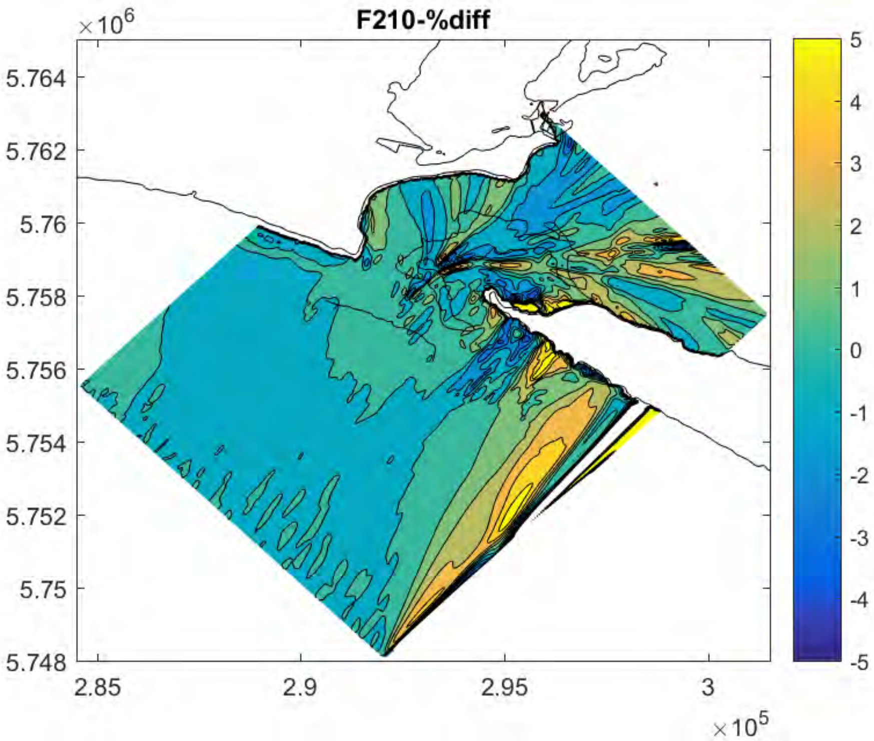

Figure 2-27 Difference in modelled significant wave height (dredged – existing) at peak flood flow expressed as a percentage change from existing.

In order to quantify the changes for all modelled cases, twenty-four extraction point locations were selected in the wave model (Figure 2-28). Changes in wave parameters at these locations, significant wave height and mean wave-direction, were extracted (Table 2-2 and Table 2-3).

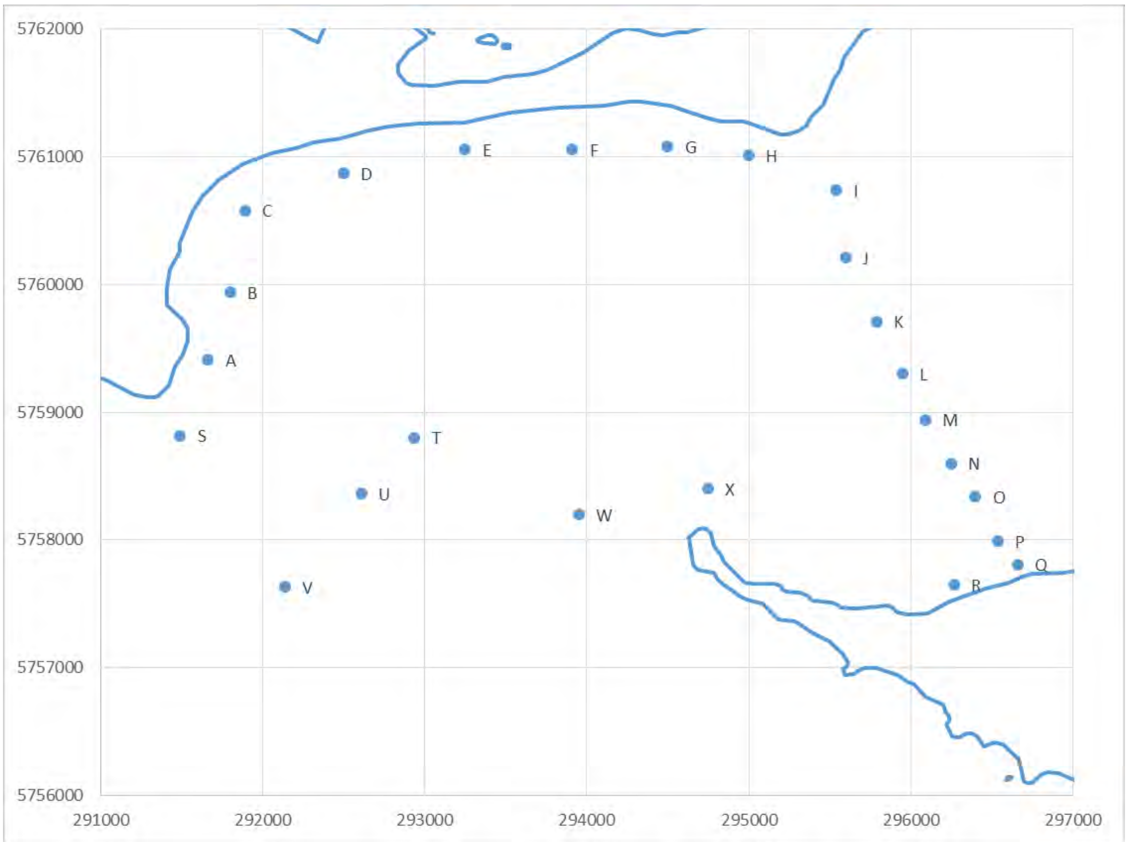

Figure 2-28 Wave model extraction points

Table 2-2 Change in significant wave height (percentage) for model extraction points for all model runs. Changes greater than 2% highlighted in yellow, greater than 5% in red.

Location	Hsig (m) Percent change (Widened - Existing)								
	Model run								
	S190	S210	S230	E190	E210	E230	F190	F210	F230
A	0.4	0.3	0.3	0.0	0.8	1.0	1.1	1.0	0.5
B	0.1	0.0	0.0	-0.3	-0.2	0.0	1.1	2.0	0.0
C	0.3	0.2	0.0	-0.6	0.4	0.3	0.0	1.4	0.1
D	-0.2	-0.1	0.0	-1.6	0.0	0.3	-0.5	-0.2	0.0
E	-0.4	0.5	1.2	-1.5	0.4	0.9	-0.5	-0.2	0.8
F	0.2	1.2	1.9	-0.9	1.1	1.6	0.3	0.9	1.9
G	1.1	0.6	0.1	0.7	0.6	0.4	-0.3	0.3	0.7
H	2.2	1.3	1.0	0.7	1.6	2.2	2.8	1.8	0.7
I	-1.1	-1.0	0.0	-0.4	0.3	3.2	-0.4	-1.0	-0.4
J	-1.5	-1.4	-0.6	-1.1	-0.4	1.9	-0.4	-1.6	-0.8
K	-1.2	-1.4	-0.8	-2.0	-2.4	-0.2	-0.7	-1.3	-0.8
L	0.1	-0.2	-0.7	1.5	-0.2	-0.9	-0.8	-1.7	-1.8
M	1.2	0.7	0.5	3.3	1.4	1.5	0.9	0.8	0.7
N	1.2	0.8	0.1	2.4	0.8	0.8	2.6	2.0	1.2
O	0.0	-0.2	-0.6	2.0	0.4	0.7	1.8	0.3	0.0
P	-0.8	-0.6	-0.8	0.8	-0.4	0.3	4.3	2.5	2.1
Q	-0.4	-0.3	-0.6	1.1	-0.2	0.1	4.3	4.7	1.6
R	0.0	-0.6	-1.3	0.7	-1.1	-0.7	1.8	4.7	-0.1
S	0.0	0.0	0.0	0.0	-0.3	0.2	0.1	0.3	0.0
T	-1.2	-0.5	0.4	-3.0	-1.2	-0.3	-0.8	-0.5	0.6
U	0.6	1.0	0.5	0.1	0.8	-0.7	0.1	0.9	0.7
V	0.0	0.0	0.0	-0.4	0.1	-0.3	0.0	0.1	0.0
W	0.3	0.7	0.4	2.4	0.6	0.3	-0.4	0.2	0.6
X	-1.4	-2.4	-3.5	-3.1	-3.9	-3.7	-1.7	-1.6	-1.3

The largest percentage changes in wave height are at points P, Q and R for the flood tide cases. These locations are on the northern shoreline of Point Nepean near Observatory Point. This is an area which has suffered erosion in the past (Cardno, 2011 and Bird, 2011) and further investigations would be required to fully assess the potential impact in this area of any widening of the channel in Port Phillip Heads. Other changes are at location X which is just north of the end of Point Nepean and also suggest more detailed investigations would be required before proceeding with widening of the channel as modelled.

Table 2-3 Change in mean wave direction (degrees) for model extraction points for all model runs. Changes greater than 1° highlighted in red.

Location	Dir (deg) Change (Developed - Existing)								
	Model run								
	S190	S210	S230	E190	E210	E230	F190	F210	F230
A	-0.1	-0.1	-0.1	-0.1	0.0	-0.1	-0.3	-0.4	-0.4
B	0.0	0.0	0.0	-0.1	-0.1	-0.1	0.0	0.0	0.0
C	0.0	0.0	0.0	0.0	-0.1	0.0	0.1	0.1	0.0
D	0.1	0.1	0.0	0.1	0.1	-0.1	0.3	0.2	0.0
E	0.0	-0.2	-0.5	-0.2	-0.4	-0.4	0.1	0.0	-0.4
F	-0.1	-0.1	-0.1	-0.2	-0.1	0.0	-0.1	-0.1	-0.2
G	-0.1	-0.1	0.0	-0.7	-0.3	0.2	0.2	0.2	0.2
H	0.0	0.0	-0.1	-0.5	-0.2	0.2	-0.1	-0.2	-0.2
I	-0.1	0.0	0.0	0.4	0.5	1.1	-0.1	0.0	0.1
J	-0.2	-0.1	0.0	0.2	0.3	0.5	-0.3	-0.2	-0.1
K	-0.1	-0.1	-0.1	0.0	0.1	0.2	-0.3	-0.2	-0.2
L	-0.1	-0.1	0.0	-0.3	-0.2	-0.1	-0.3	-0.3	-0.3
M	-0.5	-0.5	-0.4	-0.5	-0.5	-0.5	-0.8	-0.9	-0.6
N	-0.2	-0.1	0.0	-0.2	-0.1	0.0	0.4	0.0	0.0
O	-0.2	-0.1	0.0	-0.3	-0.3	-0.2	1.6	0.7	0.5
P	-0.1	0.0	0.0	-0.2	-0.2	-0.3	0.2	0.5	0.1
Q	0.0	0.0	0.0	-0.1	-0.1	-0.1	-0.4	0.1	0.0
R	-0.2	-0.1	-0.1	-0.5	-0.3	-0.3	0.6	0.5	0.1
S	0.0	0.0	0.0	-0.2	-0.5	-0.2	0.2	0.2	0.0
T	-0.2	0.0	-0.1	0.3	0.1	-0.2	-0.1	0.0	-0.2
U	0.3	0.7	0.2	0.8	0.0	-2.2	0.1	0.5	0.1
V	0.0	0.0	0.0	0.2	-0.3	-0.1	0.1	0.0	0.0
W	0.2	0.1	0.0	0.6	0.3	0.0	0.1	0.3	0.0
X	-0.6	-0.6	-1.0	-0.3	-0.3	-0.4	-0.9	0.1	-0.8

The changes in wave direction are small and isolated larger values may be due to the numerical accuracy of the modelling. However, more detailed investigations are required to confirm the impacts before undertaking the proposed works.

This preliminary modelling suggests that the proposed widening of the Great Ship Channel will not have any major impacts on the waves in and around Port Phillip Heads. However, there are some effects which warrant more detailed investigation.

2.4.4 Sediment transport

The dominant sediment transport mechanism in the Great Sands is due to strong tidal currents. As a means of screening for potential changes in sediment transport, the modelled currents have been vector-averaged over the duration of the model simulation (two months) using only those current vectors where the current speed exceeds 0.3 m/s. This calculation is a proxy for a full sediment transport computation, which is beyond the scope of this study. The calculation mimics the threshold for sediment movement for sand and then assumes a linear relation for the transport by currents above this threshold. Figure 2-29 shows the difference in the averaged current-velocity using only those current vectors where the current speed exceeds 0.3 m/s for the two cases.

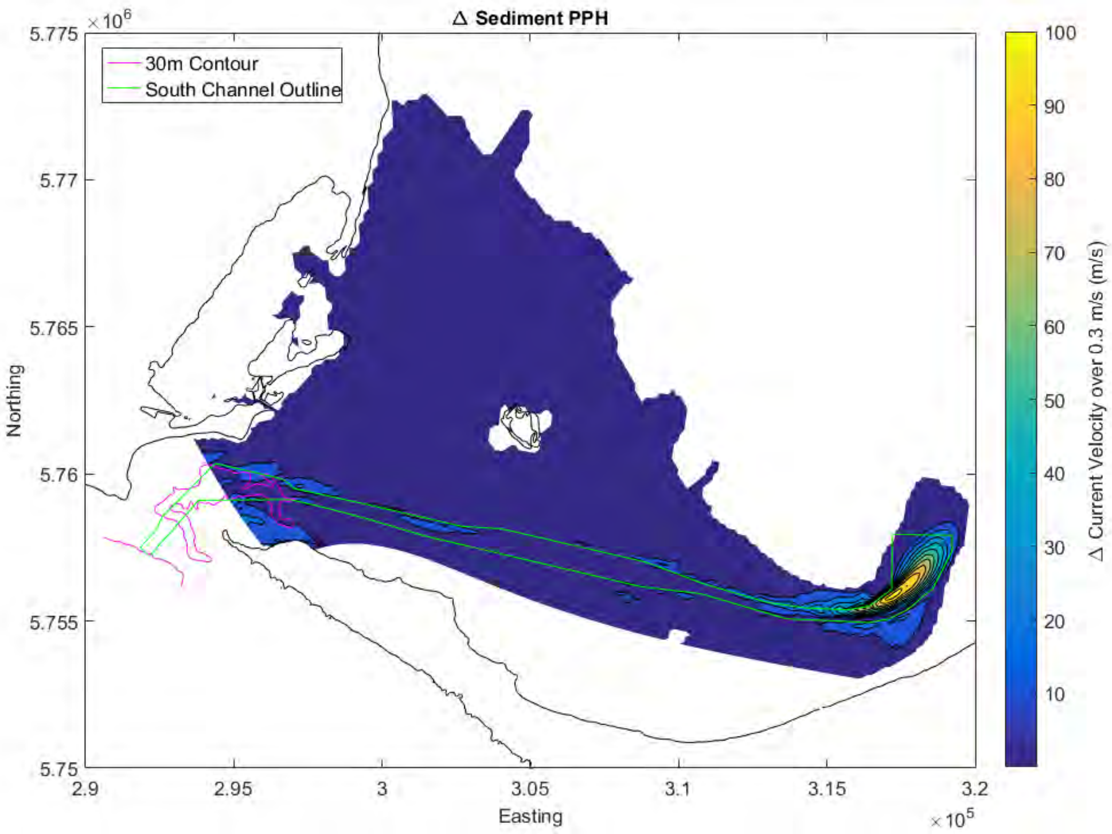

Figure 2-29 Difference in averaged current velocity for a threshold of 0.3m/s, the Great Sands, Project minus existing case.

Note that there is no consideration of the effects of waves or material availability.

The results in Figure 2-29 shows that there is increased sediment transport in the turning area around Hovell Pile due to the increased currents in the area, as discussed above. The increased flood tide currents suggest an increase in sediment movement to the north east in this area with the possibility of the formation of a bar as the current speed drops below the transport threshold and the sediment is deposited.

The other areas of change shown in Figure 2-29 are near the entrance where there is a potential increase in transport towards the Heads on the south side of the channel and into the bay on the north side. These changes are not considered large and unlikely to be significant within the natural variability and wave effects. It is of interest that these calculations do not identify any changes in the area of known sandwaves in the western end of South Channel.

While this preliminary calculation does not identify significant changes other than around Hovell Pile, more detailed sediment transport modelling would be required prior to undertaking any works.

Sediment movement on beaches is mainly driven by wave energy and thus may be effected by changes in the wave propagation caused by the project. Due the complex processes, a full coastal process modelling exercise is beyond the scope of this study, but would be required prior to undertaking any of the works included in this project. However, in general, the changes in wave energy propagation are small and unlikely to result in significant change to beach processes. However, there may be some local effects.

2.4.5 Vessel-generated waves

2.4.5.1 South Channel

The Port of Melbourne maintains warning signs for potentially large vessel-generated waves on the beaches in the south of Port Phillip, especially between Safety Beach and Rye. It is known (Gourlay, 2001) that large vessels in a confined channel can generate abnormally large waves which can propagate away from the

area of generation. These waves arise when the cross-section of the vessel is a significant proportion of the channel cross-section and thus water builds up in front of the vessel rather than flowing past it as it moves along the channel. The section of South Channel known as “The Cut’(see Figure 2-2) is a confined section of channel approximately 350 m wide with shallow banks on either side. Vessels sailing through this section can occupy a significant portion of the channel cross-section and thus it is possible for water in front of the vessel to generate a wave rather than pass down the side of the vessel. The result is a wave form known as a soliton which can travel long distances relatively unchanged, hence the warnings for large waves along the beaches. The formation of solitons occurs if the vessel Froude Number (related to speed and local water depth) exceeds a limiting value which includes the vessel cross-section, draught and channel cross-section. Values of this limiting Froude number for a range of conditions are shown in Figure 2-30.

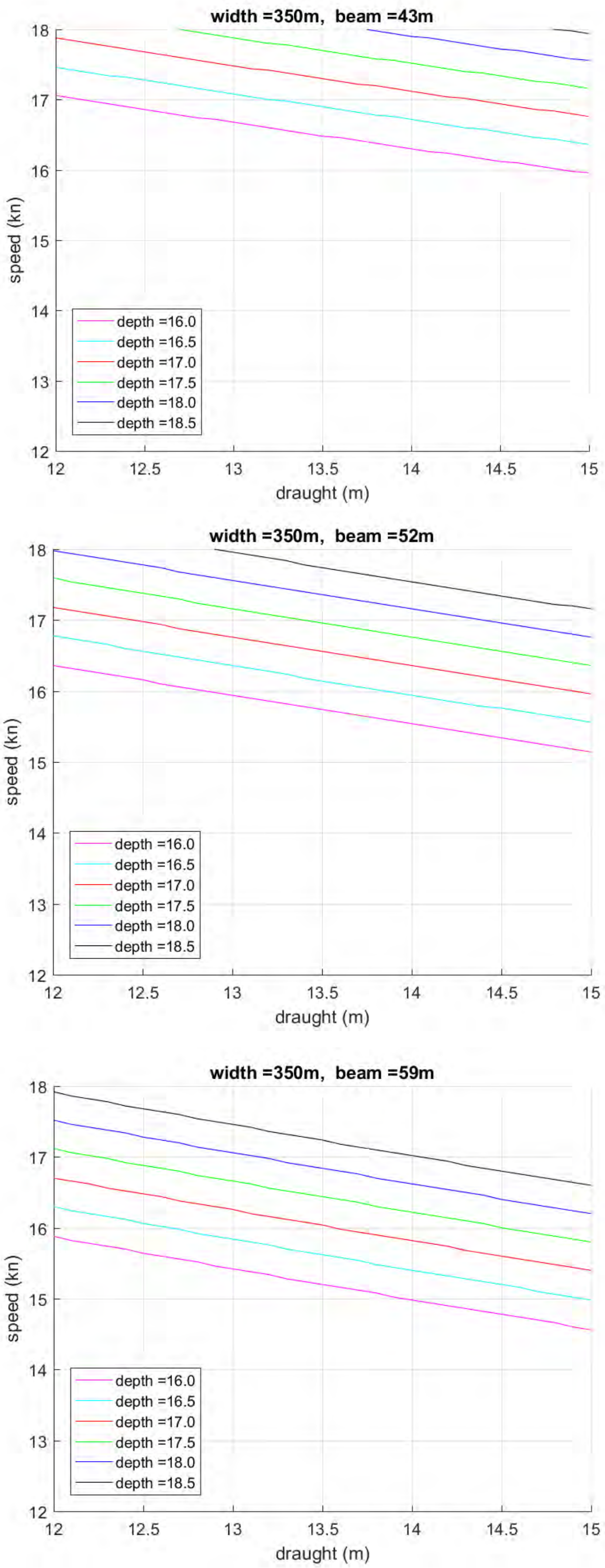

Figure 2-30 Limiting Froude numbers for generation of solitons in a shipping channel width 350 m

The data in Figure 2-30 includes a number of assumptions and approximations and requires more detailed analysis for a full assessment. However, the data shows that solitons can occur under the existing channel conditions and vessel traffic; channel width about 350 m, depth 15.5 m CD, vessel beam generally less than 40 m and draught less than 13 m (maximum 14 m). Solitons are not common, but are known to occur when vessels are near the maximum speed of 18 knots. These vessels can be very close to or exceed the theoretical limiting value.

Figure 2-30 shows that as vessel beam increases and draught increases, it is likely that vessel speeds will have to be reduced in order to avoid solitons. For example, a vessel of 59 m beam and a draught of 15 m would need to have a speed less than about 16 knots through the water if the channel depth was 17.5 m which is the minimum depth likely to be experienced in the dredged channel. This speed reduction will be required for both public safety and vessel operating efficiency as operations above the Froude Number limit require significantly more power to propel the vessel.

This analysis makes a number of assumptions and approximations. More detailed investigations would be required if larger vessels are to use South Channel. Such investigations will provide a robust basis for imposing speed restrictions for the channel based on vessel characteristics.

2.4.5.2 Yarra River Channel

A brief investigation has been undertaken into the possibility of “pressure waves”, similar to those know to occur in South Channel, being generated in the Yarra River shipping channel. The calculations carried out for South Channel were repeated using typical dimensions of the Yarra channel and representative vessel characteristics both now and projected in the future. The results for the limiting Froude number are shown in Figure 2-31 for the narrowest channel and representative vessel beams.

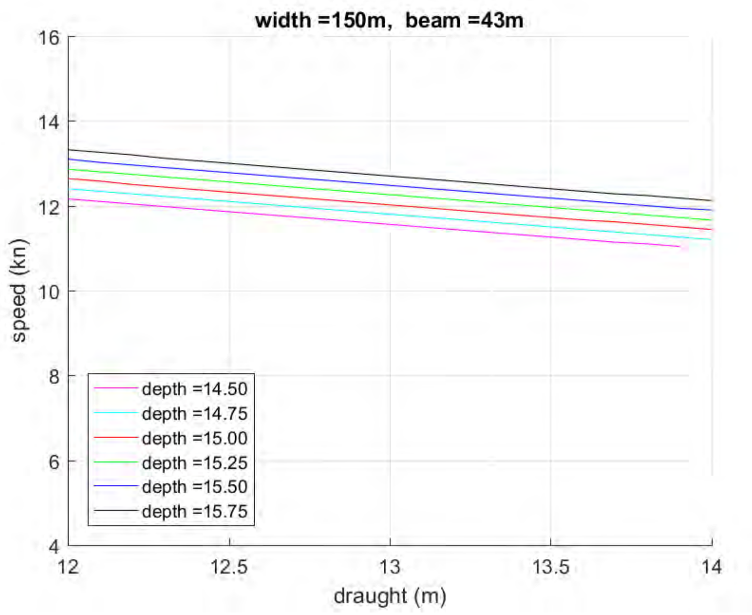

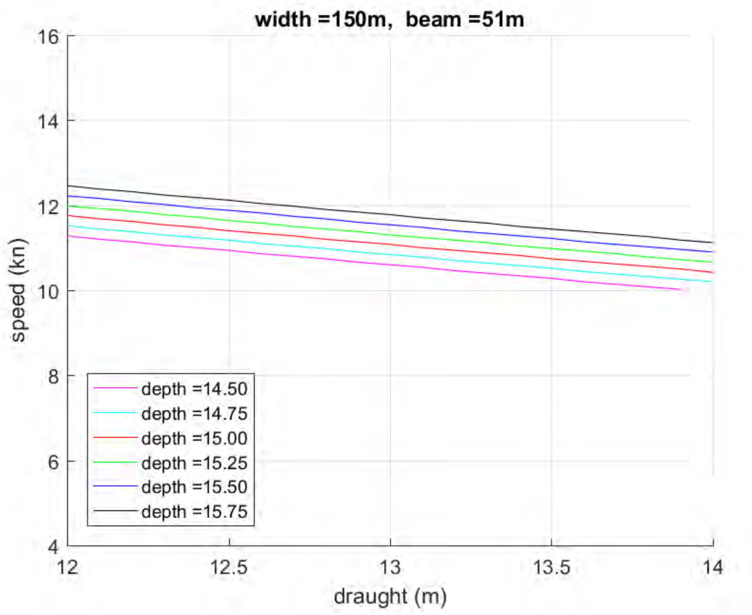

Figure 2-31 Limiting Froude numbers for generation of solitons in the Yarra River shipping channel with width 150 m for vessel beams of 43 and 51 m.

It can be seen in Figure 2-31 that for realistic underkeel clearances for vessel of 43 m beam (present day maximum), the limiting Froude numbers require vessel speeds of over about 12 knots which is well in excess of likely speeds in the Yarra. For vessels of 53 m beam, as projected in the future, the limiting Froude numbers are not reached until vessel speeds exceed about 11 knots, also well above likely practical speeds.

It is thus considered very unlikely that the "Froude number limit" type waves will occur in the Yarra, based on predictable vessel sizes and speeds.

However, there are potentially significant effects before vessels reach the limiting Froude number. As a vessel moves along a confined channel, it is displacing water ahead of it which must flow past the ship as it advances. In a very simplistic analysis, the average speed of the water flowing past the ship can be calculated by considering the volume displaced by the vessel in each second divided by the cross-section that volume must flow through in order to maintain continuity and water levels. Thus:

$$\textbf{Average current speed} = \frac{\text{(beam x draught x speed)}}{\text{(width x depth -- beam x draught)}}$$

Note that the current speed is averaged over the depth and across the channel, so that there may be higher speeds locally.

The average current speeds have been calculated for speeds of 6 and 8 knots (the existing speed limits upstream and downstream of the West Gate Bridge respectively) and for vessel beams of 43 and 51 m, as above. The results are shown for various combinations of channel width, vessel beam, water depth and vessel speed in Figure 2-32.

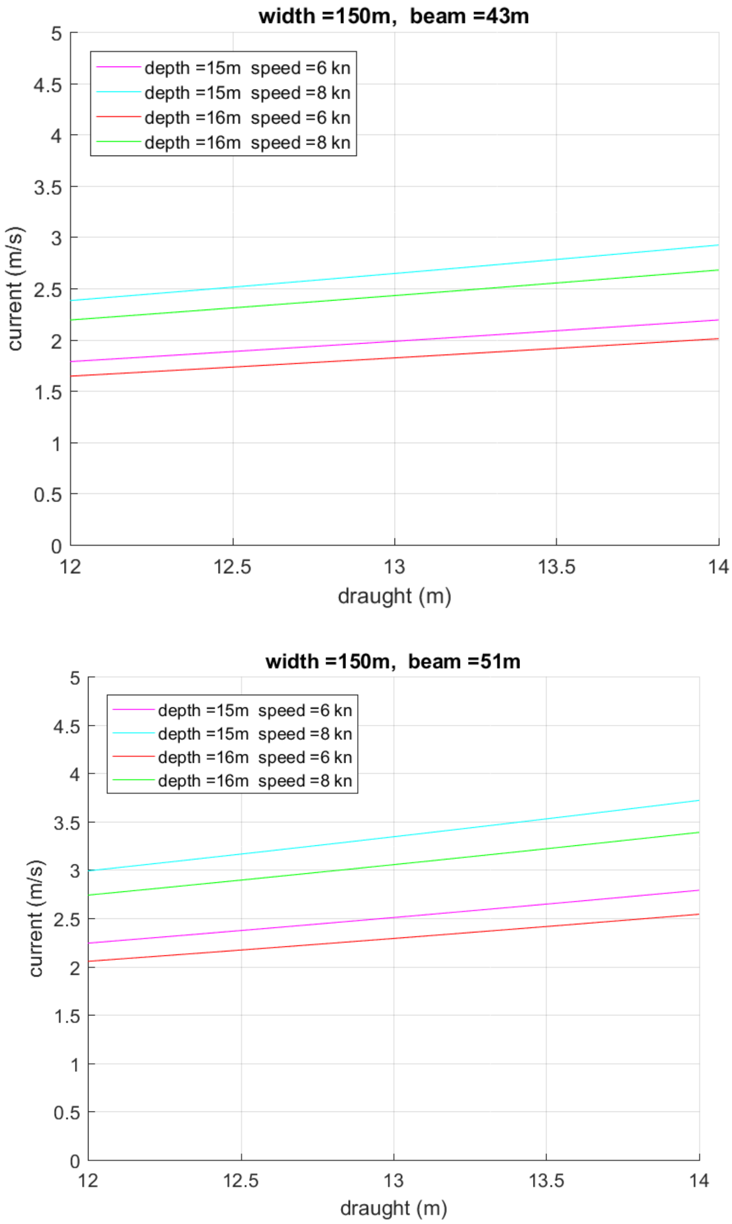

Figure 2-32 Average current speeds generated by a vessel of given beam and draught moving at speeds of 6 and 8 knots in a channel of width 150 m with depths of 15 and 16 m.

It can be seen that current speeds well in excess of 2 m/s (4 knots) are likely and in excess of 3.5 m/s (7 knots) are possible with the wider vessels. These currents would be manifest as a significant “surge” as the ship passes and may cause problems for moored vessels.

A simple estimate of the drawdown, or depression of sea level, associated with these currents shows that it is a maximum of 0.18 m associated with the current of 3.8 m/s. Noting that the drawdown depends on the current speed squared, the lower current speeds have much smaller drawdown. It is possible that the combined effects of the drawdown and surge will be identified as a “wave’ and related to issues with moored vessels.

In principle, the current-surge phenomenon is the same as the Froude-number limiting. As the current speed increases with vessel speed, the local Froude number limit becomes important and a new set of phenomena come into play.

These are preliminary calculations with a number of simplifications. The results could be refined through more detailed numerical modelling.

3 Western Port – Hastings

3.1 Western Port Bay

Western Port Bay is a large shallow embayment, see Figure 3-1. The bay entrance to Bass Strait is separated into two channels due to the presence of Phillip Island. French Island is positioned in the centre of Western Port Bay. The western channel is the dominant entrance and the one used by commercial shipping, with the eastern channel very narrow and shallow in comparison. (Cardno, 2013).

The Western Entrance and Lower North Arm sections are deep channel areas that extend up to the braided intertidal channels of the Upper North Arm (Figure 3-2). The east and north east of the bay is a depositional area with an expanse of shallow sand bars and 270 km² of intertidal mudflats (Melbourne Water, 2011). According to Marsden *et. al.* (1974) the morphology of Western Port is complex and varied, with much of the complexity attributed to the distribution of bedrock rather than the sedimentary processes, not typical of an estuary/barrier-lagoon system.

Water movements in Western Port are dominated by semi-diurnal tidal flows with a tidal range of about 2 m at the entrance and 2.6 m at the head (Tooradin). Ocean swell from Bass Strait penetrates as far as Stony Point, but further north, locally generated wind waves are the only source of wave energy.

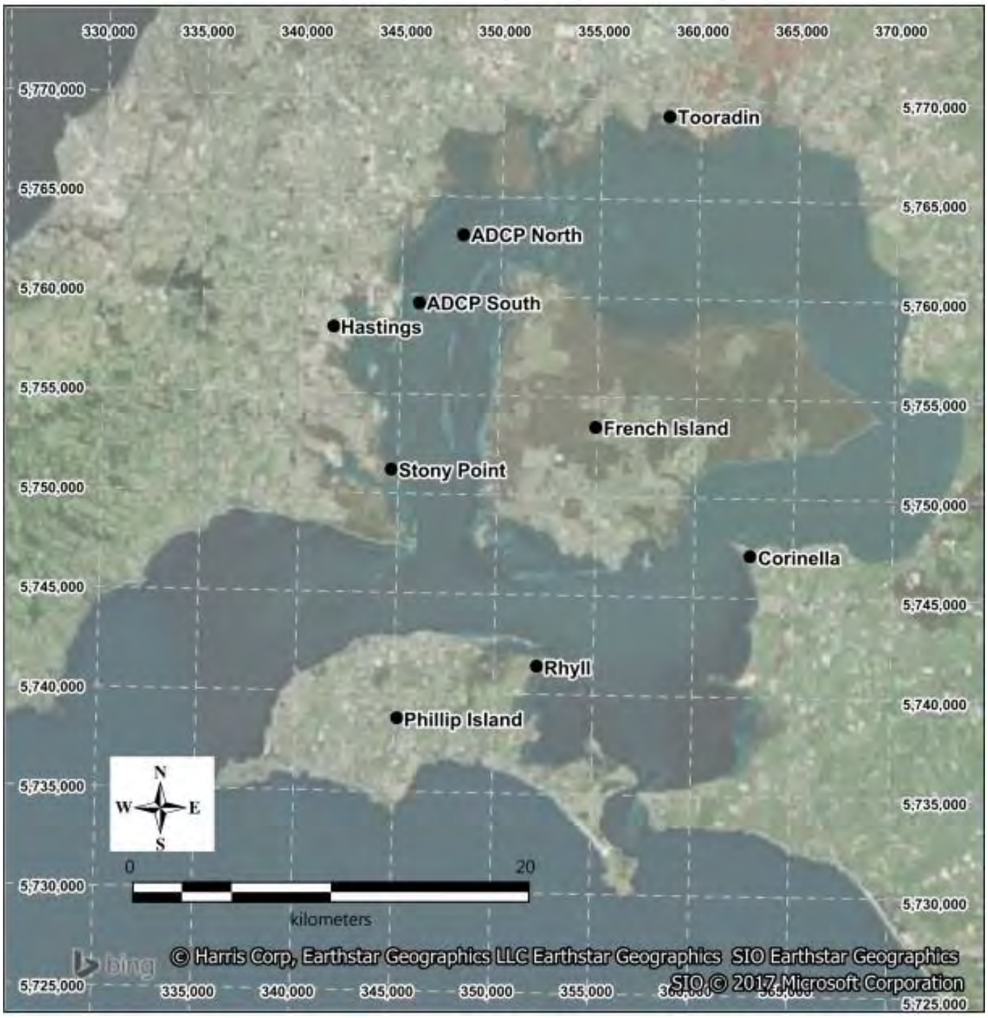

Figure 3-1 Map of Western Port Bay region.

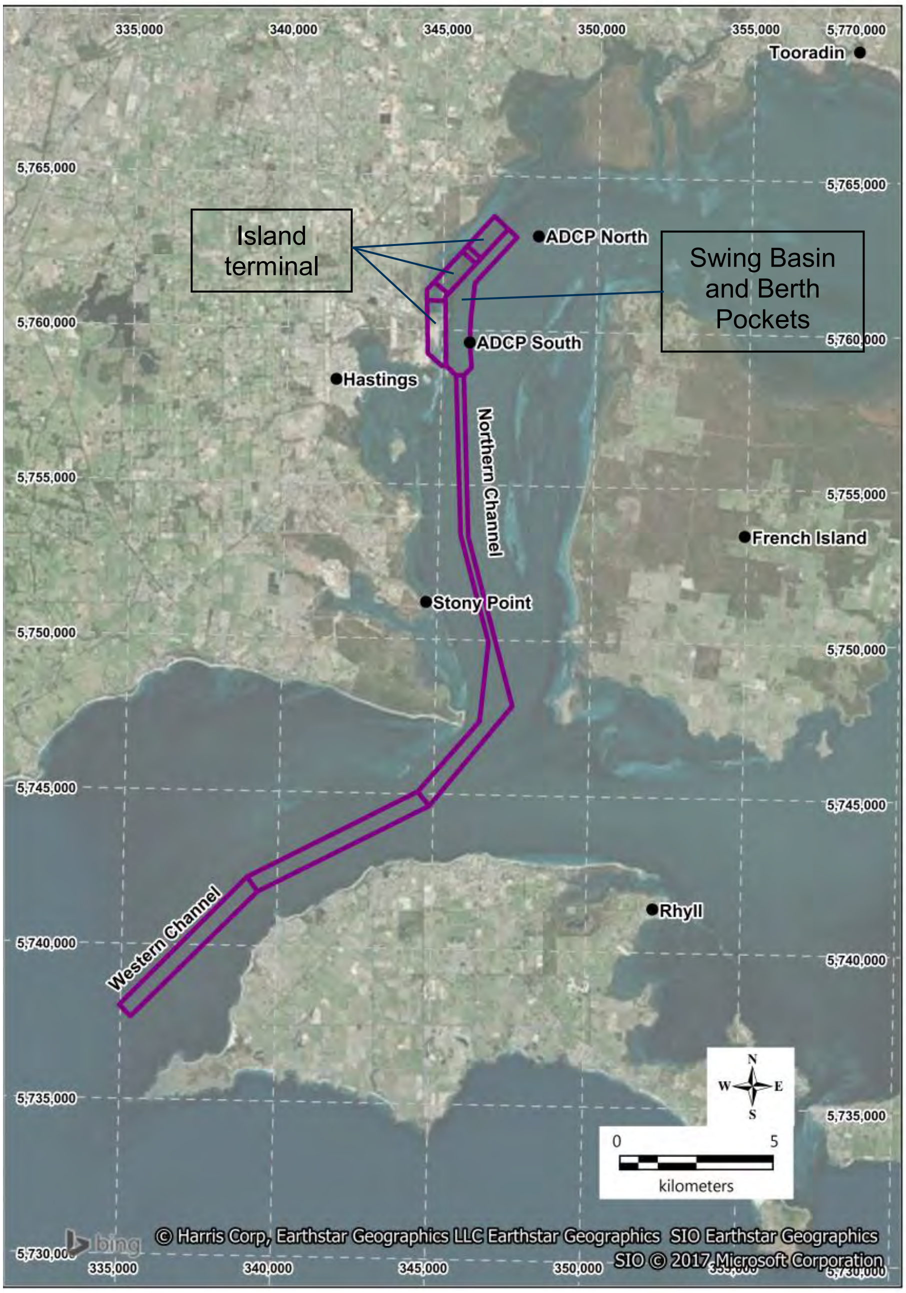

Figure 3-2 Map of Western Port Bay shipping channels

3.2 Scenario

The development of a container port in Western Port, Port of Hastings, as shown in Figure 3-2, requires construction of a land backed berth with extension to the north east, dredging of new berths and swing basin, as well as deepening existing channels with some minor re-aligning to facilitate access for larger vessels. The seaward section of the Western Channel would have a declared depth of -17.5 m CD, the remaining sections to Stony Point a declared depth of -17.0 m CD, the North Arm southern section would be -16.3 m CD, the northern section -16.2 m CD, the swing basin -16.2 m CD and the berth pockets -16.5 m CD (GHD, 2017).

The dredged material would be disposed of offshore in Bass Strait. The material used to construct the reclamation area for development of the container terminal would be sand dredged from offshore. The extension of the berth to the north east includes gaps (shown in Figure 3-2) to provide tidal exchange with the mud flats and intertidal area inshore of the terminal.

3.3 Models

3.3.1 Hydrodynamics

3.3.1.1 Description

A hydrodynamic model was developed to determine the impact of the port design scenarios for the preliminary business case investigations. This model used existing sea-level data and current measurements undertaken as part of the preliminary project. The model uses the FLOW module of the Delft3D modelling system developed by Deltares of The Netherlands. Delft3D includes a robust and efficient wetting and drying algorithm. This is particularly important for Western Port where there are extensive mangroves and intertidal areas.

Domain decomposition was applied in this study to allow efficient modelling. A far field model with coarser resolution was set up including a portion of Bass Strait which extended from Cape Schanck in the west to Cape Paterson in the east. The far field model also included the East Arm and parts of Upper North Arm. The coarse grid resolution is around 150 m and fine grid has 20 m resolution. The model extent and grids are shown in Figure 3-3.

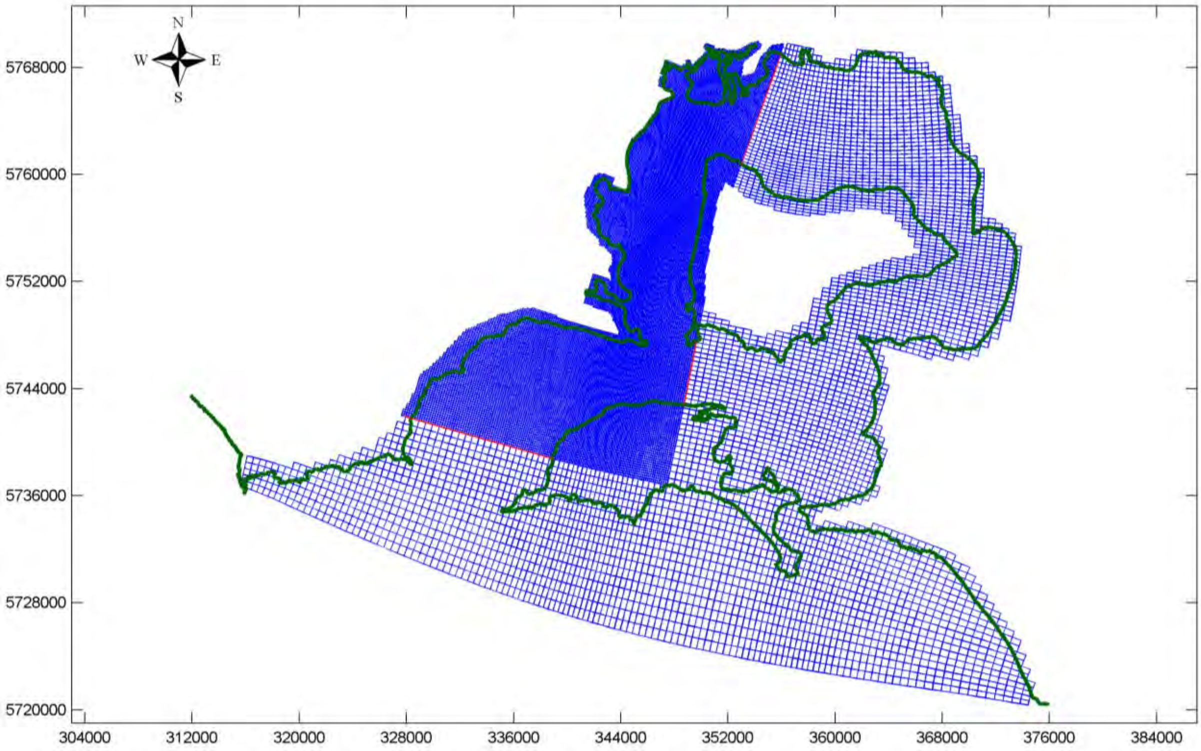

Figure 3-3 Hydrodynamic model grids used for the modelling. Note, only every 3rd grid line is plotted

Bathymetric data was used to define the model bathymetry. The bathymetry was sourced from a number of locations. High resolution (2.5 m) LADS bathymetric survey data by DSE surveyed in 2007 / 2009 were used as the basis of the bathymetry. This bathymetry was then combined with additional data from the following datasets (in order):

> 20 m Multi-beam survey data – Fugro LADS, (2010)

> Australian Bathymetry and Topography Grid, Geoscience Australia (2009).

Data read from navigation charts were used to fill gaps where other more recent data sources were unavailable, mainly the creeks in Tooradin and Warneet inlets and the channels in the Upper North Arm.

Figure 3-4 shows the model bathymetry and location of the measurements used for validation.

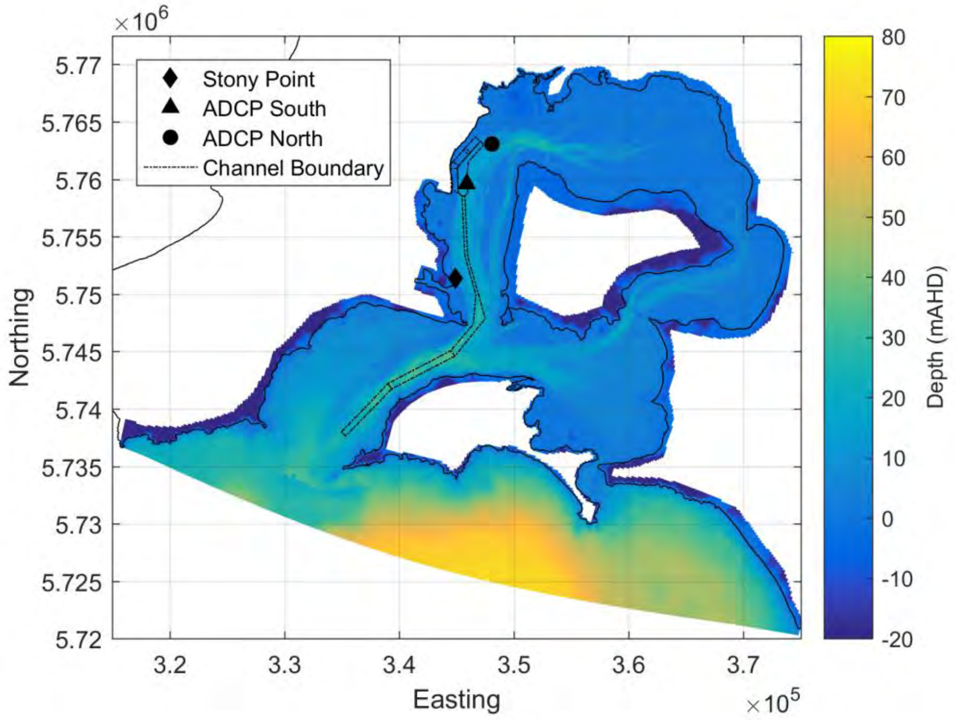

Figure 3-4 Study area showing model bathymetry and measurement locations

Following Haskoning (2014), the following values were adopted for the ends of the open boundary in Bass Strait:

> Western end = Observed Stony Point water level (m AHD) x 0.9 applied 60 minutes earlier

> Eastern end = Observed Stony Point water level (m AHD) x 0.9 applied 30 minutes earlier

The modelling and assessment for the present study used the preliminary model with updated boundary conditions, as above.

For the developed case, modifications were made to the bathymetry to account for channel dredging to accommodate 15 m draught vessels with a port development as shown in Figure 3-2 with the inclusion of the gaps to allow tidal exchange with the area inshore of the terminal.

The model was run for the time period 15 December 2012 to 15 January 2013, for both existing and developed cases.

3.3.1.2 Calibration and Validation

The hydrodynamic model results were compared with measured data to examine the performance of the model in defining the existing conditions in Western Port. As the hydrodynamics of the area are mainly driven by the astronomical tide, the model was driven by specifying the tide at the boundary, as described above. The tide levels at Stony Point, North ADCP site, South ADCP site (Figure 3-4), were compared against the model and are presented in Figure 3-5. The modelled currents were compared with the measured data at the two ADCP locations in Figure 3-6 and Figure 3-7.

The model results show a good agreement with the available data at validation sites.

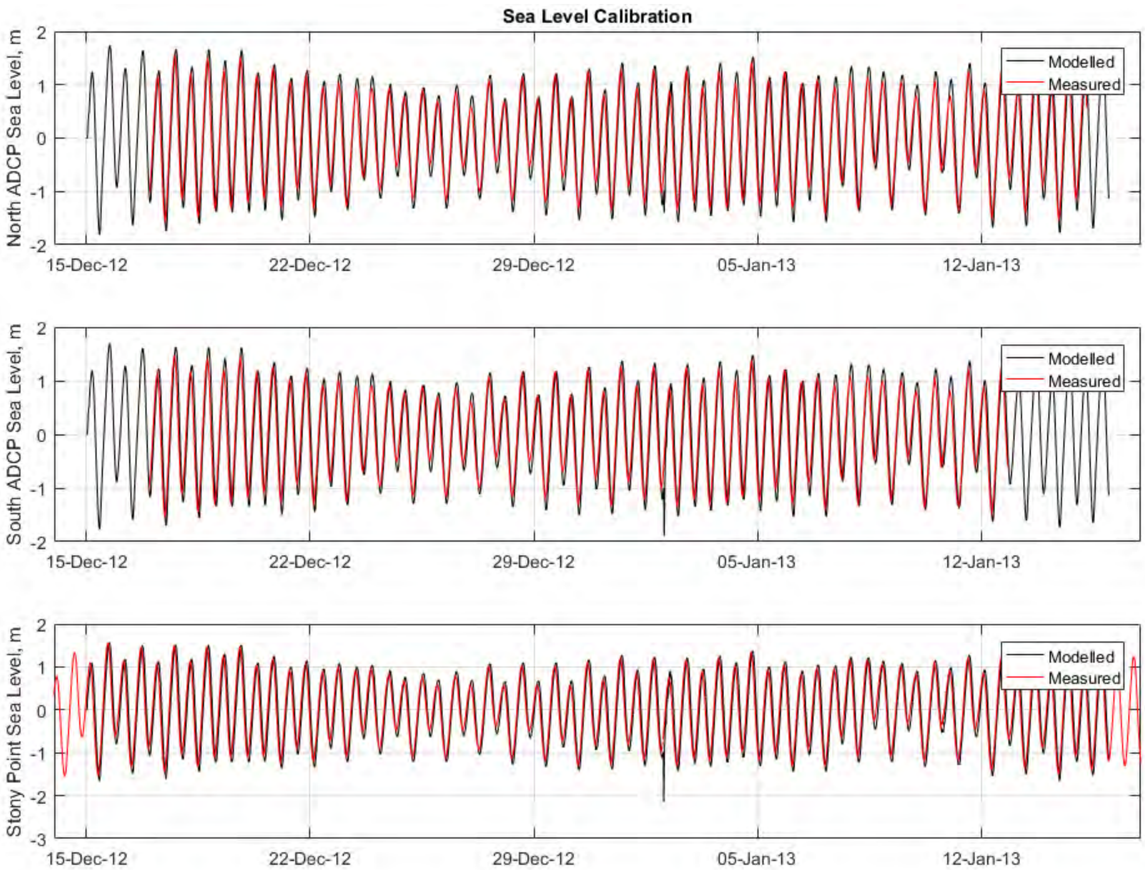

Figure 3-5 Water Level Calibration at Stony Point, ADCP North and ADCP South

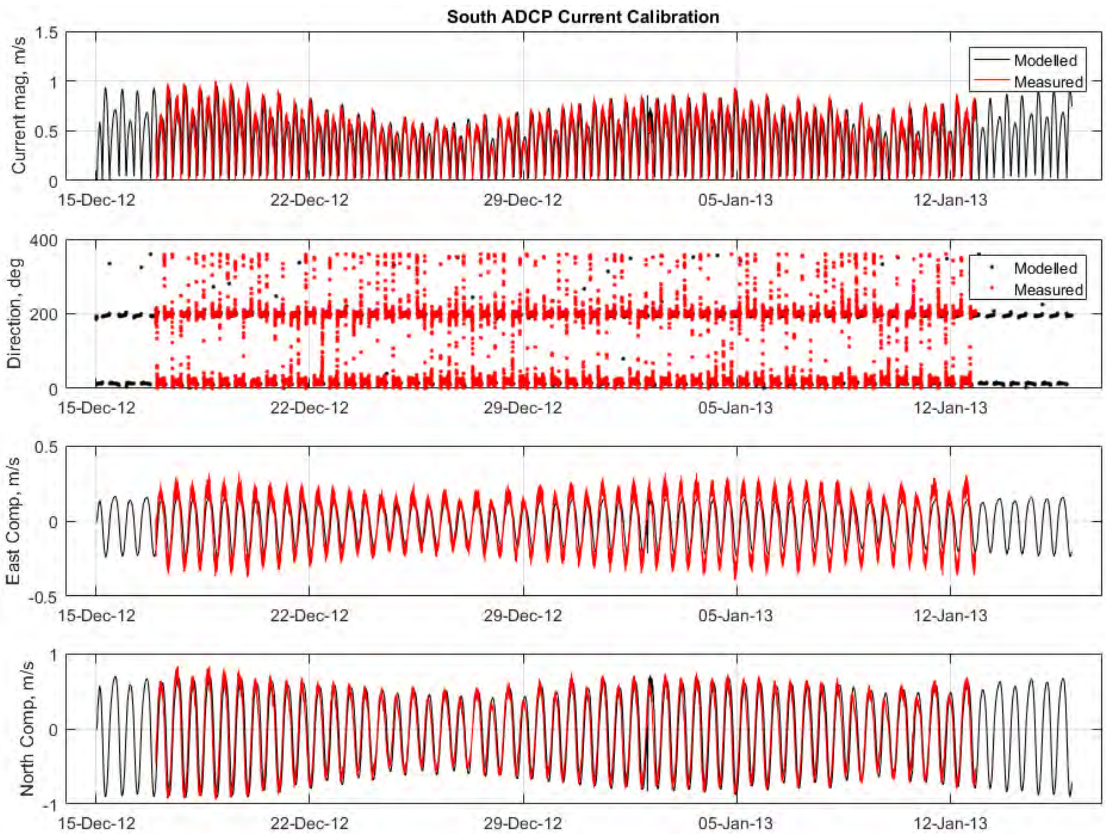

Figure 3-6 Currents Calibration at ADCP South

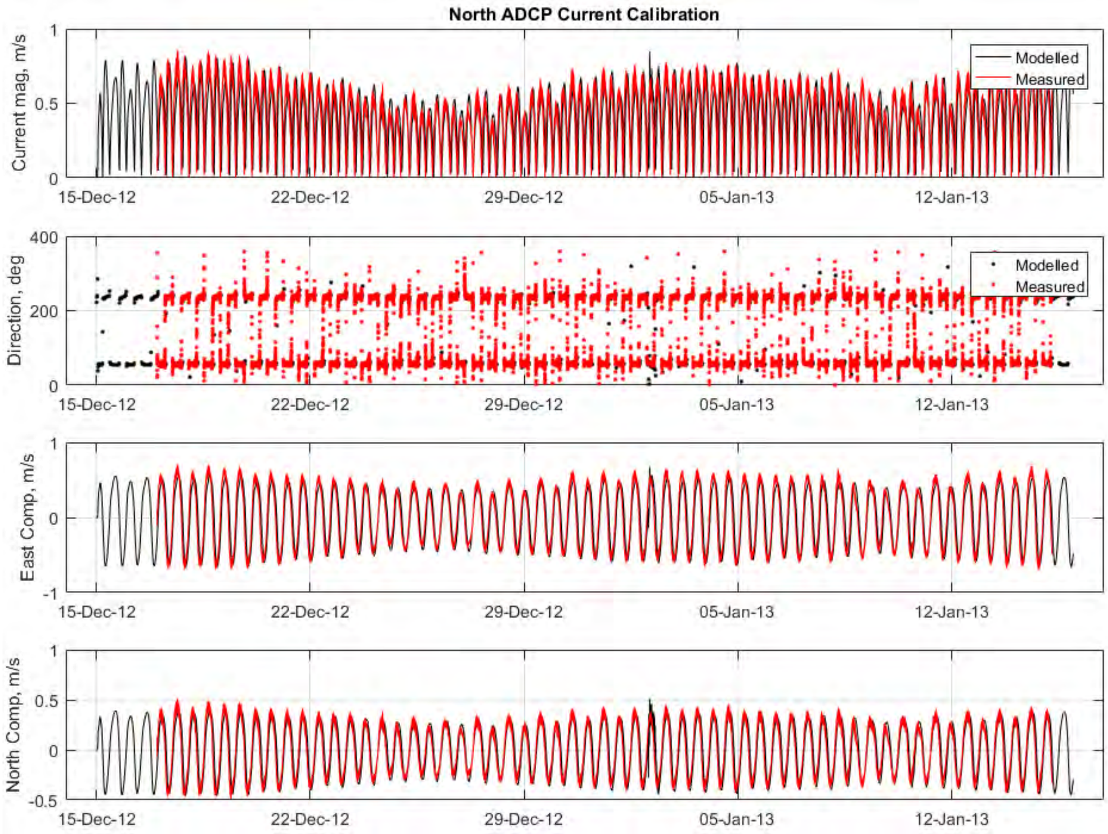

Figure 3-7 Currents Calibration at ADCP North

3.3.2 Waves

No modelling of waves was undertaken for this study. The developed case has minimal dredging of the channel south of Sandy Point and thus there will be no impact on the propagation of swell from Bass Strait into the Western entrance of Western Port.

3.4 Impact Assessment

3.4.1 Sea-level

The impact of the project on sea levels within Western Port has been assessed by computing the difference in sea level at six-minute intervals and plotting this against the existing case level for that time. An example for the North ADCP site is shown in Figure 3-8. The data indicates that there is very little change in sea-level overall, but the shape of the data plot suggests a small phase change, especially near low tide which is likely to be related to the dredging of the channels increasing the relative hydraulic efficiency of the flow as the tide level drops.

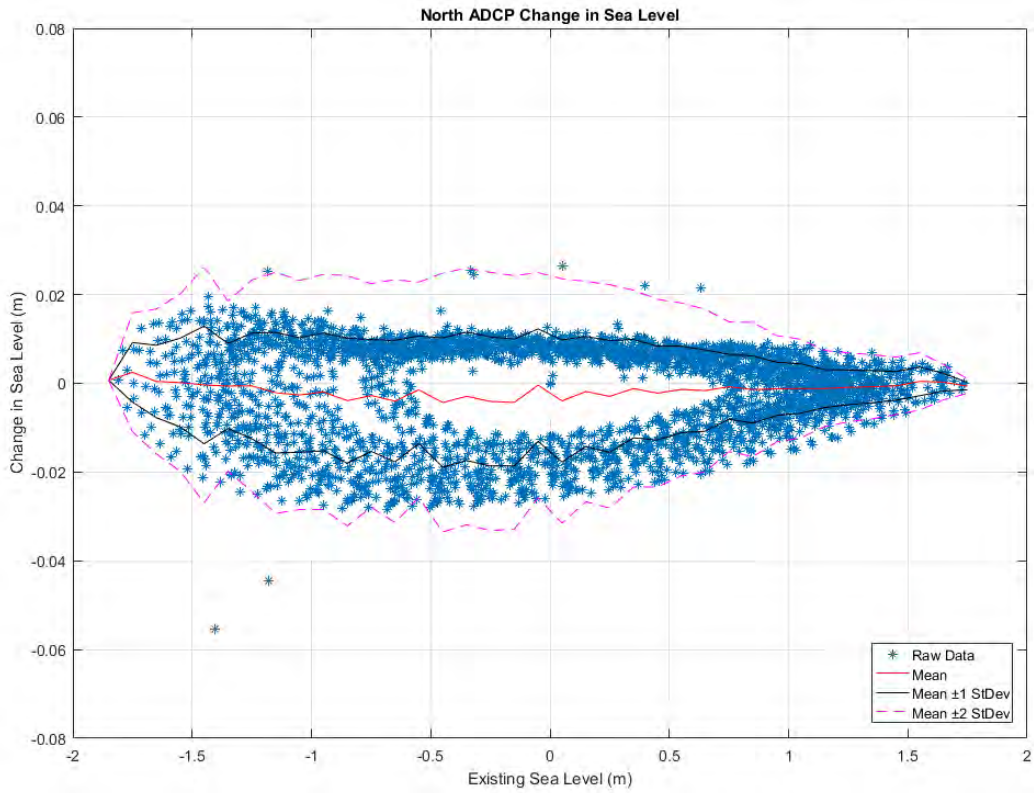

Figure 3-8 Change in sea level for the Port of Hastings development compared with existing sea level at North ADCP site

For comparison, Figure 3-9 shows a similar comparison for Corinella. In this case, there is very little change in the mean values and very little evidence of a phase change in the tide, which would show as a vertical spread in the differences on the plots, such as is evident in Figure 3-8.

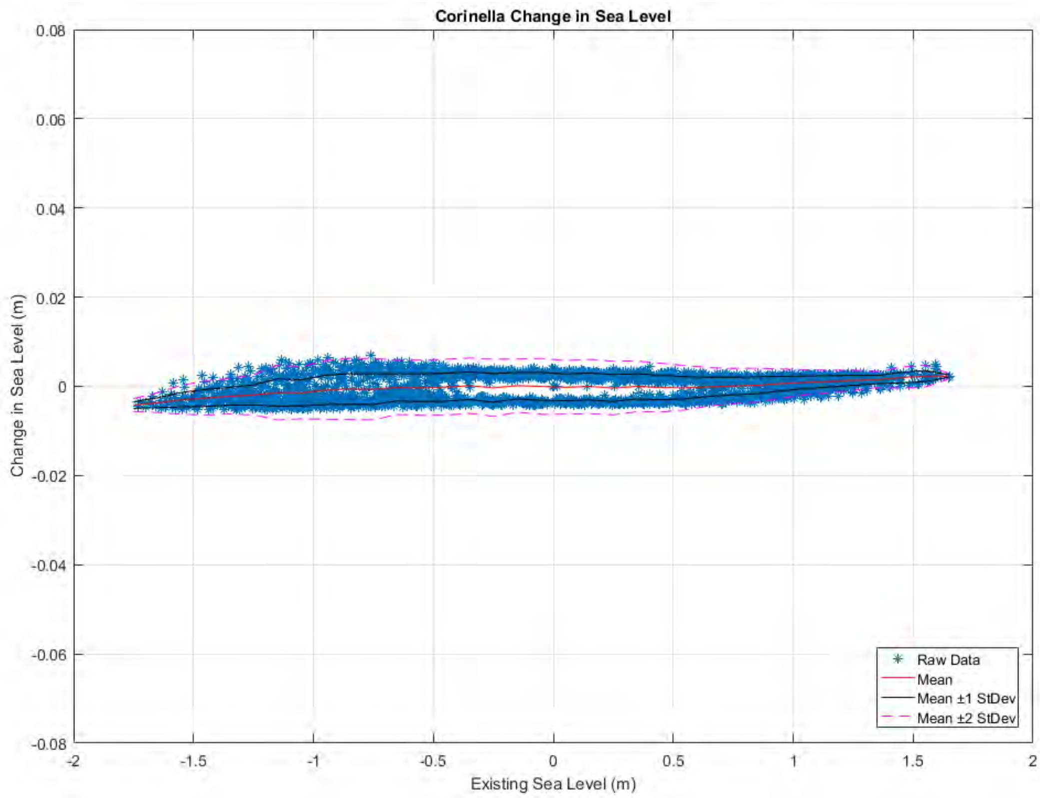

Figure 3-9 Change in sea level for the Port of Hastings development compared with existing sea level at Corinella

Table 3-1 shows the changes in the distribution of sea levels which removes the effects of small phase changes. It can be seen that the largest changes, at Tooradin, are an increase in tidal range with the 2nd percentile, the level defining the lowest 2% of sea levels, decreasing by 14.5 mm and the 98th percentile, the level defining the highest 2% of sea levels increasing by 15.9 mm. At Stony Point the corresponding levels change by about 6 mm decrease and increase respectively. The changes can be compared with the annual rates of change in sea level at Stony Point where sea level has risen by an average of 2.8 mm since 1990 and continues to rise (BoM, 2016).

Table 3-1 Impact of Port of Hastings on the distribution of sea levels (m) over the modelled period.

Location	2nd percentile	10th percentile	50th percentile	90th percentile	98th percentile
Hastings - North ADCP	-0.0251	-0.0190	0.0015	0.0094	0.0129
Hastings - South ADCP	-0.0047	-0.0032	0.0015	0.0071	0.0095
Stony Point	-0.0058	-0.0042	0.0008	0.0041	0.0064
South Channel	-0.0071	-0.0050	-0.0014	0.0009	0.0024
Corinella	-0.0046	-0.0038	0.0005	0.0030	0.0043
Tooradin	-0.0145	-0.0122	-0.0005	0.0116	0.0159
Rhyll	-0.0043	-0.0034	0.0005	0.0026	0.0038

3.4.2 Currents

The current speeds in the north-western portion of Western Port, the vicinity of the potential port development, are shown for the peak ebb flow in Figure 3-10 for both the existing and developed cases and in Figure 3-11 for the peak flood flow, again for both cases.

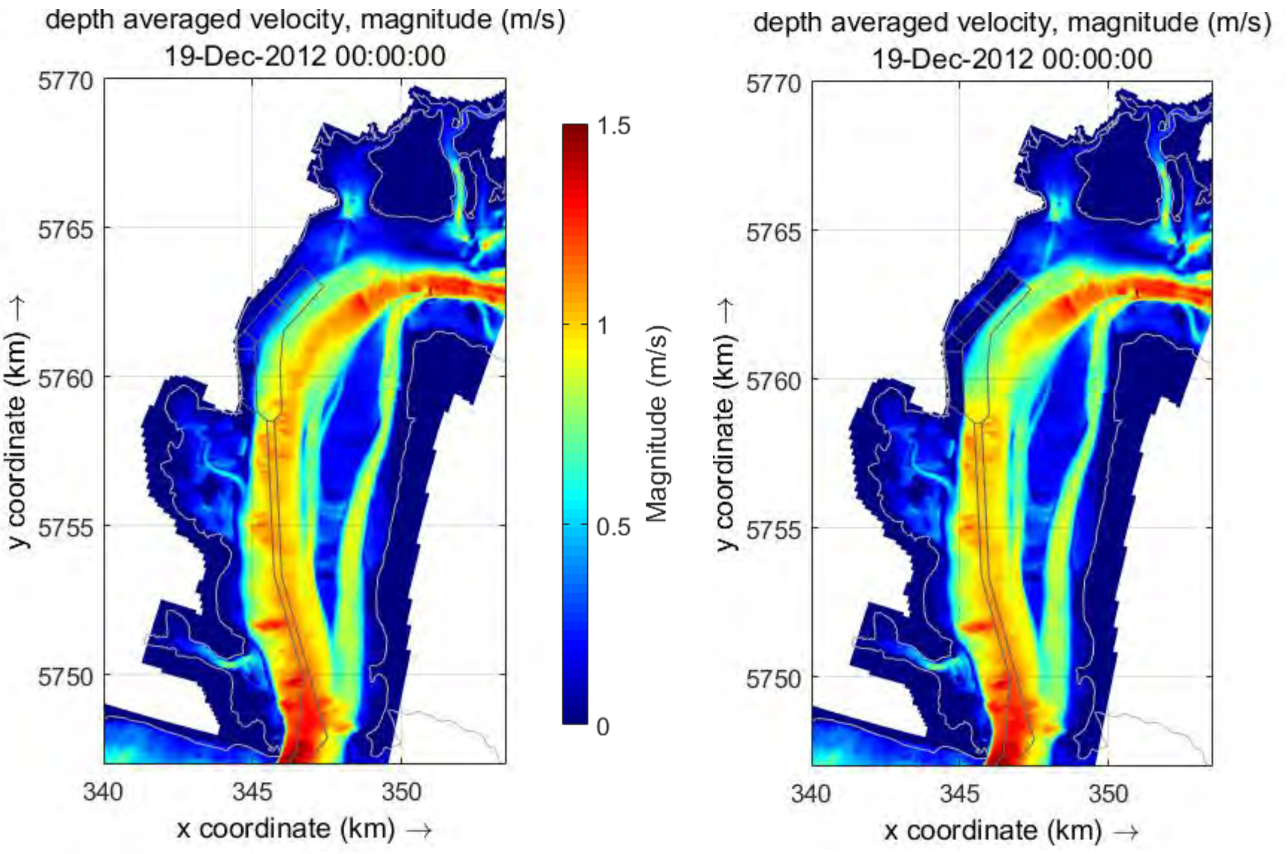

Figure 3-10 Current speed at peak ebb flow, Hastings, existing (left) and dredged case (right).

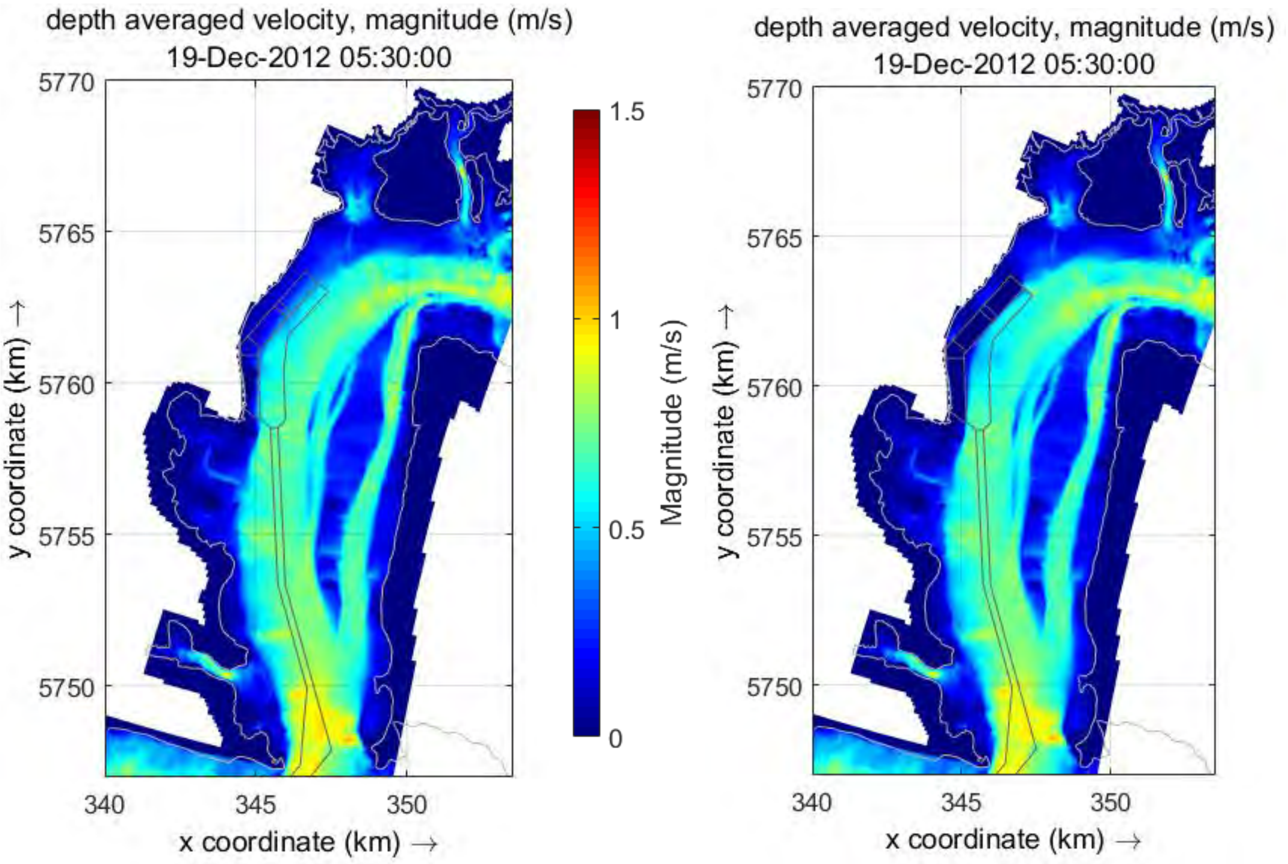

Figure 3-11 Current speed at peak flood flow, Hastings, existing (left) and dredged case (right).

Figure 3-10 and Figure 3-11 show that the ebb and flood-tide currents vary markedly across channels. This is a feature of the tidal characteristics of this area and has important consequences for sediment transport.

There are very small changes in the tidal currents overall due to the development. However there are changes in the port area where the dredging and construction of the port facilities leads to changes. These are shown as the difference in current speed (developed minus existing case) for the peak ebb (Figure 3-12) and peak flood (Figure 3-13).

The changes in the port area are small increases with accelerated flow in the gaps in the terminal structures, which are reclamation areas. The gaps are designed to allow tidal flow into the areas inshore of the terminal to maintain mudflat, mangrove and intertidal habitats. The modelling shows that this can be achieved, but there is the potential for acceleration of currents in the gaps, which may lead to scouring. Detailed engineering design will be required to mitigate this effect but still maintain the water flows.

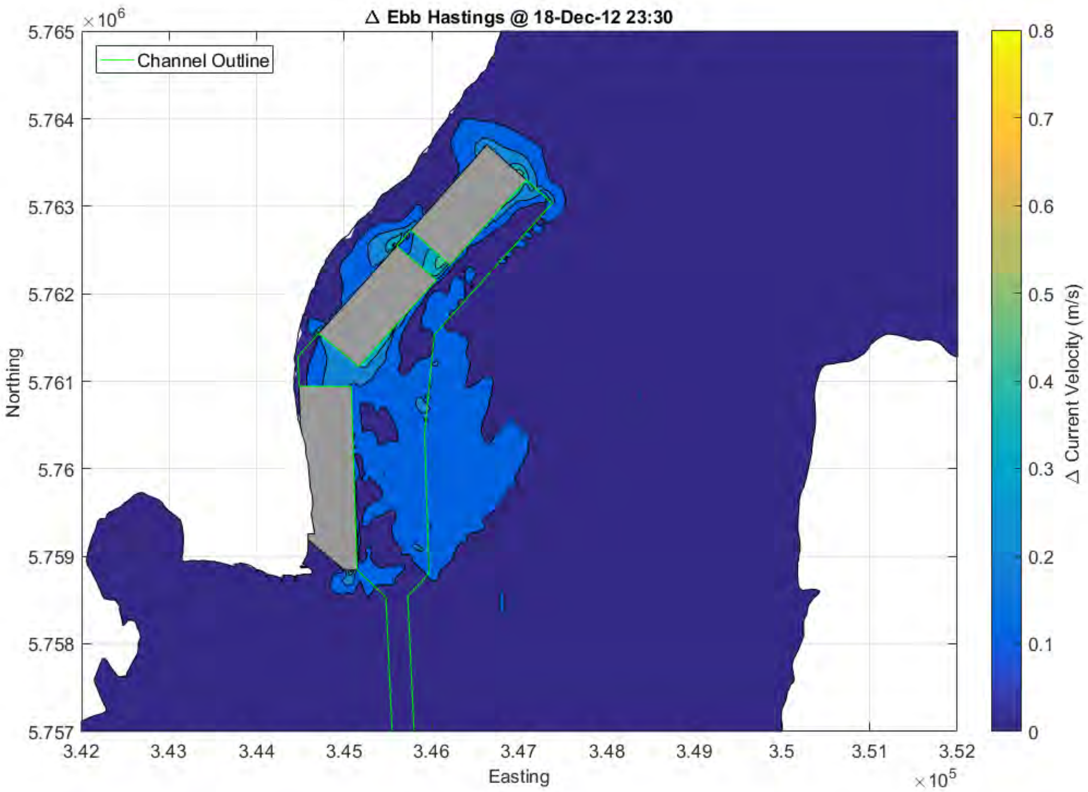

Figure 3-12 Difference in current speed at peak ebb flow, Hastings: Developed minus existing case.

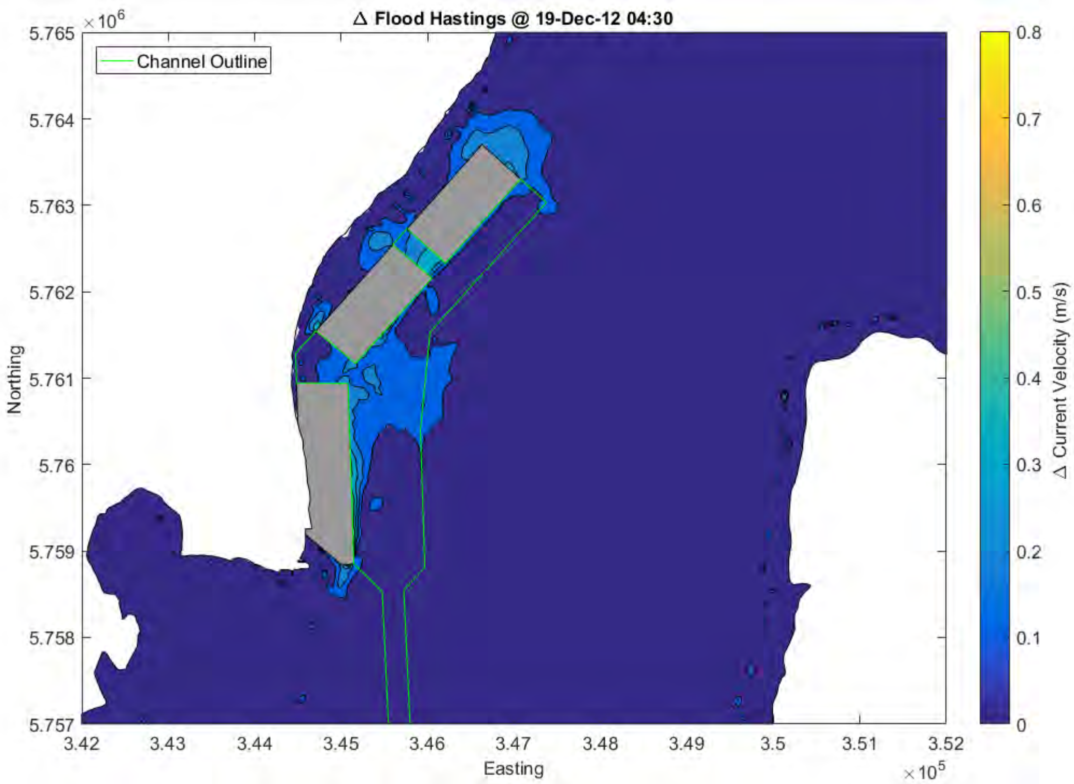

Figure 3-13 Difference in current speed at peak flood flow, Hastings: Developed minus existing case.

3.4.3 Tidal divide

The tidal divide in Western Port is the line in the north east of the bay separating the area where the rising tide brings water from the west, via North Arm, from that where the water comes from the east, via East Arm around opposite sides of French Island. A change in the position of this line may have consequences for sediment transport in this portion of the bay.

The tidal divide movement was calculated by extracting the current velocity from the hydrodynamic model. The eastward component of the current velocity at six-minute intervals over the model duration (31 days) for existing and option conditions were extracted at each grid point along a line north east of French Island, as shown in Figure 3-14. The zone of zero current speed and the line of modelled points used for determining the location of the divide are also shown in Figure 3-14.

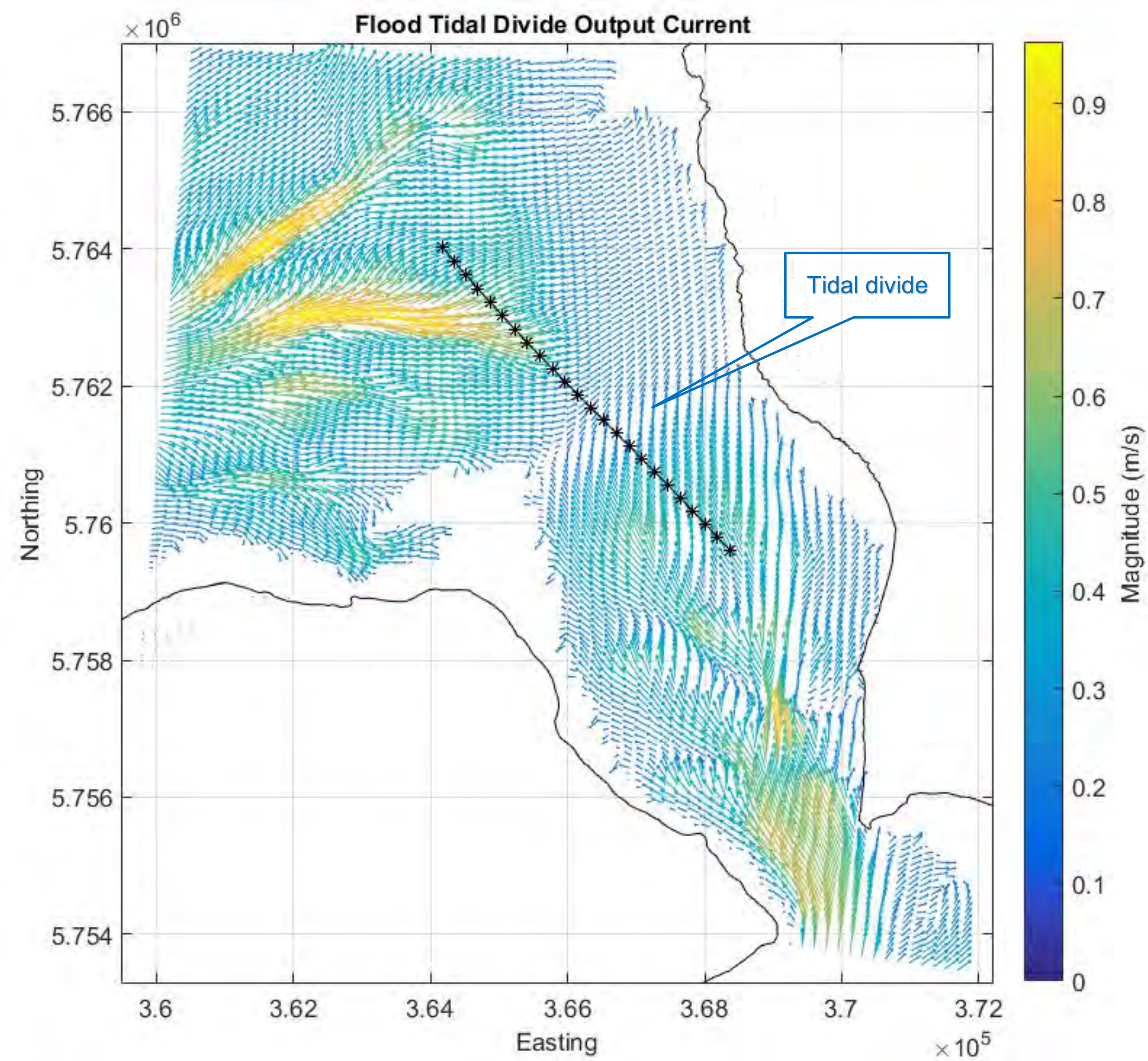

Figure 3-14 Current vectors during a flood tide north east of French Island showing the tidal divide and the line used to define the location of the divide

The analysis consisted of extracting the current component along the line indicated in Figure 3-14 and assigning a positive sign to eastward flows and negative sign to westward flows. The current component was then considered as a line as shown in Figure 3-15. The point where this line crosses zero defines the tidal divide. Such a line was developed for every model time step and the positions of the divide compared for existing and developed cases. When averaged over the one month modelled duration, it was found that the tidal divide moved to the south east, along the analysis line, by 32 m. This is within the variability of the

divide position, which had a range in movement over the modelled period between about zero and 65 m to the south east. The significance of this potential movement is not clear and would require more detailed analysis, however it would appear unlikely to be sufficient to cause a significant destabilisation of the mud flats in the area or any major change in drainage patterns.

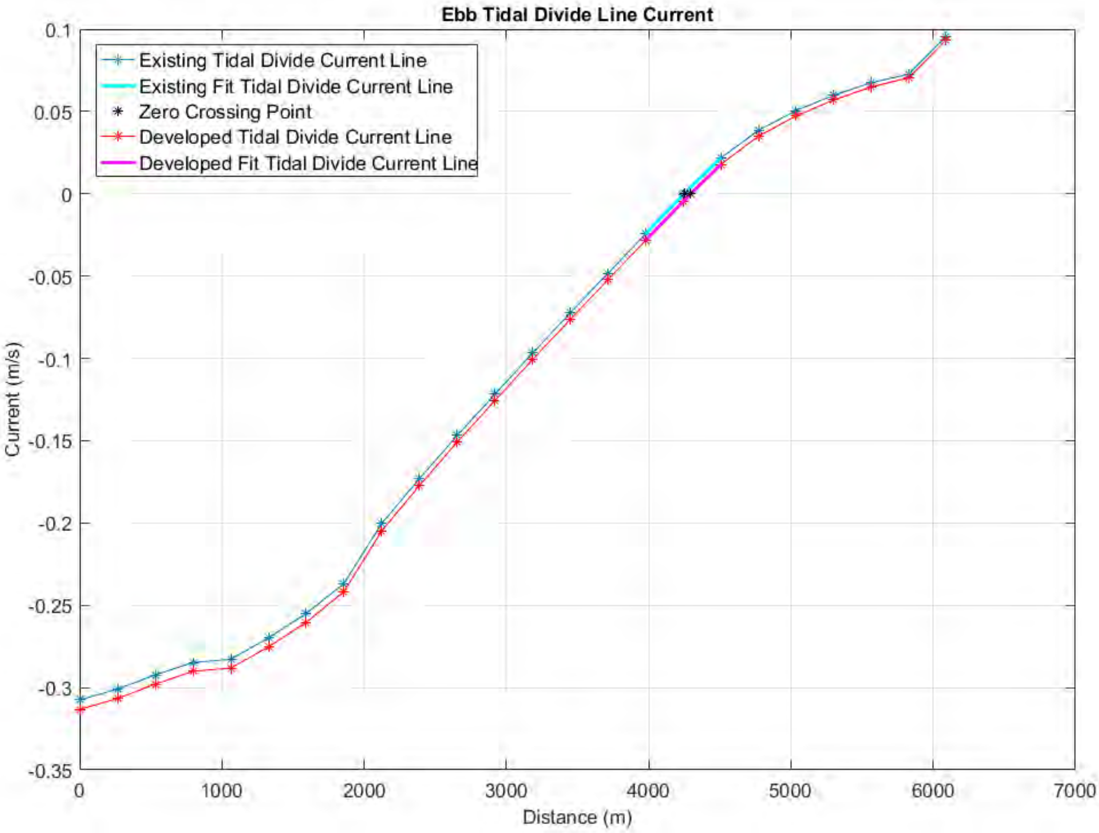

Figure 3-15 Analysis of the location of the tidal divide for the ebb tide, distances are measured positive eastwards from the western end of the line shown in Figure 3-14

3.4.4 Waves

No wave modelling has been carried out for this study. The preferred option does not involve significant dredging south of Sandy Point and none at the south-western entrance to the bay and thus there will be no changes in the swell propagation from Bass Strait.

Wind-driven waves in the port area have not been modelled, but estimated by examining the available fetch (the distance over which the wind can blow to generate waves) and wind data. The major effect of the project was shown to be the sheltering of the coast inshore of the terminal where the solid reclamation shelters the shore from wave action and thus may change the character of the habitat and thus ecology of these areas. Detailed investigation will be required to determine the magnitude and impact of these changes

3.4.5 Sediment transport

The sediment transport has been estimated in a qualitative sense by averaging the modelled currents over the duration of the model simulation using only those current vectors where the current speed exceeds 0.3 m/s (see Section 2.4.4 for more discussion). The resulting vectors for the North Channel for the existing case are shown in Figure 3-16.

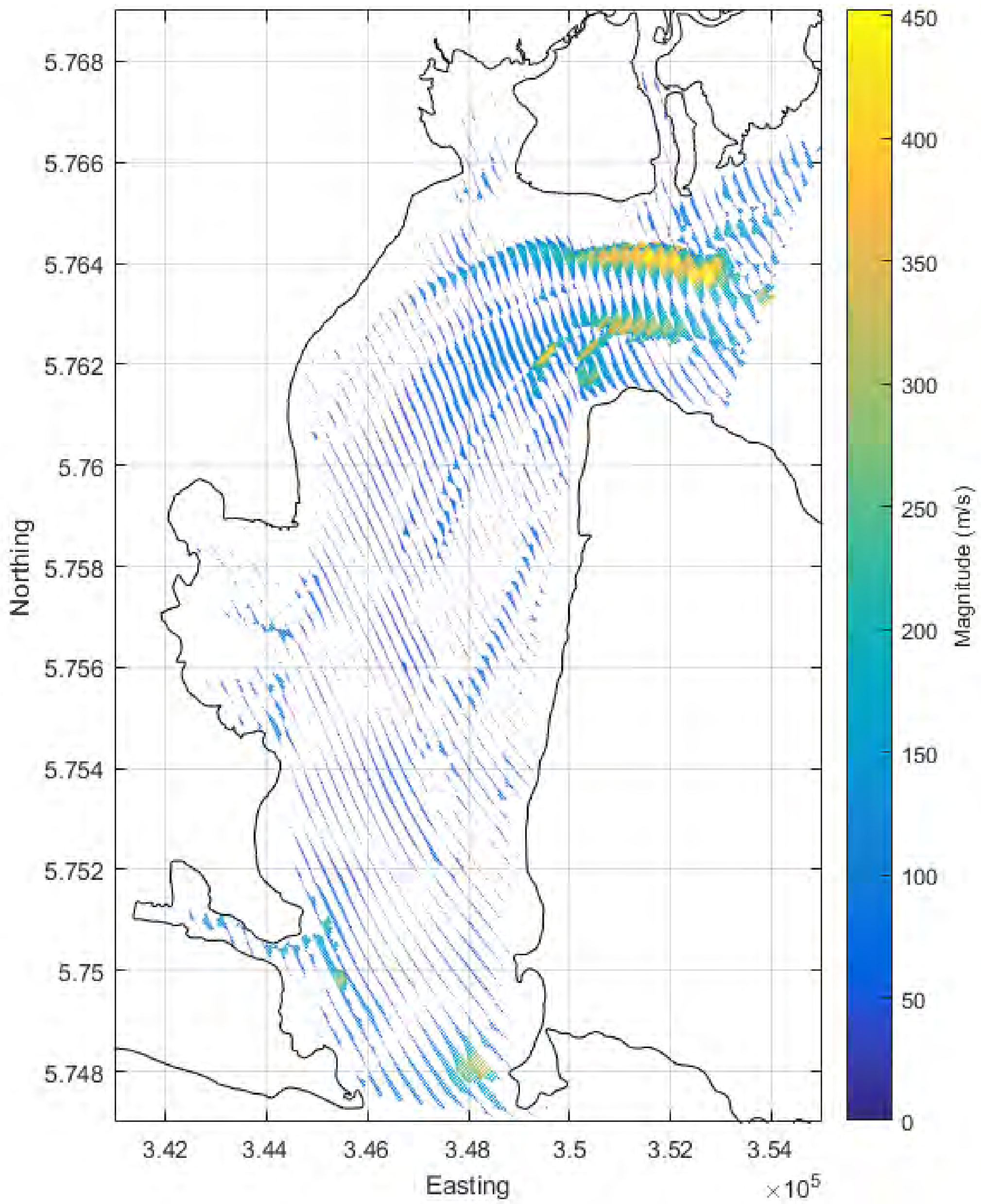

Figure 3-16 Potential sediment transport, averaged current vectors with a threshold magnitude of 0.3 m/s, North Channel

In Figure 3-16, the averaged current vectors are plotted as arrows away from the grid lines, although the detail of each arrow cannot be seen. The plot demonstrates the spatial variability in the tidal currents. For example in the channel to the north east of the port site, at the north western corner of French Island, there is an eastwards potential sediment transport on the northern side of the channel and a westwards transport on the southern side.

When the differences in potential sediment transport between the developed and existing cases are examined, the changes are confined to the immediate vicinity of the port development. This is shown in Figure 3-17. The changes are generally small, but largest in and around the dredged berth and swing basin near the port. More detailed analysis would be required to quantify the changes using a full sediment transport model during the design phase of any development such as considered in this study.

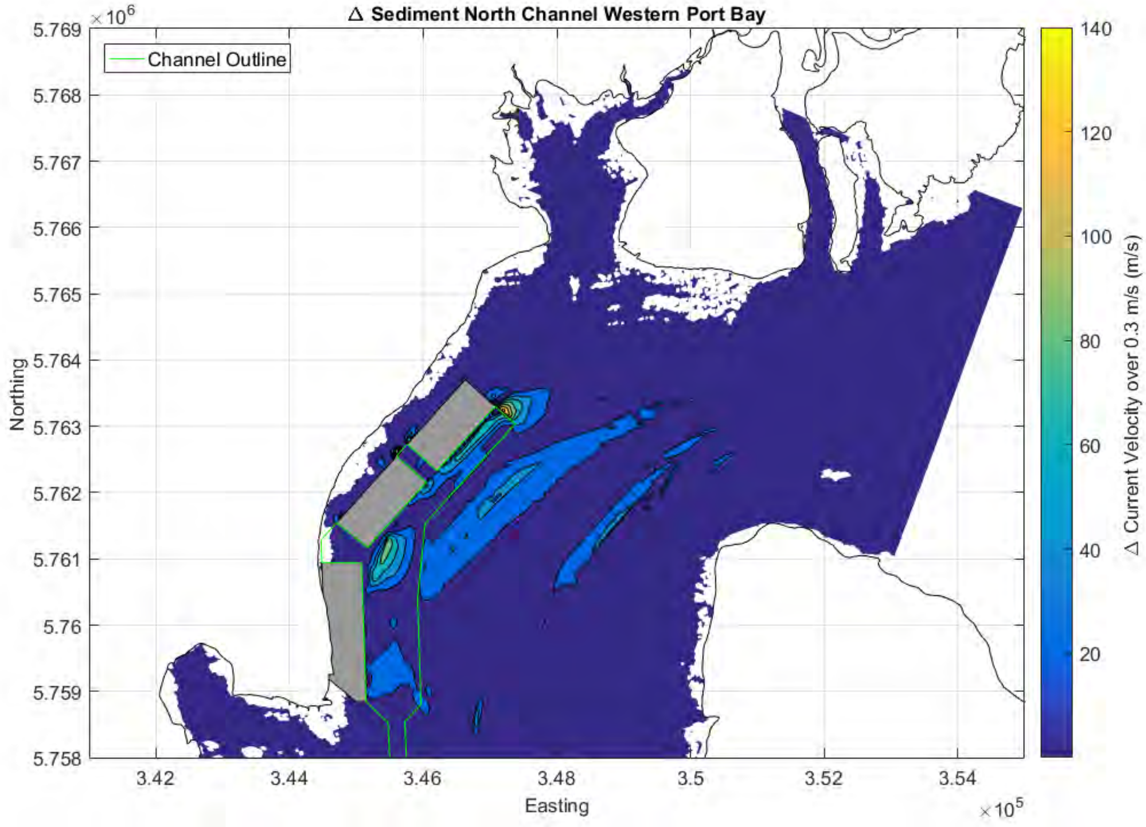

Figure 3-17 Change in potential sediment transport using the averaged current with a threshold of 0.3 m/s for the port area.

4 Conclusions

4.1 Conclusions

This study examined the potential impacts of a new container port and associated channels in Port Phillip Bay at Bay West and in Western Port Bay at Hastings.

4.1.1 Bay West

The Bay West project (see Figure 2-3 and Figure 2-4) was modelled using an existing validated model. The model included the following features of the Project:

> An island at Bay West with dredged channel, turning basin and berth pockets all dredged to -16.5 m CD

> Great Ship Channel widened from 245 m to 425 m at the existing depth of -17.3 m CD;

> South Channel deepened to -17.3 m CD within the existing toe lines;

> Turning area around Hovell Pile deepened to -17.8 m CD within the existing toe lines.

The impacts identified include those due to the dredging to widen the Entrance and deepen South Channel:

> An increase in tidal range in the body of the bay with the 2nd percentile, the level defining the lowest 2% of sea levels, decreasing by 3.7 mm and the 98th percentile, the level defining the highest 2% of sea levels, increasing by 6.3 mm. This is due mainly to the widening of the Great Ship Channel.

> An increase in the peak tidal currents in Port Phillip Heads of up to 10% in the areas where dredging occurs when the channel is widened, but generally much less than this. This is due mainly to the widening of the Great Ship Channel.

> An increase in the current speeds in a relatively small area in the turning area around Hovell Pile where peak speeds increase by up to 15% and speeds two hours after the peak flood also increase, but do not exceed the existing peak current speed. This is due mainly to the deepening of South Channel.

The current speeds in the vicinity of Bay West are low, with tidal currents less than 0.1 m/s; there are some local increases at the ends of the terminal island, but only over a small area and speeds remain below the expected threshold for sediment movement.

Waves in Port Phillip Heads were modelled for slack water, peak ebb and peak flood flow conditions and the impact of the project channel widening investigated.

> At slack water, there are some increases in wave height (1-2%) on the Lonsdale Bight beach due to refraction from the dredged area on Nepean Bank, as well as some increases and decreases in different areas of energy propagating into the south of the bay.

> At peak ebb flow, there is an increase in wave height south of the entrance due to the effects of the increased ebb-tide jet, there is some reduction in wave energy propagating into the south of the bay.

> At peak flood, there are small increases and decreases in difference areas of Lonsdale Bight beach, a reduction in energy propagating into the south of the bay with some localised increases, particularly around Observatory Point and just south of the shipping channel.

Sediment transport due to tidal currents was modelled qualitatively to identify potential changes:

> There is an increase in potential sediment transport towards the north east-in the turning area around Hovell Pile due to the increase in flood currents.

> Near the entrance where there is a potential increase in transport towards the Heads on the south side of the channel and into the bay on the north side.

> In general, the changes in wave energy propagation are small and unlikely to result in significant change to beach processes; however, there may be some local effects.

There is a potential for vessel-generated waves to impact on the beaches in the south east of the bay between Safety Beach and Rye. As larger vessels transit the channel, it may be necessary to reduce the speed-limit in sections of the channel to minimise the likelihood of the generation of large waves.

There is the potential for the currents generated by large vessels in the Yarra River to become an issue for moored vessels along the river.

4.1.2 Hastings

The development of a container port in Western Port, Port of Hastings, as shown in Figure 3-2, requires;

Construction of a land backed berth with extension to the north east.

Dredging of new berths and swing basin, the swing basin with depths -16.2 m CD and the berth pockets -16.5 m CD.

Deepening existing channels with some minor re-aligning to facilitate access for larger vessels; the seaward section of the Western Channel would have a declared depth of -17.5 m CD, the remaining sections to Stony Point a declared depth of -17.0 m CD, the North Arm southern section would be -16.3 m CD, the northern section -16.2 m CD.

The impacts of the development were modelled using an existing model.

- The greatest change in tide levels is at Tooradin where there is an increase in tidal range; the 2nd percentile, the level defining the lowest 2% of sea levels, will decrease by 14.5 mm and the 98th percentile, the level defining the highest 2% of sea levels will increase by 15.9 mm.
- At Stony Point the corresponding levels change by about 6 mm decrease and increase respectively.
- There is no change at Corinella.
- Tidal current speeds do not change apart from immediately adjacent to the new berth extension where there are local increases, especially in the gaps in the terminal reclamation.
- The tidal divide north east of French Island migrates an average of 32 m to the south east, but with a variability over the month of simulation of from 0 to 62 m.

No wave modelling was undertaken as there is minimal dredging south of Sandy Point and thus no impact on swell propagation from Bass Strait

Qualitative modelling of changes in sediment transport indicated changes in the vicinity of the port area, particularly on the edge of the dredged area and immediately adjacent to the terminal reclamation.

4.2 Impact of climate change

The major predicted consequence of climate change on the developments considered will be sea-level rise. No new modelling has been carried out for this study, however the effects were investigated in Cardno Lawson Treloar (2007a). It was shown that the impact of the Channel Deepening Project was the same, within calculation limits, for a mean sea-level rise of 0.3 m or 0.5 m as with no rise. If sea level rose further, the impact of the project reduces as the proportionate change in water depth due to dredging decreases. A similar effect would occur for both the Bay West Project and Port of Hastings Project. A relatively small increase in sea level would cause no change in the impact of the project with a larger increase in sea level resulting in a reduction in the magnitude of the impact due to the project.

5 References

AECOM, (2016). Infrastructure Victoria Second Container Port Advice, Navigation Study. Report prepared for Infrastructure Victoria by AECOM Australia Pty Ltd, ref 60521932.

Bird, E. (2011). Changes on the Coastline of Port Phillip Bay. Report by Eric Bird for the Office of the Environmental Monitor, Victorian Government Department of Sustainability and Environment

BoM (2016). Monthly Data Report – October 2016. Australian Baseline Sea Level Monitoring Array. Australian Bureau of Meteorology. http://www.bom.gov.au/ntc/IDO60201/IDO60201.201610.pdf

Cardno Lawson Treloar (2007a). Hydrodynamic and Coastal Processes, Head Technical Report. Report prepared for Maunsell Australia Pty Ltd on behalf of the Port of Melbourne Corporation, Report RM2124, ver 1.2. Technical Appendix 45 of the PoMC Supplementary Environment Effects Statement of the Channel Deepening Project

Cardno Lawson Treloar (2007b). Hydrodynamic and Wave Model Calibration and Validation. Report prepared for Maunsell Australia Pty Ltd on behalf of the Port of Melbourne Corporation, Report RM2127, ver 1.1. Technical Appendix 44 of the PoMC Supplementary Environment Effects Statement of the Channel Deepening Project

Cardno (2011). The Great Sands and Adjacent Coast and Beaches. Report prepared from Port of Melbourne Corporation, report RM2289_LJ5518, ver 1.0

Cardno (2013). Port of Hastings 2013 Description Report – Hydrodynamics. Port of Hastings Development Project Preliminary Base Case Phase. Report NA49913530, R04 Final ver1.0 prepared for the Port of Hastings Development Authority by Cardno Victoria Pty Ltd.

Cardno (2015). Port Phillip Bay Sea Level. Report prepared for the Association of Bayside Municipalities under the Port Phillip Bay Managing Better Now project. Cardno report 59914543_R01

Fugro (2010). Report of survey 2009-10 Western Port bathymetry project Contract number: PO 424675.Report by Fugro LADS Corporation Pty Ltd for Victorian Department of Sustainability and Environment (DSE). Document Reference No: TLCS00.026.001

Geoscience Australia (2009). *Australian Bathymetry and Topography Grid,* 2 DVD set.

GHD, (2017). Infrastructure Victoria Second Container Port Advice, Concept Options - Bay West and Hastings. Report prepared for Infrastructure Victoria by GHD Pty Ltd, ref 255163.

Gourlay T. (2001). The supercritical bore produced by a high-speed ship in a channel. J. Fluid Mech. 434, 399-409

Haskoning, (2014). Early Hydrodynamic Modelling for Port of Hastings Development Project. Report HAS-CEP0-HY-REP-0012-C Final Draft (Issue C) prepared for the Port of Hastings Development Authority by Haskoning Australia Pty Ltd

Marsden, M.A.H., Mallett, C.W. & Donaldson, A.K. (1979). Geological and Physical Setting, Sediments and Environments, Western Port, Victoria. Marine Geology, 30:11-46.Marsden, M.A.H. & Mallett, C.W., (1974). Morphology and sediment distribution, Western Bay. Prepared for the Westernport Bay Environmental Study.

Melbourne Water (2011). Understanding the Western Port Environment – A summary of current knowledge and priorities for future research.

Ris , R.C., Booij, N. and Holthuijse4n, (1999). A third-generation wave model for coastal regions, Part II: verification. J Geophys. Research, 104, C4, 7667-7681.

Hydrodynamics
Infrastructure Victoria
Second Container Port Advice

APPENDIX
A

Port Phillip Model Validation

Cardno
Shaping the Future

Port Phillip Heads – Model Validation

Port Phillip Heads Current Modelling

59916502

Prepared for
Port of Melbourne Corporation

April 2016   Abridged February 2017

Cardno
Shaping the Future

Contact Information

Cardno Victoria Pty Ltd
ABN 47 106 610 913

Level 4 , 501 Swanston Street
Melbourne, VIC 3000

Telephone: (03) 8415 7777
Facsimile: (03) 8415 7788
International: +61 3 8415 7777

www.cardno.com.au

Author(s): David Provis
Senior Principal,
Oceanography

Approved By: Phebe Bicknell
Experienced Engineer

Document Information

Prepared for	Port of Melbourne Corporation
Project Name	Port Phillip Heads Current Modelling
File Reference	59917507_R1_AppA.docm
Job Reference	59916502
Date	23 February 2017
Version Number	Rev 0.1
Effective Date	23 February 2017
Date Approved:	23 February 2017

Document History

Version	Effective Date	Description of Revision	Prepared by:	Reviewed by:
Rev A	11/01/2016	Working Draft	DGP / PJB	
Rev B	19/02/2016	Draft for PoMC	DGP / PJB	
Rev 0	06/04/2016	Update figures, include PoMC comments	DGP / PJB	MH
Rev 0.1	16/2/2017	Abridged to remove commercially sensitive material	DGP	

Executive Summary

The Port of Melbourne Corporation (PoMC) requires updated information on the speed and direction of currents in Port Phillip Heads to assist in the safe navigation of commercial vessels through the entrance to Port Phillip from Bass Strait. Cardno has been commissioned to generate the required information including any additional data collection required for validation of the outputs.

This report describes the setup of the numerical model, the results of the measurements undertaken for this project and the resulting validation of the numerical model with the measured data.

The numerical model of the hydrodynamics of Port Phillip Heads has been validated against measured data, including spatial measurements of currents. The validation demonstrates that the model's performance is "fit for purpose" for predicting the tidal streams in Port Phillip Heads.

There are some small systematic differences between the model results and the measured data and these need to be taken into consideration with small "calibration factors" included if required to maximise the agreement between the outputs and measured data.

Table of Contents

Appendices

Tables

Figures

1 Introduction

1.1 General

The Port of Melbourne Corporation (PoMC) requires updated information on the speed and direction of currents in Port Phillip Heads to assist in the safe navigation of commercial vessels through the entrance to Port Phillip from Bass Strait. Cardno has been commissioned to generate the required information including any additional data collection required for validation of the outputs.

This report describes the setup of the numerical model, the results of the measurements undertaken for this project and the resulting validation of the numerical model with the measured data.

1.2 Scope of work

The scope of work for the project, as defined in PoMC Contract C3732, including Cardno's response to Request for tender RFT 448:

1. Analysis of existing data and modelling, including analysis of existing measurements and re-establishment and calibration of an existing numerical model.
2. Additional data, in particular measurements of currents using an Acoustic Doppler Current Profiler from a vessel steaming along transects in Port Phillip Heads.

1.3 Qualifications

The model and measurements described in this report have been developed in response to a specific request. The model and measured data should not be used for other purposes without confirmation by Cardno of their suitability.

2 Background

2.1 Analysis of existing data and modelling.

There are significant existing measurements from a number of locations along the centreline of the great Ship Channel which provide a sound basis for this project. These data will be used to re-calibrate and validate an existing numerical model of the hydrodynamics of the south of Port Phillip and adjacent waters of Bass Strait.

2.2 Additional data

Additional data will be required to expand the spatial coverage of the current measurements and thus extend the model validation beyond the sites of the fixed measurement locations. These data will be gathered using Acoustic Doppler Current Profiling (ADCP) from a moving vessel in conjunction with accurate positioning of the survey vessel. The aim is to undertake a number of transects and thus measure the currents along these transects to define the spatial variability of the currents.

Each transect (measurements along a straight-line segment) will be analysed and the vessel position compared with the ADCP bottom track to allow accurate correction for the vessel effect on the instrument compass. The currents along each transect can then be compared with model output for the same location and time by using measured tide-gauge data to drive the model. By undertaking transects in sensitive areas, such as across the tidal jet and through eddy structures, this process allows validation of the model and demonstrated performance. This results in user confidence in the final product.

The outcome of items 2.1 and 2.2 will be a numerical model which can be used with confidence to generate values for the current speed and direction across the Entrance and the south of Port Phillip.

3 Model

3.1 Modelling system

The numerical model which calculates the hydrodynamics of Port Phillip, including the entrance and adjacent waters of Bass Strait, is a development of that used for the CDP and described in Cardno Lawson Treloar (2007). The model calculates the water level and current speed and direction over the model domain which is shown in Figure 3-1. A curvilinear grid with variable grid size is used in the horizontal and five layers are used in the vertical, each of a fixed thickness of 20 m vertically starting from 2 m above mean sea level, taken as 0.0 m AHD. (This is termed a “z-layer” modelling system).

The model uses the FLOW module of the Delft3D modelling system developed by Deltares of The Netherlands.

3.2 Model inputs

3.2.1 Bathymetry

The bathymetry used in the model is primarily derived from data provided by PoMC for modelling after the completion of dredging for the CDP (Cardno, 2011a, b). These data included survey from LADs and multibeam echo-soundings as well as historical survey data from the body of the bay. For offshore areas, not covered by PoMC surveys, the bathymetry was derived from the Australian Bathymetry and Topography Grid, Geoscience Australia (2009) which has a resolution of 9 arc seconds. (~ 250 m at the equator).

The model extent and bathymetry is shown in Figure 3-1.

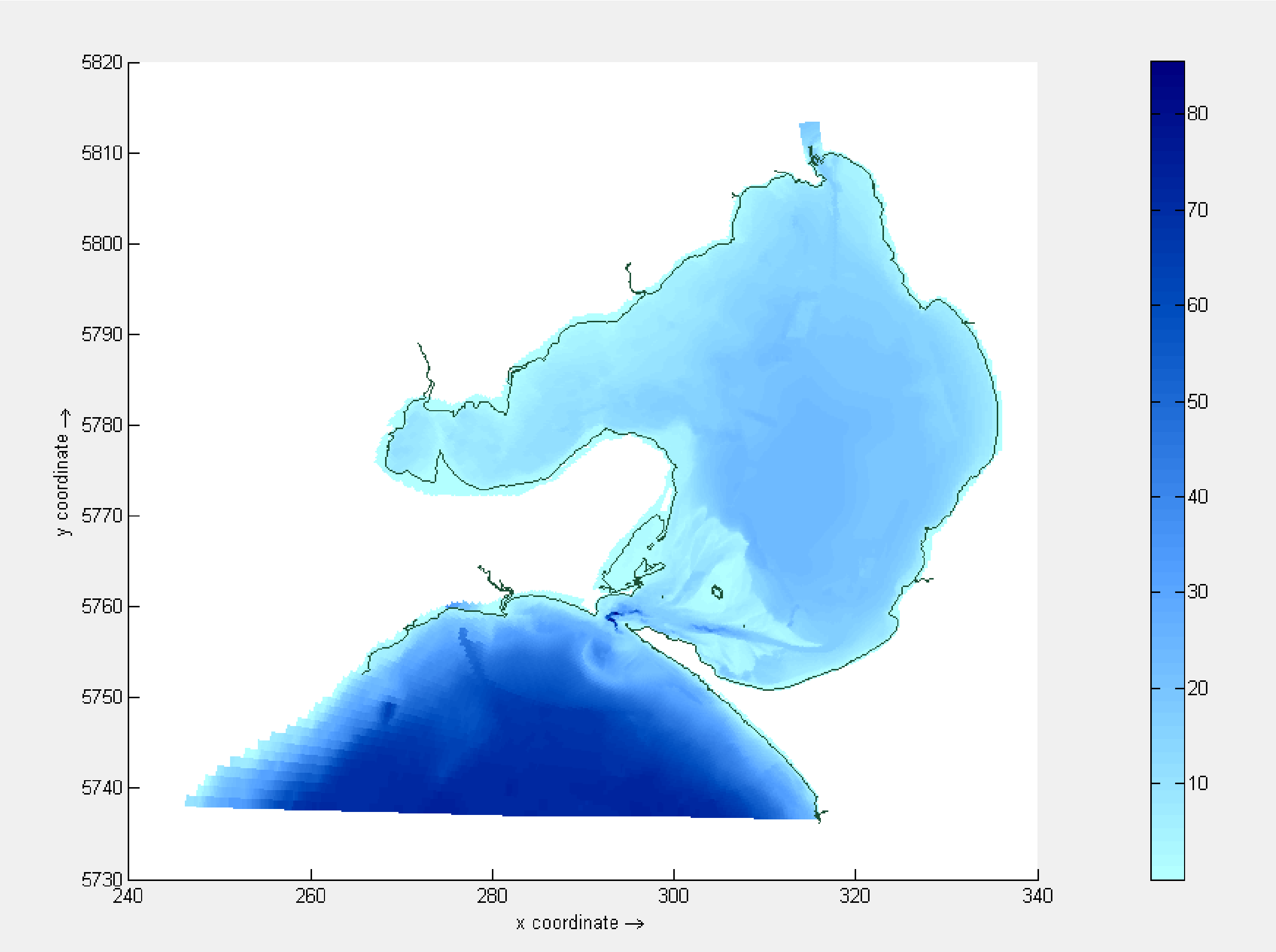

Figure 3-1 Model domain and bathymetry (in metres below 0.0 AHD)

3.2.2 Parameters

There are a number of model parameters used in establishing the model

3.2.2.1 Grid resolution

The model uses a curvilinear grid and is three-dimensional with 5 layers in the vertical. The layers are "z-layers", that is, they are of fixed thickness. The layers are each 20 m thick with the top layer starting at 2 m above mean sea level, taken to be 0.0 m AHD. In this way, all the vertical motion of the tides is contained within the top layer which extends to either the sea bed or -18 m AHD, whichever is deeper. The currents required for the tidal streams are then taken as those from this top layer which represent the depth-averaged currents in this layer and for much of Port Phillip this includes the total depth. In areas where the water is deeper than -18 m AHD, the model allows the vertical structure of the currents to develop. Thus in the Entrance Deep, the model allows for the currents to flow in different directions in the different layers, as is known to occur in the field.

The model grid resolution in Port Phillip Heads is approximately 100 m and is shown in Figure 3-2.

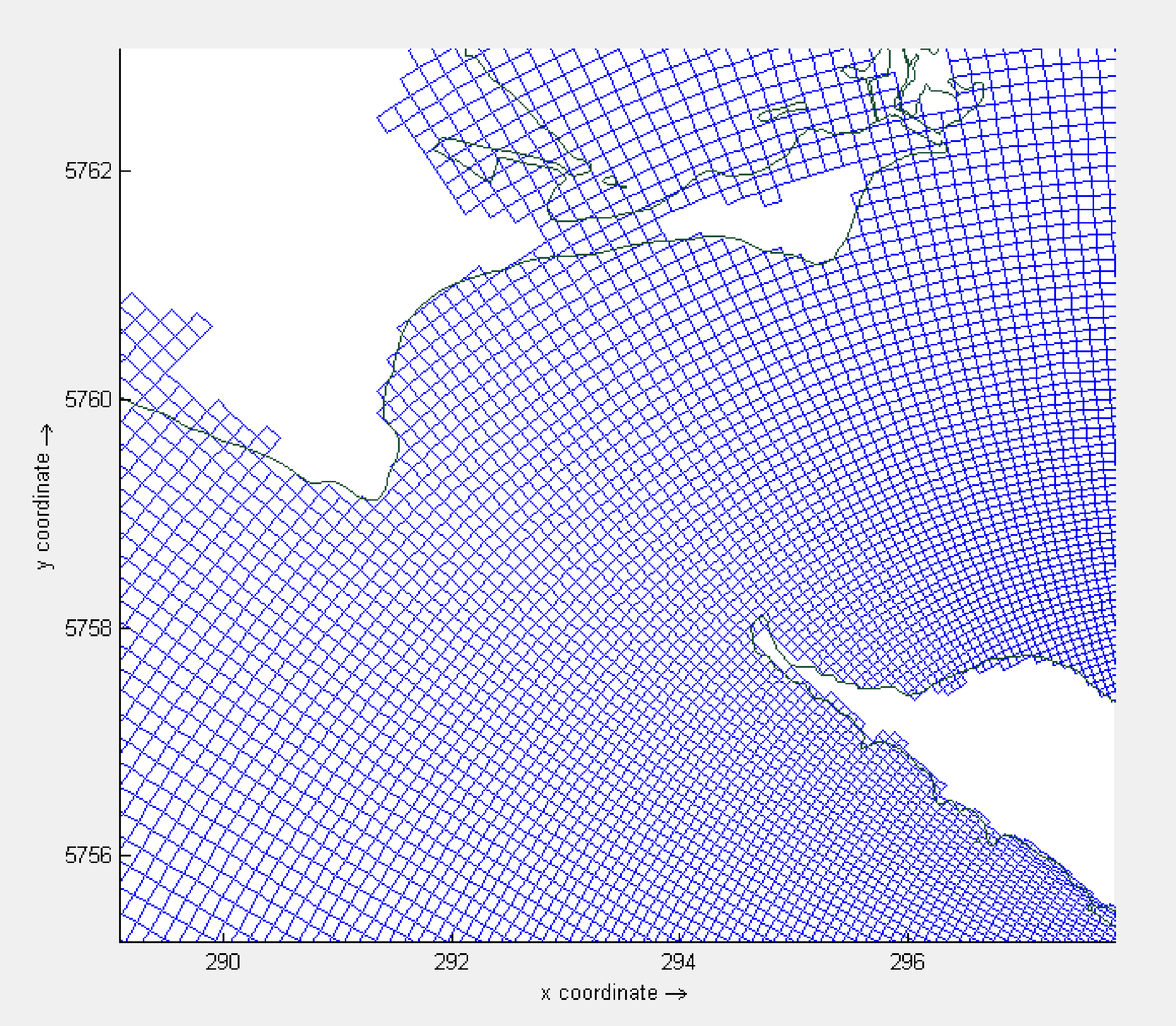

Figure 3-2 Model grid in Port Phillip Heads, including the land boundary

3.2.2.2 Time step

The model uses a time step of 1 minute

3.2.2.3 Bottom friction

Bottom friction is specified as a Mannings “n” coefficient and follows the approach of Cardno Lawson Treloar (2007). The values used in the Heads are shown in Figure 3-3.

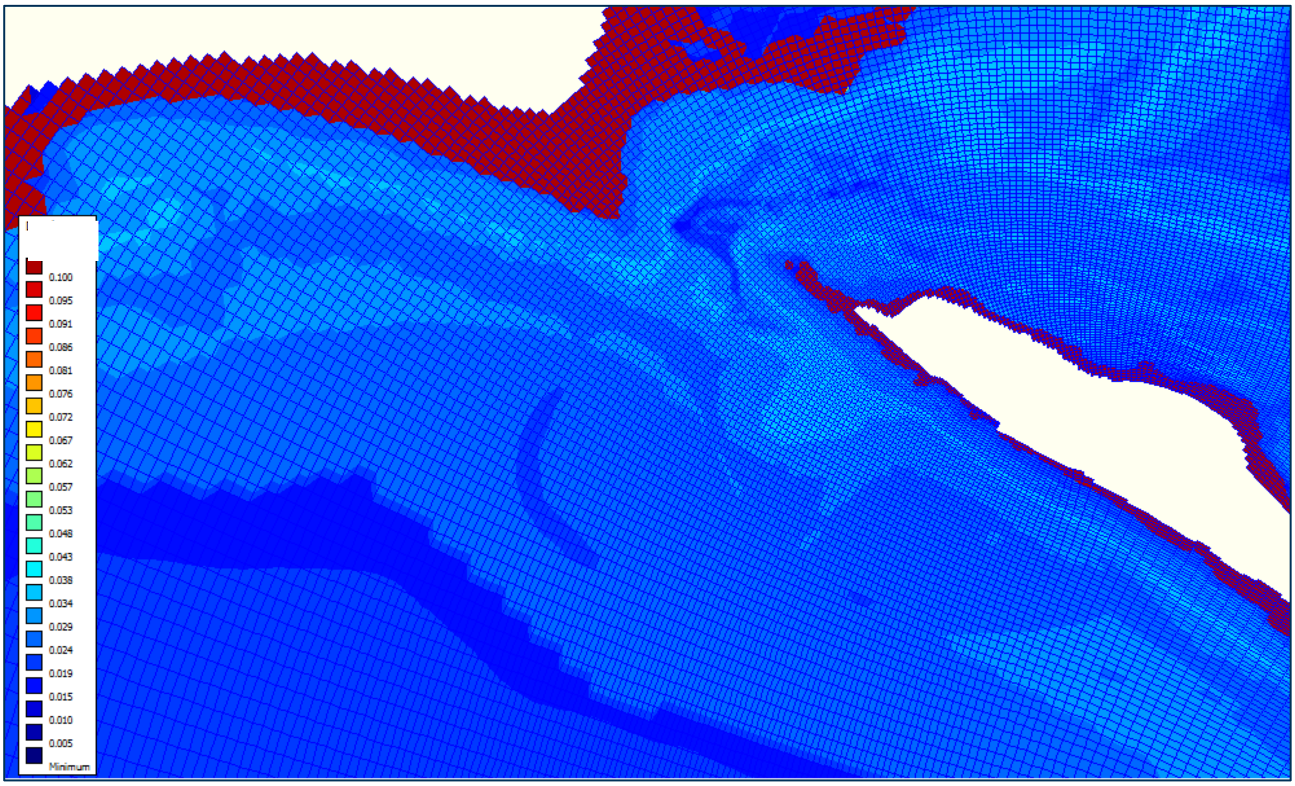

Figure 3-3 Bottom friction in the Heads specified as Mannings “n”.

3.2.2.4 Eddy viscosity and mixing

Horizontal eddy viscosity is set using a background eddy viscosity of 1 m^2/s with sub-grid scale turbulence computed by the model’s built-in Horizontal Large Eddy Simulator. Three dimensional turbulence is computed using a k-epsilon scheme.

3.2.3 Boundary conditions

The model has an open boundary in Bass Strait running east from Lorne to the coast just north of Cape Schanck. The model is driven by prescribing the water level along this boundary. At the western end, sea levels at Lorne are specified and at the eastern end the levels at Lorne are used with a time lag and an increase in amplitude to account for the propagation of the tide into Bass Strait. The sea level at Lorne can be the predicted tide derived from harmonic constituents or measured data. All the runs reported in this report use measured sea level from Lorne at 6 minute intervals with some smoothing. The advantage of using these data is that non-tidal variations in sea level due to meteorological effects are captured and this allows comparison with measured sea-levels from sites within the model domain to be used for comparison and validation of model performance.

4 Measurements

4.1 Time series

4.1.1 Sea level

Measurements of sea level are available from a number of sites and the sources used in this study are shown in Table 4-1.

Table 4-1 Sources of sea-level data used in this investigation

Location	Instrument	Data available
Lorne	Tide gauge	6 minute values of sea level relative to Chart Datum
Offshore Bank	Bottom-mounted ADCP	Hourly values of sea level derived from pressure, relative to mean over the record
Rip Bank Outer	Bottom-mounted AWAC	Hourly values of sea level derived from pressure, relative to mean over the record
Rip Bank Centreline	Bottom-mounted AWAC	Hourly values of sea level derived from pressure, relative to mean over the record
Nepean Bank	Bottom-mounted AWAC	Hourly values of sea level derived from pressure, relative to mean over the record
Queenscliff	Tide gauge	6 minute values of sea level relative to Chart Datum
Hovell Pile	Tide gauge	6 minute values of sea level relative to Chart Datum

The locations of the bottom-mounted instruments are shown in Figure 4-1

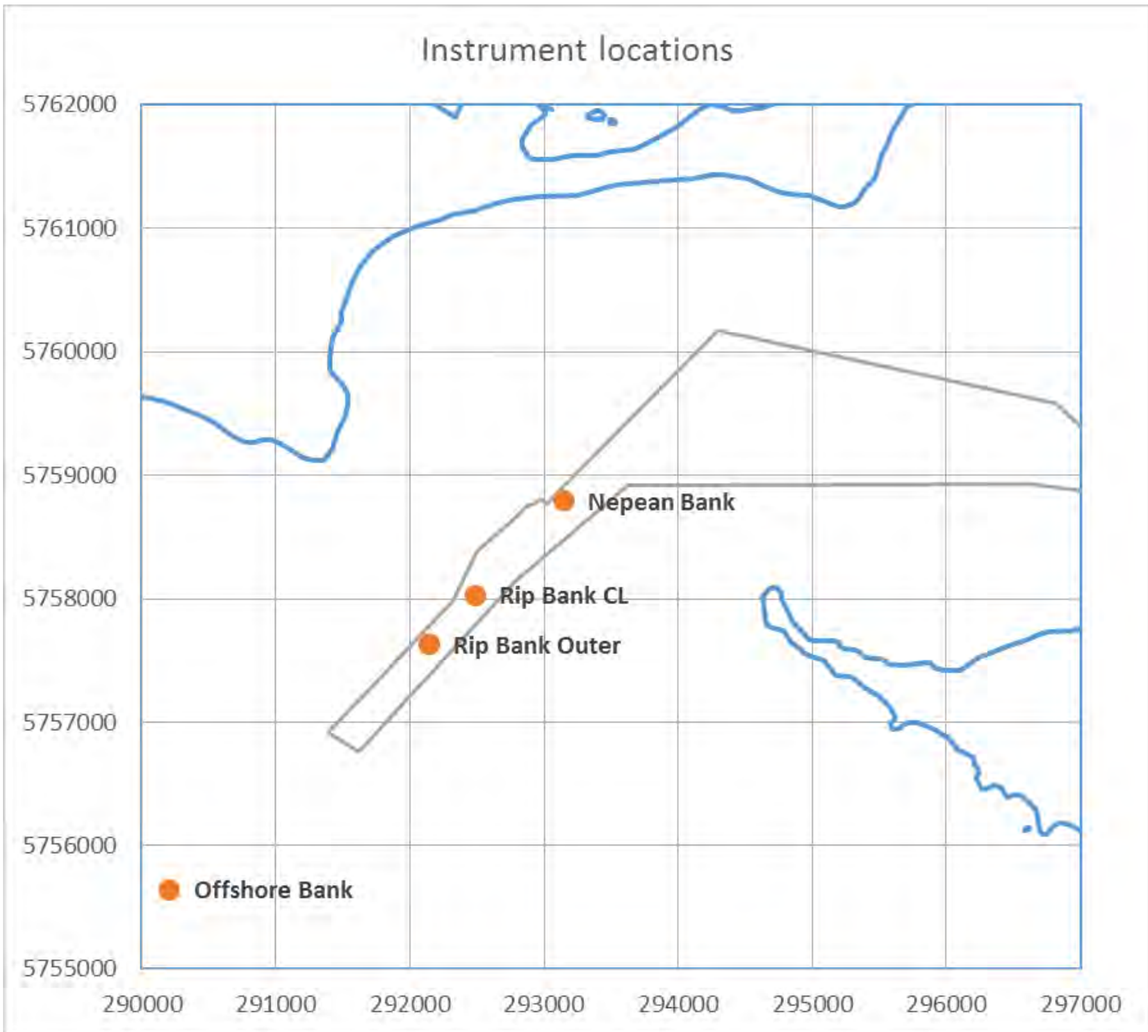

Figure 4-1 Location of bottom-mounted instrument measurements including the outline of the shipping channel

4.1.2 Currents

Current measurements are available from the bottom-mounted instruments listed in Table 4-1. These consist of hourly values taken as providing depth-averaged currents at each of the sites.

4.2 Spatial variability of currents

In order to expand the spatial coverage of the current measurements and thus extend the model validation beyond the sites of the fixed measurement locations, current measurements were undertaken from a moving vessel along transects in and around Port Phillip Heads. This data was gathered using an Acoustic Doppler Current Profiler mounted on a survey vessel in conjunction with accurate positioning of the vessel. The aim was to undertake a number of transects and thus measure the currents along these transects to define the spatial variability of the currents.

A summary of the field work is contained in a memorandum included in Appendix A

5 Validation

5.1 Time series

5.1.1 Model skill

The performance of the model has been assessed using the measure of model skill derived by Wilmott et al. (1984) where the model skill is defined by:

$$ModelSkill = 1 - \frac{\sum \left[X_{model} - X_{observed}\right]^2}{\sum \left(\left[X_{model} - \overline{X}_{observed}\right] + \left[X_{observed} - \overline{X}_{observed}\right]\right)^2}$$

With this definition, the model skill is 1 for perfect agreement and 0 for no agreement.

5.1.2 Sea level

Comparisons of measured and modelled sea levels are shown in Figure 5-1 and Figure 5-2

For the data in Figure 5-1, the model skill scores are shown in Table 5-1.

Table 5-1 Model skill for sea-level data shown in Figure 5-1 and Figure 5-2

Location	Model skill
Offshore Bank	0.98
Rip Bank Outer	0.98
Rip Bank Centre Line	0.98
Nepean Bank	0.75
Queenscliff	0.99
Hovell Pile	0.98

The scores for the three more offshore sites indicates excellent agreement, as can be seen in the figures. The lower skill score at Nepean Bank is reflected in the plotted data and indicates the sensitivity of the model skill parameter

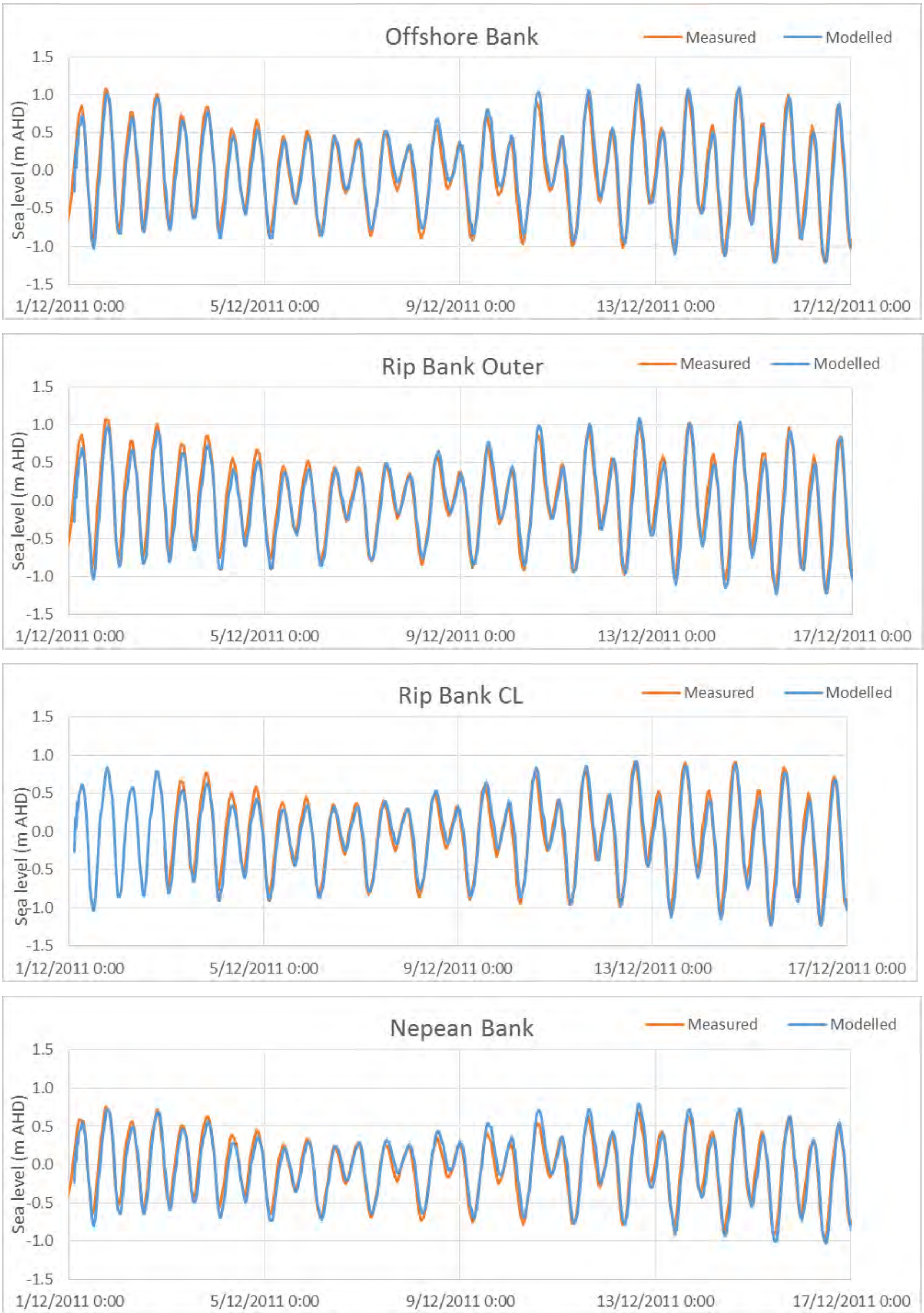

Figure 5-1 Comparison of modelled data with sea level from bottom-mounted instruments

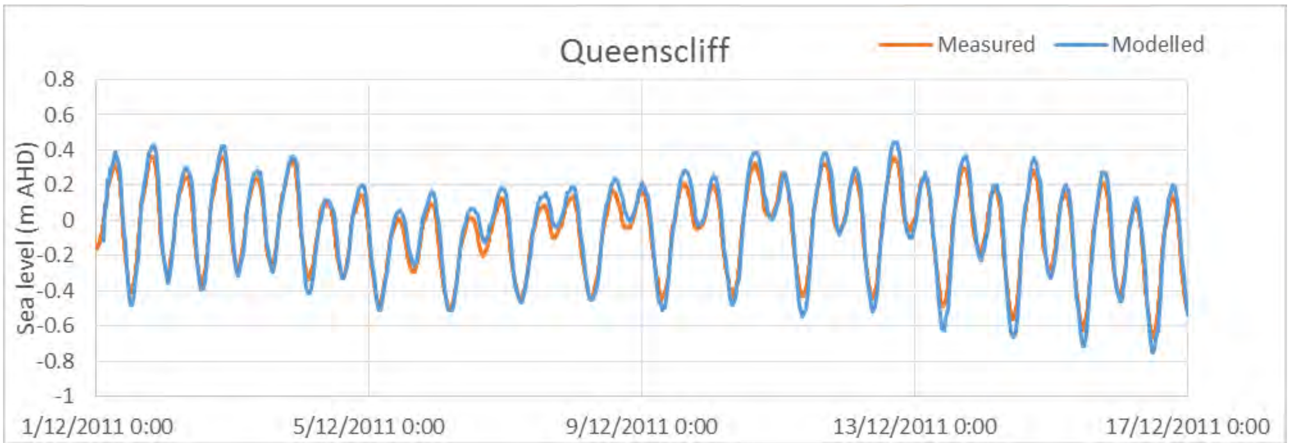

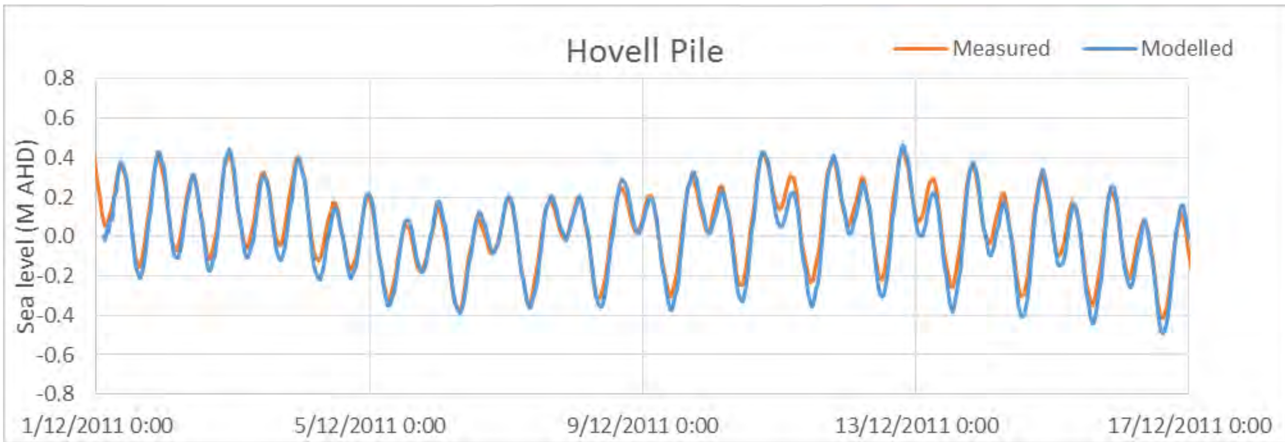

Figure 5-2 Comparison of modelled data with sea level from tide gauges

5.1.3 Currents

Comparison of modelled and measured currents are shown for Offshore Bank in Figure 5-3, for Rip Bank Outer in Figure 5-4, Rip Bank Centre Line in Figure 5-5 and Nepean Bank in Figure 5-6.

The results for the model skill using the data shown in the figures are shown in Table 5-2.

Table 5-2 Model skill for data shown in the figures, based on east and north components of currents

Location	East component	North component
Offshore Bank	0.95	0.86
Rip Bank Outer	0.98	0.98
Rip Bank Centre Line	0.99	0.99
Nepean Bank	0.96	0.98

The model skill shows excellent performance at the sites in the Heads with satisfactory performance at the Offshore Bank where very complex current patterns are found due to the interaction of eddies from the ebb-tide flow. This complex structure can be seen in Figure 5-3. For the other sites, the figures demonstrate the excellent model performance with very good reproduction of both current speed and direction

In Figure 5-7, the current speed is plotted with flood flows as positive, ebb flows as negative to give a continuous tidal variation. This format highlights the complexity of the tidal flow at Offshore Bank, a slight under prediction by the model of current speeds at Rip Bank Outer, a slight under prediction by the model of the ebb tide at Rip Bank Centre Line and an over prediction of the flood and under prediction of the ebb at Nepean Bank.

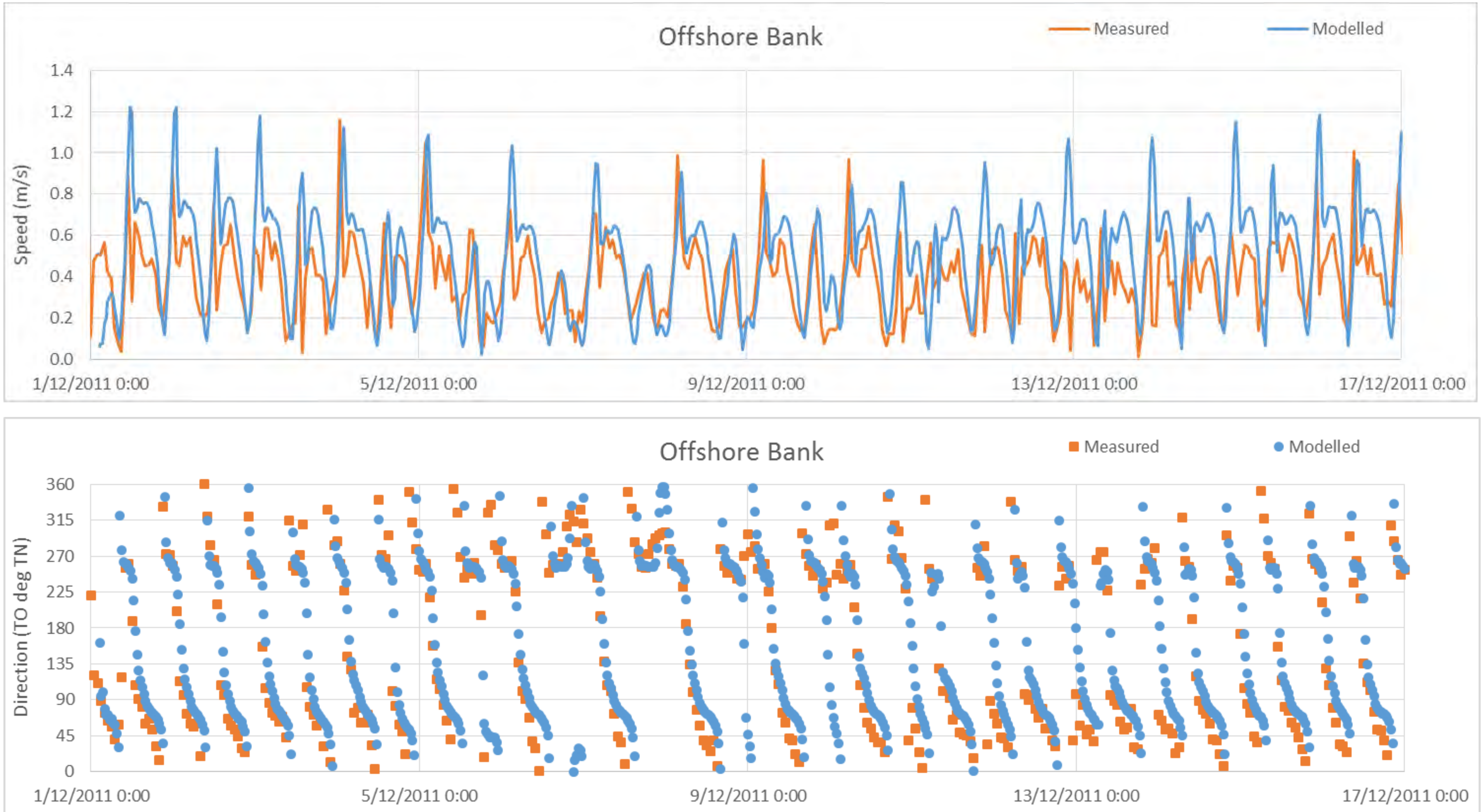

Figure 5-3 Comparison of modelled and measured current speed (upper panel) and direction (lower panel) from the Offshore Bank site

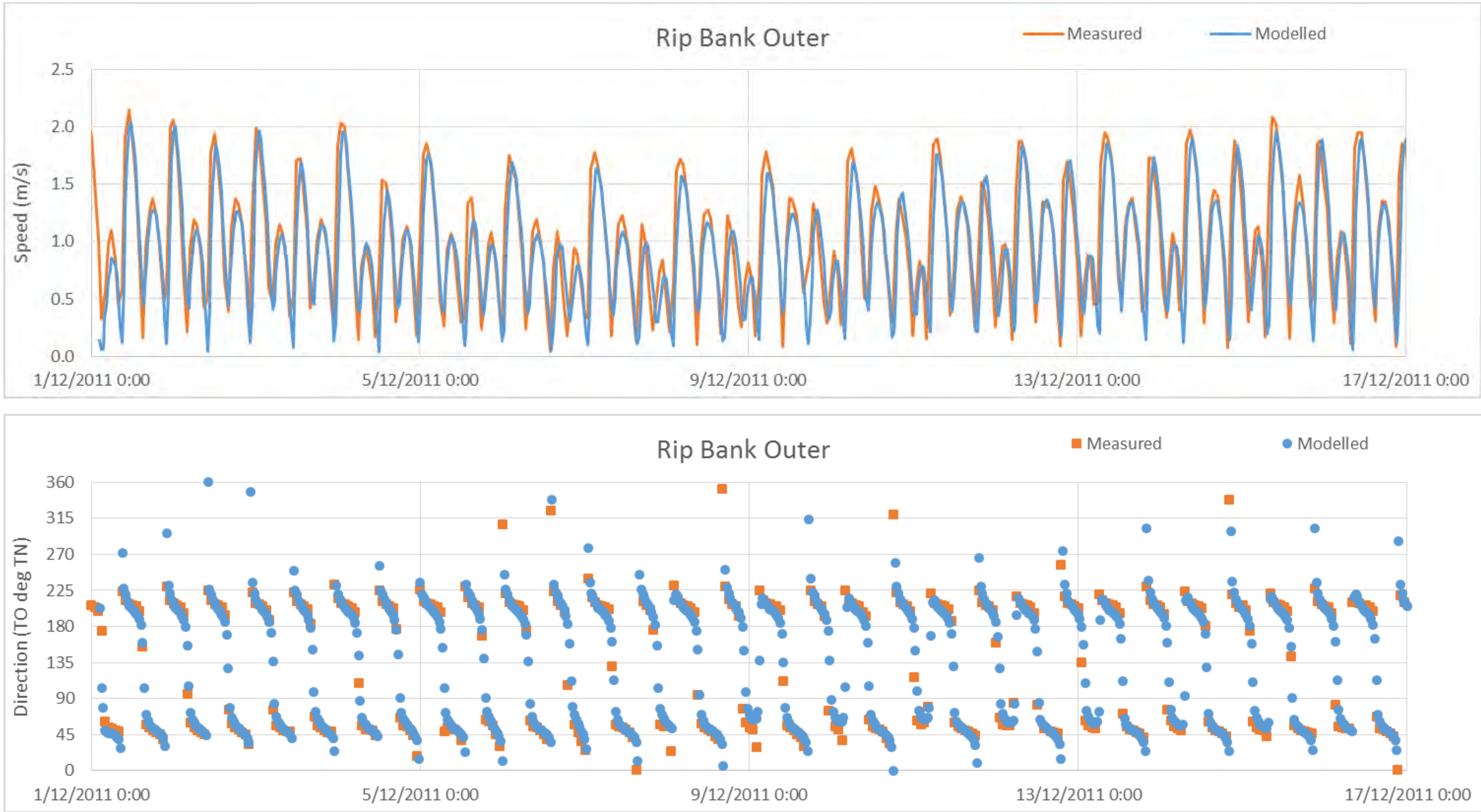

Figure 5-4 Comparison of modelled and measured current speed (upper panel) and direction (lower panel) from the Rip Bank Outer site

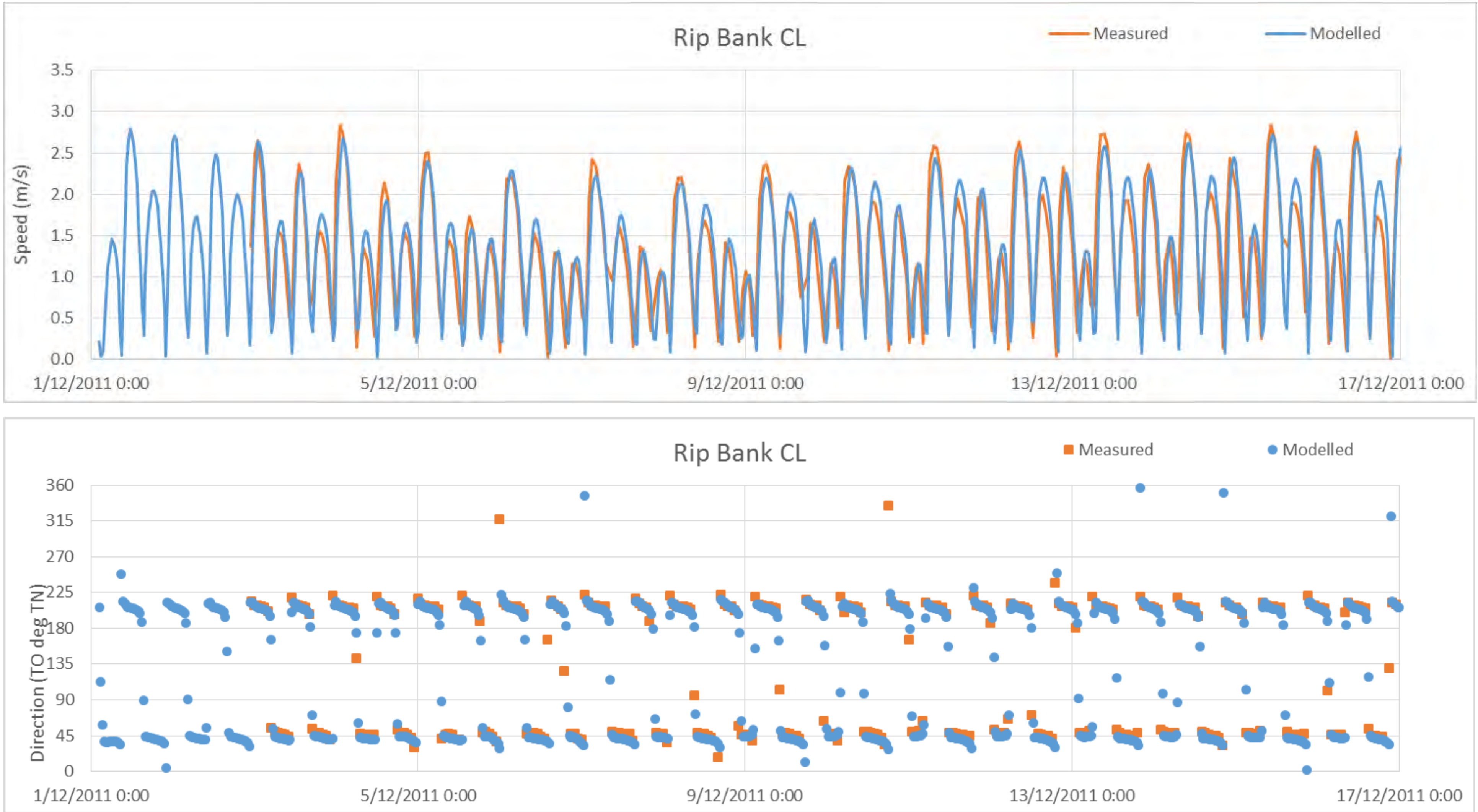

Figure 5-5 Comparison of modelled and measured current speed (upper panel) and direction (lower panel) from the Rip Bank Centre Line site

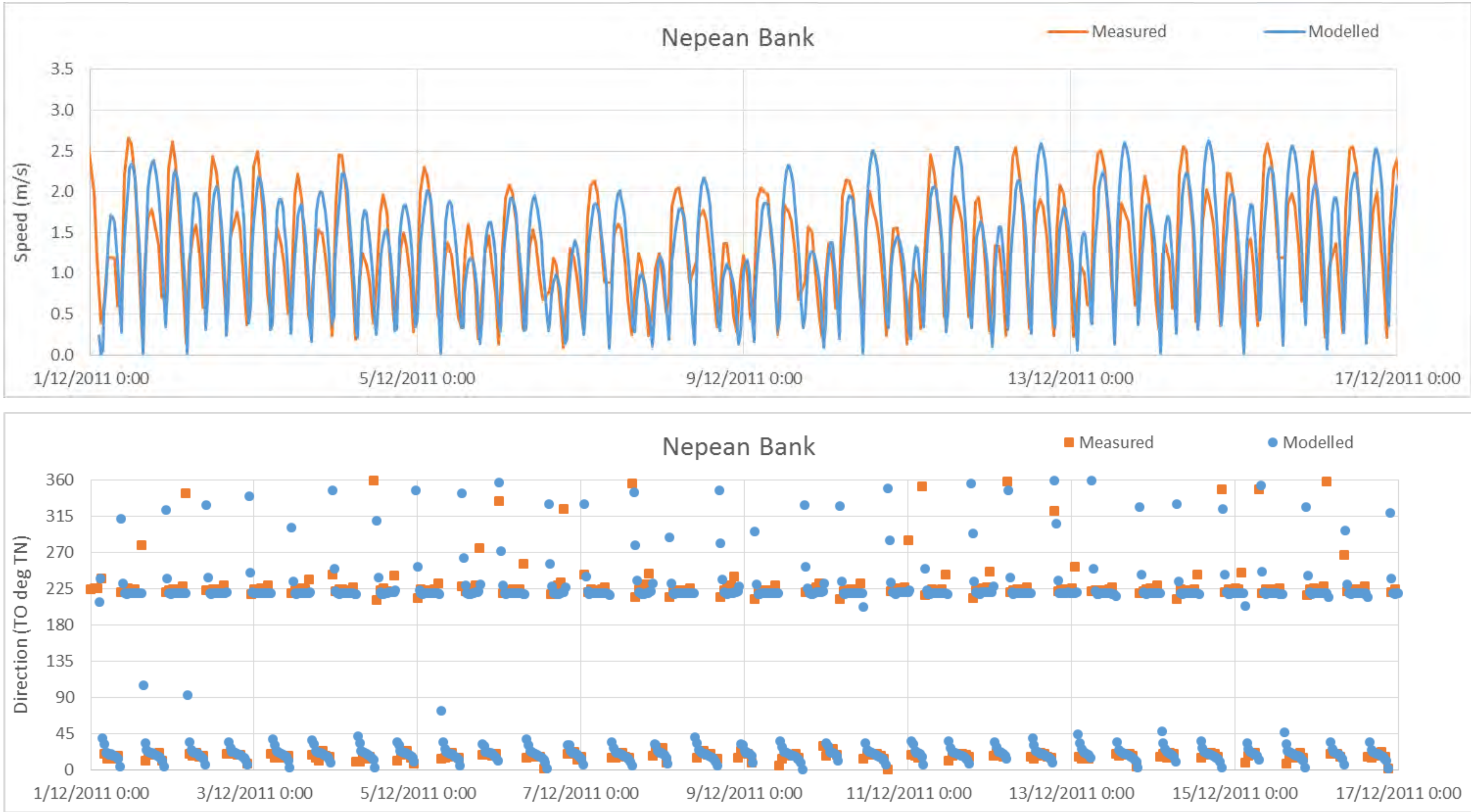

Figure 5-6 Comparison of modelled and measured current speed (upper panel) and direction (lower panel) from the Nepean Bank site

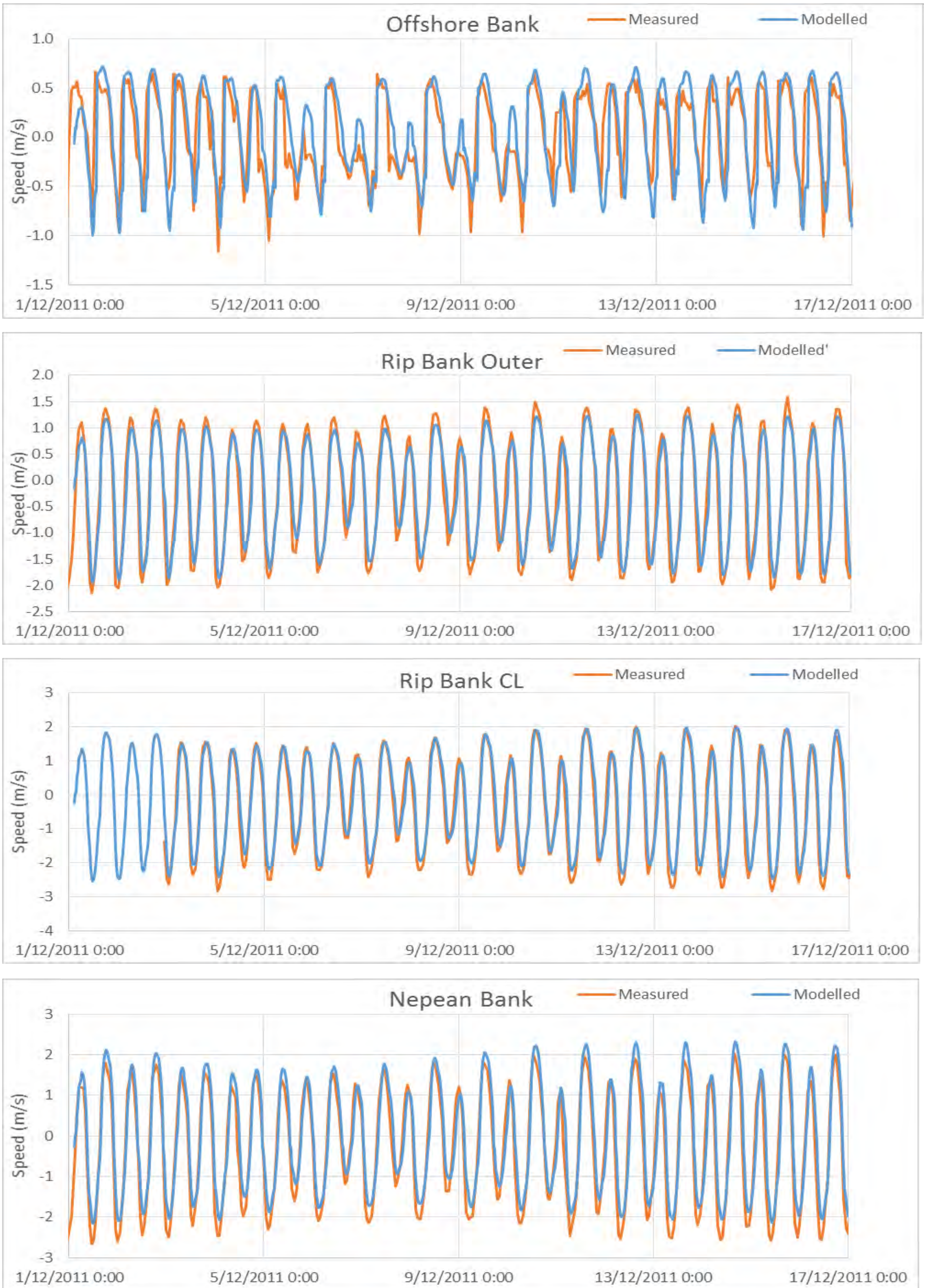

Figure 5-7 Comparison of measured and modelled current speed plotted as flood positive, ebb negative

Overall, the performance of the model is excellent when compared to the measured data available. The model is considered “fit for purpose”.

5.2 Spatial variability

The ability of the modelled results to represent the spatial distribution of currents was assessed by comparing measured currents from the ADCP transects with modelled results for the same period. The model was run using the measured sea-levels from Lorne as described in Section 3.2.3.

The measured current data were averaged to produce depth averages over the top 20 m of the water column, or the available depth when less than this. The data were also averaged temporally to reduce the number of readings and smooth the results to account for instrument noise due to vessel motion and small scale variability. This also produced results at a comparable spatial resolution to that of the numerical model. The model results for the time closest to the midpoint of each transect were then plotted as a vector field and the ADCP transect vectors overlaid. The measured speed and direction at points along each transect were also compared with the modelled speed and direction interpolated to the same points. The results for all transects are included in Appendix B. Some examples of the ebb and flood tide transects are shown in Figure 5-8 and Figure 5-9.

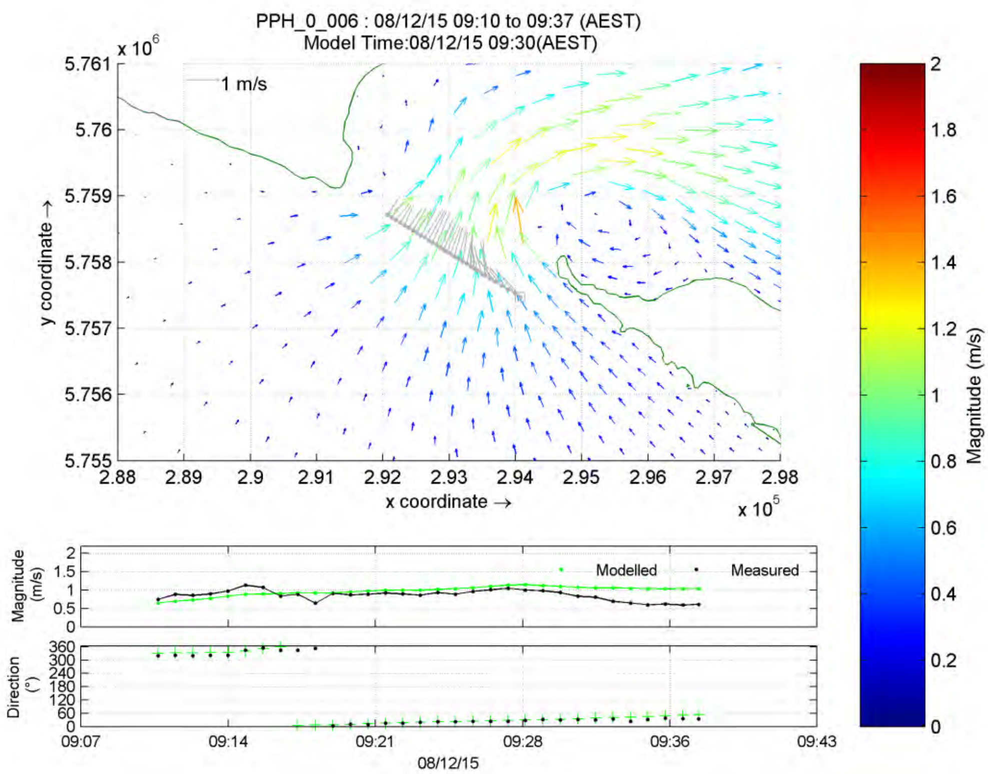

Figure 5-8 Typical ADCP transect taken during the flood tide – Modelled vs Measured

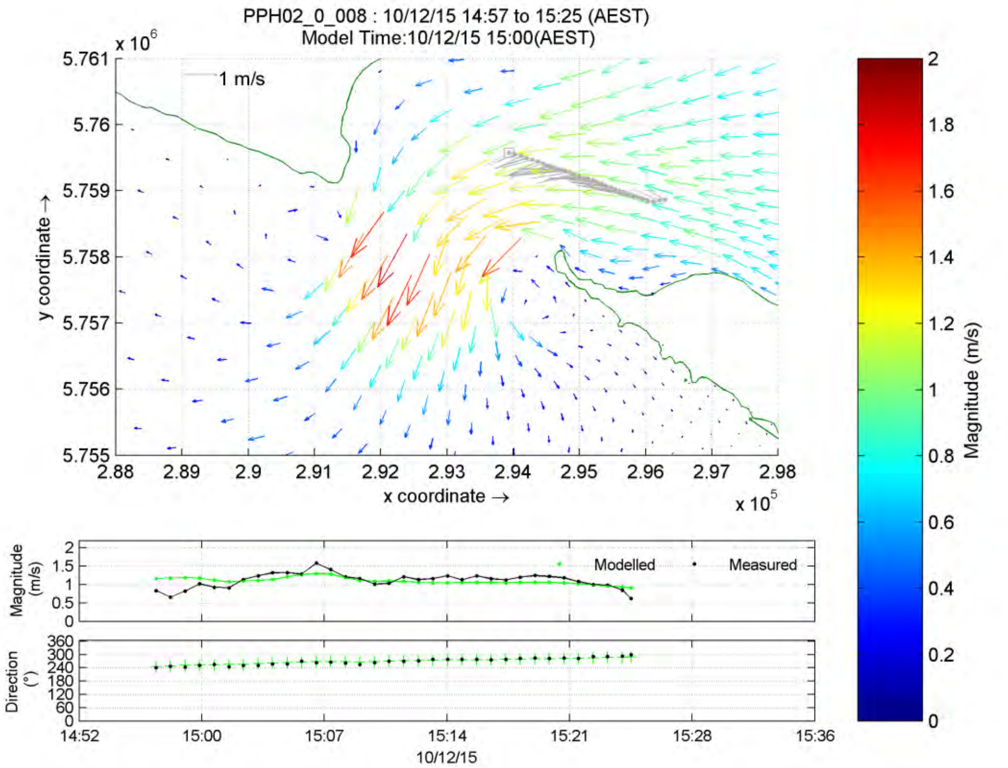

Figure 5-9 Typical ADCP transect taken during the ebb tide – Modelled vs Measured

6 Conclusions and Recommendations

6.1 Conclusions

The numerical model of the hydrodynamics of Port Phillip Heads has been validated against measured data, including spatial measurements of currents undertaken explicitly for this project. The validation demonstrates that the model's performance is "fit for purpose" for predicting the tidal streams in Port Phillip Heads.

6.2 Recommendations

There are some small systematic differences between the model results and the measured data and these need to be taken into consideration when generating predictions with small "calibration factors" included if required to maximise the agreement between the predictions and measured data in certain locations.

7 References

Cardno Lawson Treloar, 2007. *Hydrodynamic and wave model calibration and validation*. Report prepared for Maunsell Australia Pty Ltd on behalf of Port of Melbourne Corporation. Report LJ5508/RM2127, Technical Appendix 44 to the Supplementary Environment Effects Statement for the Channel Deepening Project.

Cardno (2011a). *The Great Sands and adjacent coasts and beaches*. Report RM2289_LJ5518, 137p. Report prepared for Port of Melbourne Authority.

Cardno (2011b). *Sediment Transport Modelling. Great Sands, Port Philip*. Report RM2271_LJ5518, 78p. Report prepared for Port of Melbourne Authority.

Geoscience Australia (2009). *Australian Bathymetry and Topography Grid,* 2 DVD set.

Willmott CJ 1984, 'On the evaluation of model performance in physical geography', in GL Gaile & CJ Willmott (eds), *Spatial Statistics and Models*, D Reidel Publishing Company, Dordrecht, pp. 443–60.

Port Phillip Heads
Current Modelling

APPENDIX

A

Fieldwork
Memorandum

Cardno
Shaping the Future

Memorandum

To:	Jake Shackleton (jake.shackleton@portofmelbourne.com) Peter Gibb (peter.gibb@portofmelbourne.com)
Company:	Port of Melbourne Corporation
From:	Phebe Bicknell (phebe.bicknell@cardno.com.au)
Date	18/12/2015 (minor typographical corrections 30/3/2016, abridged Feb 2017 for inclusion in Infrastructure Victoria Ports Study)

ADCP Data Collection at Port Phillip Heads

Cardno were commissioned by POMC to develop a system to generate maps of current speed and direction which allow mariners to know the strength and spatial variations in the tidal streams they will encounter during a passage through the Heads. As part of developing this process, Cardno is using existing calibrated and validated numerical models which include the effects of Channel Deepening, to determine current speed and direction throughout Port Phillip, including the Heads, using data from Lorne and Queenscliff tide gauges.

In order to further validate these models, currents measurements were taken at the Heads. Additional data was required to expand the spatial coverage of the current measurements and thus extend the model validation beyond the sites of the fixed measurement locations. This data was gathered using Acoustic Doppler Current Profiling from a moving vessel in conjunction with accurate positioning of the survey vessel. The aim was to undertake a number of transects and thus measure the currents along these transects to define the spatial variability of the currents.

This memorandum provides a summary of the fieldwork undertaken. It is intended to provide an overview of the fieldwork and does not include any analysis of the measurements at this stage.

1 Instrumentation

A Workhorse Sentinel ADCP (Acoustic Doppler Current Profiler), manufactured by Teledyne RD Instruments, was used to take transects at the Heads from 7th December 2015 to 11th December 2015. The instrument was secured to a mount, designed for the vessel *John Norgate* during previous ADCP measurements for POMC, fixing the instrument 1.5 m below the water surface, and downward facing to the seabed. The ADCP instrument also has bottom-track to determine the vessel position and velocity relative to the sea bed during the transect.

Computer software developed by the manufacturer for use with the ADCP, *Win River II*, allowed visualisation of the measurements in real-time, enabling an immediate knowledge of the values and quality of the data being obtained. This allowed field practices to be amended according to the conditions being experienced at that time.

2 Transects

Each transect (measurements along a straight-line segment) is recorded separately and the vessel position compared with the ADCP bottom track to allow accurate correction for the vessel effect on the instrument compass. The currents along the transect can then be compared with model output for the same location and time by using measured tide-gauge data to drive the model. By undertaking transects in sensitive areas, such as across the tidal jet and through eddy structures, this process allows validation of the model and demonstration of its performance. This results in user confidence in the final outputs.

Using existing model results, the location and timing of the transects was determined, prioritising areas and states of the tide that demonstrated notable current behaviours, such as tidal jets and eddies. Figure 1 shows the approximate locations at which transects were undertaken. These locations were used as a guide for the

vessel's path for each transect, and variation from these lines exists in the actual measurements. Current measurements were undertaken at various stages of the tide, to use in the validation of the model.

Figure 1- Approximate transect locations

Table 1 shows a summary of the transects that were recorded and the state of the tide at that time. A total of 43 transects were recorded, as well as some additional instrument calibration test transects, during the four day fieldwork period. Note that not all transects were required for each tidal state, with particular locations prioritised based on the model results.

Calm conditions are preferable to obtain clear, high quality measurements when recording ACPD transects. Given the nature of condition at Port Phillip Heads, this was not always easily achieved. Due to the wind and wave conditions, the quality of some results were found to be varied, particularly outside the Heads. As a result, not every transect could be obtained in entirety. The presence of passing ships in the channel also had to be considered in transect timing. However, every effort was taken to obtain a suitable coverage of the study area by shortening transects where necessary.

Table 1- Summary of transects and the state of the tide

Transect	Ebb	Flood	Slack		Transect	Ebb	Flood	Slack
A to B		1	1		E to C2	1	1	
A to F		1			E to D	1		
A to F2	2	1			F to C	1	1	1
A to H	1				F to G	2	1	
B to E	1				F2 to F	1		
B2 to F2		1			F2 to K	1		
C to C2		1			G to A	1		
C to D	1	1			G to H	2	2	
C to E	1				H to J	1	1	
C to K		1	1		I to J	1	1	
C2 to G		2			J to G	2		
E to B2		1			K to A	1		
K to G		1	1					

3 Data Obtained

Figure 2 gives an example of the information that can be gained from the current measurements. This figure is a screen shot of the software of the screen interface as the instrument was transmitting data during a transect. While the measurements have not been assessed in any detail at this stage, preliminary observations through graphical visualisation of the data during the measurements, indicated that the fieldwork should provide suitable values to be incorporated into the analysis and used in validating the numerical model.

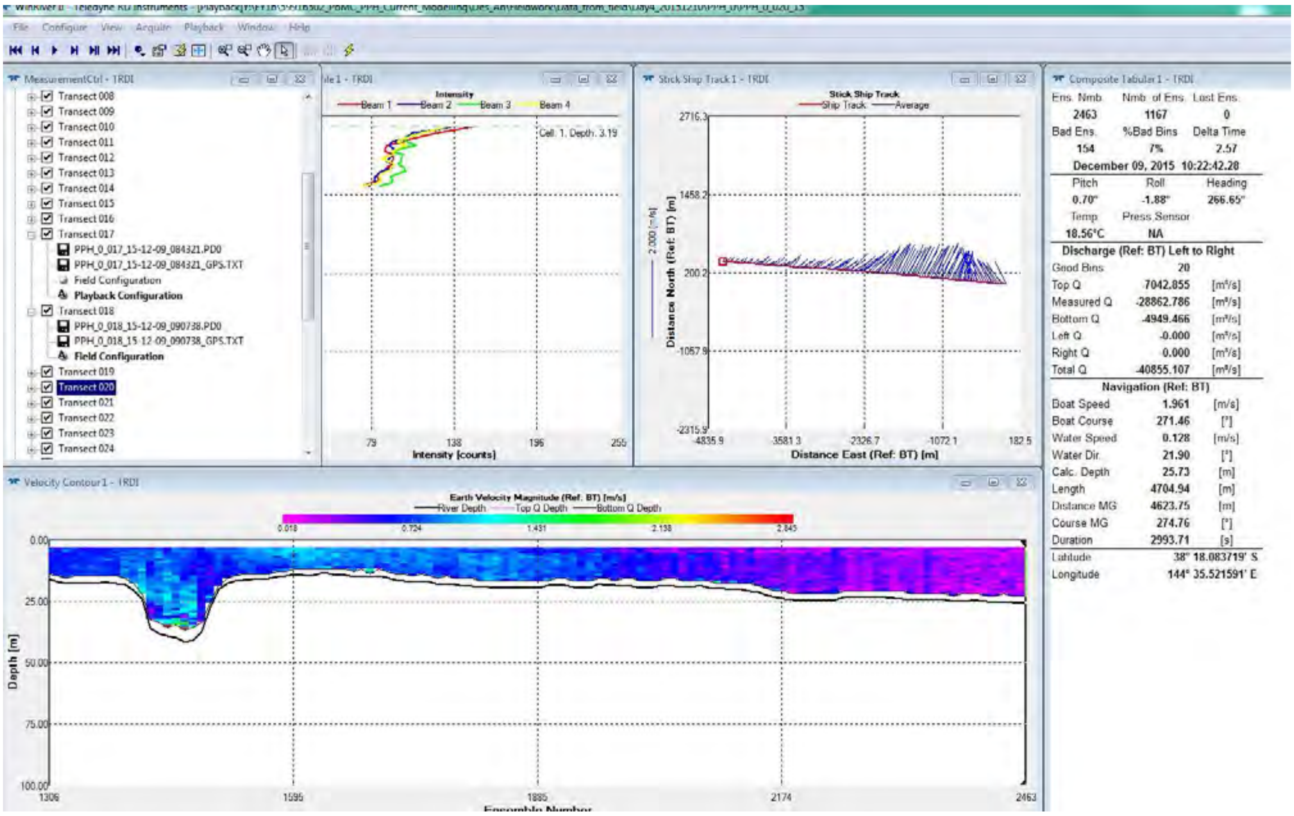

Figure 2- Screenshot showing typical current measurements

Port Phillip Heads
Current Modelling

APPENDIX B

Transect Figures: Modelled and Measured Currents

Cardno
Shaping the Future

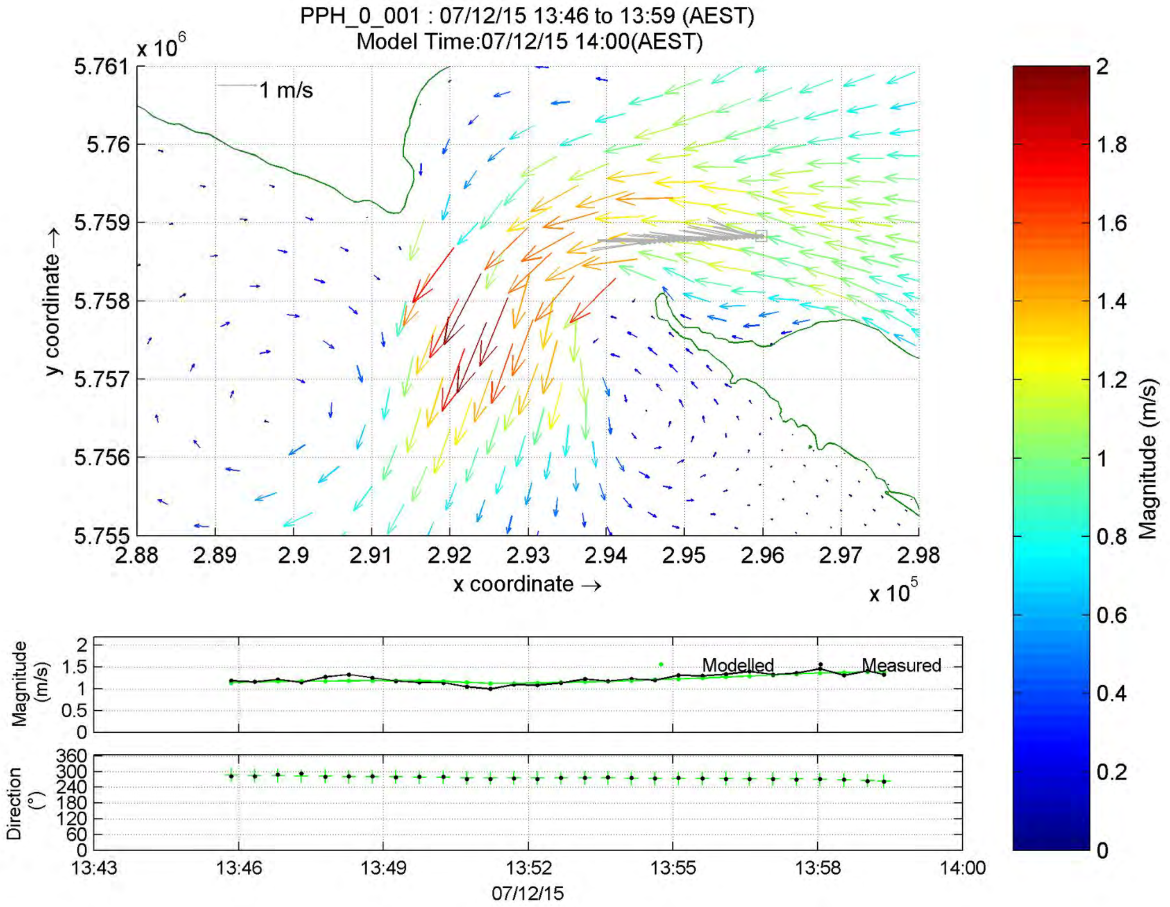
PPH_0_001 : 07/12/15 13:46 to 13:59 (AEST)
Model Time:07/12/15 14:00(AEST)
x 10^6
1 m/s
5.761
5.76
5.759
5.758
5.757
5.756
5.755
y coordinate →
2.88
2.89
2.9
2.91
2.92
2.93
2.94
2.95
2.96
2.97
2.98
x coordinate →
x 10^5
Magnitude (m/s)
2
1.8
1.6
1.4
1.2
1
0.8
0.6
0.4
0.2
0
Modelled
Measured
Magnitude (m/s)
Direction (°)
360
300
240
180
120
60
0
13:43
13:46
13:49
13:52
13:55
13:58
14:00
07/12/15

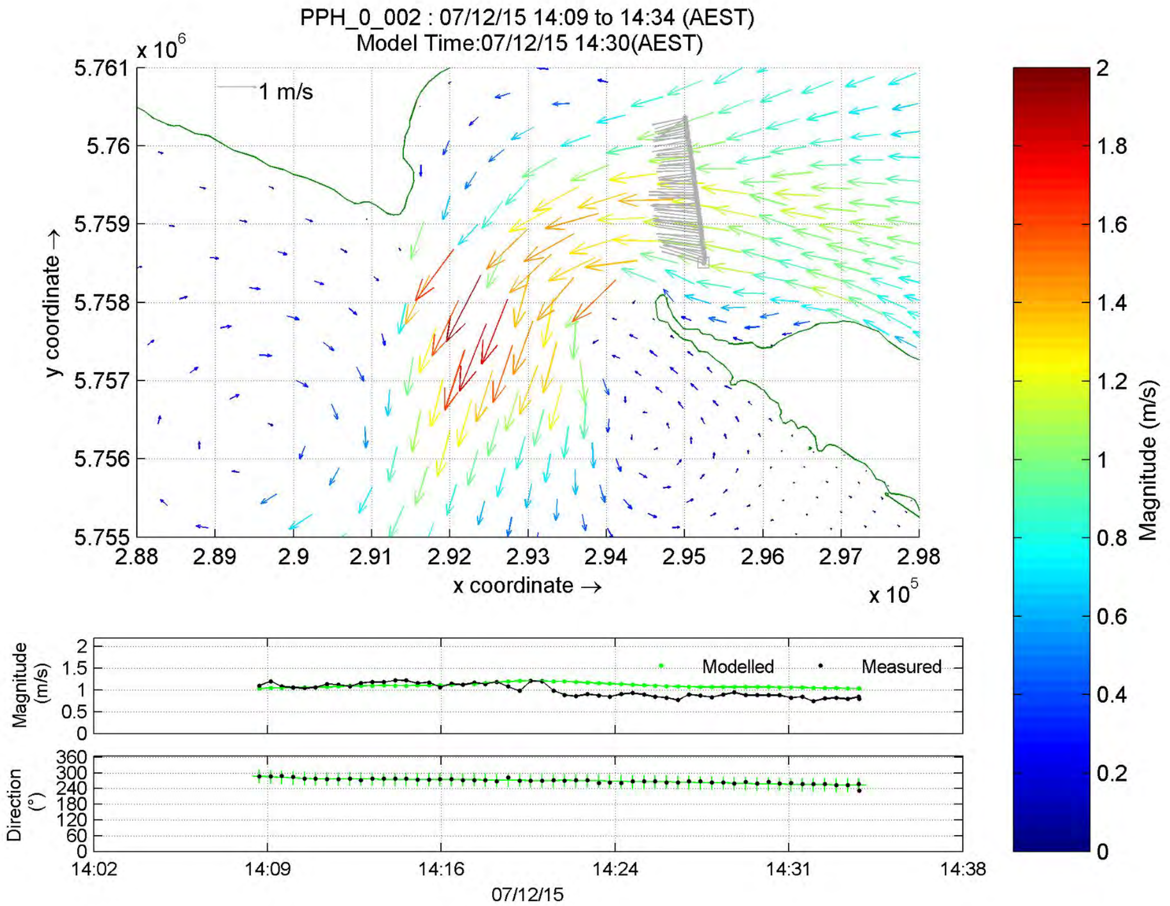
PPH_0_002 : 07/12/15 14:09 to 14:34 (AEST)
Model Time:07/12/15 14:30(AEST)
x 10^6
1 m/s
5.761
5.76
5.759
5.758
5.757
5.756
5.755
y coordinate →
2.88
2.89
2.9
2.91
2.92
2.93
2.94
2.95
2.96
2.97
2.98
x coordinate →
x 10^5
Magnitude (m/s)
2
1.8
1.6
1.4
1.2
1
0.8
0.6
0.4
0.2
0
Modelled
Measured
Magnitude (m/s)
Direction (°)
360
300
240
180
120
60
0
14:02
14:09
14:16
14:24
14:31
14:38
07/12/15

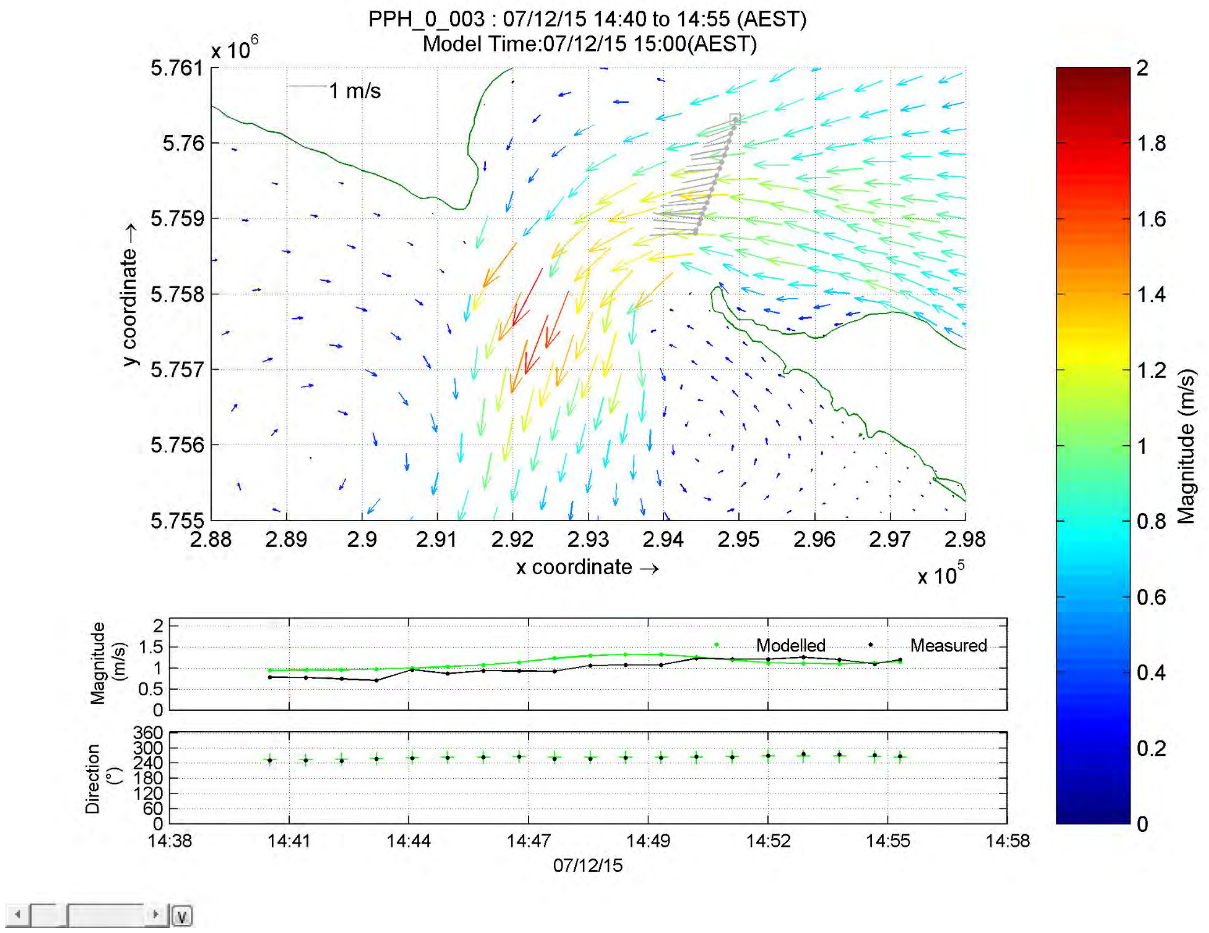
PPH_0_003 : 07/12/15 14:40 to 14:55 (AEST)
Model Time:07/12/15 15:00(AEST)
1 m/s
y coordinate →
x coordinate →
x 10^6
x 10^5
Magnitude (m/s)
Modelled
Measured
Magnitude (m/s)
Direction (°)
07/12/15

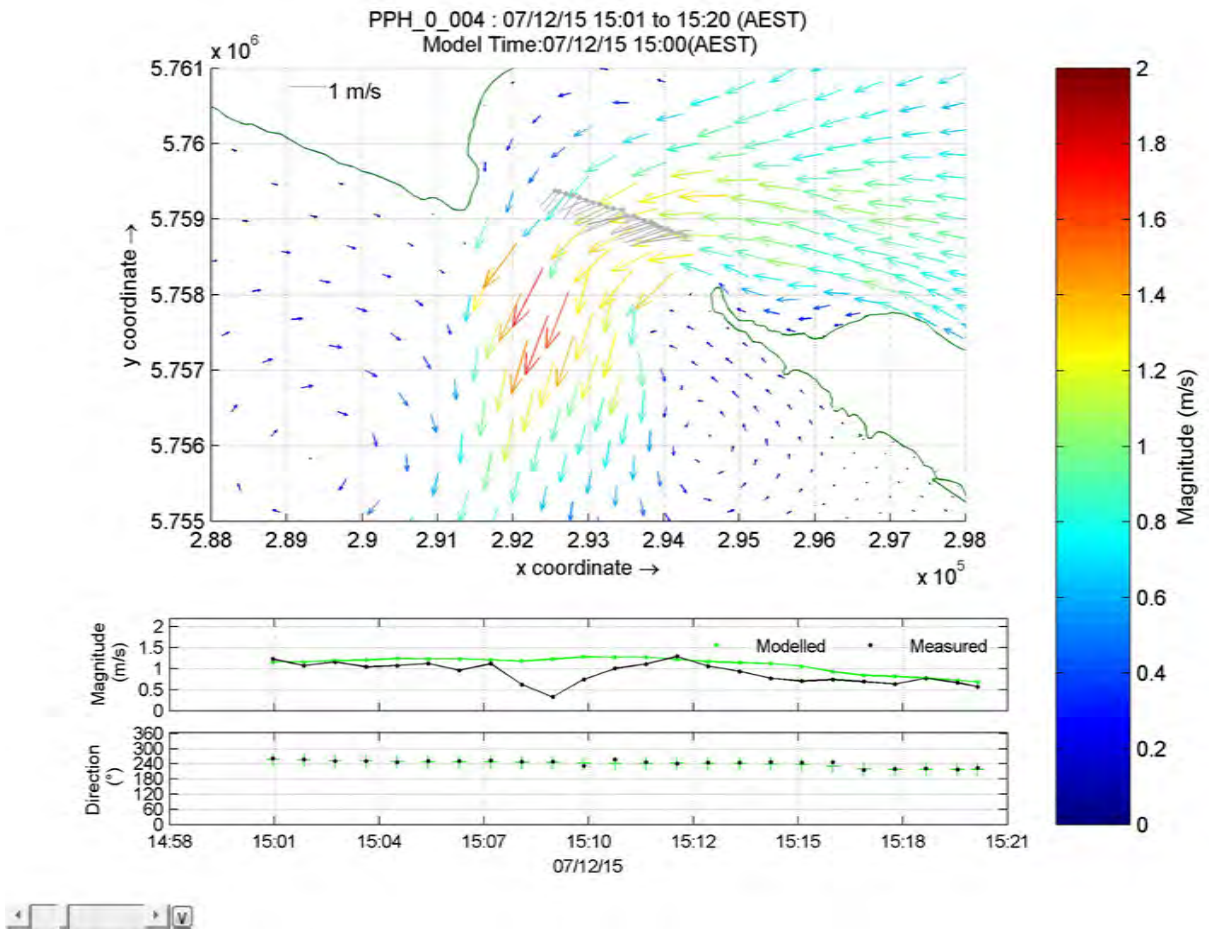
PPH_0_004 : 07/12/15 15:01 to 15:20 (AEST)
Model Time:07/12/15 15:00(AEST)
1 m/s
y coordinate →
x coordinate →
x 10^6
x 10^5
Magnitude (m/s)
Modelled
Measured
Magnitude (m/s)
Direction (°)
07/12/15

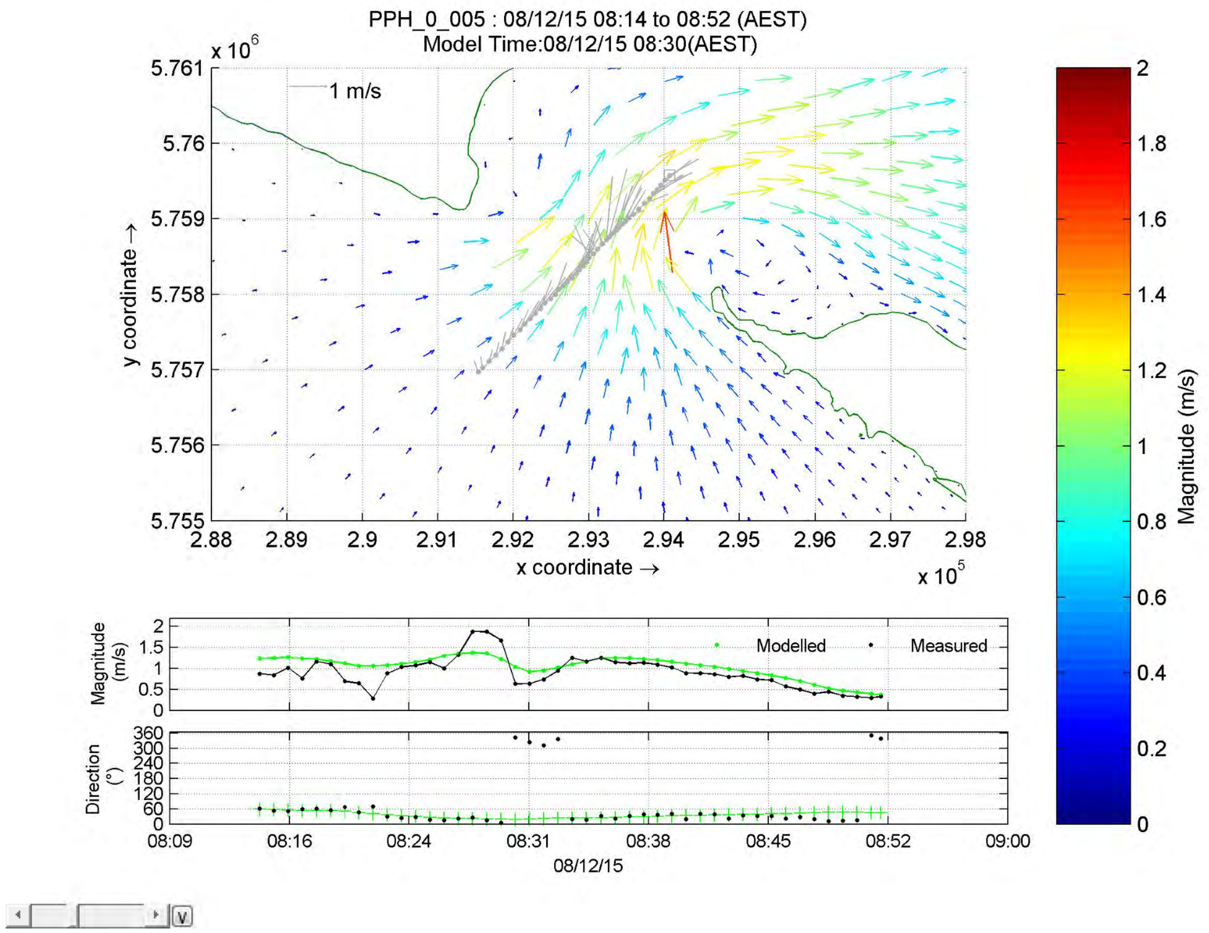
PPH_0_005 : 08/12/15 08:14 to 08:52 (AEST)
Model Time:08/12/15 08:30(AEST)
1 m/s
y coordinate →
x coordinate →
x 10^6
x 10^5
Magnitude (m/s)
Modelled
Measured
Direction (°)
08/12/15

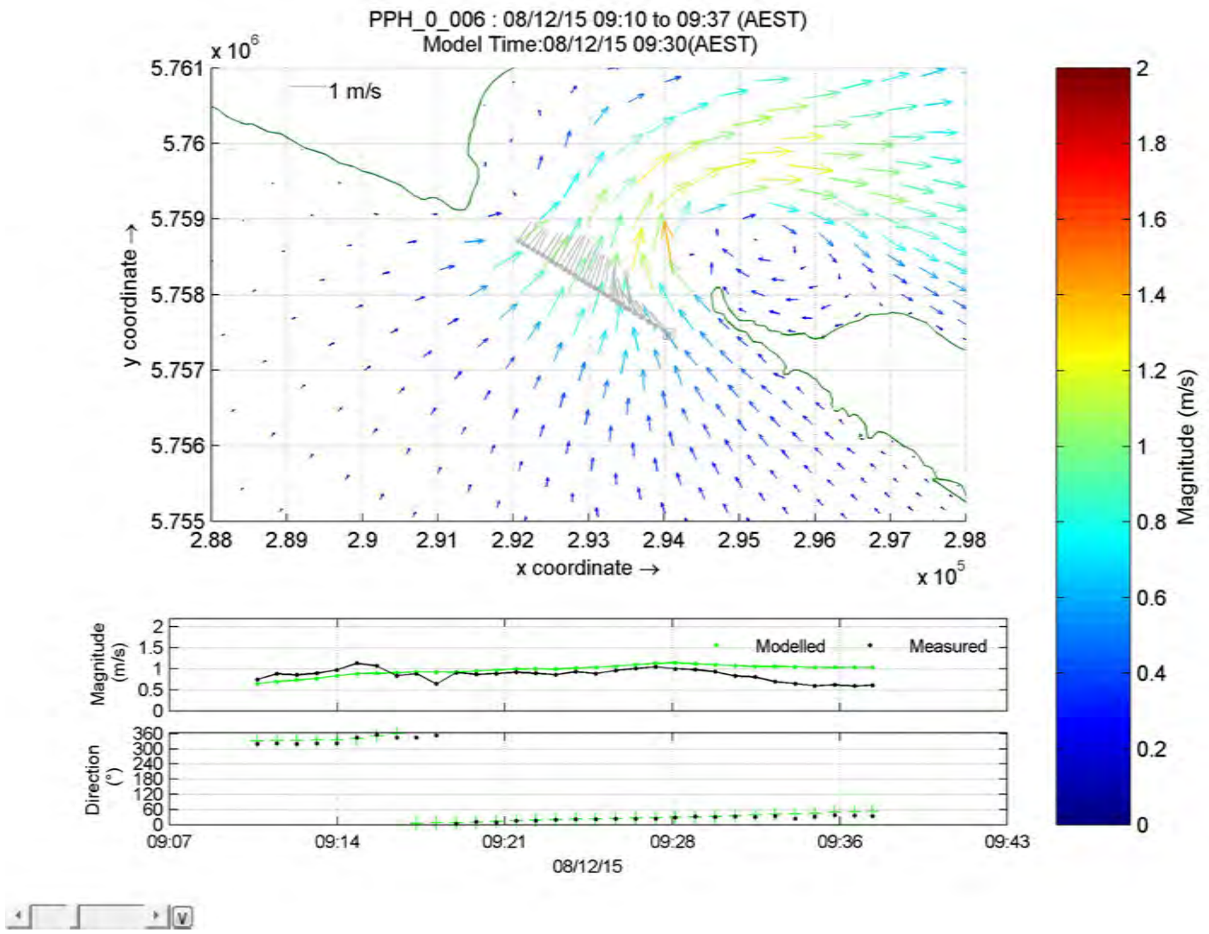
PPH_0_006 : 08/12/15 09:10 to 09:37 (AEST)
Model Time:08/12/15 09:30(AEST)
1 m/s
y coordinate →
x coordinate →
x 10^6
x 10^5
Magnitude (m/s)
Modelled
Measured
Direction (°)
08/12/15

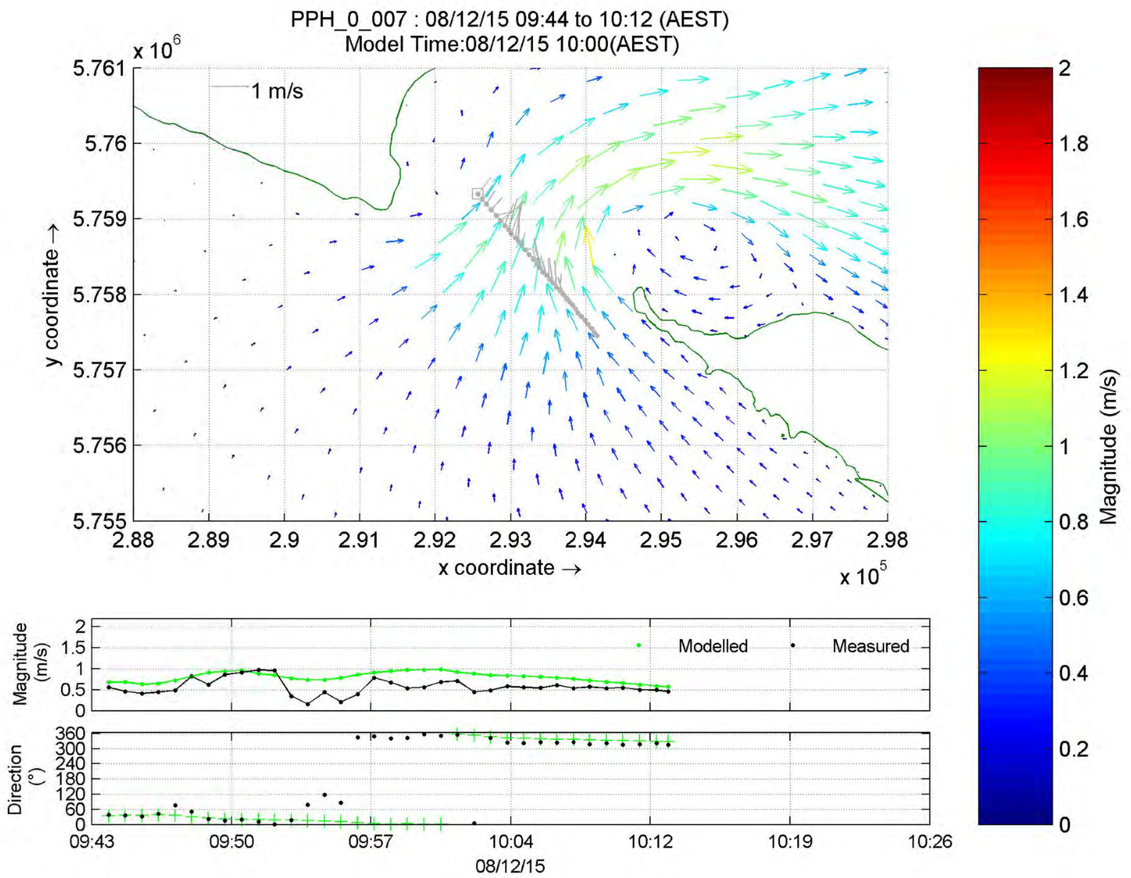
PPH_0_007 : 08/12/15 09:44 to 10:12 (AEST)
Model Time:08/12/15 10:00(AEST)
x 10^6
1 m/s
y coordinate →
x coordinate →
x 10^5
Magnitude (m/s)
Modelled
Measured
Magnitude (m/s)
Direction (°)
09:43
09:50
09:57
10:04
10:12
10:19
10:26
08/12/15

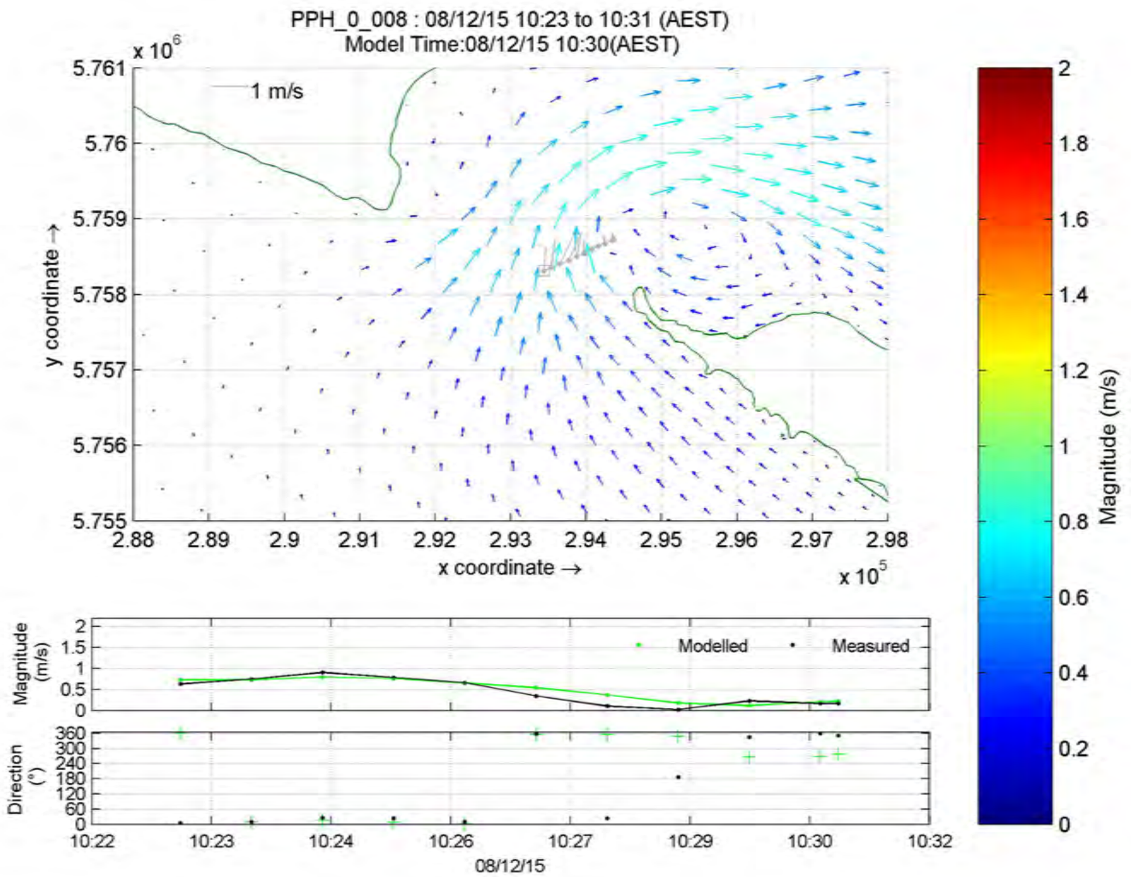
PPH_0_008 : 08/12/15 10:23 to 10:31 (AEST)
Model Time:08/12/15 10:30(AEST)
x 10^6
1 m/s
y coordinate →
x coordinate →
x 10^5
Magnitude (m/s)
Modelled
Measured
Magnitude (m/s)
Direction (°)
10:22
10:23
10:24
10:26
10:27
10:29
10:30
10:32
08/12/15

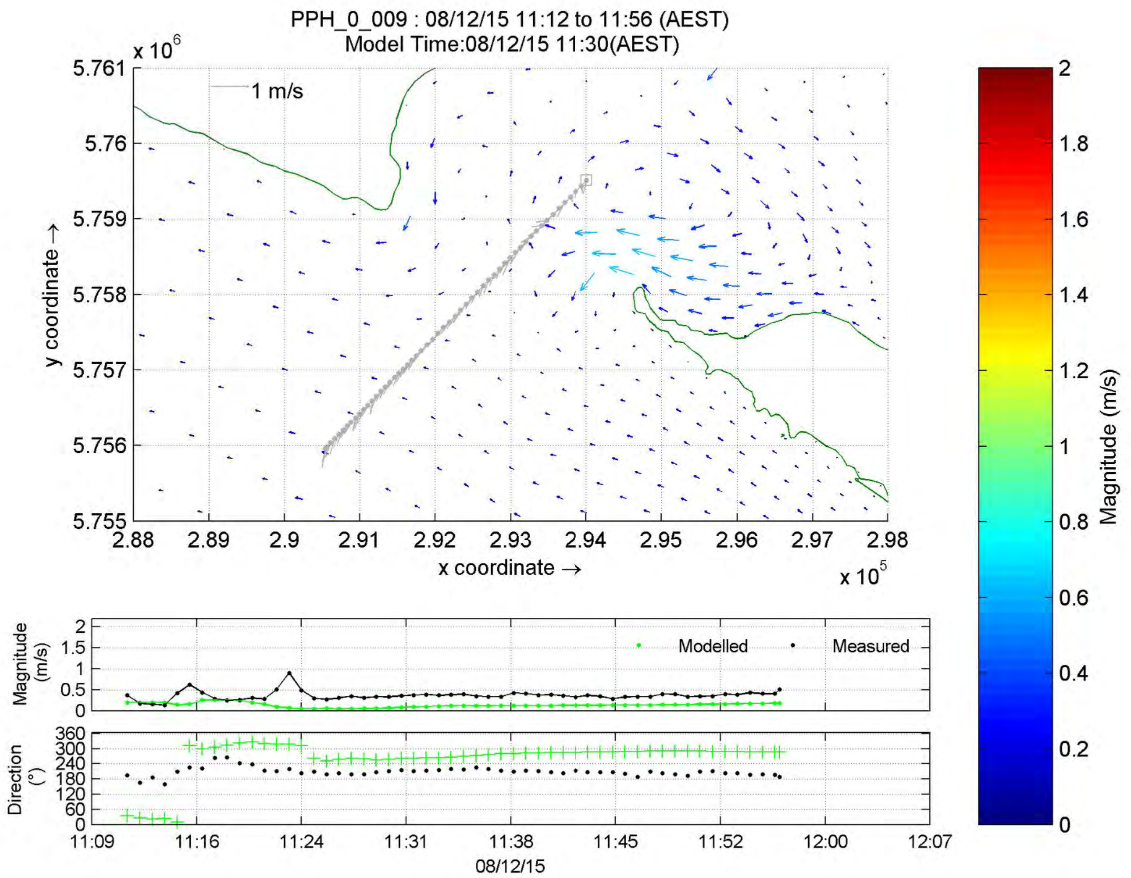
PPH_0_009 : 08/12/15 11:12 to 11:56 (AEST)
Model Time:08/12/15 11:30(AEST)
x 10^6
1 m/s
5.761
5.76
5.759
5.758
5.757
5.756
5.755
y coordinate →
2.88 2.89 2.9 2.91 2.92 2.93 2.94 2.95 2.96 2.97 2.98
x coordinate →
x 10^5
Magnitude (m/s)
2 1.8 1.6 1.4 1.2 1 0.8 0.6 0.4 0.2 0
Magnitude (m/s)
2 1.5 1 0.5 0
Modelled
Measured
Direction (°)
360 300 240 180 120 60 0
11:09 11:16 11:24 11:31 11:38 11:45 11:52 12:00 12:07
08/12/15

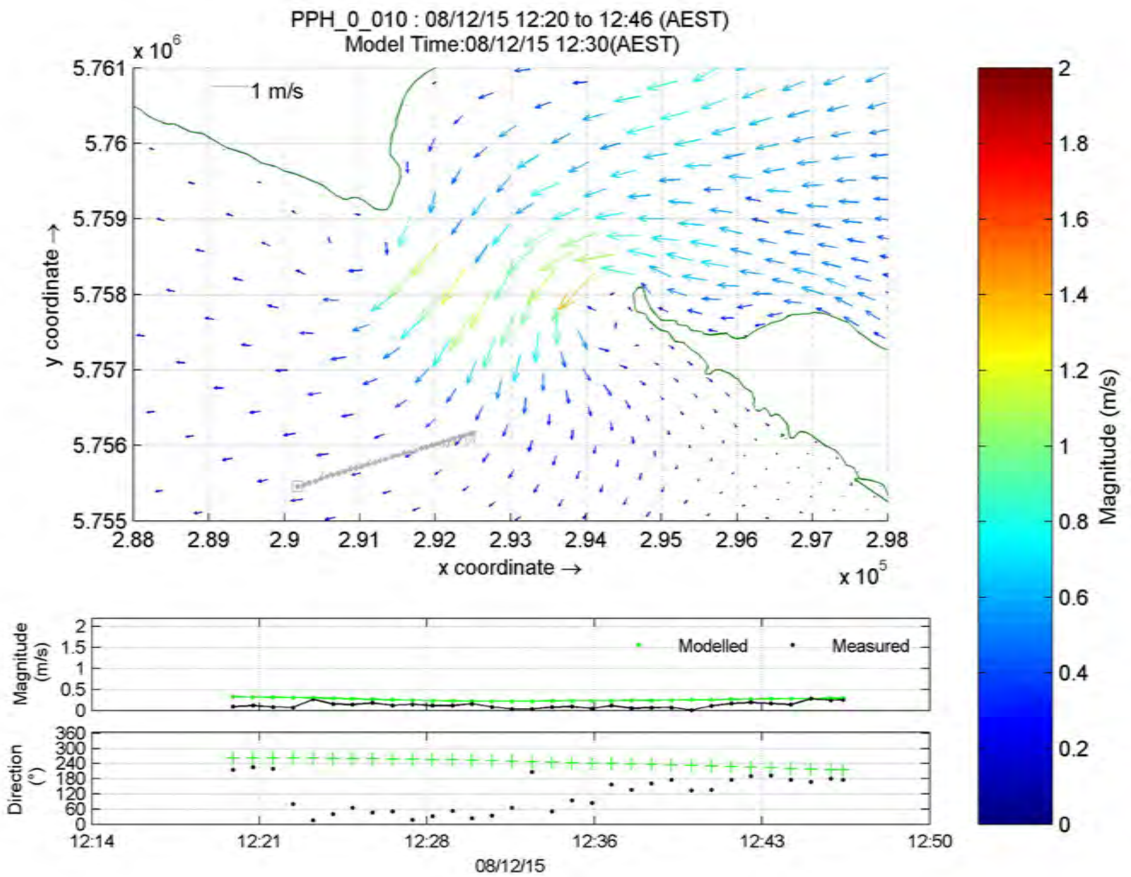
PPH_0_010 : 08/12/15 12:20 to 12:46 (AEST)
Model Time:08/12/15 12:30(AEST)
x 10^6
1 m/s
5.761
5.76
5.759
5.758
5.757
5.756
5.755
y coordinate →
2.88 2.89 2.9 2.91 2.92 2.93 2.94 2.95 2.96 2.97 2.98
x coordinate →
x 10^5
Magnitude (m/s)
2 1.8 1.6 1.4 1.2 1 0.8 0.6 0.4 0.2 0
Magnitude (m/s)
2 1.5 1 0.5 0
Modelled
Measured
Direction (°)
360 300 240 180 120 60 0
12:14 12:21 12:28 12:36 12:43 12:50
08/12/15

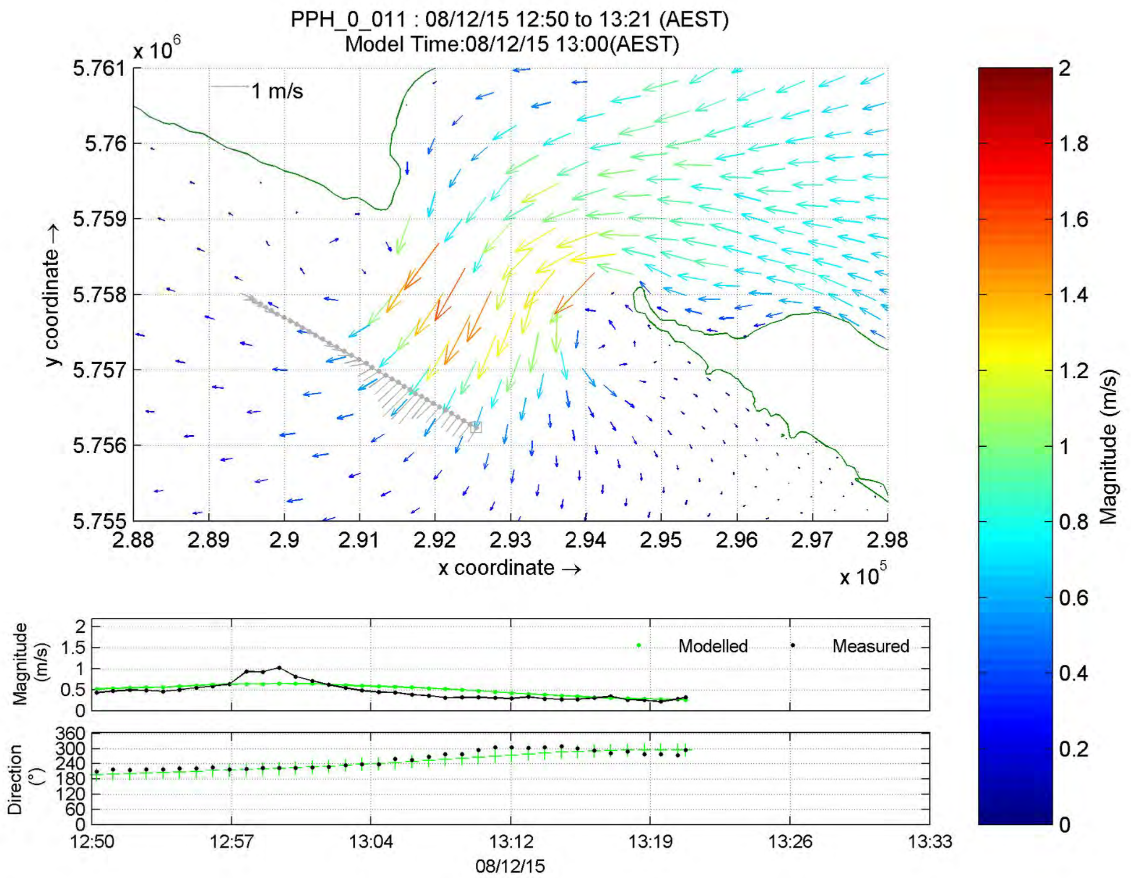
PPH_0_011 : 08/12/15 12:50 to 13:21 (AEST)
Model Time:08/12/15 13:00(AEST)
1 m/s
y coordinate →
x coordinate →
Magnitude (m/s)
Modelled
Measured
Direction (°)
08/12/15

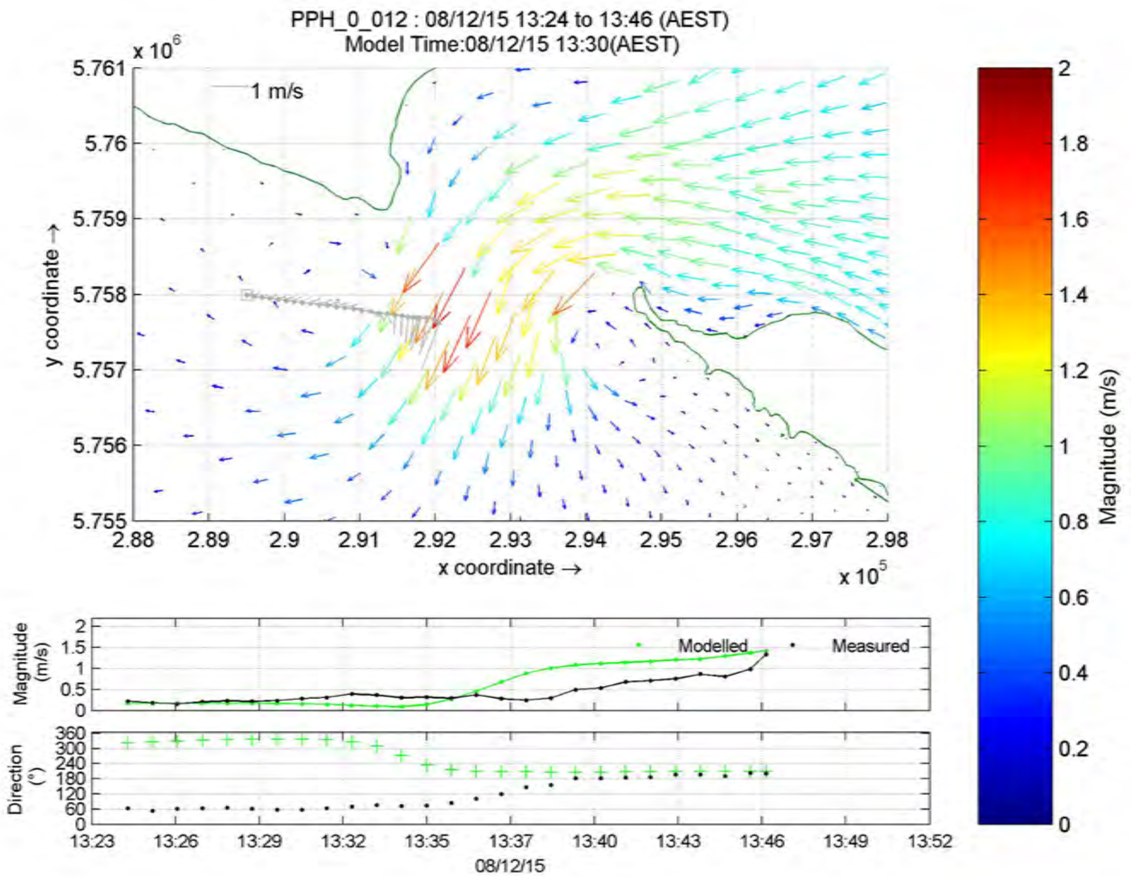
PPH_0_012 : 08/12/15 13:24 to 13:46 (AEST)
Model Time:08/12/15 13:30(AEST)
1 m/s
y coordinate →
x coordinate →
Magnitude (m/s)
Modelled
Measured
Direction (°)
08/12/15

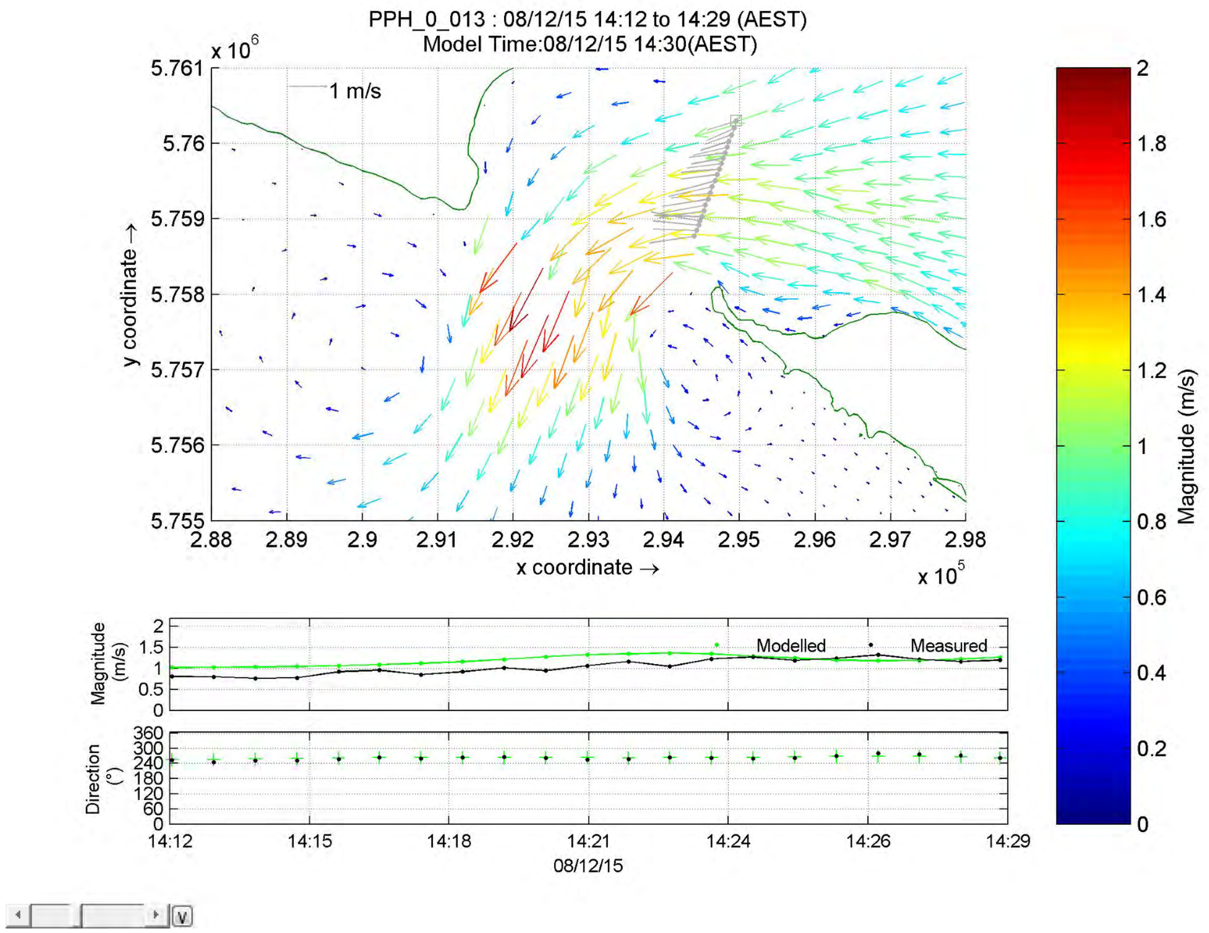
PPH_0_013 : 08/12/15 14:12 to 14:29 (AEST)
Model Time:08/12/15 14:30(AEST)
1 m/s
y coordinate →
x coordinate →
Magnitude (m/s)
Modelled
Measured
Direction (°)
14:12
14:15
14:18
14:21
14:24
14:26
14:29
08/12/15

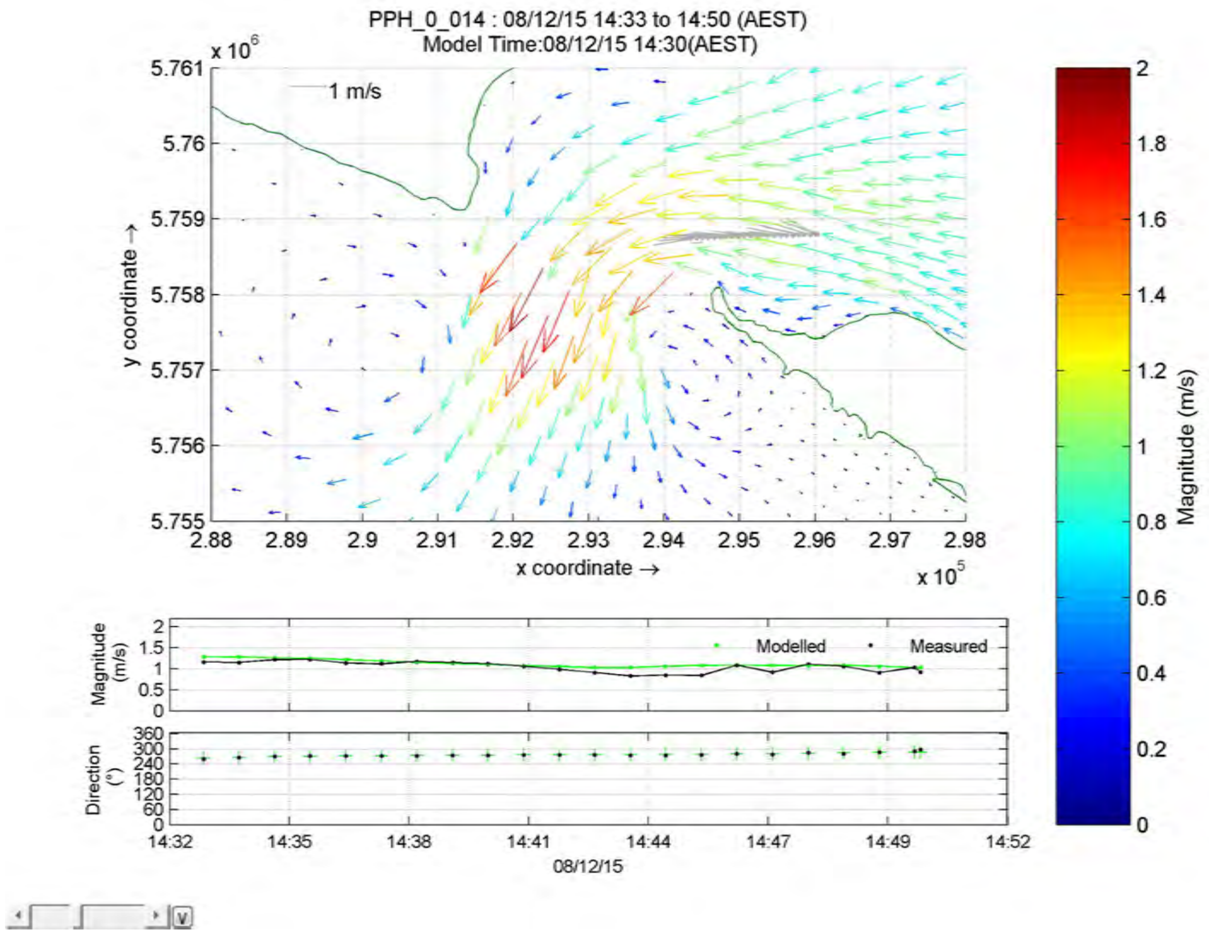
PPH_0_014 : 08/12/15 14:33 to 14:50 (AEST)
Model Time:08/12/15 14:30(AEST)
1 m/s
y coordinate →
x coordinate →
Magnitude (m/s)
Modelled
Measured
Direction (°)
14:32
14:35
14:38
14:41
14:44
14:47
14:49
14:52
08/12/15

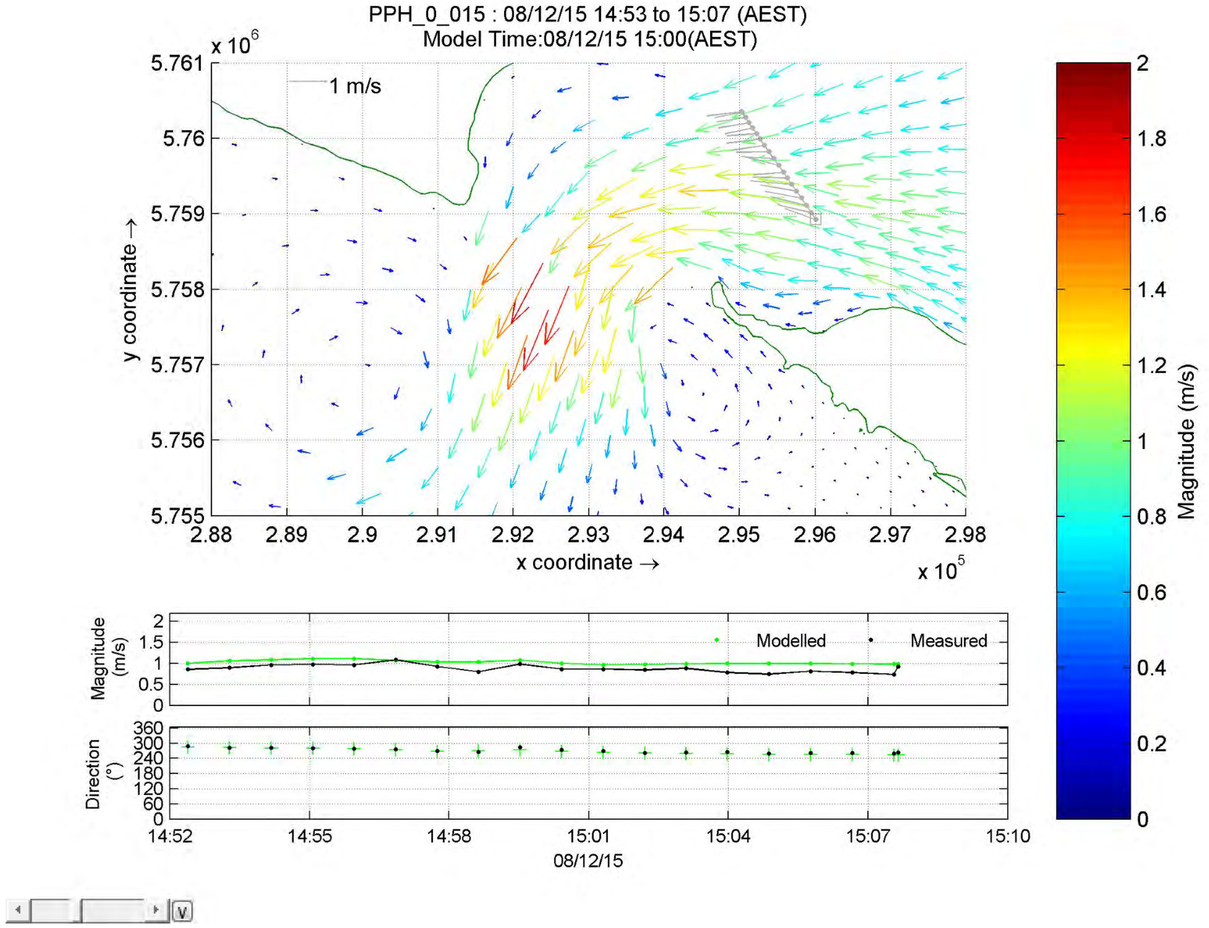
PPH_0_015 : 08/12/15 14:53 to 15:07 (AEST)
Model Time:08/12/15 15:00(AEST)
x 10^6
1 m/s
5.761
5.76
5.759
5.758
5.757
5.756
5.755
y coordinate →
2.88
2.89
2.9
2.91
2.92
2.93
2.94
2.95
2.96
2.97
2.98
x coordinate →
x 10^5
2
1.8
1.6
1.4
1.2
1
0.8
0.6
0.4
0.2
0
Magnitude (m/s)
Magnitude (m/s)
Modelled
Measured
Direction (°)
14:52
14:55
14:58
15:01
15:04
15:07
15:10
08/12/15

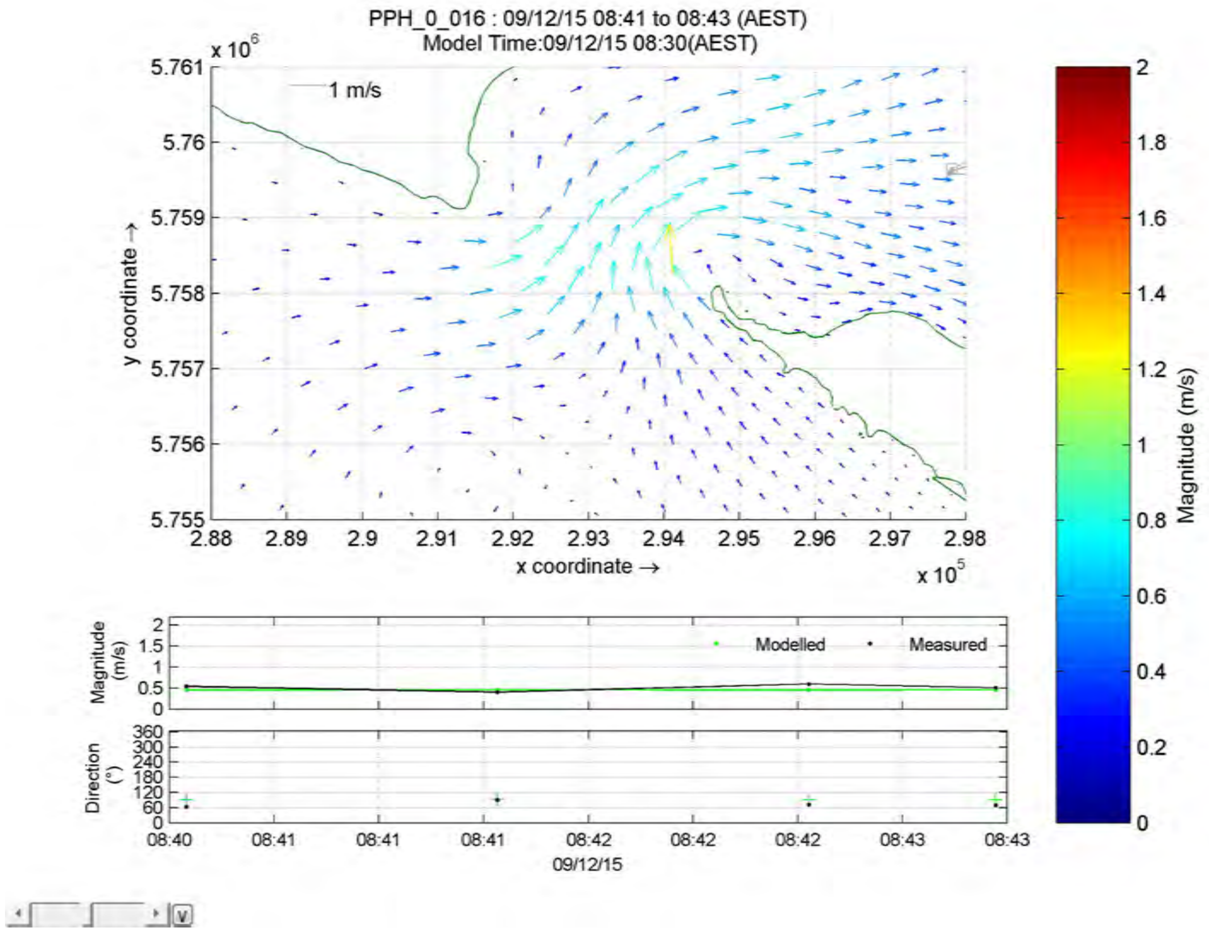
PPH_0_016 : 09/12/15 08:41 to 08:43 (AEST)
Model Time:09/12/15 08:30(AEST)
x 10^6
1 m/s
5.761
5.76
5.759
5.758
5.757
5.756
5.755
y coordinate →
2.88
2.89
2.9
2.91
2.92
2.93
2.94
2.95
2.96
2.97
2.98
x coordinate →
x 10^5
2
1.8
1.6
1.4
1.2
1
0.8
0.6
0.4
0.2
0
Magnitude (m/s)
Magnitude (m/s)
Modelled
Measured
Direction (°)
08:40
08:41
08:41
08:41
08:42
08:42
08:42
08:43
08:43
09/12/15

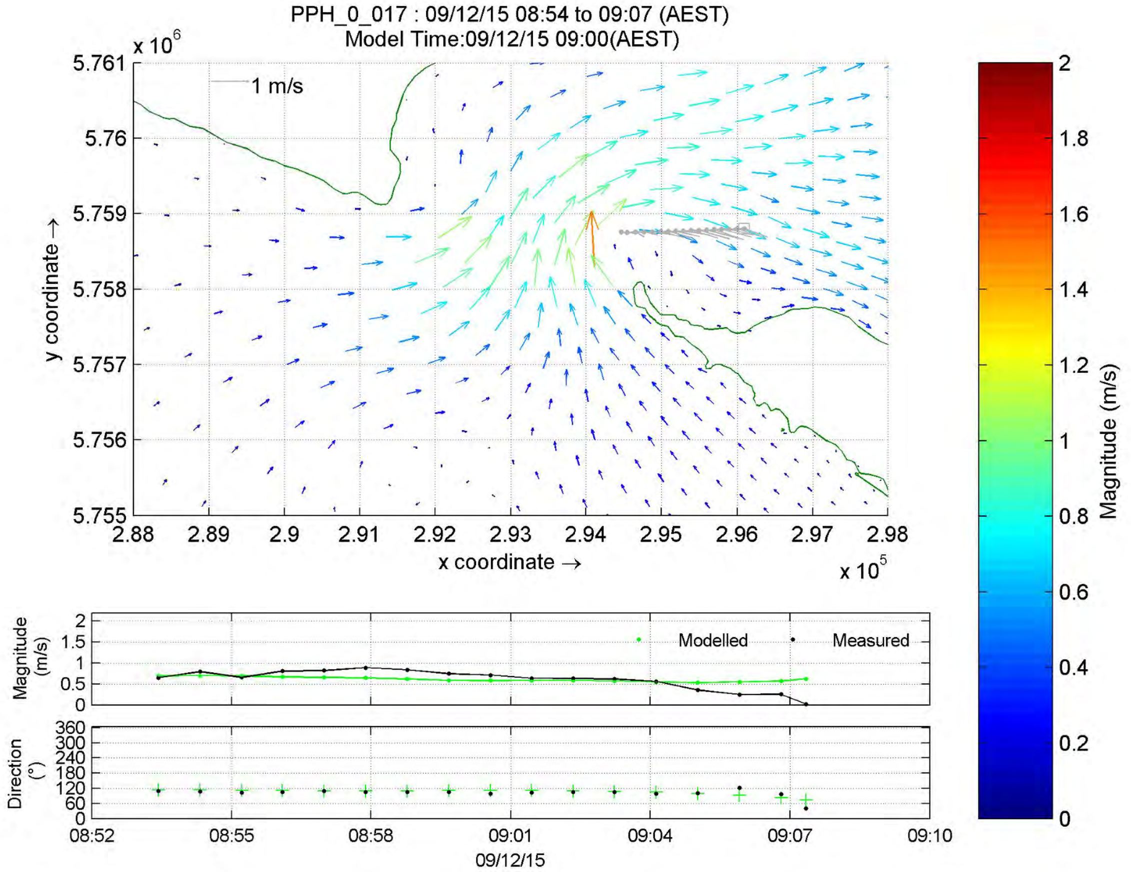
PPH_0_017 : 09/12/15 08:54 to 09:07 (AEST)
Model Time:09/12/15 09:00(AEST)
x 10^6
1 m/s
y coordinate →
x coordinate →
x 10^5
Magnitude (m/s)
Modelled
Measured
Direction (°)
08:52
08:55
08:58
09:01
09:04
09:07
09:10
09/12/15

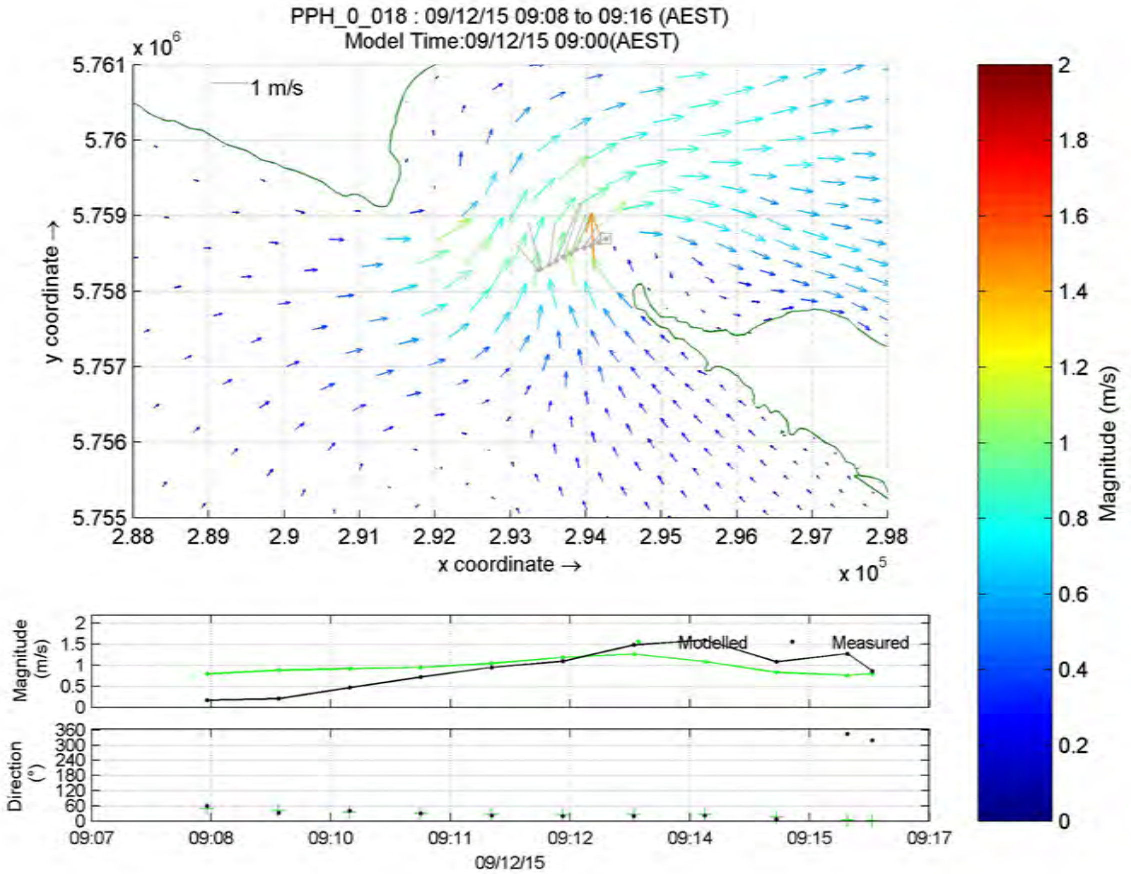
PPH_0_018 : 09/12/15 09:08 to 09:16 (AEST)
Model Time:09/12/15 09:00(AEST)
x 10^6
1 m/s
y coordinate →
x coordinate →
x 10^5
Magnitude (m/s)
Modelled
Measured
Direction (°)
09:07
09:08
09:10
09:11
09:12
09:14
09:15
09:17
09/12/15

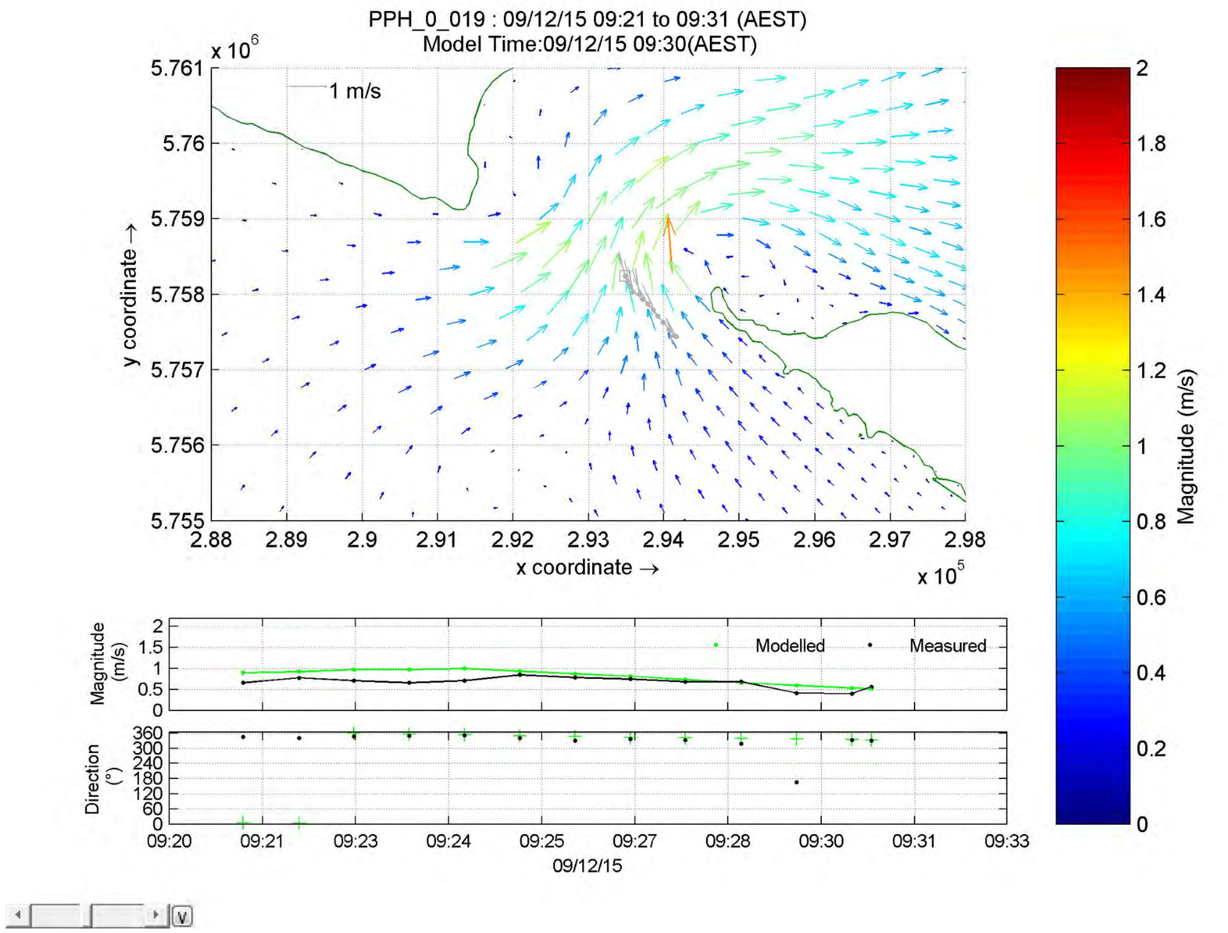
PPH_0_019 : 09/12/15 09:21 to 09:31 (AEST)
Model Time:09/12/15 09:30(AEST)
1 m/s
y coordinate →
x coordinate →
x 10^6
x 10^5
Magnitude (m/s)
Modelled
Measured
Direction (°)
09/12/15

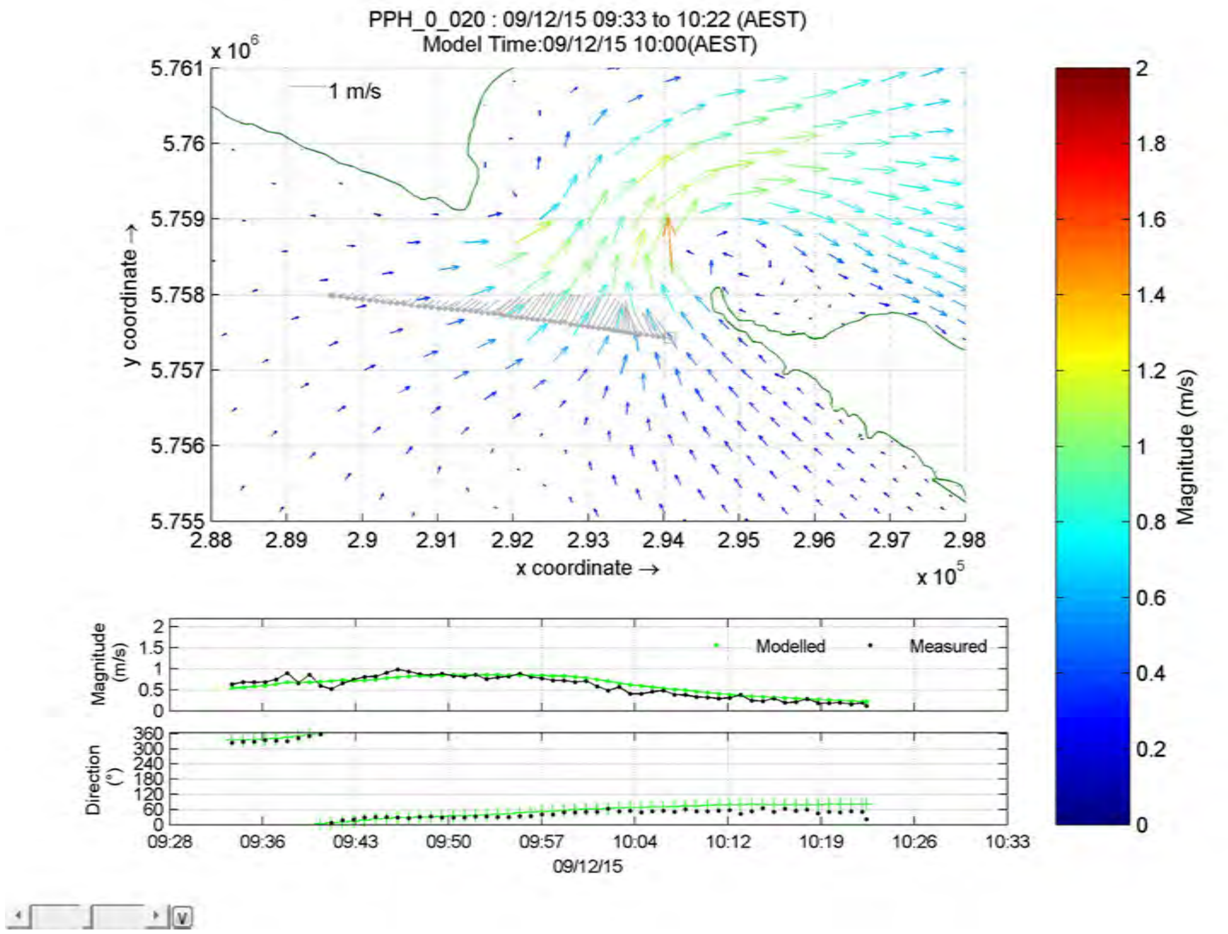
PPH_0_020 : 09/12/15 09:33 to 10:22 (AEST)
Model Time:09/12/15 10:00(AEST)
1 m/s
y coordinate →
x coordinate →
x 10^6
x 10^5
Magnitude (m/s)
Modelled
Measured
Direction (°)
09/12/15

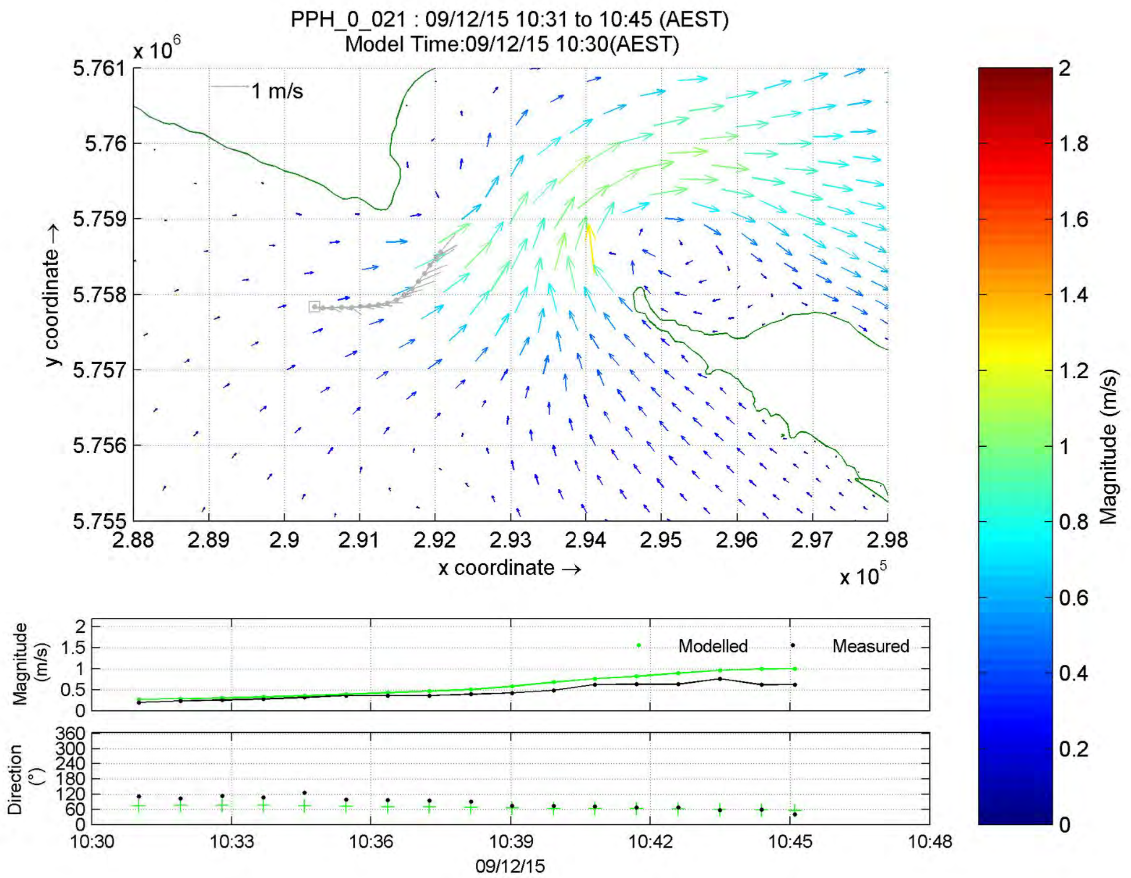
PPH_0_021 : 09/12/15 10:31 to 10:45 (AEST)
Model Time:09/12/15 10:30(AEST)
x 10^6
1 m/s
5.761
5.76
5.759
5.758
5.757
5.756
5.755
y coordinate →
2.88
2.89
2.9
2.91
2.92
2.93
2.94
2.95
2.96
2.97
2.98
x coordinate →
x 10^5
Magnitude (m/s)
2
1.8
1.6
1.4
1.2
1
0.8
0.6
0.4
0.2
0
Magnitude (m/s)
Modelled
Measured
Direction (°)
360
300
240
180
120
60
0
10:30
10:33
10:36
10:39
10:42
10:45
10:48
09/12/15

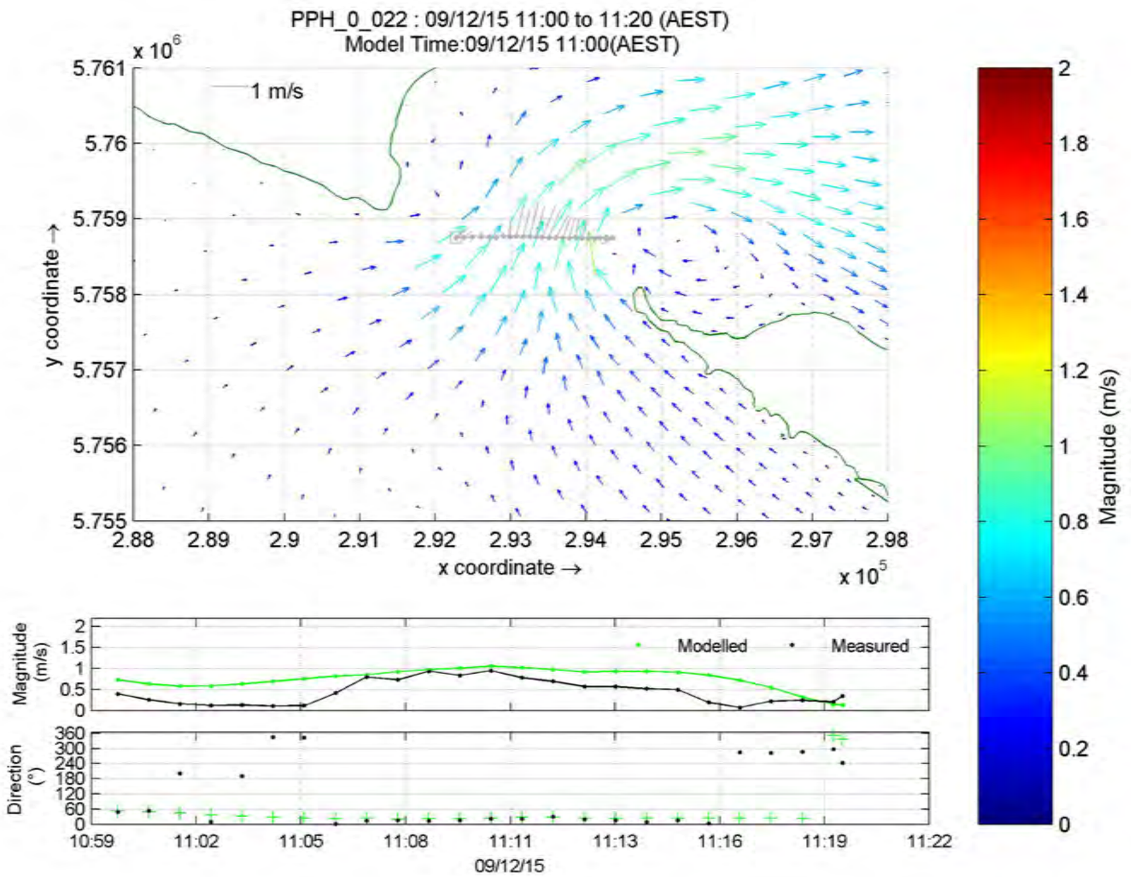
PPH_0_022 : 09/12/15 11:00 to 11:20 (AEST)
Model Time:09/12/15 11:00(AEST)
x 10^6
1 m/s
5.761
5.76
5.759
5.758
5.757
5.756
5.755
y coordinate →
2.88
2.89
2.9
2.91
2.92
2.93
2.94
2.95
2.96
2.97
2.98
x coordinate →
x 10^5
Magnitude (m/s)
2
1.8
1.6
1.4
1.2
1
0.8
0.6
0.4
0.2
0
Magnitude (m/s)
Modelled
Measured
Direction (°)
360
300
240
180
120
60
0
10:59
11:02
11:05
11:08
11:11
11:13
11:16
11:19
11:22
09/12/15

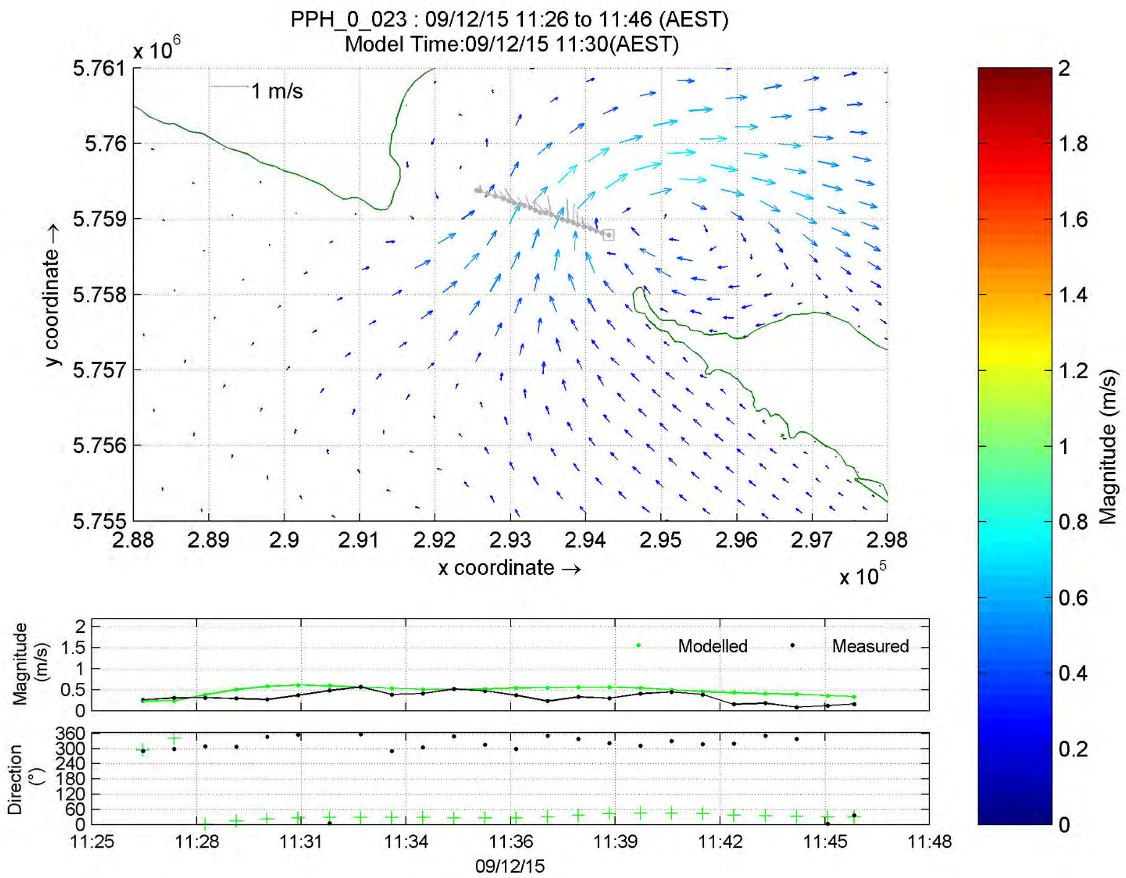
PPH_0_023 : 09/12/15 11:26 to 11:46 (AEST)
Model Time:09/12/15 11:30(AEST)
1 m/s
y coordinate →
x coordinate →
x 10^6
x 10^5
Magnitude (m/s)
Modelled
Measured
Direction (°)
09/12/15

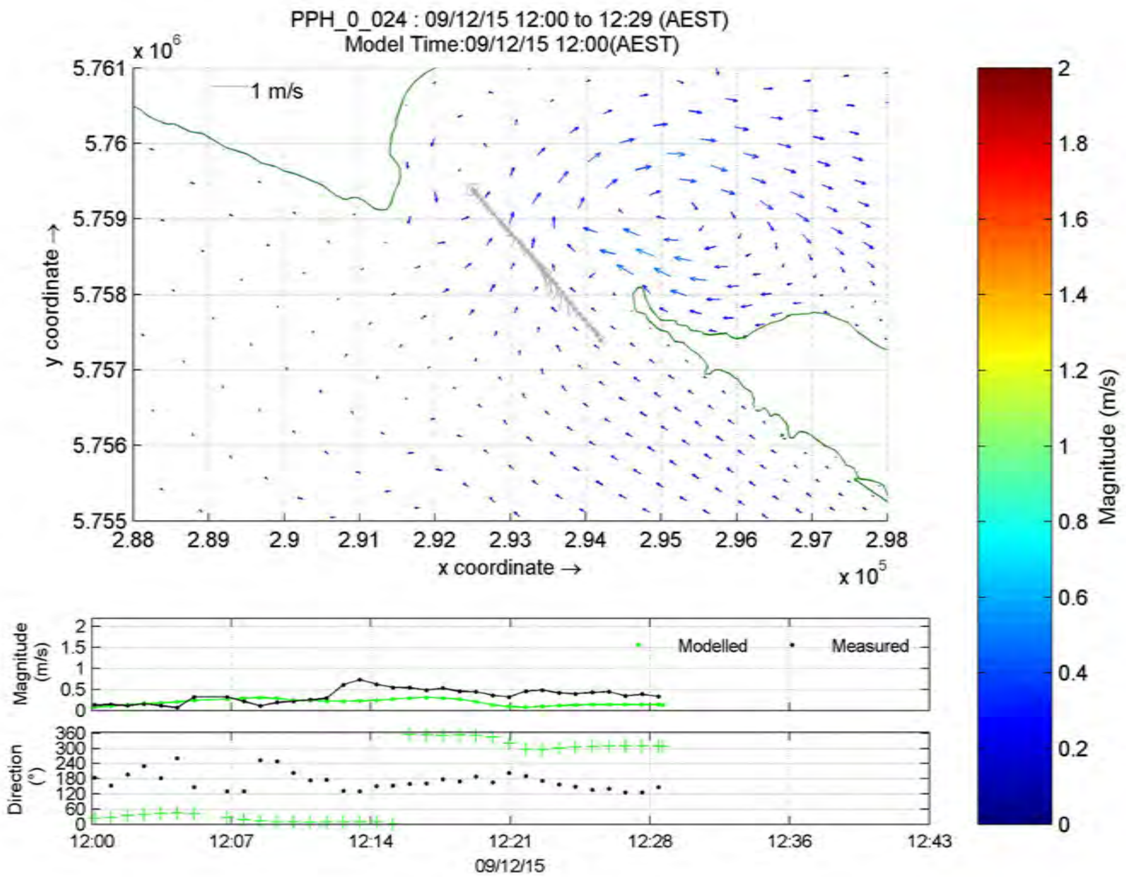
PPH_0_024 : 09/12/15 12:00 to 12:29 (AEST)
Model Time:09/12/15 12:00(AEST)
1 m/s
y coordinate →
x coordinate →
x 10^6
x 10^5
Magnitude (m/s)
Modelled
Measured
Direction (°)
09/12/15

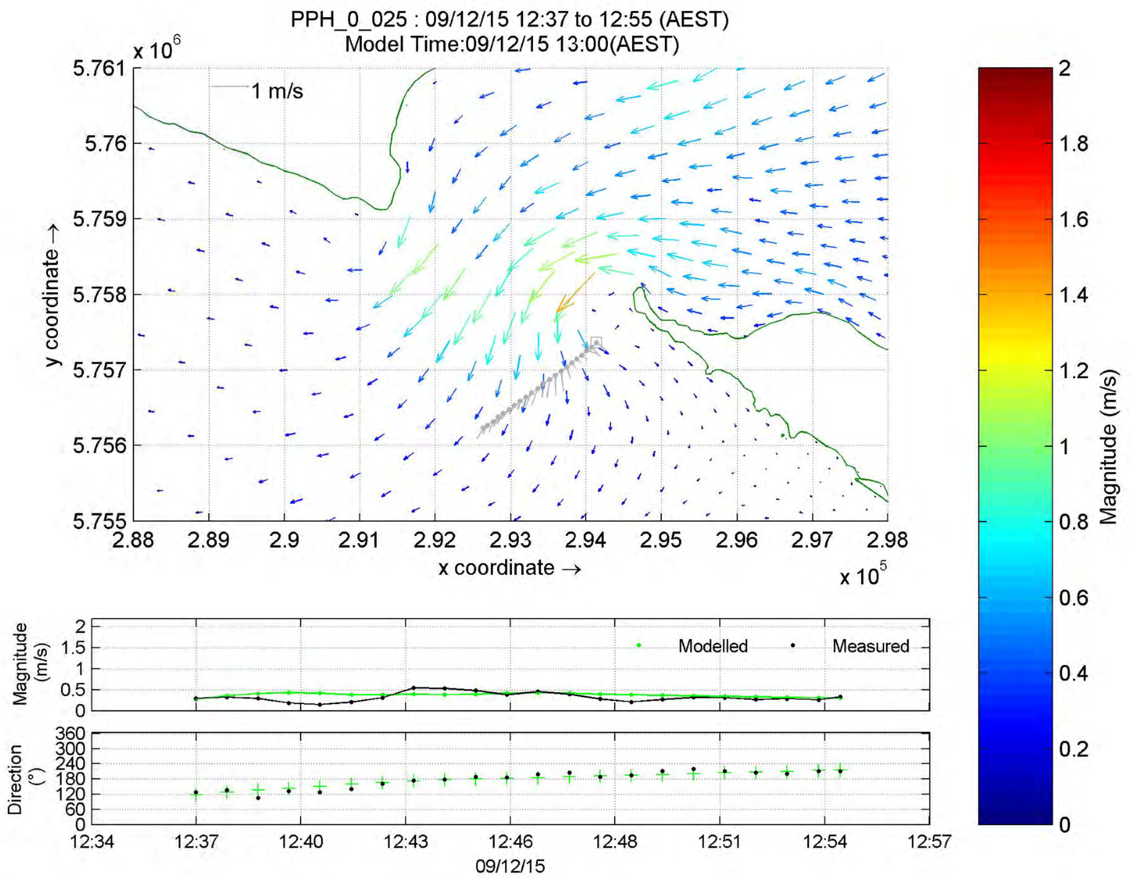
PPH_0_025 : 09/12/15 12:37 to 12:55 (AEST)
Model Time:09/12/15 13:00(AEST)
x 10^6
1 m/s
y coordinate →
x coordinate →
x 10^5
Magnitude (m/s)
Modelled
Measured
Direction (°)
09/12/15

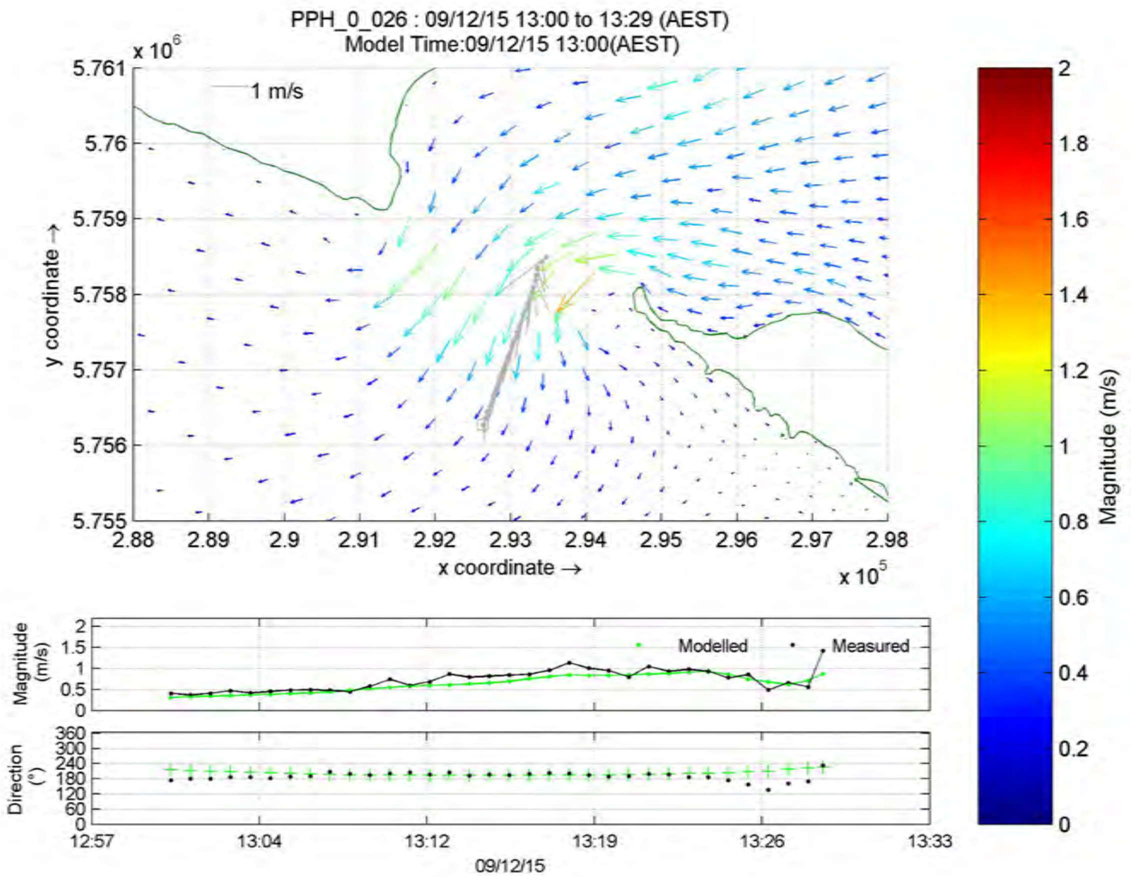
PPH_0_026 : 09/12/15 13:00 to 13:29 (AEST)
Model Time:09/12/15 13:00(AEST)
x 10^6
1 m/s
y coordinate →
x coordinate →
x 10^5
Magnitude (m/s)
Modelled
Measured
Direction (°)
09/12/15

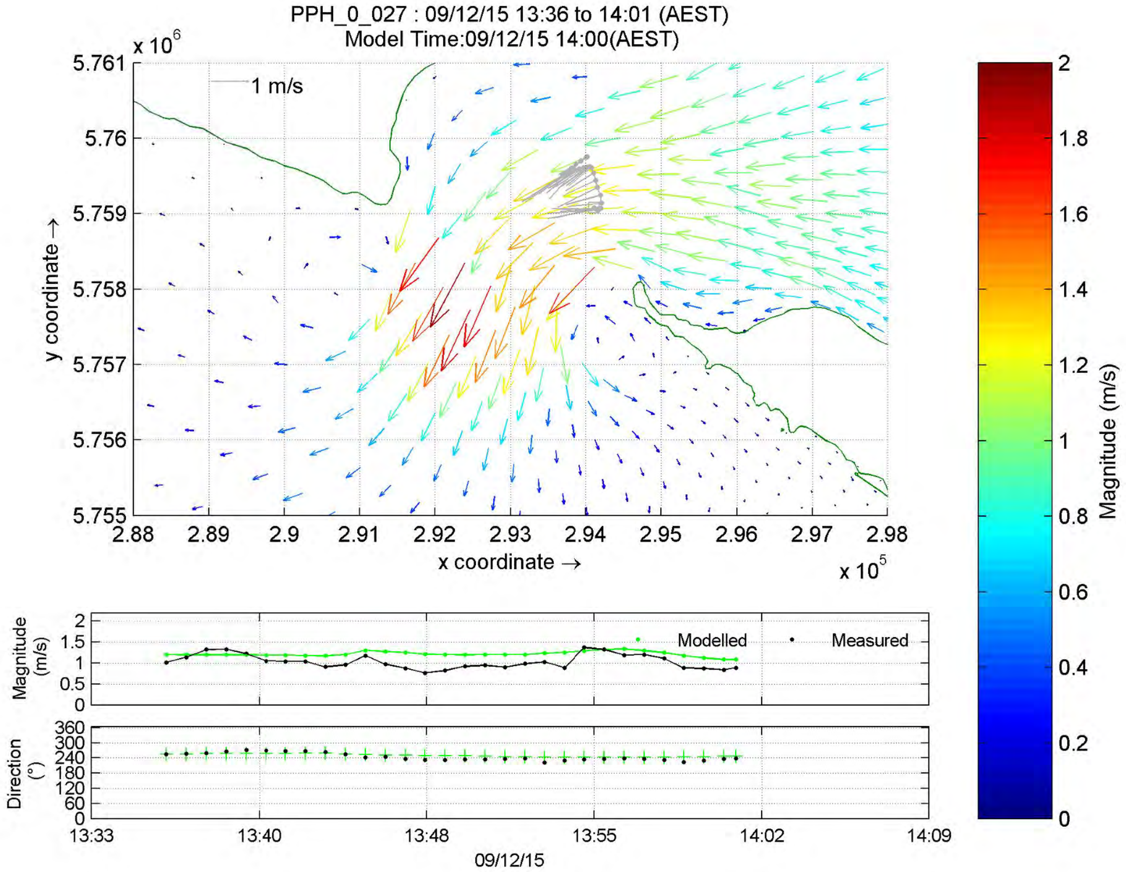
PPH_0_027 : 09/12/15 13:36 to 14:01 (AEST)
Model Time:09/12/15 14:00(AEST)
x 10^6
1 m/s
y coordinate →
x coordinate →
x 10^5
Magnitude (m/s)
Modelled
Measured
Direction (°)
13:33
13:40
13:48
13:55
14:02
14:09
09/12/15

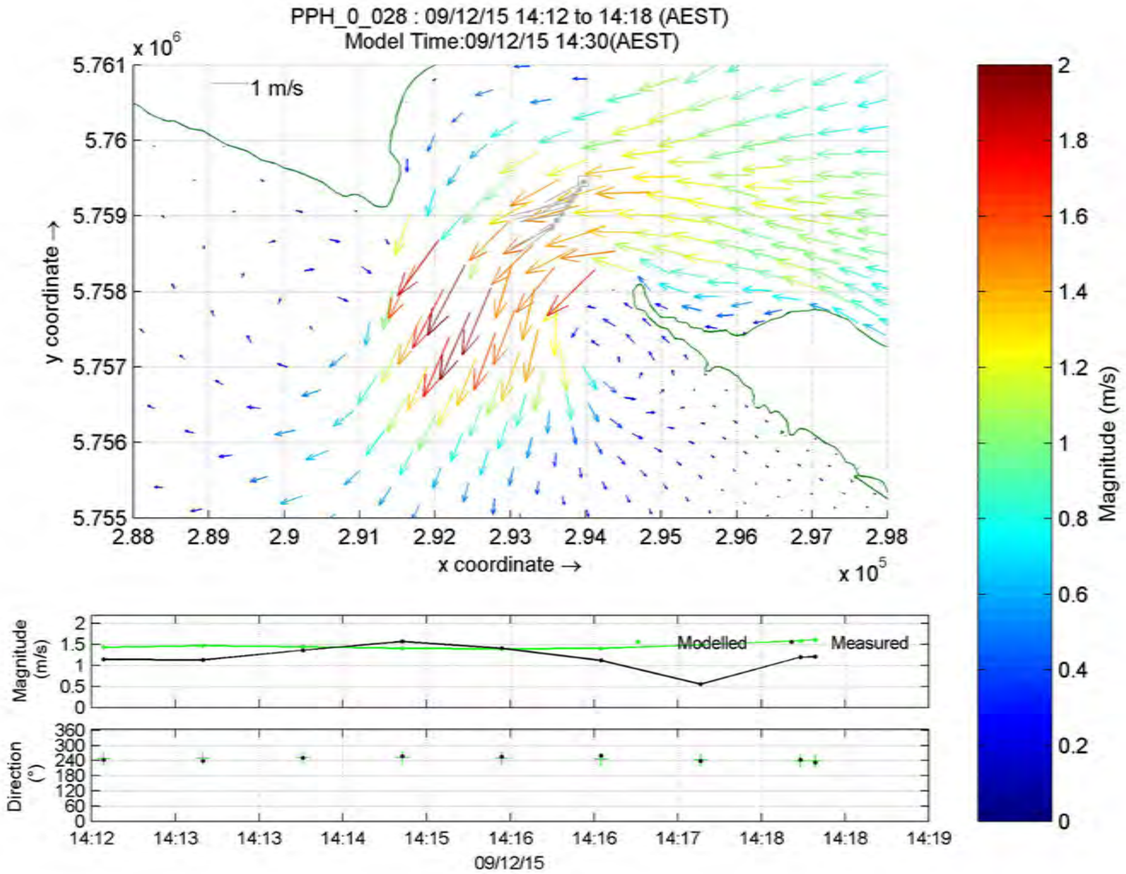
PPH_0_028 : 09/12/15 14:12 to 14:18 (AEST)
Model Time:09/12/15 14:30(AEST)
x 10^6
1 m/s
y coordinate →
x coordinate →
x 10^5
Magnitude (m/s)
Modelled
Measured
Direction (°)
14:12
14:13
14:13
14:14
14:15
14:16
14:16
14:17
14:18
14:18
14:19
09/12/15

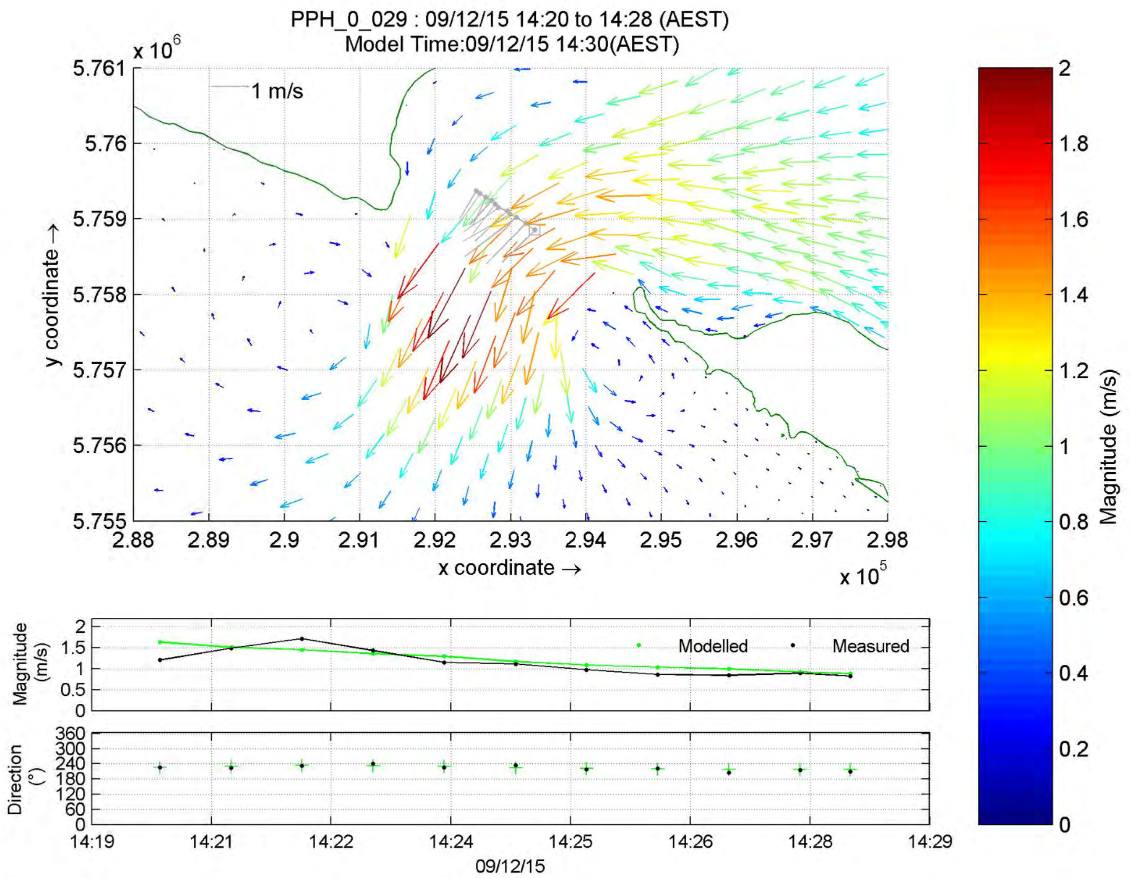
PPH_0_029 : 09/12/15 14:20 to 14:28 (AEST)
Model Time:09/12/15 14:30(AEST)
1 m/s
y coordinate →
x coordinate →
Magnitude (m/s)
Magnitude (m/s)
Modelled
Measured
Direction (°)
14:19
14:21
14:22
14:24
14:25
14:26
14:28
14:29
09/12/15

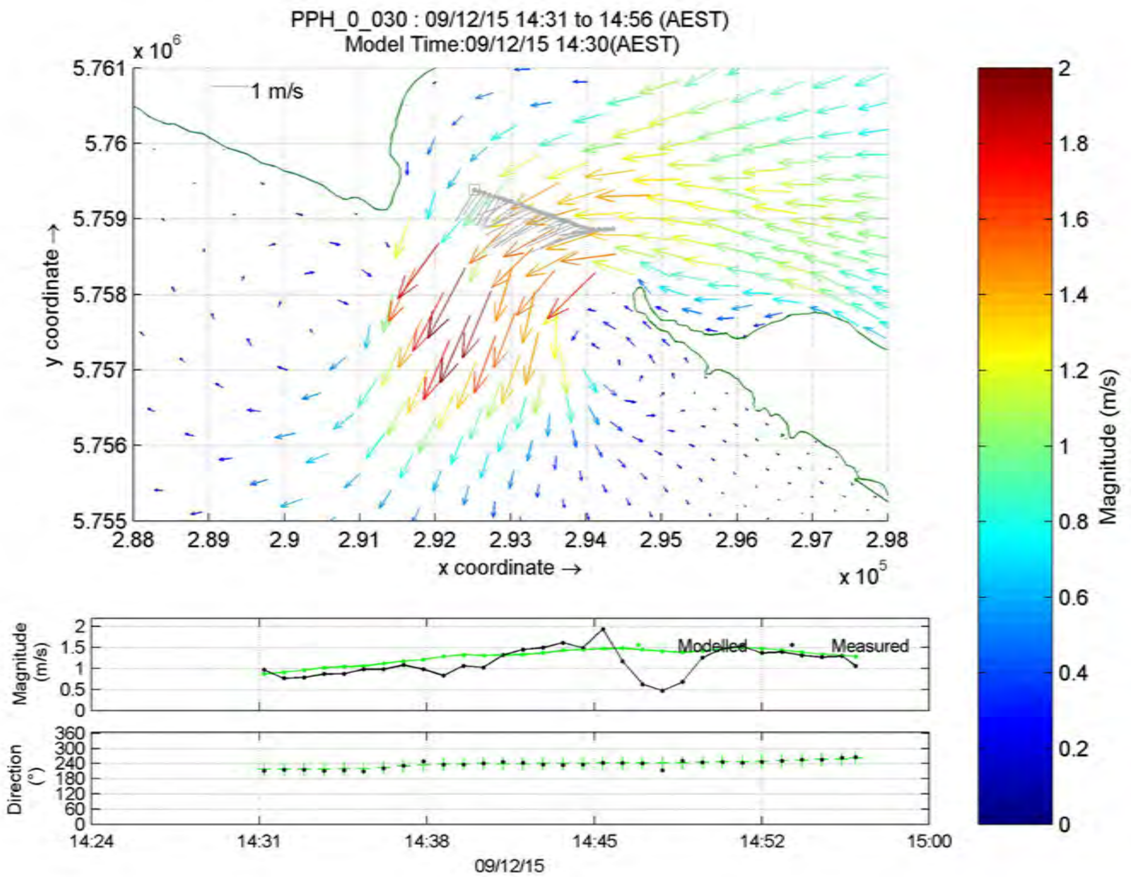
PPH_0_030 : 09/12/15 14:31 to 14:56 (AEST)
Model Time:09/12/15 14:30(AEST)
1 m/s
y coordinate →
x coordinate →
Magnitude (m/s)
Magnitude (m/s)
Modelled
Measured
Direction (°)
14:24
14:31
14:38
14:45
14:52
15:00
09/12/15

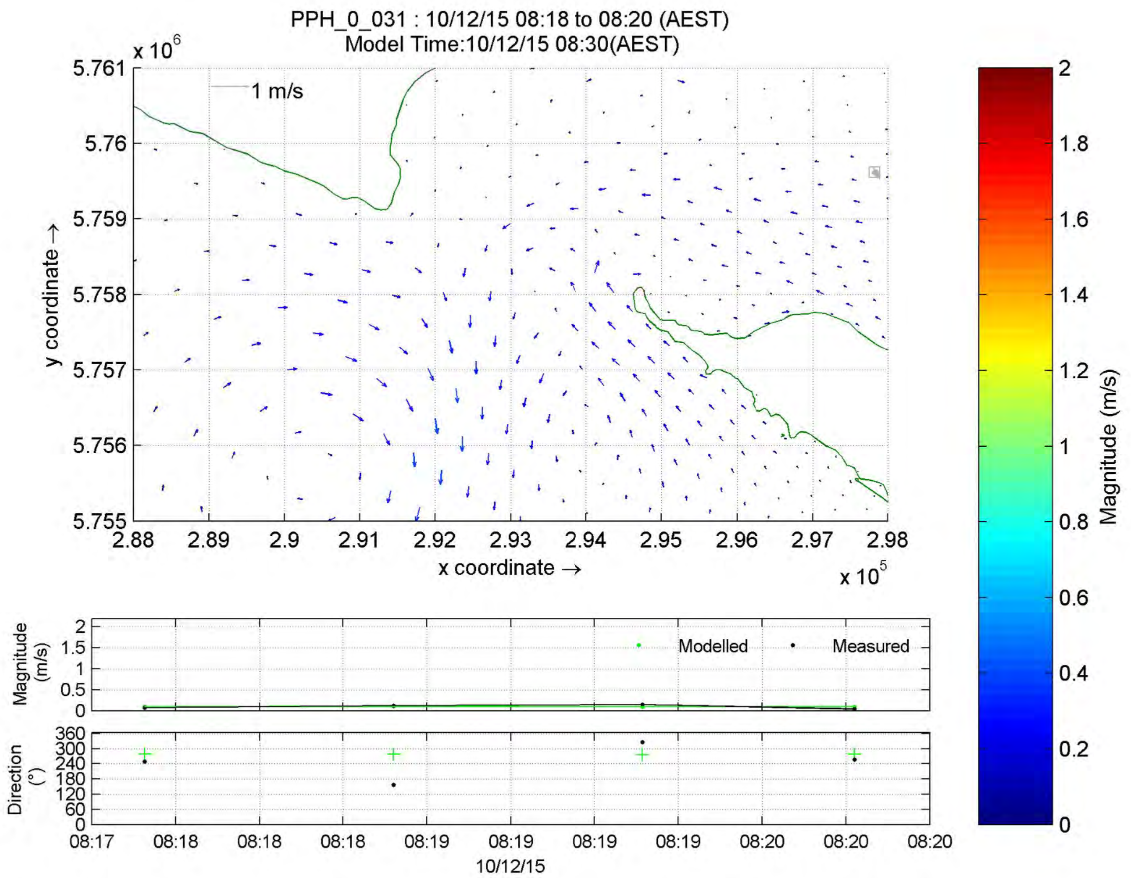
PPH_0_031 : 10/12/15 08:18 to 08:20 (AEST)
Model Time:10/12/15 08:30(AEST)
1 m/s
y coordinate →
x coordinate →
x 10^6
x 10^5
Magnitude (m/s)
Modelled
Measured
Direction (°)
10/12/15

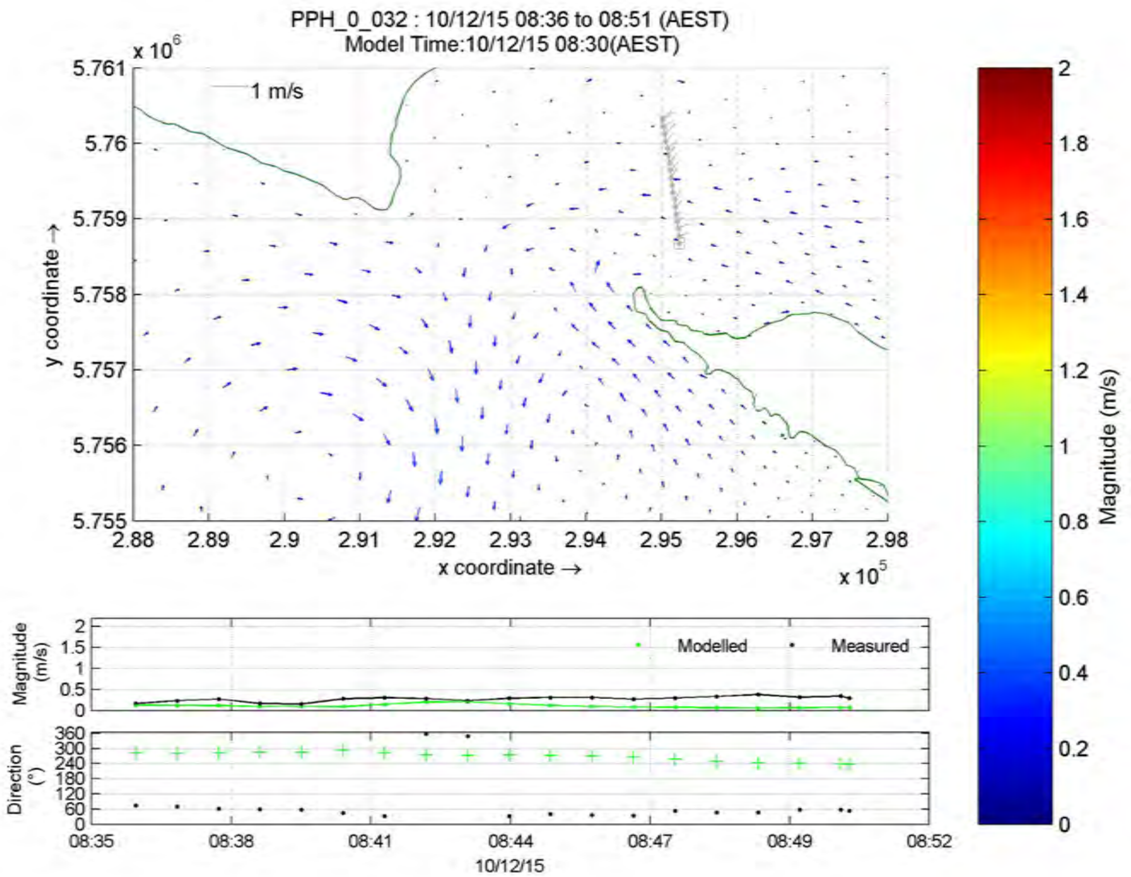
PPH_0_032 : 10/12/15 08:36 to 08:51 (AEST)
Model Time:10/12/15 08:30(AEST)
1 m/s
y coordinate →
x coordinate →
x 10^6
x 10^5
Magnitude (m/s)
Modelled
Measured
Direction (°)
10/12/15

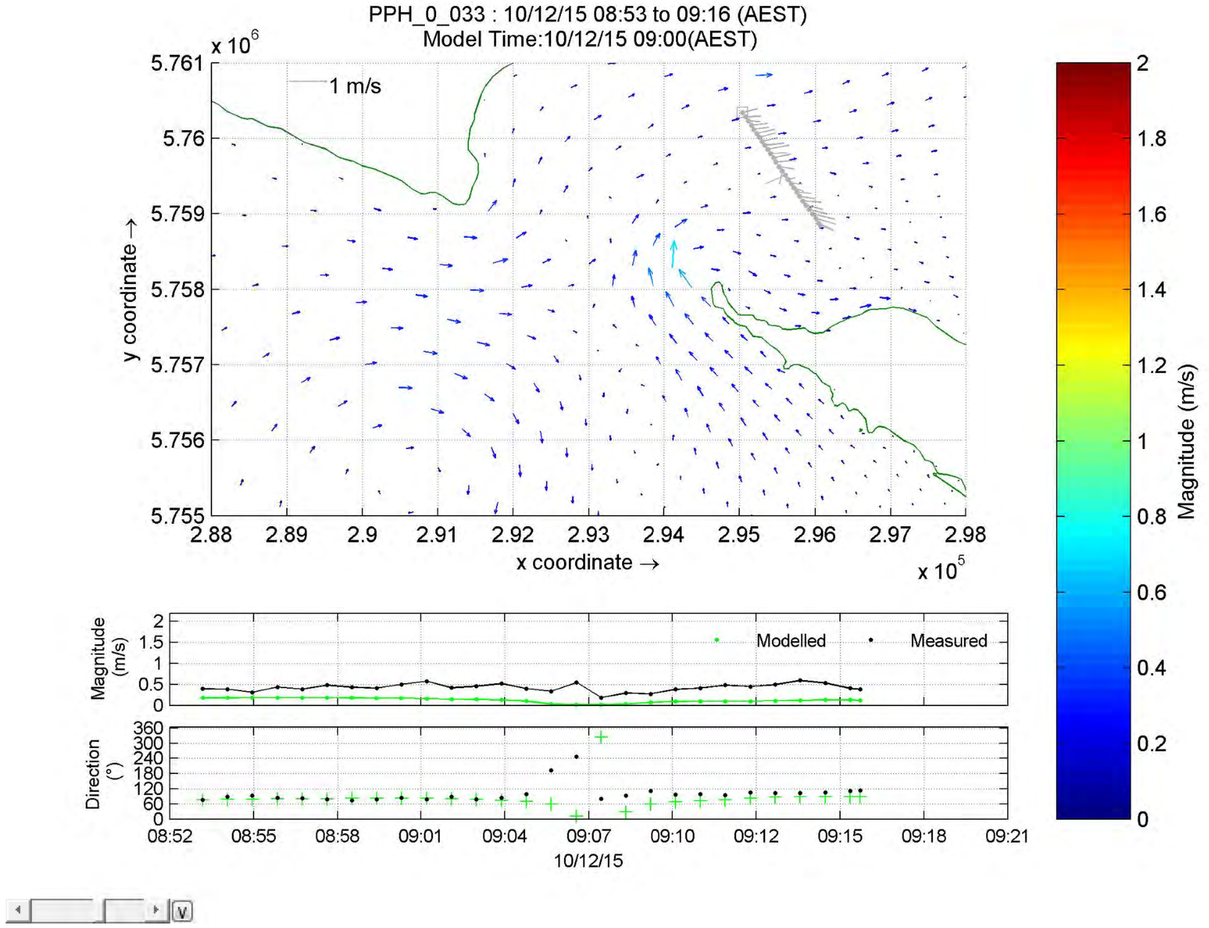
PPH_0_033 : 10/12/15 08:53 to 09:16 (AEST)
Model Time:10/12/15 09:00(AEST)
1 m/s
y coordinate →
x coordinate →
x 10^6
x 10^5
Magnitude (m/s)
Magnitude (m/s)
Modelled
Measured
Direction (°)
10/12/15

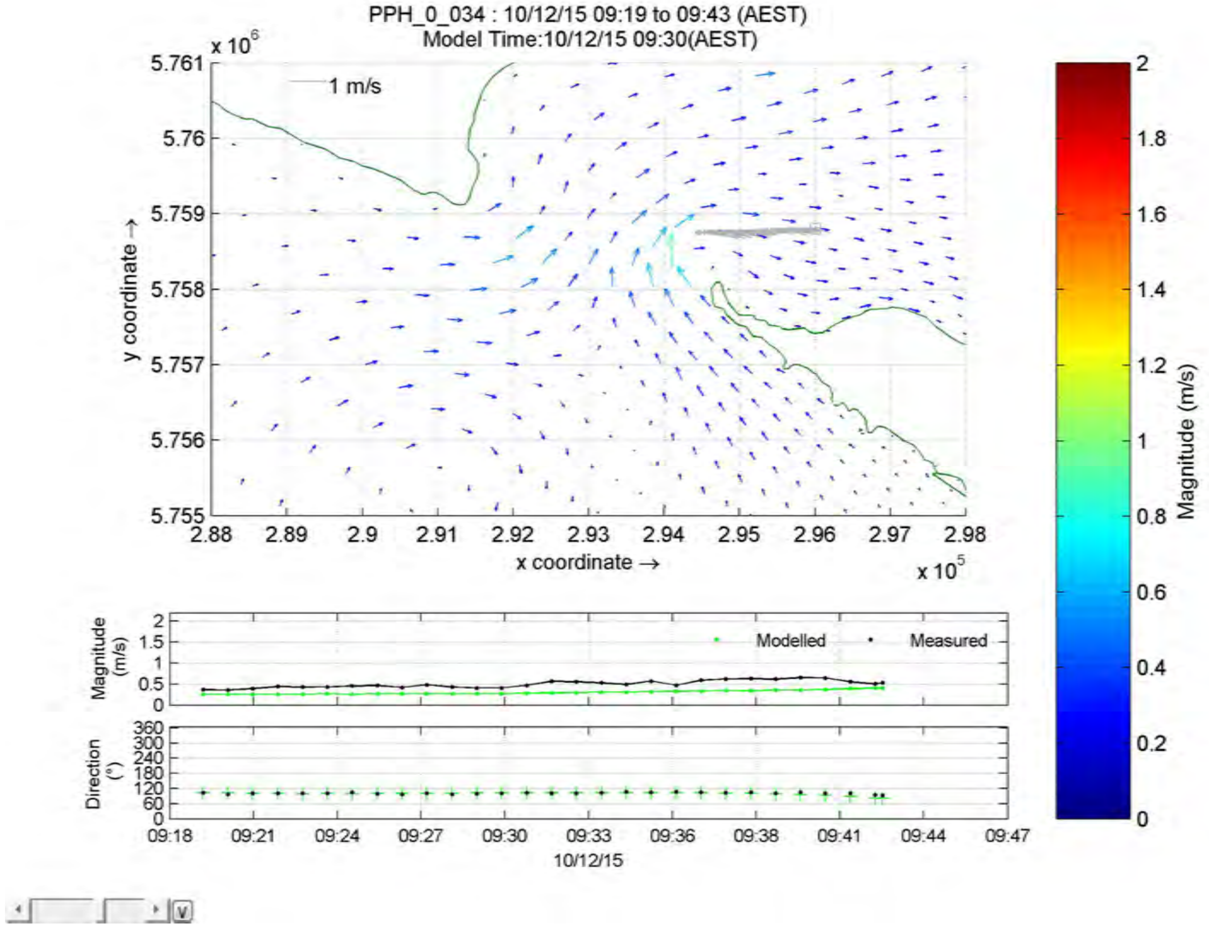
PPH_0_034 : 10/12/15 09:19 to 09:43 (AEST)
Model Time:10/12/15 09:30(AEST)
1 m/s
y coordinate →
x coordinate →
x 10^6
x 10^5
Magnitude (m/s)
Magnitude (m/s)
Modelled
Measured
Direction (°)
10/12/15

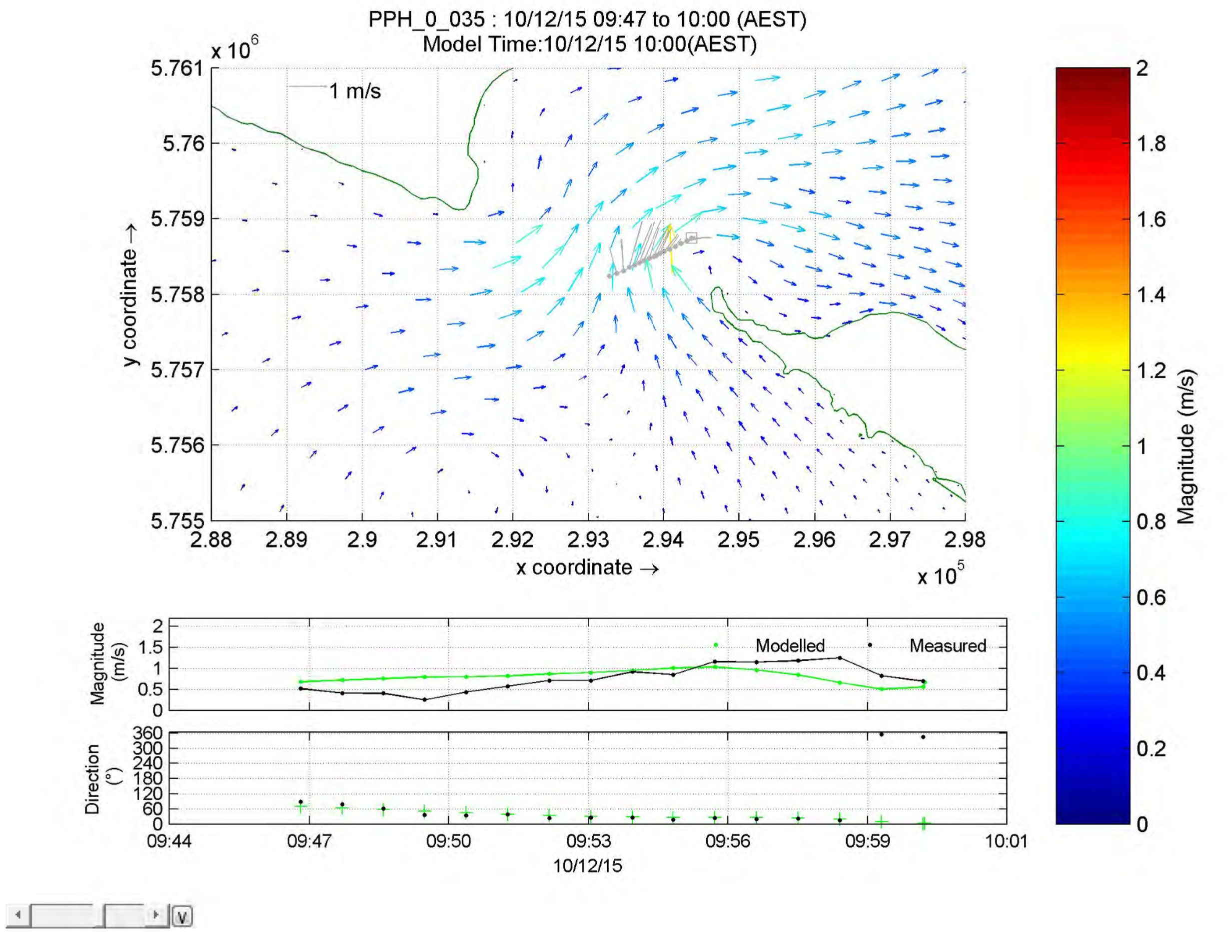
PPH_0_035 : 10/12/15 09:47 to 10:00 (AEST)
Model Time:10/12/15 10:00(AEST)
1 m/s
y coordinate →
x coordinate →
x 10^6
x 10^5
Magnitude (m/s)
Modelled
Measured
Direction (°)
09:44
09:47
09:50
09:53
09:56
09:59
10:01
10/12/15

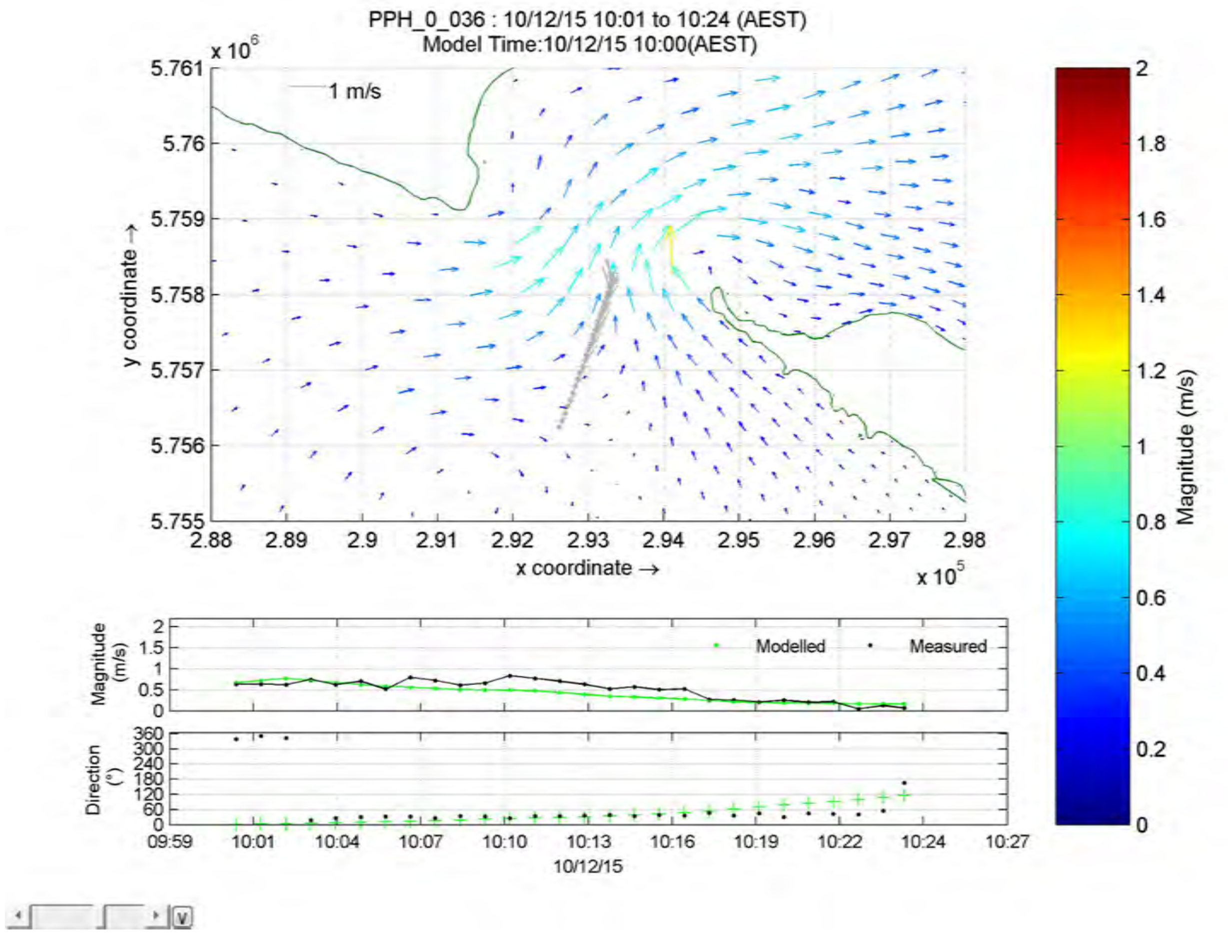
PPH_0_036 : 10/12/15 10:01 to 10:24 (AEST)
Model Time:10/12/15 10:00(AEST)
1 m/s
y coordinate →
x coordinate →
x 10^6
x 10^5
Magnitude (m/s)
Modelled
Measured
Direction (°)
09:59
10:01
10:04
10:07
10:10
10:13
10:16
10:19
10:22
10:24
10:27
10/12/15

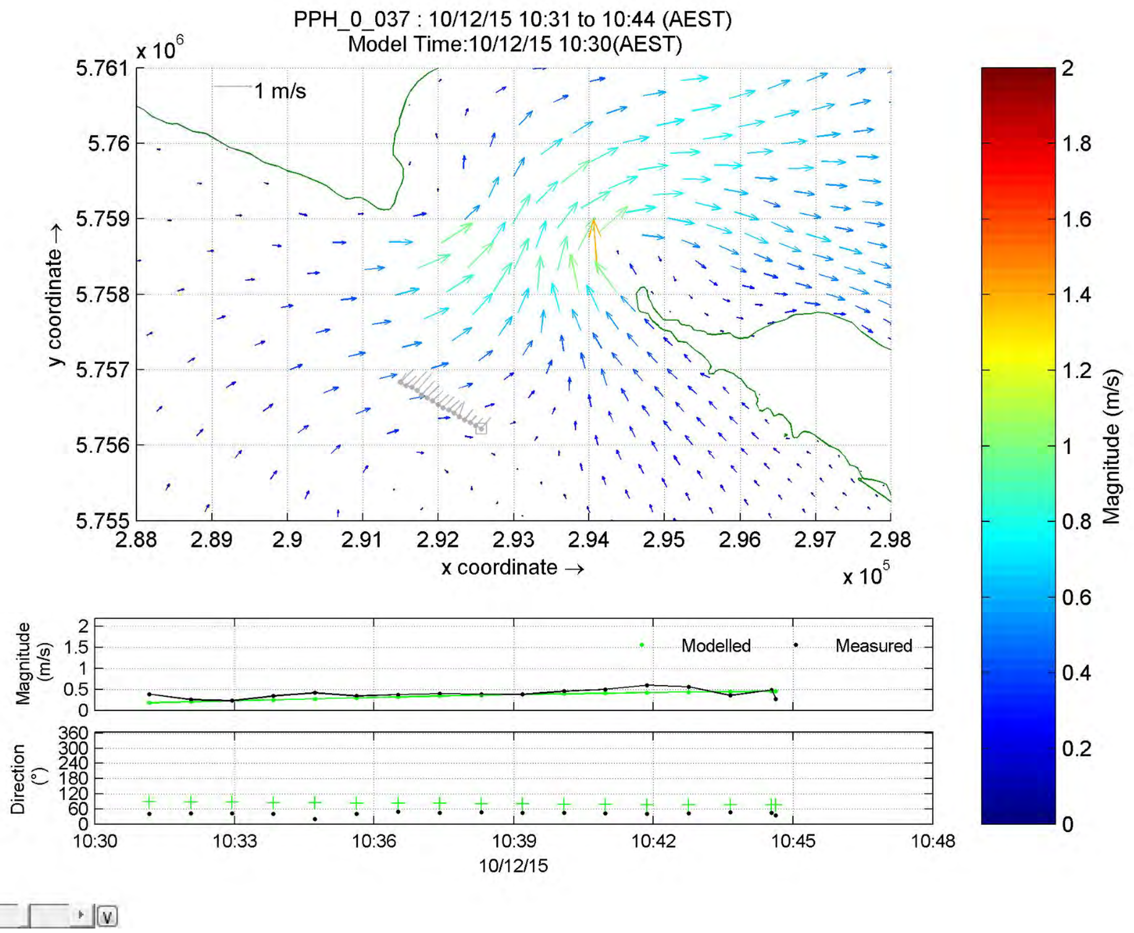
PPH_0_037 : 10/12/15 10:31 to 10:44 (AEST)
Model Time:10/12/15 10:30(AEST)
1 m/s
y coordinate →
x 10^6
x coordinate →
x 10^5
Magnitude (m/s)
Modelled
Measured
Direction (°)
10/12/15

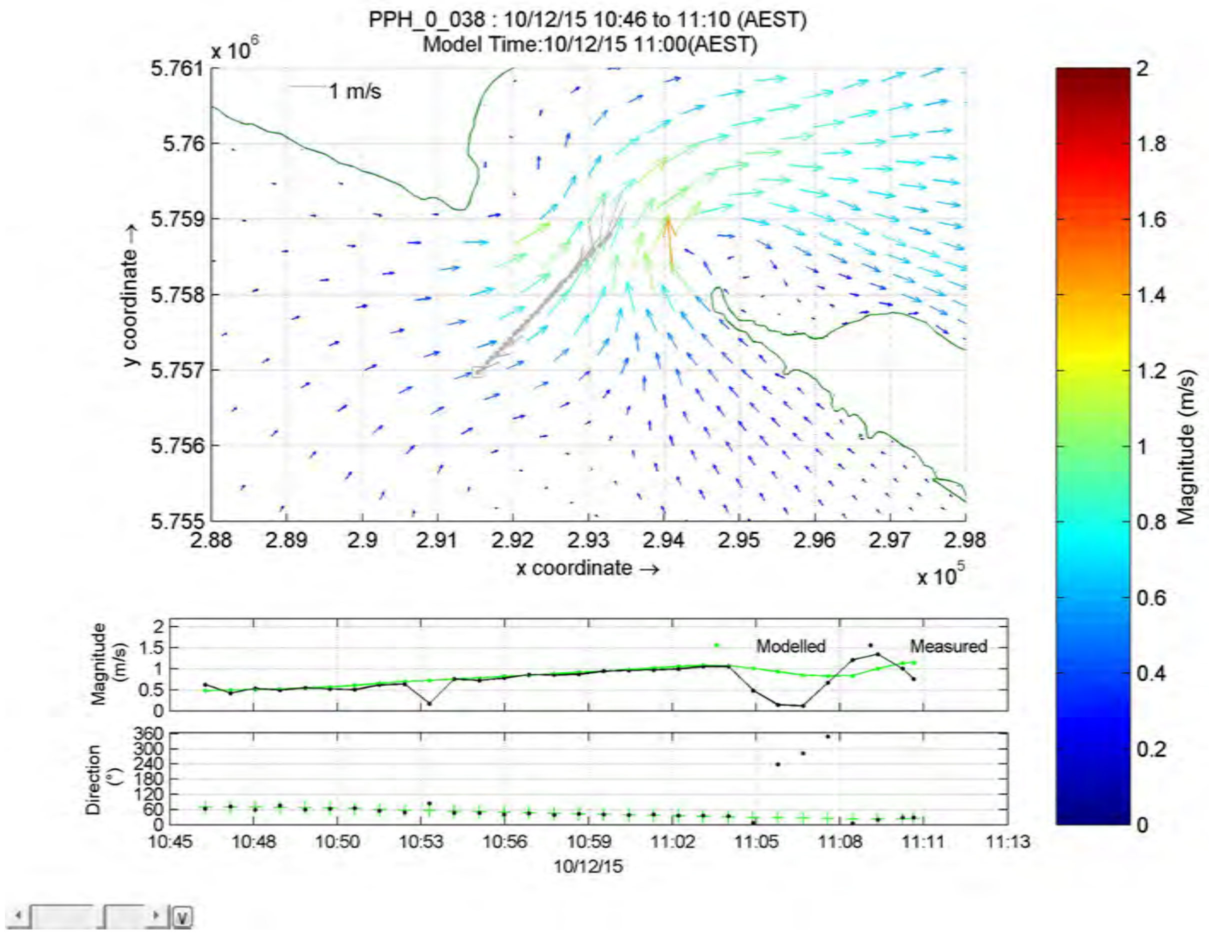
PPH_0_038 : 10/12/15 10:46 to 11:10 (AEST)
Model Time:10/12/15 11:00(AEST)
1 m/s
y coordinate →
x 10^6
x coordinate →
x 10^5
Magnitude (m/s)
Modelled
Measured
Direction (°)
10/12/15

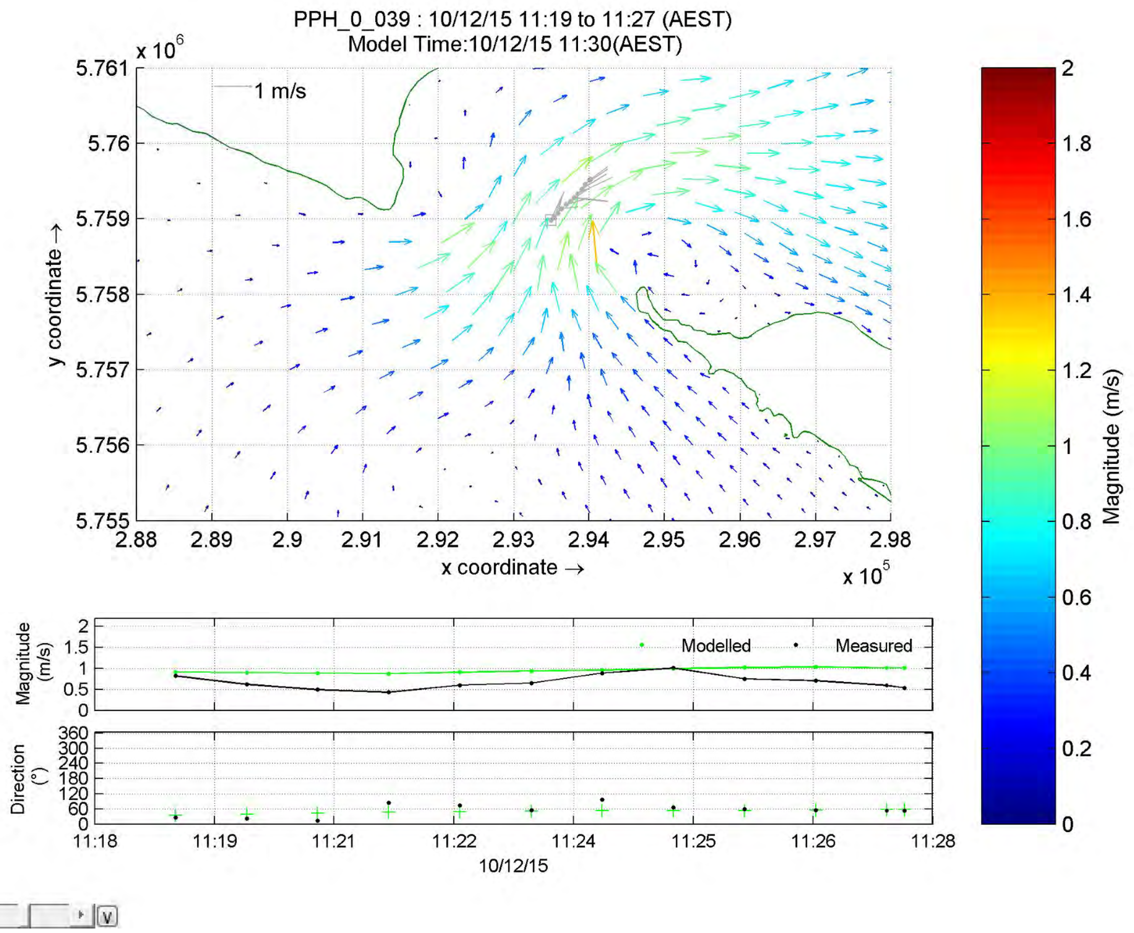
PPH_0_039 : 10/12/15 11:19 to 11:27 (AEST)
Model Time:10/12/15 11:30(AEST)
x 10^6
1 m/s
5.761
5.76
5.759
5.758
5.757
5.756
5.755
y coordinate →
2.88
2.89
2.9
2.91
2.92
2.93
2.94
2.95
2.96
2.97
2.98
x coordinate →
x 10^5
Magnitude (m/s)
2
1.8
1.6
1.4
1.2
1
0.8
0.6
0.4
0.2
0
Magnitude (m/s)
Modelled
Measured
Direction (°)
360
300
240
180
120
60
0
11:18
11:19
11:21
11:22
11:24
11:25
11:26
11:28
10/12/15

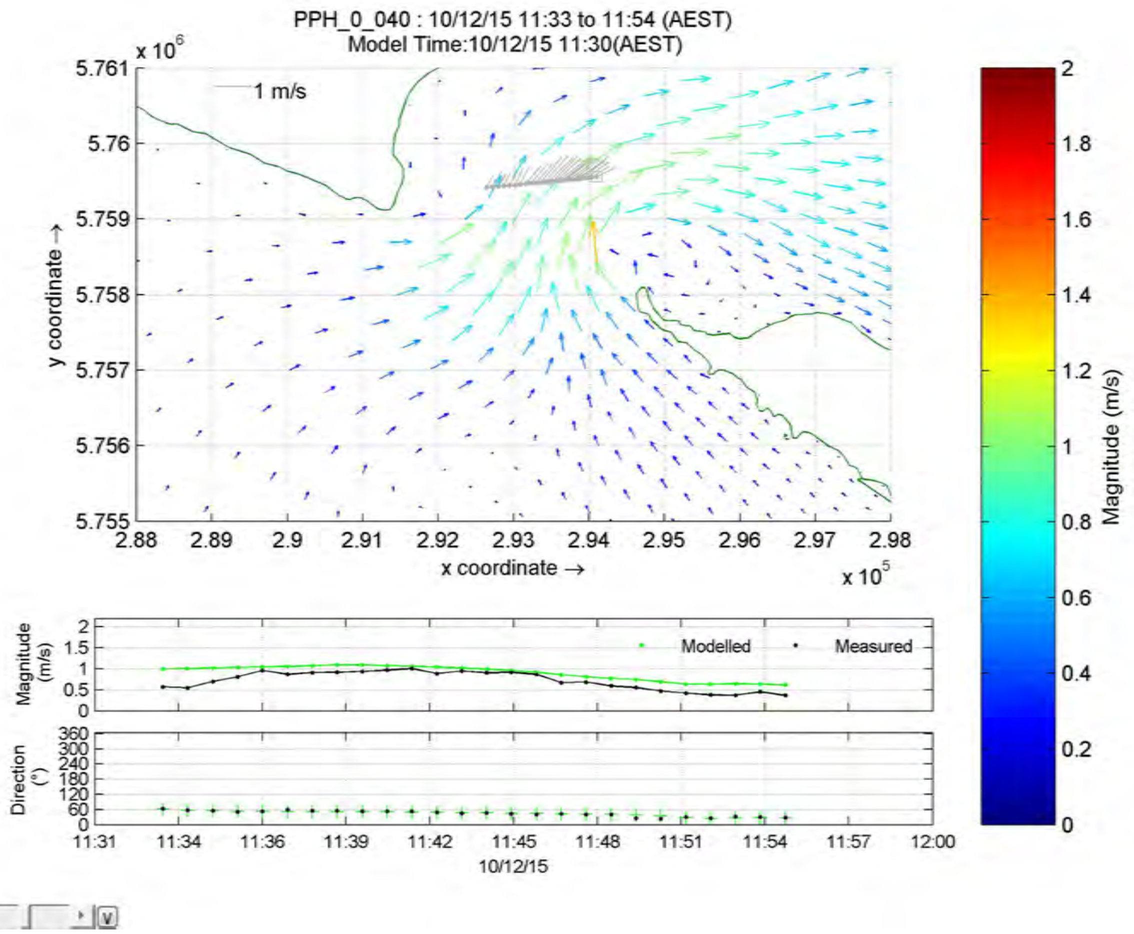
PPH_0_040 : 10/12/15 11:33 to 11:54 (AEST)
Model Time:10/12/15 11:30(AEST)
x 10^6
1 m/s
5.761
5.76
5.759
5.758
5.757
5.756
5.755
y coordinate →
2.88
2.89
2.9
2.91
2.92
2.93
2.94
2.95
2.96
2.97
2.98
x coordinate →
x 10^5
Magnitude (m/s)
2
1.8
1.6
1.4
1.2
1
0.8
0.6
0.4
0.2
0
Magnitude (m/s)
Modelled
Measured
Direction (°)
360
300
240
180
120
60
0
11:31
11:34
11:36
11:39
11:42
11:45
11:48
11:51
11:54
11:57
12:00
10/12/15

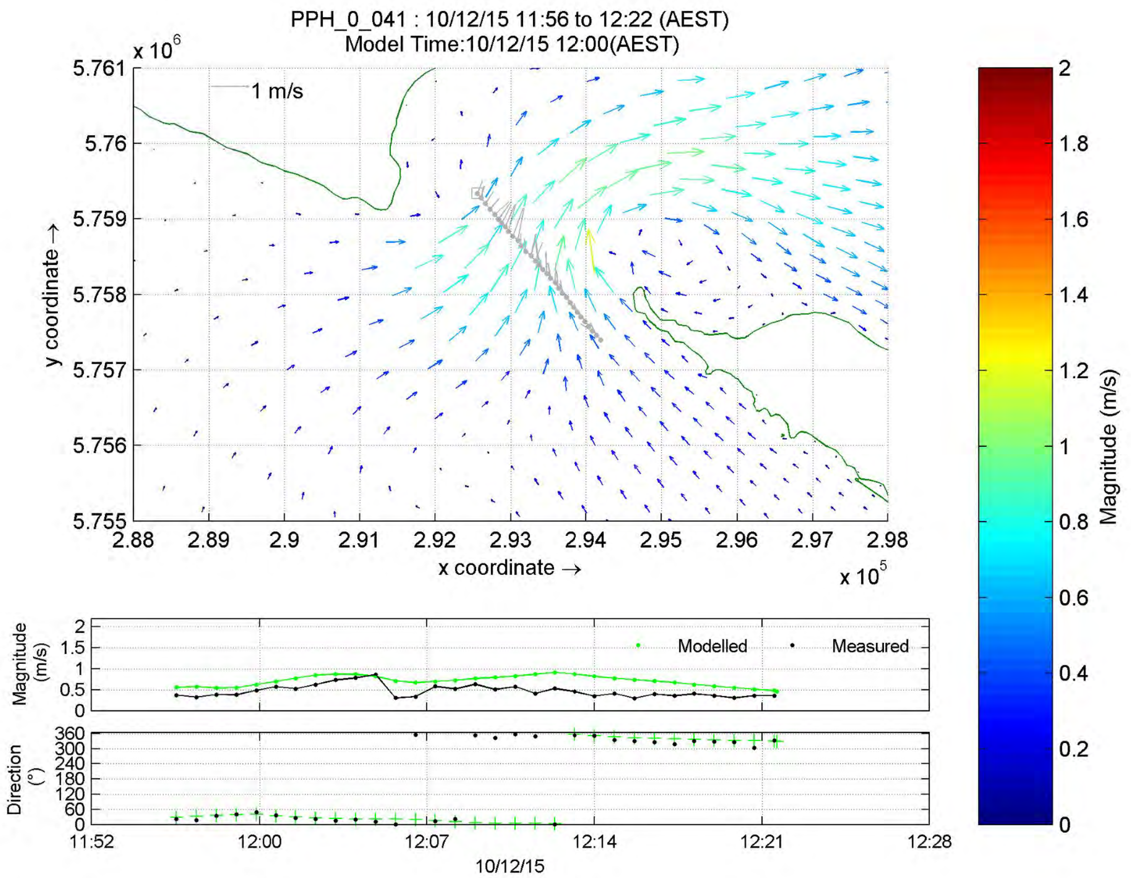
PPH_0_041 : 10/12/15 11:56 to 12:22 (AEST)
Model Time:10/12/15 12:00(AEST)
1 m/s
y coordinate →
x coordinate →
Magnitude (m/s)
Modelled
Measured
Direction (°)
10/12/15

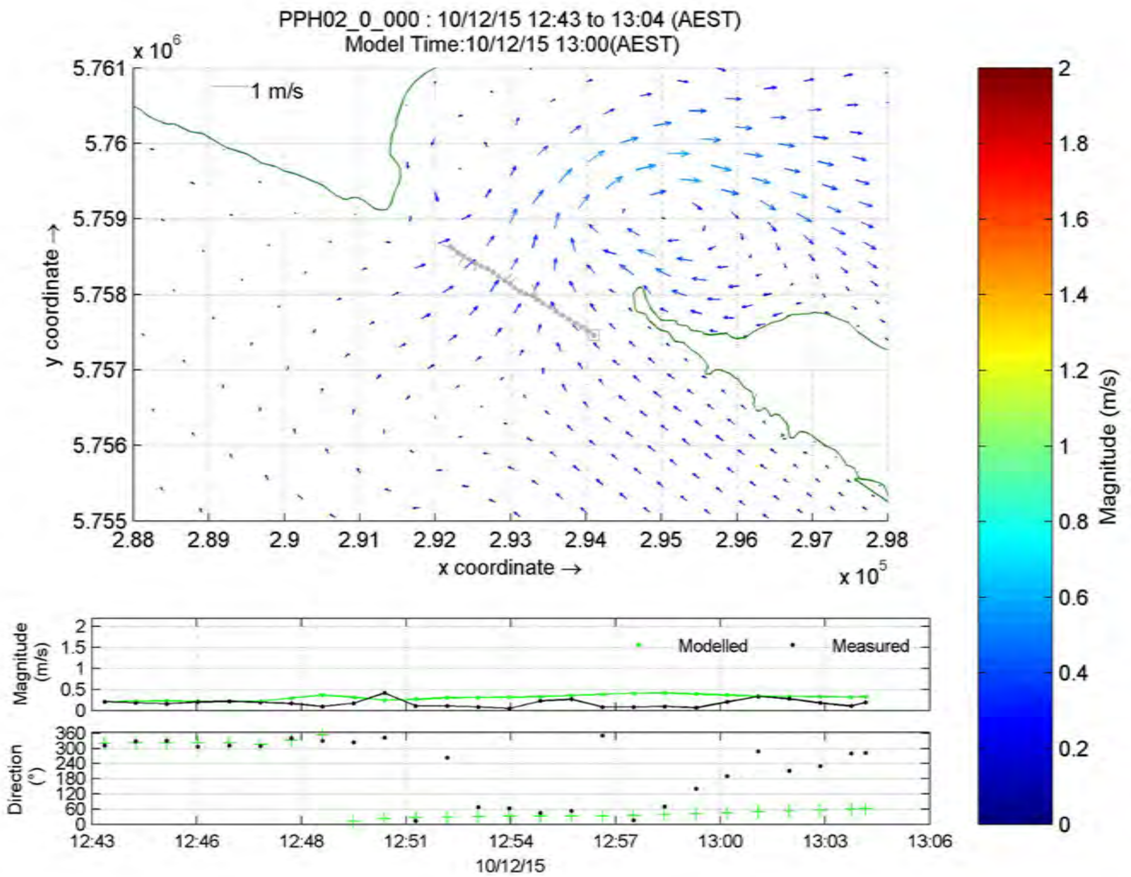
PPH02_0_000 : 10/12/15 12:43 to 13:04 (AEST)
Model Time:10/12/15 13:00(AEST)
1 m/s
y coordinate →
x coordinate →
Magnitude (m/s)
Modelled
Measured
Direction (°)
10/12/15

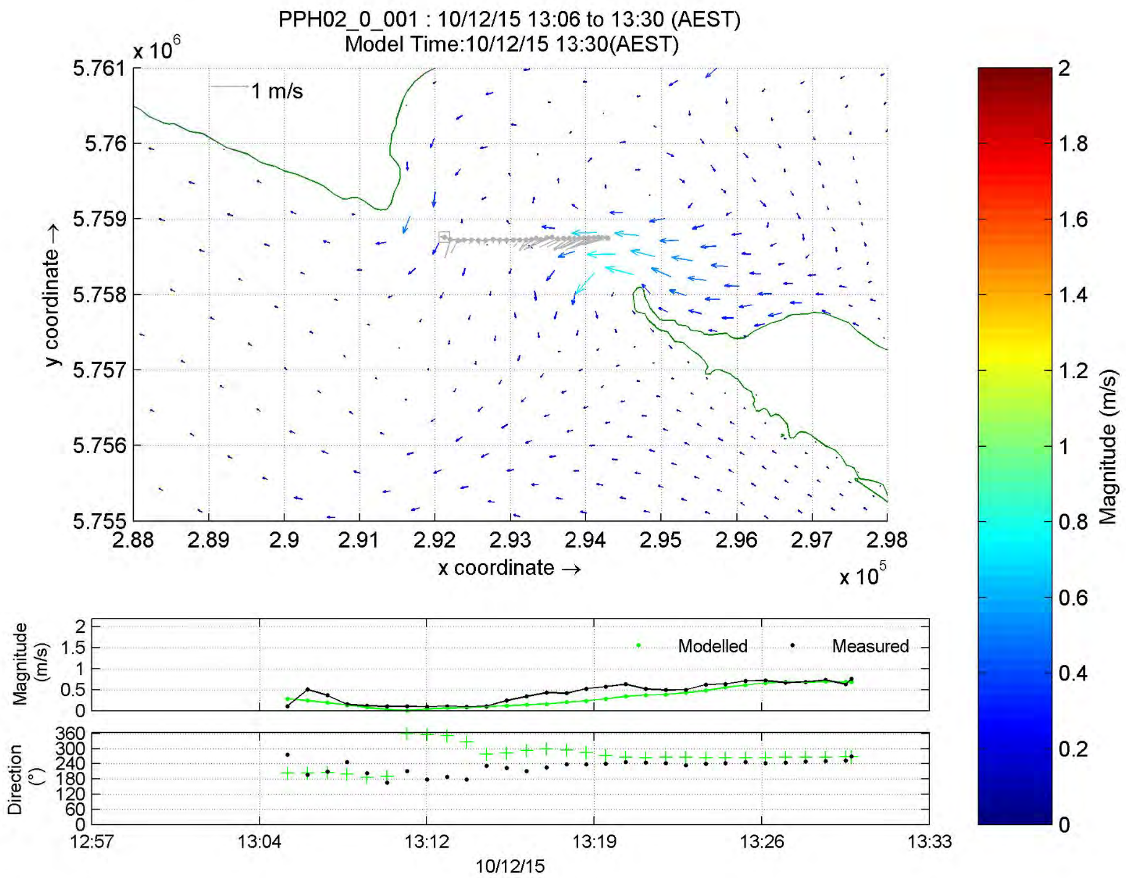
PPH02_0_001 : 10/12/15 13:06 to 13:30 (AEST)
Model Time:10/12/15 13:30(AEST)
x 10^6
1 m/s
y coordinate →
x coordinate →
x 10^5
Magnitude (m/s)
Modelled
Measured
Direction (°)
10/12/15
12:57
13:04
13:12
13:19
13:26
13:33

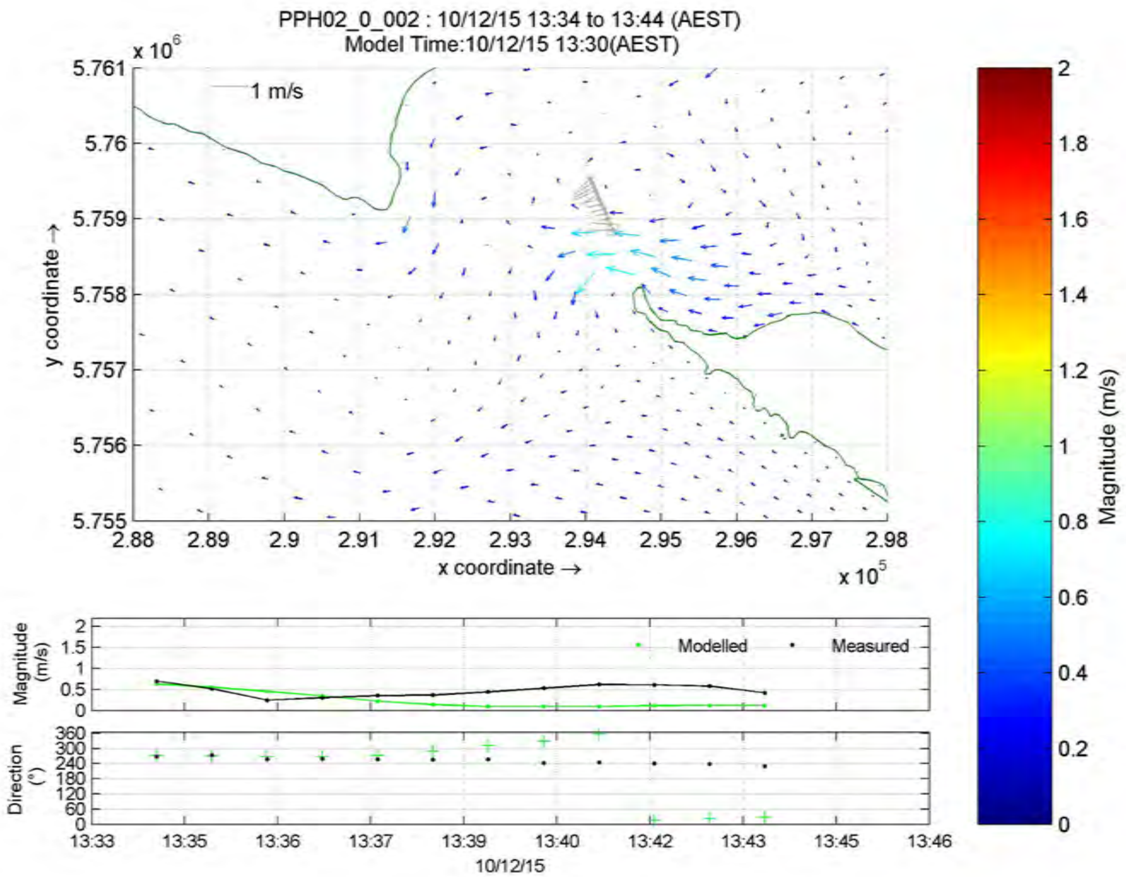
PPH02_0_002 : 10/12/15 13:34 to 13:44 (AEST)
Model Time:10/12/15 13:30(AEST)
x 10^6
1 m/s
y coordinate →
x coordinate →
x 10^5
Magnitude (m/s)
Modelled
Measured
Direction (°)
10/12/15
13:33
13:35
13:36
13:37
13:39
13:40
13:42
13:43
13:45
13:46

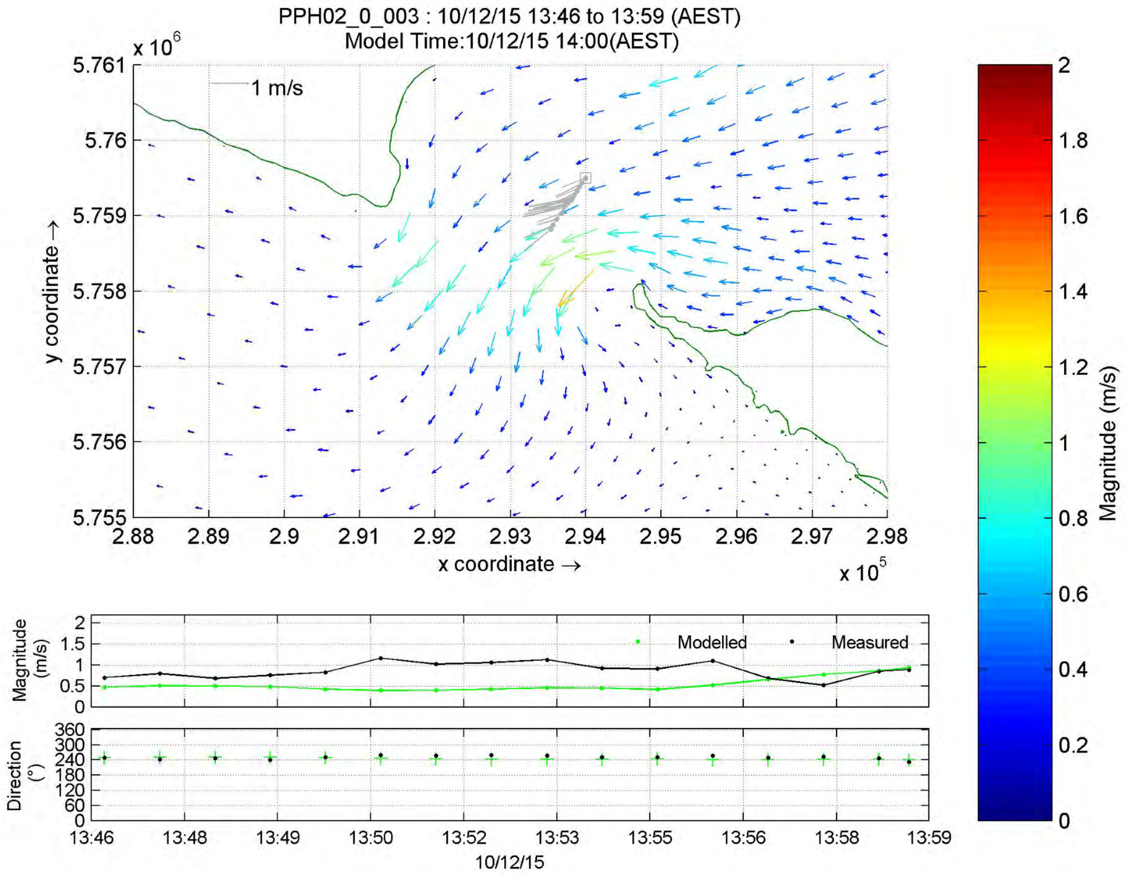
PPH02_0_003 : 10/12/15 13:46 to 13:59 (AEST)
Model Time:10/12/15 14:00(AEST)
1 m/s
y coordinate →
x coordinate →
Magnitude (m/s)
Modelled
Measured
Direction (°)
10/12/15

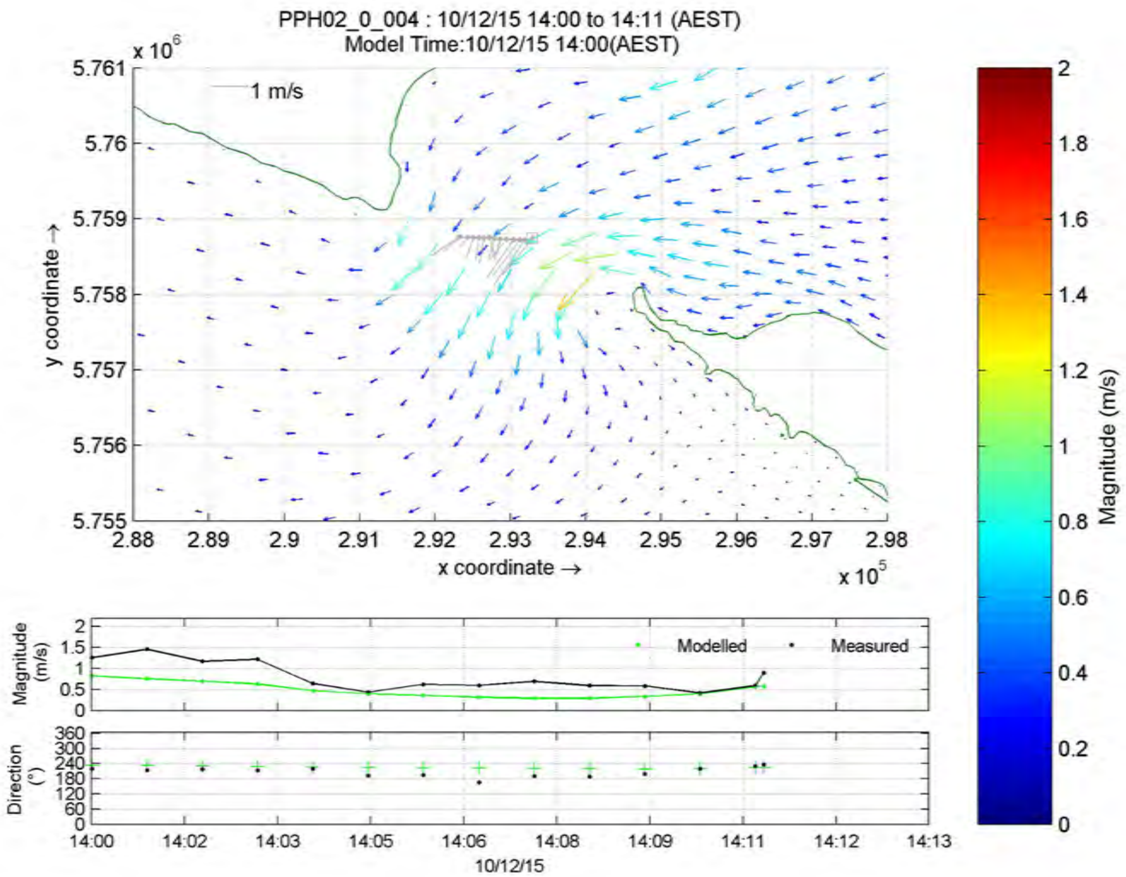
PPH02_0_004 : 10/12/15 14:00 to 14:11 (AEST)
Model Time:10/12/15 14:00(AEST)
1 m/s
y coordinate →
x coordinate →
Magnitude (m/s)
Modelled
Measured
Direction (°)
10/12/15

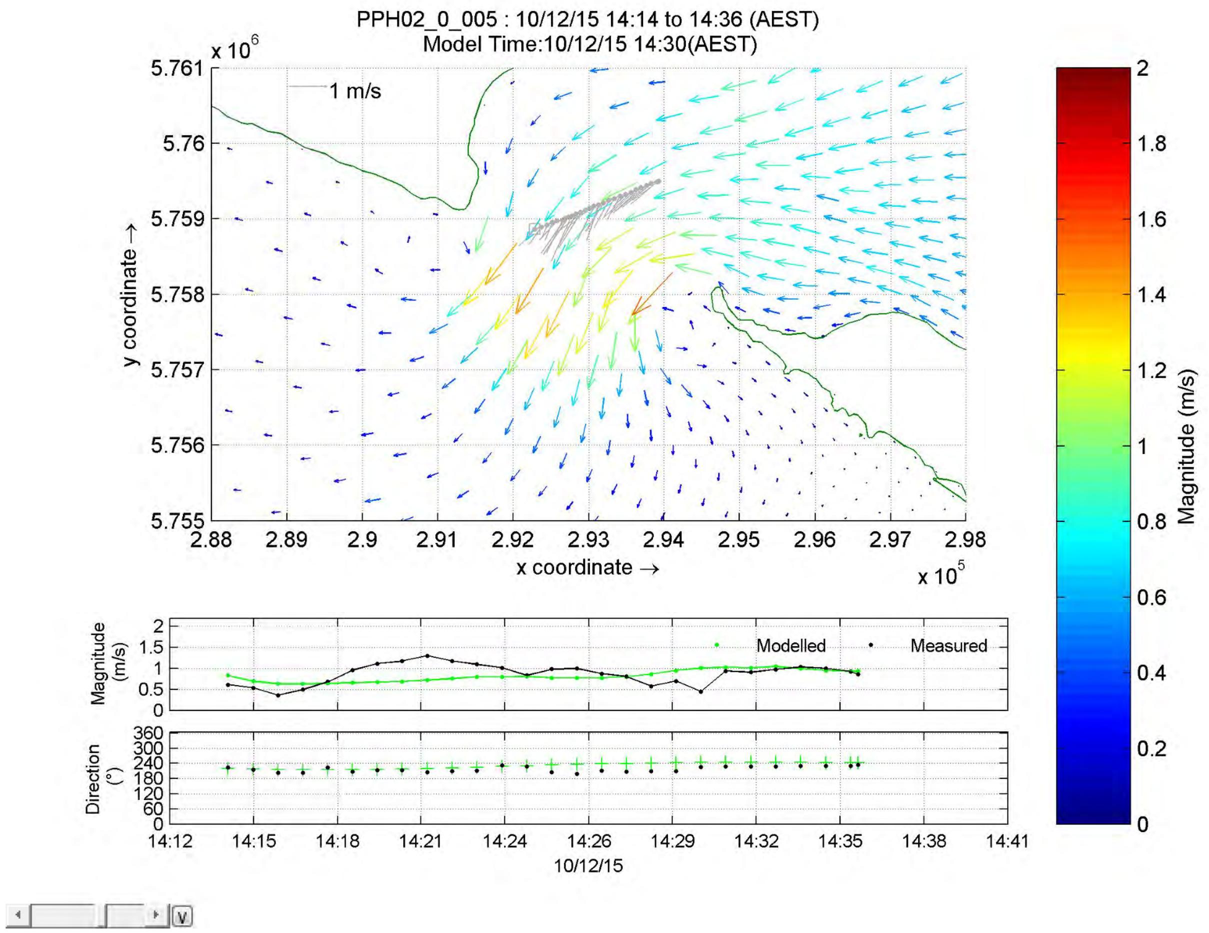
PPH02_0_005 : 10/12/15 14:14 to 14:36 (AEST)
Model Time:10/12/15 14:30(AEST)
1 m/s
y coordinate →
x coordinate →
Magnitude (m/s)
Modelled
Measured
Direction (°)
10/12/15

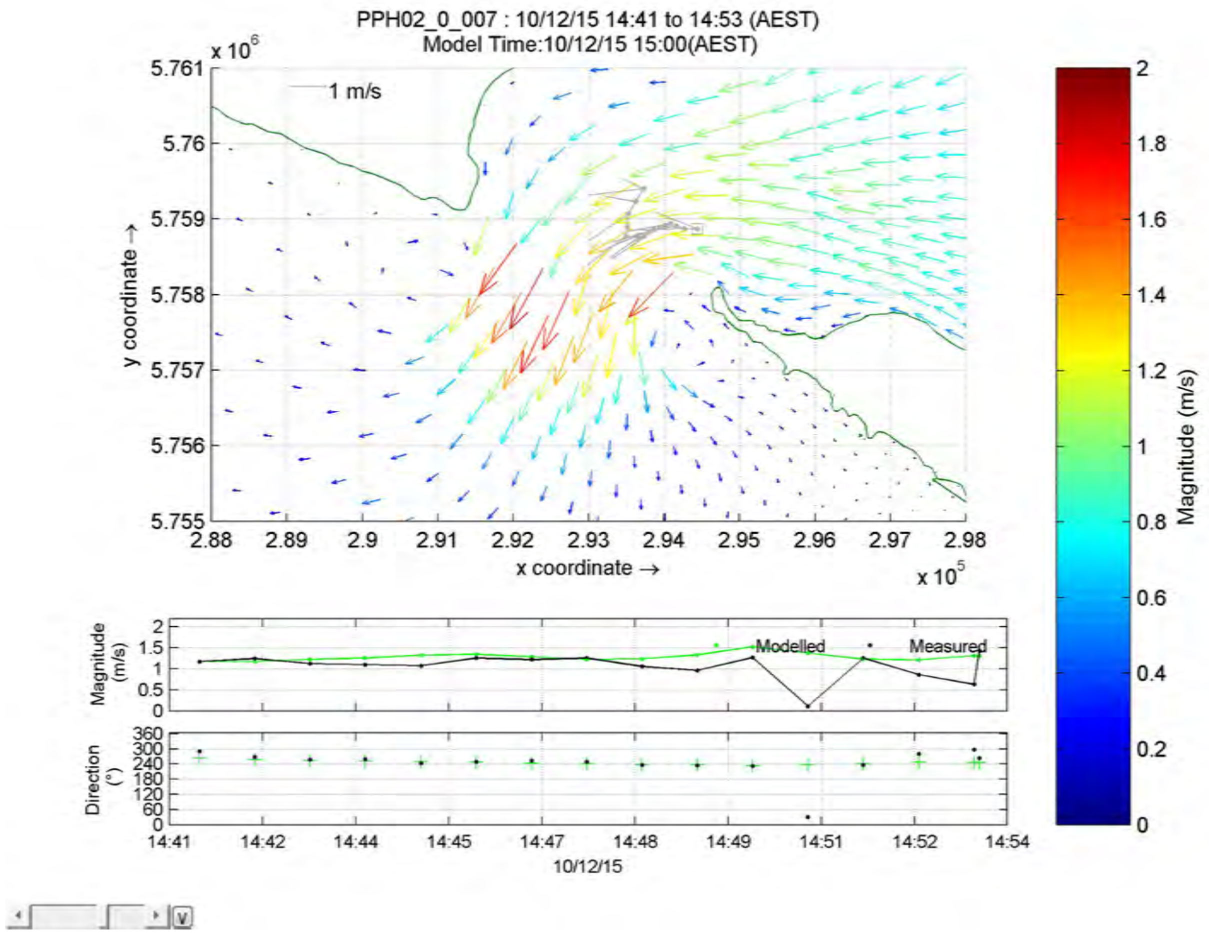
PPH02_0_007 : 10/12/15 14:41 to 14:53 (AEST)
Model Time:10/12/15 15:00(AEST)
1 m/s
y coordinate →
x coordinate →
Magnitude (m/s)
Modelled
Measured
Direction (°)
10/12/15

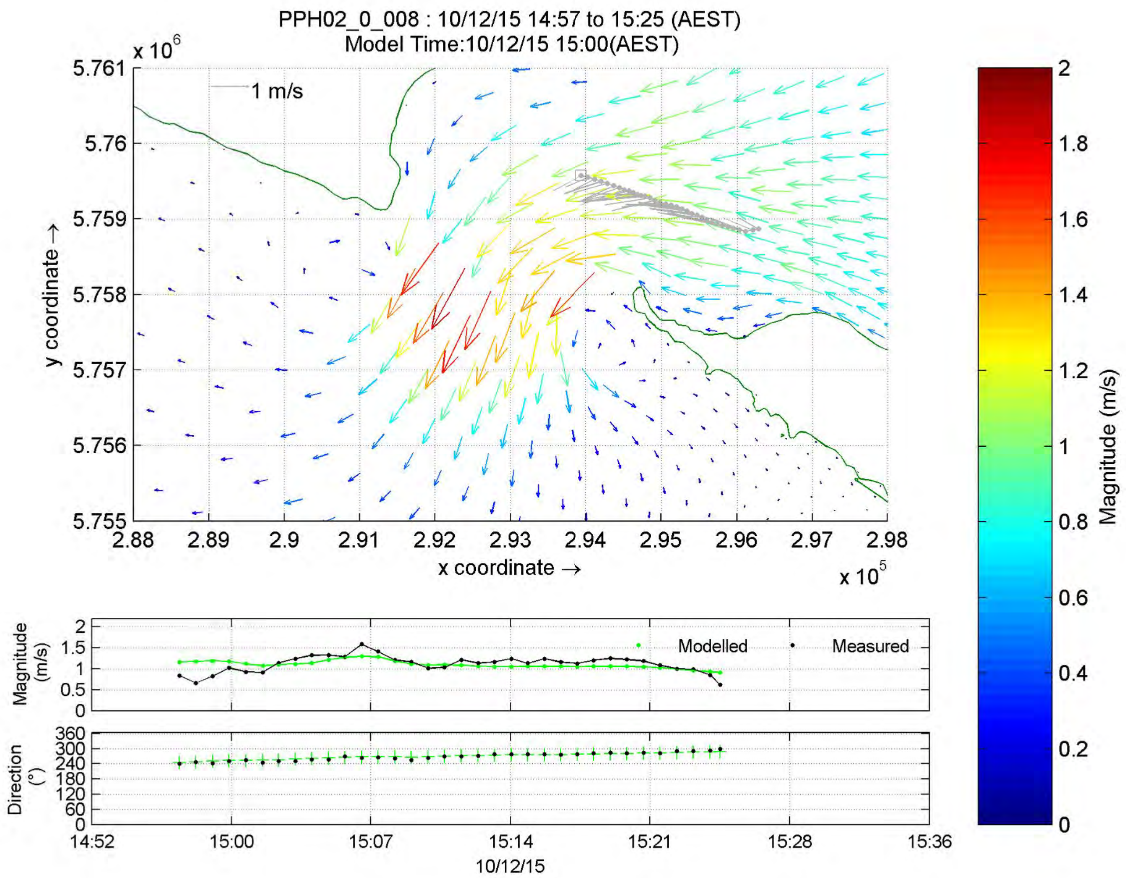
PPH02_0_008 : 10/12/15 14:57 to 15:25 (AEST)
Model Time:10/12/15 15:00(AEST)
x 10^6
1 m/s
5.761
5.76
5.759
5.758
5.757
5.756
5.755
y coordinate →
2.88
2.89
2.9
2.91
2.92
2.93
2.94
2.95
2.96
2.97
2.98
x coordinate →
x 10^5
Magnitude (m/s)
Modelled
Measured
Direction (°)
14:52
15:00
15:07
15:14
15:21
15:28
15:36
10/12/15
2
1.8
1.6
1.4
1.2
1
0.8
0.6
0.4
0.2
0

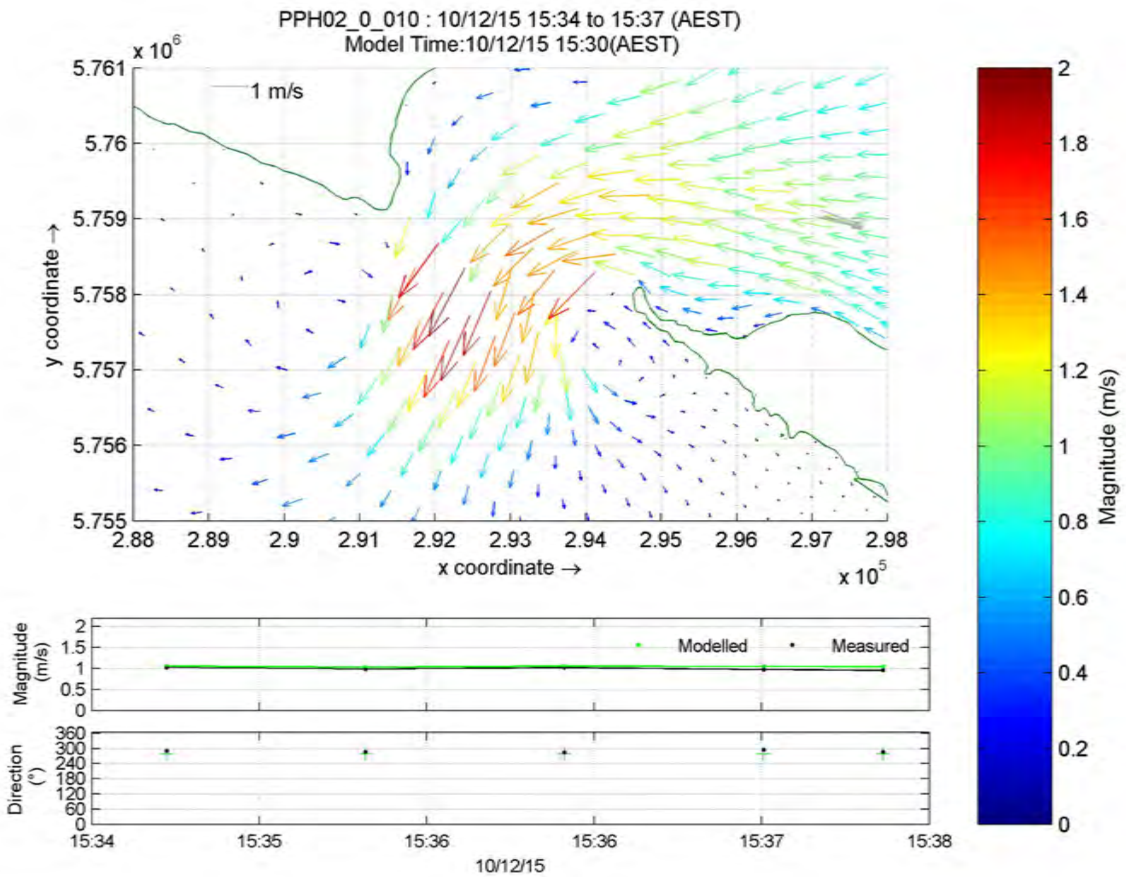
PPH02_0_010 : 10/12/15 15:34 to 15:37 (AEST)
Model Time:10/12/15 15:30(AEST)
x 10^6
1 m/s
5.761
5.76
5.759
5.758
5.757
5.756
5.755
y coordinate →
2.88
2.89
2.9
2.91
2.92
2.93
2.94
2.95
2.96
2.97
2.98
x coordinate →
x 10^5
Magnitude (m/s)
Modelled
Measured
Direction (°)
15:34
15:35
15:36
15:36
15:37
15:38
10/12/15
2
1.8
1.6
1.4
1.2
1
0.8
0.6
0.4
0.2
0